CHARACTERIZATION AND INTERVENTION OF *CAMPYLOBACTER JEJUNI* PERSISTENCE AND BIOFILM FORMATION

by

Jinsong Feng

MSc, Zhejiang University, 2013

A THESIS SUBMITTED IN PARTIAL FULFILLMENT OF

THE REQUIREMENTS FOR THE DEGREE OF

DOCTOR OF PHILOSOPHY

in

THE FACULTY OF GRADUATE AND POSTDOCTORAL STUDIES

(FOOD SCIENCE)

THE UNIVERSITY OF BRITISH COLUMBIA

(Vancouver)

March 2018

Abstract

The hard-to-treat chronic bacterial infection is one of the most significant challenges to conventional antibiotic therapy. These chronic infections represent an elevated risk for the development of severe clinical consequences. Bacteria can form biofilms or persister cells to withstand harsh stresses and antibiotic treatment. In addition, both biofilm and persister cells can restore the bacterial population upon the removal of stresses and antibiotic treatment. Hence, biofilm and persister cells are proposed to be one of the major survival strategies that associate chronic bacterial infections. As one of the major causes of human gastroenteritis in the world, *Campylobacter jejuni* was frequently identified in food production as well as in the environment. However, how can this microaerophilic microbe survive in the aerobic environment and disseminate throughout the food chain to eventually cause campylobacteriosis is not fully understood yet. We argued that bacterial biofilm and persister cells be two particular survival state of *C. jejuni* that contribute to the prevalence of *C. jejuni*. In this dissertation, particular survival modes of *C. jejuni*, known as biofilm and persister cells, were characterized. We found that *C. jejuni* could form both mono- and multispecies biofilms and biofilm formation was significantly influenced by environmental stresses. The extracellular DNA was the factor that mediated this influence. In addition, we identified the presence of *C. jejuni* persister cells which accounted for ~ 0.01% of the total population. The transcriptome analysis of persister cells indicated that the low metabolic activity and bacterial dormancy could play an important role in the formation of persister cells. In the end, a synergistic treatment using ajoene and Al_2O_3/TiO_2 nanoparticles in a combined manner was applied to generate a significant antimicrobial effect against *C. jejuni*. In this study, we comprehensively investigated the two major bacterial survival strategies, namely biofilm and persister cells, and applied innovative antimicrobial treatment to

inactivate *C. jejuni*. The knowledge from this study provides insight to understand the survival and distribution of *C. jejuni* and aids in the development of intervention strategies to reduce the prevalence of *C. jejuni* and other pathogens.

Lay Summary

Campylobacter jejuni is a leading foodborne pathogen. It is a fragile microaerophilie but widely distributed in the natural environment. The survival mechanism of *C. jejuni* is not clear yet. *C. jejuni* could form a complex matrix which was known as biofilm by excreting extracellular polymeric substances. Within a biofilm, *C. jejuni* could survive under stresses. In addition, dormant *C. jejuni* also demonstrated a survival advantage. This particular state was known as persister cells. *C. jejuni* persister cells were a small proportion of normal growing cells that could survive under antibiotic treatment at lethal concentration. We speculated that biofilm and persister cells could be important survival strategy of *C. jejuni*. By combining a plant-based bioactive compound and metal oxide nanoparticles, we developed a synergistic antimicrobial approach that efficiently inactivated *C. jejuni*. This thesis provided insight into understanding the survival of *C. jejuni* and aided in the development of alternative antimicrobial strategies.

Preface

The following sections are mainly based on the publications and submitted manuscripts.

Chapter 2 is the work of using biochemical and biophysical techniques to characterize *C. jejuni* biofilms: Feng, J., Lamour, G., Xue, R., Mirvakliki, M.N., Hatzikiriakos, S.G., Xu, J., Li, H., Wang, S. and Lu, X. Chemical, physical and morphological properties of bacterial biofilms affect survival of encased *Campylobacter jejuni* F38011 under aerobic stress. *International Journal of Food Microbiology* (2016) 238: 172-182. Dr. Lu was responsible for the design of the experiment and helped edit the manuscript. Dr. Li and Dr. Lamour provided the technical support on the application of atomic force microscopy. Dr. Mirvakliki and Dr. Hatzikiriakos provided the technical assistance for the performance of contact angle measurement. I was responsible for performing experiments, analyzing the data and drafting the manuscript.

Chapter 3 is the application of confocal micro-Raman microfluidic platform for the characterization of bacterial biofilm, which was published as Feng, J., De La Fuente-Núñez, C., Trimble, M.J., Xu, J., Hancock, R.E. and Lu, X. An *in situ* Raman spectroscopy-based microfluidic "lab-on-a-chip" platform for non-destructive and continuous characterization of *Pseudomonas aeruginosa* biofilms. *Chemical Communications* (2015) 51: 8966-8969. Dr. Lu was responsible for the design of the experiment and helped edit the manuscript. Dr. Xu provided technical support on the fabrication of the microfluidic device. Dr. Hancock, Dr. Trimble, and Dr. de la Fuente-Núñez provided technical assistance on the application of confocal laser scanning microscope and helped edit the manuscript. I was responsible for performing experiments, analyzing the data, and drafting the manuscript.

Chapter 4 is a follow-up study of using confocal micro-Raman microfluidic platform to study the biofilm formation of *C. jejuni*. The results have been published as Feng, J., Ma, L., Nie,

J., Konkel, M.E., Lu, X. Environmental stress-induced bacterial lysis and extracellular DNA release contribute to *Campylobacter jejuni* biofilm formation *Applied and Environmental Microbiology* (2018) 84: E:02068-17. I was responsible for experimental design under the guidance of Dr. Lu, performed the experiments, analyzed the data and drafted the manuscript. Nie helped conduct the antimicrobial tests. Dr. Lu, Dr. Ma, and Dr. Konkel helped edit the manuscript.

Chapter 5 is related to the investigation of *C. jejuni* persister cells. The result will be submitted for publication: Feng, J., Xue, R., Ma, L., Wang, Y., Konkel, M.E., Lu, X. Characterization and transcriptome analysis of *Campylobacter jejuni* persister cells. I was responsible for the design of experiment under the guidance of Dr. Lu, performed experiments, analyzed the data and drafted the manuscript. Xue and Wang helped to conduct tests. Dr. Lu, Dr. Ma, and Dr. Konkel helped to edit the manuscript.

Chapter 6 is related to the investigation of synergistic antimicrobial strategy against *C. jejuni,* which has been submitted for publication: Feng, J., Xue, R., Wang, S., Konkel, M.E., Lu, X. Whole transcriptome sequencing analysis of the synergistic antimicrobial effect of metal oxide nanoparticle and ajoene against *Campylobacter jejuni*. Dr. Lu was responsible for experimental design and helped edit the manuscript. Xue and I performed the experiments. I analyzed the data and drafted the manuscript. Dr. Konkel and Dr. Wang helped edit the manuscript.

All published contents including text, figures, and tables are used with permission.

Table of contents

List of tables

List of figures

List of supplementary materials

Table A-1 was the supplementary material of RNA-seq data for **chapter 5**.

Table A-2 was the supplementary material of RNA-seq data for **chapter 6**.

Both **Table A-1** and **Table A-2** were linked to this dissertation in clRcle.

List of abbreviations

AFM – atomic force microscope

AMP - Ampicillin

ANOVA – Analysis of variance

BLAST – Basic local alignment search tool

CCD – Charge-coupled device

cDNA – Complementary deoxyribonucleic Acid

CFU – Colony forming unit

CIP - Ciprofloxacin

CJS index – *Campylobacter jejuni* share index

CLSM – Confocal laser scanning microscope

Cm - Chloramphenicol

Cm^R – Chloramphenicol resistance

Ct – Cycle threshold

DAPI – 4',6-diamidino-2-phenylindole

DEG – Differentially expressed genes

DMSO – Dimethyl sulfoxide

DNA – Deoxyribonucleic acid

eDNA – Extracellular deoxyribonucleic acid

EDTA –Ethylenediaminetetraacetic acid

ELISA – Enzyme-linked immunosorbent assay

EPS – Extracellular polymeric substance

FDA – Food and drug administration

FDR – False discovery rate

GBS – Guillain-Barré syndrome

gDNA – genomic DNA

GFP – Green fluorescent protein

KD – Kilo daltons

Kan - Kanamycin

Kan^R – Kanamycin resistance

LB agar/broth – Luria-Bertani agar/broth

MDK – Minimum duration of killing

MH agar/broth – Mueller-Hinton agar/broth

MIC – Minimum inhibitory concentration

mRNA – Messenger ribonucleic acid

NC membrane – Nitrocellulose membrane

OD – Optical density

PBS – Phosphate buffered saline

PCA – Principal component analysis

PC – Principal component

PCR – Polymerase chain reaction

PDMS – Polydimethylsiloxane

PI – Propidium iodide

PLSR – Partial least-squares regression

RFP – Red fluorescent protein

RMS roughness – Root mean square roughness

RNA – Ribonucleic acid

rRNA – Ribosomal ribonucleic acid

RNA-seq – Ribonucleic acid sequencing

ROS – Reactive oxygen species

RT-qPCR – Real-time quantitative polymerase chain reaction

SEM – Scanning electron microscopy

TCA cycle– Tricarboxylic acid

Tn insertion –Transposon insertion

ToF-SIMS – Time-of-flight secondary ion mass spectrometry

TSB – Tryptic soy broth

UTI – Urinary tract infections

TA system – Toxin-antitoxin system

UV-vis – Ultraviolet-visible

VBNC state– Viable but non-culturable state

XLD agar – Xylose lysine deoxycholate agar

Acknowledgements

I want to express my sincere gratitude to my supervisor, Dr. Xiaonan Lu, for his invaluable mentorship, patience, encouragement, and support throughout the time of my Doctor of Philosophy program. His rigorous attitude to research and immense passion for challenges set an example for me to be a good scientist.

I would also like to thank my committee members, Dr. Eunice Li-Chan, Dr. Robert Hancock, and Dr. Jie Xu, who have been providing professional advices and selfless help throughout my research project. Their comments and suggestions remarkably improve the quality of the entire research projects.

I also want to thank the members in Lu's lab, Dr. Lina Ma, Shaolong Feng, Yaxi Hu, Mohammed Hakeem, Luyao Ma, Jiaqi Li, Gracia Windiasti, Lu Han, Vivian Nie, Gianna Wang, for their technical support, thoughtful help, encouragement, patience, and friendship.

I want to thank the financial support from China Scholarship Council.

Lastly, I would like to thank my family for their endless love and support. They are my core motivation throughout this journey.

Dedication

This thesis is dedicated to my family for their endless love and support.

Chapter 1: Literature review

1.1 *Campylobacter*

Campylobacter jejuni has been recognized as one of the leading causes of human gastrointestinal diseases worldwide. In the United States, approximately 1.4-2.3 million cases of *Campylobacter* infections were reported per year during the past several decades (Samuel et al., 2004). Among the 18 species of *Campylobacter* identified to date, *C. jejuni* is responsible for over 80% of *Campylobacter*-associated illnesses, and *C. coli* accounts for approximately 10% of the cases. Recently, *C. lari* is recognized as an emerging species that is responsible for less than 1% of the infection cases (Teh et al., 2014). *C. jejuni*-mediated diseases, known as campylobacteriosis, generally occurs several days after the ingestion of *Campylobacter* and are usually featured by fever, nausea, abdominal pain, loose to watery stools containing blood and fecal leukocytes (Butzler and Oosterom, 1991). The infectious dose of *C. jejuni* can be as low as 500 cells (Wilson et al., 2008). Campylobacteriosis is one of the most frequently reported foodborne illnesses in Canada, outnumbering the cases caused by other common foodborne pathogens, such as *Listeria monocytogenes*, *Salmonella*, and Shiga toxigenic *Escherichia coli* (Kalmokoff et al., 2006). According to a report from European Center for Disease Prevention and Control, campylobacteriosis remained to be the most reported zoonotic infection in humans in Europe since 2005 (Team, 2012). Campylobacteriosis usually is self-limiting, but up to 10% of the cases require medical intervention, and the symptoms can last for several weeks. Severe chronic sequelae of campylobacteriosis shows a close association with a high incidence of Guillain-Barré syndrome (GBS), an autoimmune disease as one of the leading causes of flaccid paralysis in the post-polio era. Poultry product is the primary source of foodborne *Campylobacter* infections due to poor processing practice or direct contamination of raw

materials (Bryan and Doyle, 1995). It was estimated that *C. jejuni* contaminated over 90% of the domestic chicken carcasses at the time of sale (Kramer et al., 2000).

The paradox associated with *C. jejuni* is that this microbe is frequently isolated from food products and difficult to remove from the agri-food systems; however, *C. jejuni* is a microaerophilic bacterium and regarded as fragile towards the stresses. It is challenging for *C. jejuni* to survive in the aerobic environment (Park, 2002; Young et al., 2007). The understanding of the survival mechanism of *C. jejuni* in the unfavorable environment is of highly interest.

Bacterial stress response system is one of the most well recognized survival strategies that facilitate *C. jejuni* to adapt to and survive under different stress conditions. *C. jejuni* has various stress response systems that are regulated by different regulators, such as the heat-shock response regulator *dnaK* (Thies et al., 1999), the stringent response regulator *spoT* (Gaynor et al., 2005), and oxidative stress regulators *csrA* and *ahpC* (Baillon et al., 1999; Fields and Thompson, 2008). Moreover, *C. jejuni* can form a mono-species biofilm or reside in the multi-species biofilm. *C. jejuni* cells residing in a biofilm matrix are more tolerant to the stresses than its planktonic state (Reeser et al., 2007; Ica et al., 2012). In the natural environment, biofilms may arise in water supplies and plumbing systems of animal husbandry facilities and food processing plants, which may explain the prevalence of *C. jejuni* in the food system either directly or indirectly via farm animals (Buswell et al., 1998; Siringan et al., 2011). In addition, *C. jejuni* cells were identified to enter a state with a low metabolic activity that is highly tolerant to the environmental stresses as well as antimicrobial treatments (Cappelier et al., 1999a; Cappelier et al., 1999b).

1.2 Survival mechanism of *C. jejuni*

1.2.1 Bacterial stress response

In the natural environment, bacteria struggle with various stresses, such as temperature fluctuation, nutrient deficiency, availability of oxygen and the presence of toxic chemicals. Bacterial survival is the process of adaptation to these environmental stresses. Bacterial stress response system enables bacteria to respond to stresses by regulating the expression of metabolically associated genes, such as heat-shock response, cold-shock response, oxidative response, and stringent response. The specific regulations of stress response system in different bacteria vary significantly. For example, the oxidative stress response of microaerophilic bacteria is more complex than that of aerobic bacteria. Typically, bacterial stress response systems follow several distinctive regulatory patterns: (1) Stress response is mediated by sigma factors (σ factor), a protein that serves as a transcription initiation factor for the synthesis of RNA. Sigma factors are activated by stresses. They will specifically recognize and interact with the promoter of stress-associated genes to regulate the transcription. For example, sigma factors *sigH* is responsible for the regulation of heat shock in *Mycobacterium tuberculosis*. The heat shock response is triggered by high temperature. The activation of *sigH* will specifically recognize and positively regulate the expression of heat shock genes *dnak* and *clpB*, which enables *M. tuberculosis* to adapt to the high-temperature environment (Raman et al., 2001); (2) DNA repressors mediate bacterial stress response by binding to DNA controlling element and regulating the expression profile of associated genes. For example, *Bacillus subtilis* contains a transcriptional repressor *hrcA*, which can bind to DNA controlling element via a helix-turn-helix motif. The *hrcA* is triggered in response to heat shock and it will in turn conduct transcriptional regulation on heat-shock operons *dnaK* and *groESL* (Wiegert and Schumann, 2003); (3) Stress

response can be mediated by intracellular proteolysis. For example, inner membrane protein RseA is the central regulatory factor of signal transduction cascade in *E. coli*. The extracytoplasmic stress can induce proteolysis of RseA that rapidly activates the stress response (Ades et al., 1999); (4) Small RNAs can regulate bacterial stress response. Small RNAs are a type of non-coding RNA in the range of 50-250 nucleotides. Some small RNAs can specifically target at the mRNAs of stress response regulons, which stimulates or inhibits the translation. Many well-recognized stress response regulons in *E. coli* are identified under the regulation of small RNAs. For example, RyhB 90-nt RNA is responsible for bacterial response to iron starvation. RyhB 90-nt RNA will inhibit the translation of a set of iron-storage and iron-usage genes in response to the low availability of iron. This process is critical for *E. coli* to adapt to iron starvation (Massé and Gottesman, 2002).

C. jejuni possesses essential stress response operons that enable the survival of this microbe under different stress conditions, but not all well-recognized stress response operons have been identified in *C. jejuni* (**Table 1-1**). In the natural environment, both high oxygen level (~21% oxygen) and starvation (nutrient deficiency) are the primary negative factors on the survival of *C. jejuni*. Hence, both oxidative stress response and starvation response are critical to the survival and fitness of *C. jejuni* in the environment and agri-food systems.

Table 1-1. Summary of critical stress response genes that are present in other model bacterial species but absent in *C. jejuni* (Park, 2002)

Genes	Functions	Distribution		
		C. jejuni	*E. coli*	*B. subtilis*
Oxidative stress				
soxRS	positively regulates the response to superoxide stress	-	+	-
oxyR	positively regulates the response to peroxide stress	-	+	-
sodA	Manganese cofactor of superoxide dismutase in response to superoxide stress	-	+	+
katG	catalase-peroxidase in response to peroxide stress	-	+	-
Osmotic stress				
proU or *opuC*	Osmotic regulatory uptake of compatible solutes	-	+	+
osAB	synthesis of osmotic regulatory trehalose	-	+	-
betAB or *gbsAB*	synthesis of osmotic regulatory choline-glycine betaine pathway	-	+	+

Genes	Functions	Distribution		
		C. jejuni	*E. coli*	*B. subtilis*
Starvation				
rpoS	sigma factor is involved in stationary phase and general stress	-	+	-
relA	stringent response regulator is involved in response to amino acid, glucose, and oxygen starvation	-	+	+
Heat and cold shock				
rpoH	alternative sigma factor regulates the response to heat shock	-	+	-
cspA	essential protein for cold shock	-	+	+
Global regulation				
lrp	Global regulator for general metabolism	-	+	+

"-" indicates the absence of specific gene in the corresponding bacteria; "+" indicates the presence of specific gene in the corresponding bacteria

1.2.1.1 Response of *C. jejuni* to starvation

Individual nutrient deficiency can trigger the starvation response. In response to starvation, Bacteria conduct a series of physiological regulations, such as low metabolic activity, delayed growth, occurrence of proteolysis (Moore, 2001) and the shrink of cell volume (Dykes et al.,

2003). The activation of the starvation response not only increases the bacterial adaptation to the nutrient-limited environment, but also elevates bacterial tolerance to a wide range of stresses, such as heat shock, oxidative stress, and osmotic stress (Rees et al., 1995). Hence, the starvation response is critical to the fitness and adaption of bacteria in the unfavorable environment. Most of the Gram-negative bacteria contain sigma factor *rpoS* and homolog of *relA/spoT* were the regulators that responsible for the starvation response (Loewen et al., 1998). However, both sigma factor *rpoS* and *relA* homolog are absent in the genome of *C. jejuni* model strain NCTC 11168 (Parkhill et al., 2000). The absence of these two sigma factors might be the reason why most of *C. jejuni* strains are more susceptible to heat shock and oxidative stress in the stationary phase and nutrient-deprived environment than other bacteria (Kelly, 2001). Currently, *spoT* is the only well-characterized general regulator in *C. jejuni* that is responsible for the stringent response. The *spoT*-mediated response is critical for *C. jejuni* to survive under the nutrient-deprived or high oxygen level environment (Gaynor et al., 2005).

1.2.1.2 Response of *C. jejuni* to oxidative stress

Exposure to a high oxygen environment can induce the generation and accumulation of reactive oxygen species (ROS) in bacteria, which will impact the intracellular redox balance and subsequently damage the intercellular biomacromolecules (*e.g.*, lipids, nucleic acids, and proteins). Accordingly, bacteria have a series of responses that can neutralize ROS, reduce the oxidative stress and repair the damage. As a microaerophilic bacterium, *C. jejuni* can grow in the presence of a certain level of oxygen. The adaption to aerobic metabolisms indicates that *C. jejuni* possesses inherent cellular defense against the oxidative stress (Jones et al., 1993). *C. jejuni* contains three enzymes that have been identified to be essential for antioxidant, including

superoxide dismutase encoded by *sodB* (Pesci et al., 1994), catalase encoded by *katA* (Grant and Park, 1995), and alkyl hydroperoxide reductase encoded by *ahpC* (Baillon et al., 1999). The regulatory pattern of these genes was well recognized in *E. coli*. Both *soxRS* and *oxyR* were identified to be involved in the antioxidant of *E. coli.* Specifically, the *soxRS* regulons are responsible for the neutralization of superoxide or nitric oxide stress (Greenberg et al., 1990; Nunoshiba et al., 1992) while the *oxyR* regulon is responsible for the neutralization of peroxide stress (Storz and Imlayt, 1999). However, these oxidative stress regulators and their homologs have not been identified in *C. jejuni* yet. Instead, *C. jejuni* possesses several alternative regulators to combat the oxidative stress. For example, *C. jejuni* contains *perR* that can sense and respond to the peroxide stress. Transcriptomic analysis indicated that *perR* regulon can conduct the regulation of a total of 104 genes involved in a variety of physiological metabolisms, including energy metabolism, DNA repair, multidrug efflux pumps and synthesis of antioxidants (Palyada et al., 2009). In addition, several putative regulons, such as *cosR* (Hwang et al., 2011) and *csrA* (Fields and Thompson, 2008) have also be identified in *C. jejuni* that can mediate its response to oxidative stress.

1.2.2 Biofilm formation of *C. jejuni*

1.2.2.1 Overview of bacterial biofilms

In the natural environment, bacteria typically survive as a community, such as films, mats, sludge or biofilms, rather than as dispersed single cells (Joshua et al., 2006). Previous studies indicated that biofilm formation was a dynamic biological cycle, including several distinct stages (**Figure 1-1**): (1) initial attachment: planktonic cells attach to a substrate; (2) irreversible attachment: the attached cells are immobilized; (3)-(4) maturation and maintenance: bacterial

cells multiply and continuously secrete extracellular polymer substances (EPS) to develop the biofilm from a thin mono-layer to a thick multi-layer structure; (5) dispersal: biofilm structure breaks down and the sessile bacterial cells are released into the environment to colonize new sites.

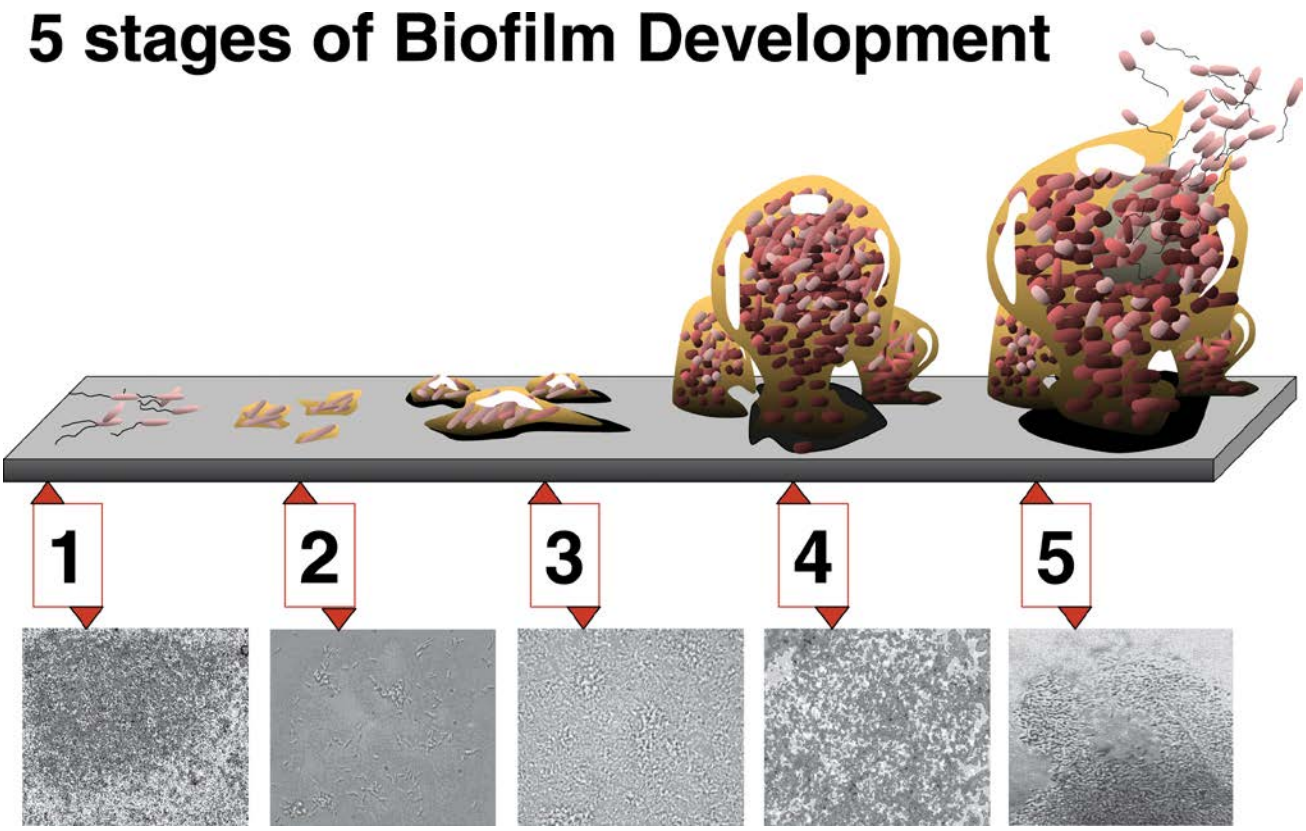

Figure 1-1. The schematic figures demonstrate distinct stages of biofilm formation. Stage 1 initial attachment: bacteria attach to the substrate; Stage 2 irreversible attachment: the initial attachment is reinforced; Stage 3: bacteria start secreting extracellular polymeric substances (EPS) that lead to the formation of a thin mono-layer biofilm structure; Stage 4 biofilm maturation: bacteria multiply and progressively secrete EPS that lead to the formation of a thick multi-layer biofilm structure; Stage 5 biofilm dispersal: the structure of biofilm is broken down, and cells in the biofilm are released and dispersed into the environment to colonize new sites. The photograph is derived from a developing biofilm by *Pseudomonas aeruginosa* (Monroe, 2007).

Initial attachment is critical for biofilm formation and can be influenced by many factors, such as mechanical properties of the substrate, hydrodynamic condition of the environment, metabolic activity of bacteria cells and the presence of adherence organelles (*e.g.*, flagella, pili, and capsules). For example, hydrophobic substrate with a rough surface is more likely to facilitate bacterial attachment. In addition, the pre-coating of biomacromolecules (*e.g.*, nucleic acids, proteins, lipids, and polysaccharides) on the substrate also contributes to the immobilization of bacterial cells. In contrast, the presence of surfactants that reduce the surface hydrophobicity will prevent the bacterial attachment (Chae et al., 2006; Patel et al., 2007; Simões et al., 2008). Hydrodynamic condition is a critical environmental factor that influences bacterial initial attachment. For example, both high flow velocity (*e.g.*, turbulent flow) and strong shear force can prevent the initial attachment by washing the reversibly attached cells away from the substrate (Stoodley et al., 1999; Simões et al., 2007). Moreover, bacteria contain adherence organelles (*e.g.*, flagella and pili) and produce EPS that can contribute to bacterial attachment (Pratt and Kolter, 1998; Vatanyoopaisarn et al., 2000; Parsek and Greenberg, 2005). The factors that influence bacterial initial attachment are summarized in **Table 1-2**.

Table 1-2. Summary of factors that affect biofilm initial attachment (Donlan, 2002).

Adhesion surface	Fluidic environment	Bacterial cell
texture or roughness	fluidic velocity	cell surface hydrophobicity
hydrophobicity	liquid pH	extracellular organelles (*i.e.* flagella)
surface chemistry	temperature	extracellular polymeric substances
surface charge	presence of antimicrobials	quorum sensing
surface conditioning	cations	cell surface charge

1.2.2.2 Hydrodynamic condition, bacterial physiological properties, EPS and biofilms

In the natural environment, biofilm formation is usually identified in hydrodynamic condition. However, in most of the studies, biofilms were cultivated in static conditions, such as in a 96-well microplate, in a glass tube, or on different packaging materials. The static cultivation cannot include the influence of shear flow and nutrient exchange on biofilm formation. In contrast, hydrodynamic cultivation can simulate the real hydrodynamic condition as natural settings for biofilm formation (Purevdorj et al., 2002; Kirisits et al., 2007). For example, the biofilm formation of *rpoS*-deficient *E. coli* in a flow condition demonstrated a considerable difference compared to that in static cultivation. The structure variation between the biofilms formed in hydrodynamic condition and that in static condition might be associated with a few factors. For example, continuous flow prevented the accumulation of cell signaling molecules, impaired the quorum sensing effect, and subsequently inhibited the biofilm formation (Ito et al., 2008). Several commercially available macro-scale flow chambers have been applied in the

studies of bacterial biofilms. However, most of these flow chambers shared similar disadvantages, such as inaccurate control of hydrodynamic parameters, consumption of large volumes of reagents, and low compatibility to advanced detection techniques (Ica et al., 2012). “Lab-on-a-chip” is also known as microfluidic chip when it applied small volumes of fluids to interconnect various laboratory functions on a single integrated chip. Compared to macro-scale chambers, microfluidic chips demonstrate numerous advantages, such as precise and high-efficient control of hydrodynamic parameters, consumption of small volumes of reagents, flexibility of customized design and high compatibility to different detection and characterization techniques. All of these make microfluidic chips to be a desired platform for the cultivation and characterization of bacterial biofilms (Kim et al., 2012).

The surface hydrophobicity and adherence organelles of bacteria (*e.g.,* hydrophobicity and extracellular filamentous appendages) are critical factors that can influence bacterial biofilm formation. The chemical composition of the bacterial cell membrane is related to the surface hydrophobicity. Moreover, both bacterial aggregation and attachment are highly dependent upon hydrophobic interactions. A high proportion of non-polar hydrophobic domains on bacterial surface can enhance the initial attachment of bacteria to the substrate due to the strong hydrophobic interaction between bacteria and the adhesion surface (Donlan, 2002).

Bacteria have different types of extracellular organelles, such as flagella, pili, capsule, and fimbriae, all of which are responsible for bacterial adherence and motility. Flagella are helical structures that originate from cytoplasm and extend through the cell wall and are responsible for bacterial motility. Flagella can generate a driving force to overcome the repulsive force during bacterial attachment (Fang et al., 2000; Donlan, 2002). In addition, flagellum can bind to both biotic and abiotic materials by forming adhesive interactions (Newell et al., 1985;

Vatanyoopaisarn et al., 2000). Other filamentous appendages, such as pili and fimbriae, also demonstrate adherence capability. Previous studies indicated that pili and pilus could generate electrostatic adsorption in certain environment to bind bacterial cell onto the substrate (Keizer et al., 2001; Craig et al., 2006). Hence, bacteria with adherence organelles usually have a better attachment than those without adherence organelles (Sauer et al., 2000).

EPS are the major constituents of biofilm and account for up to 90% of total volume of biofilm (Røder et al., 2016). EPS are comprised of macromolecules, such as polysaccharides, nucleic acids, proteins, and lipids. The composition of EPS in different bacterial biofilms extensively varies from each other. For example, exopolysaccharides and proteins are the major components of EPS in biofilms formed by *E. coli*, *Staphylococcus*, *Streptococcus* and *Vibrio* (Vu et al., 2009). One previous study reported that 75-89% of the EPS are comprised of exopolysaccharides and proteins (Tsuneda et al., 2003). In some cases, extracellular DNA is the major constituents of biofilm EPS, such as *P. aruginosa* biofilm (Whitchurch et al., 2002), although the specific role of these individual EPS molecules is not fully clear yet. EPS demonstrate various physiological advantages for the survival of bacteria in biofilms, such as storage of nutrient, maintenance of hydration, prevention and inhibition of the penetration of antimicrobials (Sutherland, 2001; Davies, 2003). Hence, identification and characterization of EPS components provide insights into understanding the mechanism of the protection of biofilm to the encased bacteria.

The identification and characterization of EPS is highly dependent on the isolation methods. Centrifugation, filtration, sonication and enzymatic treatment are the commonly used methods for the isolation of EPS from bacterial biofilms. Ion exchange resin is also applied under certain circumstances to isolate proteins and carbohydrates from EPS (Tapia et al., 2009). However,

most of these isolation methods can only extract specific components. In addition, some EPS fractions are tightly bound to bacterial cells. Harsh extraction procedures may damage cell membrane and introduce artifacts due to the release of bacterial intracellular substances. For example, extraction using high concentration of sodium hydroxide released cytoplasmic components into the extracts (Brown and Lester, 1980).

Staining is an alternative method that has been applied to investigate the chemical compositions of EPS and their spatial distribution within a biofilm. Crystal violet (CV) is one of the well recognized staining methods that can nonspecifically stain EPS as well as the sessile bacterial cells in the biofilms. The result of CV staining can only reflect the formation level of a biofilm but not the chemical composition of EPS (Reeser et al., 2007). Confocal laser scanning microscope (CLSM) coupled with fluorescent dyes is another important tool for *in-situ* identification of specific EPS compositions in the biofilms. In addition, CLSM can also be used to investigate the viability of the encased cells in biofilms when it is coupled with live/dead bacterial cell staining (SYTO 9 for live cells and propidium iodide for dead cells) (Joshua et al., 2006). Other advanced techniques, such as super-resolution imaging, also demonstrate the potential for the study of bacterial biofilm (Berk et al., 2012). However, none of these aforementioned techniques can identify and characterize biofilm EPS in a non-destructive manner. Raman spectroscopy can determine the chemical composition of a biological system without any sample preparation. When it is coupled with a confocal microscope and a digital stage for mapping, Raman spectroscopy can be used to determine the chemical composition *in-situ* (Ivleva et al., 2008) as well as the spatial distribution (Ivleva et al., 2009) within a biofilm in a non-destructive manner.

The structure of biofilm can influence the survival of the bacterial cells in the biofilms. For example, the compacted multi-layer EPS can usually lead to the development of a thick biofilm that efficiently delays the penetration and diffusion of antimicrobials (Mah and O'Toole, 2001). In addition, a biofilm with compacted structure will more likely to have a good water holding capacity which is critical to the survival of bacterial cells in the biofilms under desiccation. (Tang et al., 2011). Biomechanical properties of EPS are closely associated with the biofilm structure. Therefore, the biomechanical profiles of EPS will be valuable for the characterization of a bacterial biofilm. Atomic force microscopy (AFM) is one of the promising tools that can investigate the topographic information of a biological sample (*e.g.*, a biofilm) in the scale of nanometers. In addition, AFM can also be applied to determine the mechanical properties of biological samples. Several studies have successfully characterized a series of mechanical parameters of bacterial biofilms using AFM, including cohesive strength, hydrophobicity, and surface elasticity (Ahimou et al., 2007; Scheuring and Dufrêne, 2010).

1.2.2.3 *Campylobacter* biofilms

Campylobacter can form biofilms on different materials, such as stainless steel, glass and plastics (Dykes et al., 2003; Asakura et al., 2007b). The capability of biofilm formation is different among various *Campylobacter* species (Sulaeman et al., 2010) and strains (Kim et al., 2017). For example, both clinical isolates *C. jejuni* F38011 (Feng et al., 2016) and NCTC 11168 (Kalmokoff et al., 2006) can form relatively intensive biofilms under different environmental conditions. In contrast, *C. jejuni* strain RM 1221 can barely form a biofilm even under the optimal laboratory condition (Brown et al., 2015b).

Biofilm formation of *C. jejuni* is influenced by various factors. A previous study reported that the formation of *C. jejuni* biofilm was significantly inhibited under thermophilic and high osmotic conditions (Reeser et al., 2007). Reuter and colleagues identified that *C. jejuni* developed a biofilm more rapidly under the aerobic condition than that under the microaerobic condition (Reuter et al., 2010), and this observation was recently confirmed by another study (Turonova et al., 2015). In addition, food residues, such as chicken juice (Brown et al., 2014) and pork juice (Li et al., 2017), could also enhance the formation of *C. jejuni* biofilms.

Molecular understanding of *C. jejuni* biofilm formation is still in its infancy, even though several genes have been identified to regulate biofilm formation, such as the flagella synthesis genes and stress response genes (Kalmokoff et al., 2006; Reeser et al., 2007; Svensson et al., 2014). Reeser and others identified that the biofilm formation by flagella knockout mutant (Δ*flaAB*) of *C. jejuni* was significantly lower compared to that of the wild-type counterpart (Reeser et al., 2007). Furthermore, the genes responsible for survival during stationary phase or under the starvation condition also influence the biofilm formation of *C. jejuni*. Deletion of these genes could increase the formation level of *C. jejuni* biofilms (Candon et al., 2007; McLennan et al., 2008).

Campylobacter can co-develop a biofilm with other bacteria. A previous study reported that a mixture of *C. jejuni*, *Enterococcus faecalis*, and *Staphylococcus simulans* could develop an intensive multi-species biofilm (Teh et al., 2010). Multi-species *Campylobacter* biofilms and mono-species *Campylobacter* biofilms are significantly different from physiological and mechanical perspectives (Teh et al., 2014). For example, mono-species *C. jejuni* biofilms consumed less oxygen and were more susceptible to strong shear stress compared to that of multi-species *C. jejuni* biofilms (Ica et al., 2012). Another study identified that *Campylobacter*

could co-exist with *P. aeruginosa* in a dual-species biofilm. The formation level of this multi-species biofilm was significantly higher than that of mono-species *C. jejuni* biofilm (Hilbert et al., 2010).

Besides forming a biofilm alone, *C. jejuni* can also reside in a pre-established biofilm. Hanning and colleagues inoculated *C. jejuni* in the mature biofilms isolated from a poultry farm. *C. jejuni* cells could survive for a longer time in this biofilm under aerobic condition compared to that as the planktonic cells (Hanning et al., 2008). In another study, Trachoo and others validated that *C. jejuni* could reside in a multi-species biofilm isolated from a poultry house. *C. jejuni* cells in this multi-species biofilm could withstand a dramatic temperature fluctuation (*i.e.*, 12°C and 23°C) and maintained their viability over a week (Trachoo et al., 2002). A similar result was obtained in another study that *C. jejuni* could be incorporated into the biofilm formed by aquatic microorganisms. Within this biofilm, *C. jejuni* could survive a longer period under stresses compared to floating single cells (Buswell et al., 1998).

1.2.3 *Campylobacter* dormancy

1.2.3.1 Overview of bacterial dormancy

The survival of bacteria in nature is usually challenged by various stresses, such as high oxygen condition, desiccation, temperature fluctuation and the presence of antimicrobial compounds. Bacteria can accordingly develop different survival strategies to adapt to these stresses. Bacterial dormancy is a period that bacteria minimize the metabolic activity and stop the growth (Lewis, 2007). Entering an inactive state will aid bacteria in conserving energy and withstanding different types of stresses. As a result, the dormant bacteria are difficult to be eradicated, potentially leading to the recurrent human infections, such as *E. coli*-associated

urinary tract infections (UTI) (Jacobsen et al., 2008) and *Mycobacterium tuberculosis*-associated lung diseases (Parrish et al., 1998).

Bacterial persisters and bacterial "viable but non-culturable state" (VBNC) are two well-known types of bacterial dormancy. Both persister cells and VBNC cells demonstrate high tolerance against antimicrobial treatment as well as environmental stresses. A recent review paper drafted by Ayrapetyan and others for the first time argued that these two types of bacterial dormancy are closely related to each other as part of the "dormancy continuum" (Ayrapetyan et al., 2015). For example, both persister cells and VBNC cells were identified at a high level in similar conditions, such as in the microenvironment of a biofilm (*e.g.*, low oxygen, high acidity and limited nutrients) (Stewart and Franklin, 2008). It was suspected that bacteria cells might firstly turn into persisters in response to a short period of stress and then enter VBNC state if the stress is maintained for an elevated period. According to a previous study, the viability of the encased bacterial cells in the biofilm progressively switched from the culturable state (*i.e.*, normal growing cells and persister cells) to non-culturable state (VBNC cells) under a long-term exposure to stress, indicating the transition from normal growing cells and persister cells to VBNC cells (Feng et al., 2016). The relationship between biofilms, VBNC cells, and persister cells is summarized in **Figure 1-2**.

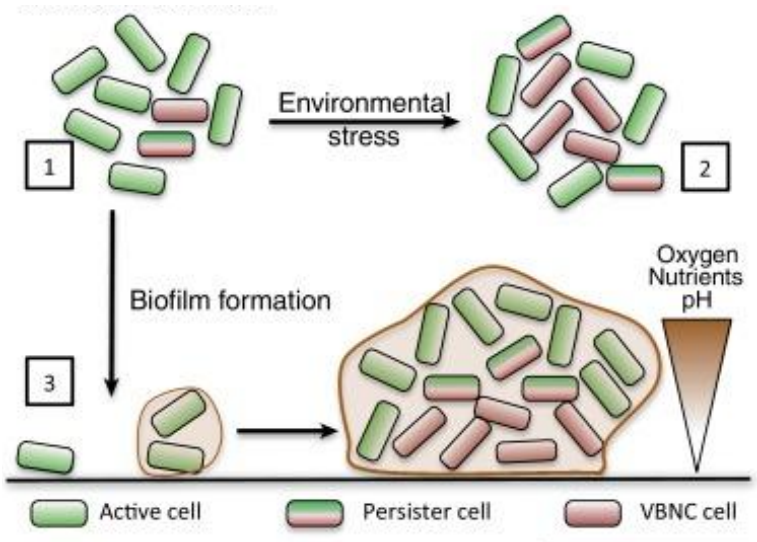

Figure 1-2. The stressful microenvironment of biofilm stimulates the transition of bacteria from the normal growing cells to VBNC and persister cells: (1) VBNC cells and persister cells stochastically present in planktonic culture at low level; (2) environmental stresses (*i.e.*, starvation, oxidative stress, temperature fluctuation) can induce the transition of bacteria from normal growing cells to VBNC and persister cells; (3) the microenvironment of biofilm is acidic and has limited oxygen, which can also stimulate the transition of bacteria from the normal growing cells to VBNC and persister cells (Ayrapetyan et al., 2015).

1.2.3.2 Persister cells

Bacterial cells can survive under the antibiotic treatment without developing resistance. These cells are known as persisters or persister cells. Generally, persisters are a small fraction of the bacterial population. In some case, persisters can account for approximately 1% of the total population (Keren et al., 2004b). The number of persister cells in a specific bacterial population might vary significantly due to different growth states (*i.e.*, lag phase, log phase, stationary phase, and death phase) and cultivation conditions. For example, persister cells comprise only a small

proportion of exponentially growing bacterial cells. In contrast, the ratio and the amount of the persister cells can be high in the population at stationary phase as well as in a biofilm (Wood et al., 2013).

Persister cells were firstly identified from *S. aureus*, in which ~1% of the *S. aureus* cells survived under the treatment by lethal-dose penicillin. The survived cells were able to restore the population after the removal of penicillin without acquiring resistance (Lewis, 2010). Compared to antibiotic-resistant cells whose resistance capacity is due to genetic mutation, persister cells have the identical genetic background to the normal growing cells. It was proposed that persisters were in a dormancy state. Due to the slow growth and low metabolic activity, they were more tolerant to antibiotic treatment compared to the normally growing cells (Lewis, 2012). Brauner and colleagues systematically analyzed and discussed the difference between antibiotic-resistant cells and persister cells (Brauner et al., 2016). The mechanism of resistance was mainly due to the mutation of antibiotic binding targets. In contrast, persister cells still contain the active antibiotic-binding targets. Hence, the tolerance of persister cells must occur due to a distinctive mechanism. Two critical parameters, namely minimum inhibitory concentration (MIC) and minimum duration of killing (MDK), can be used to differentiate between normal growing cells, resistant cells and persister cells (**Figure 1-3**). Persister cells shared the similar MIC and MDK_{99} (minimal duration required to kill 99% of the cells) as that of the normal growing cells when they were challenged using antibiotics. The complete inactivation of persister cells required a more extended period of treatment, leading to a higher $MDK_{99.99}$ (minimal duration required to kill 99.99% of the cells) than that of the normal growing cells. Accordingly, the killing curve of persister cells under antibiotic treatment follows an obvious biphasic killing curve with a distinctive survival plateau. Theoretically, resistant bactterial cells could grow in the presence of

antibiotics. Hence, the MIC of resistant cells will be much higher than that of persister cells as well as normal growing cells.

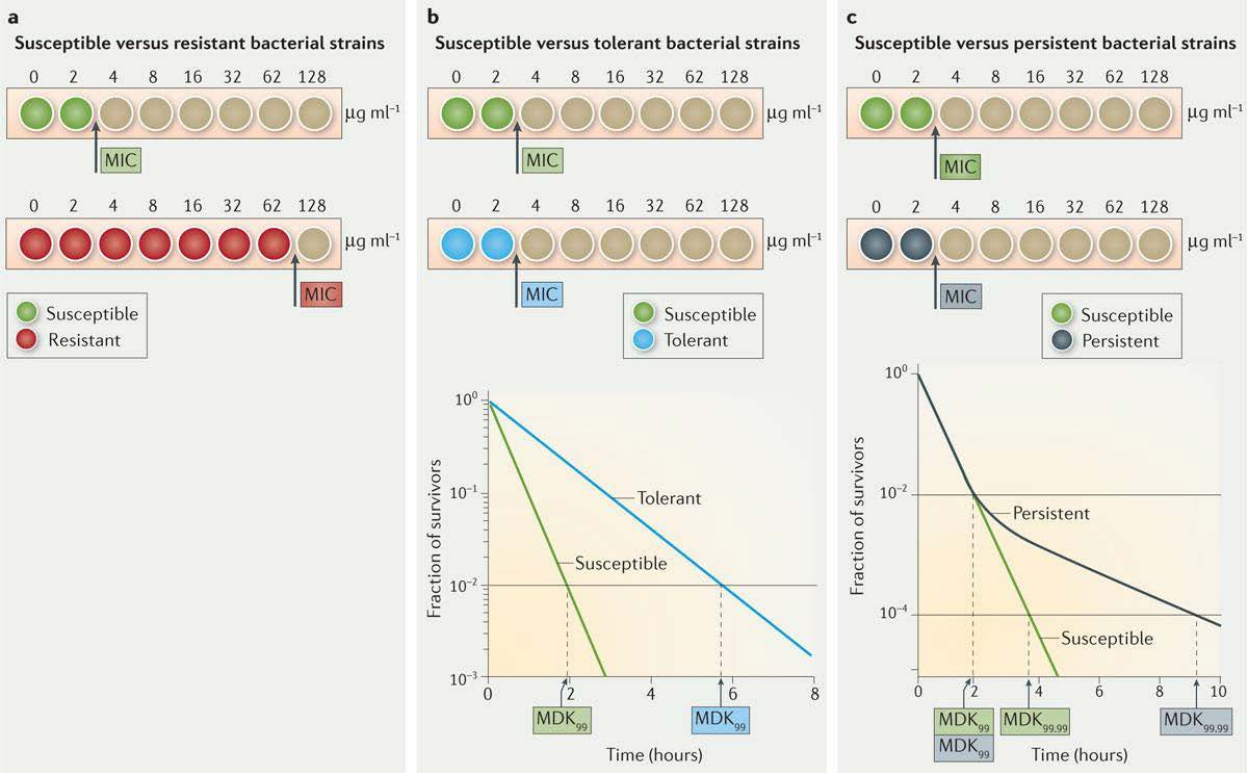

Figure 1-3. Time-kill kinetics of resistant cells, tolerant cells and persister cells challenged using antibiotic treatment. The antibiotic susceptibility of these cells is totally different. a) The minimum inhibitory concentration (MIC) of resistant cells is substantially higher than that of the susceptible cells. Colored wells represent the growth of bacterial cells, whereas wells in light brown represent the complete inhibition of bacterial growth due to the presence of antibiotics. b) MIC of the tolerant cells is almost the same as that of the susceptible cells; however, the MDK_{99} (minimum duration for killing 99% of bacterial cells in the population) of tolerant cells is substantially higher than that of the susceptible cells. c) The population of persister cells comprises a fraction of susceptible cells and a faction of tolerant cells. Hence, MIC and MDK_{99} of persister population is almost the same as that of the susceptible cells. However, the $MDK_{99.99}$ of persister cells is substantially higher than that of the susceptible cells. Concentrations and timescales are selected for illustration purposes only (Brauner et al., 2016).

The mechanism of the formation of persister cells has not been well characterized yet (Lewis, 2010). Currently, two possible mechanisms have been proposed, including the stochastic mechanism and the responsive mechanism (Harms et al., 2016).

Many bacteria have evolved a stochastic protection mechanism, known as bet-hedging strategy, to increase their fitness in stresses, such as lethal dose of antibiotic treatment, high level of oxidative stress and dramatic temperature fluctuation (Veening et al., 2008a; Veening et al., 2008b). For example, the bet-hedging strategy was responsible for the sporulation of *B. subtilis* which ensured the preservation of clonal lineage under stresses (Chung et al., 1994; González-Pastor et al., 2003; Maamar et al., 2007). Bacterial persistence have been documented as an example of a bacterial bet-hedging strategy. Because persister cells are phenotypic variants of normal growing cells which have the identical genetic background as their kin population. In addition, the switch from normal growing cells to persister cells usually occur stochastically. It is reasonable to believe that the stochastic mechanism can possibly lead to the formation of persister cells (Keren et al., 2004b; Germain et al., 2015).

Bacteria can adapt to and survive in adverse environment by adjusting metabolism, and this process is known as an active response (Chung et al., 1994). The responsive mechanisms of the formation of persister cells depend upon the active response. Transposon (Tn) insertion mutation is one efficient method to investigate the active response associated persister cells formation by screening the candidate genes, predicting the corresponding functions, and analyzing the metabolic pathways. The application of Tn for *S. aureus* persister cells identified 13 genes that were mainly distributed among the metabolism of oxidative phosphorylation, tricarboxylic acid (TCA) cycle, cell cycle, and glycolysis. The insertion mutation of these genes could significantly reduce the formation level of *S. aureus* persister cells (Wang et al., 2015). A

similar experiment was conducted for *E. coli* persister cells. The application of Tn sequencing revealed a set of genes involved in motility and amino acid biosynthesis that were closely associated with the formation of gentamicin-tolerant persister cells. Deletion of these genes significantly reduced the formation level of *E. coli* persister cells but did not influence the MIC of the mutants against gentamicin (Shan et al., 2015). The size of Tn mutant library is important for the screening of the candidate genes. A small set of Tn mutant library only contains the representative genes or region of interest which may loss critical genes or relevant regions. Keio collection could significantly improve the efficiency and accuracy of Tn screening by generating a large size of the mutant library. Hansen and colleagues applied Keio collection to investigate the candidate genes for the formation of *E. coli* persister cells. They generated a library of 3985 *E. coli* deletion strains and identified that most of the candidate genes were global regulators, such as *dnaKJ* (chaperones), *hns* (global regulator), and *dksA* (regulator of rRNA transcription). This study provided supporting evidence to the responsive mechanism of the formation of persister cells (Hansen et al., 2008).

The influence of toxin-antitoxin (TA) systems on the formation of persister cells is another supporting evidence to the responsive mechanism. TA systems comprise a pair of closely linked genes to encode a stable “toxin” protein and a cognate “antitoxin” (protein for type II, IV, V TA system; antisense RNA for type I, III TA system). The concept of TA systems is originally identified in plasmids as a gene-stable and transferable element that enables the daughter generations to inherit plasmid after cell division. The absence of plasmid will induce the degradation of antitoxin and the release of toxin. The released toxin will then kill the dividing cells, known as post-segregational killing (Hayes, 2003). TA systems have been correlated to the formation of persister cells. Keren and colleagues applied transcriptome analysis to plot the gene

expression profile of *E. coli* persister cells. The expression of RelE toxin was significantly higher in *E. coli* persister cells than that in the normal growing cells (Keren et al., 2004a). Another transcriptome analysis showed a similar result that the overexpression of MazF toxin was along with a higher formation level of persister cells (Vázquez-Laslop et al., 2006). Although the activation of TA systems was usually under the control of transcriptional and post-transcriptional regulations, the details of different regulations might vary due to different types of TA systems. For example, the type I TA system *tisAB* in *E. coli* is under the control of SOS response. The deletion mutation on this SOS-TA locus (*tisAB-istR*) could significantly increase the formation level of persister cells (Dörr et al., 2010). In addition, the type II TA systems can be activated by intercellular proteolysis (degradation by intracellular proteases, such as Lon and ClpP) (Brzozowska and Zielenkiewicz, 2013). Generally, the release of toxins can adjust bacterial physiology and induce bacteriostatic growth state that enhances the tolerance of cells against antibiotics. However, deletion mutation of a single TA locus did not show any persisters-like phenotype, indicating that individual TA system only had considerable influence on the formation of persister cells (Hansen et al., 2008; De Groote et al., 2009). Conlon and colleagues recently confirmed this hypothesis using a 10 TA loci deletion mutant of *E. coli*. They observed a cumulative decrease of the formation of persister cells along with the progressive deletion of these 10 TA (Conlon et al., 2016). Therefore, there may be a synergistic effect among different TA loci that together influence the formation of persister cells.

1.2.3.3 VBNC cells

Bacteria can enter a dormant state, called “viable but non-culturable” (VBNC) state. VBNC cells are alive but cannot form colonies on the routine laboratory media (Oliver, 2005).

VBNC cells are typically more tolerant to different stresses, such as starvation, temperature fluctuation, and oxidative stress, than the normal growing cells. VBNC cells have a low metabolic activity as characterized by the reduction of nutrient transport, weak respiration and low level of biosynthesis (Oliver and Bockian, 1995). Compared to the dead cells, VBNC cells have a much higher level of free adenosine triphosphate (ATP), indicating that VBNC cells are still alive (Tholozan et al., 1999).

Currently, the investigation of VBNC cells is still in its infancy. The investigation of molecular perspectives has identified several candidate genes that can influence the formation of VBNC *E. coli* O157:H7 cells, including *stx1*, *rfbE*, *mobA* and 16S rRNA genes (Yaron and Matthews, 2002). A comprehensive transcriptome analysis of *Vibrio cholerae* persister cells demonstrated that toxic (*e.g.*, *ctxAB, rtxA* and *hlyA*) and virulence (*e.g.*, *tcpA* and *TTSS*) genes were still expressed in its VBNC state (Vora et al., 2005). Thus, VBNC pathogenic cells are regarded as virulent. This statement was supported by another study in which enterotoxigenic *E. coli* H10407 was identified to produce enterotoxin and retain pathogenicity in the VBNC state (Pommepuy et al., 1996).

1.2.3.4 *Campylobacter* persister cells and VBNC cells

The existence of *Campylobacter* persister cells has not been reported yet. However, VBNC state of *Campylobacter* cells has been identified and reported in the previous studies. Tholozan and coauthors reported that *C. jejuni* was able to survive in the microcosm water in VBNC state. The subsequent analysis revealed that these *C. jejuni* VBNC cells demonstrated a lower membrane potential and internal potassium content than that of the normal growing cells (Tholozan et al., 1999). In another study, normal growing *C. jejuni* cells were identified to turn

into VBNC cells during the incubation in phosphate buffered saline at 4°C (Magajna and Schraft, 2015b). In addition, starvation and low temperature were more efficient to induce the normal growing *C. jejuni* cells to enter VBNC state (Magajna and Schraft, 2015a).

1.3 Linkage of *Campylobacter* dormancy and biofilm formation to food safety

Campylobacter can survive a longer period in the biofilm or in the dormant state (*i.e.*, VBNC cells and persister cells) compared to the normal growing single cells. This indicates the potential health risk of *C. jejuni* biofilm and dormant cells. Currently, the linkage between *Campylobacter* dormancy (*i.e.*, VBNC cells and persister cells) and biofilm formation was not clear yet. The microenvironment in the biofilm is able to induce the formation of persister cells and VBNC states of bacteria. For example, the microenvironment in biofilm has limited nutrients and is highly acidic, both of which could induce the formation of dormant *Campylobacter* cells. Therefore, biofilm is supposed to be one of the important reservoirs that not only induces the formation of dormant *Campylobacter* cells but also offers additional protection to the encased dormant cells against various stress conditions (Ayrapetyan et al., 2015).

Epidemiological studies have revealed that many campylobacteriosis cases are linked to the poor processing practice and cross-contamination of poultry products. Fresh produce is recently reported to be responsible for a relatively large amount of campylobacteriosis cases (Sivapalasingam et al., 2004). Contamination of fresh produce can occur during harvesting, processing, packaging, distribution, and at the retail level. Thus, the presence of *Campylobacter* in food processing environment can be a source for its contamination to agri-food products.

Bacteria can form biofilms in the food processing environment, such as fish processing, poultry processing, dairy processing, and ready-to-eat food processing environment (Srey et al.,

2013). Commercial sanitizers may fail to completely inactivate *C. jejuni* residing in the biofilms (Chmielewski and Frank, 2003). The compact structure of biofilm can physically reduce the penetration of sanitizers. Some EPS components can neutralize sanitizers via chemical reactions. In addition, cells in a biofilm are in a state of low metabolic activity and are more tolerant to sanitizers than the planktonic cells. Hence, biofilm formation and bacteria in a low metabolic activity can enable *Campylobacter* to survive in food processing environment and potentially contribute to the dissemination of this microbe in agri-food systems.

1.4 General hypothesis, objectives, and rationale

1.4.1 General hypothesis

Biofilm formation and persister cells are tolerant to stresses that enable the survival of *C. jejuni* in the unfavorable environment.

1.4.2 Objectives

The overall objective of this study is to identify and characterize biofilm formation and persister cells of *C. jejuni* and develop effective antimicrobial strategies against *C. jejuni.* The individual objectives are listed as below.

Objective 1: To identify and characterize mono- and multi-species *C. jejuni*-containing biofilms

Objective 2: To investigate the relationship between stress response and biofilm formation of *C. jejuni* under different environmental stresses

Objective 3: To identify and characterize *C. jejuni* persister cells

Objective 4: To investigate effective antimicrobial strategies that can inactivate *C. jejuni*

1.4.3 Rationale

C. jejuni is a fragile microaerophilic bacterium, but it is the one of the leading causes of foodborne illness worldwide. The mechanism of how this microbe can successfully survive under the stress conditions and be transported via foods is not fully known yet. Biofilm and persister cells are particular survival states that enable bacteria to survive in the unfavorable environmental conditions. It is reasonable to hypothesize that *C. jejuni* may survive in the biofilm or as persister cells in response to different stress conditions.

Chapter 2: Chemical, physical and morphological properties of bacterial biofilms affect survival of encased *Campylobacter jejuni* F38011 under aerobic stress

2.1 Summary

Campylobacter jejuni is a microaerophilic pathogen and leading cause of human gastroenteritis. The presence of *C. jejuni* biofilms might be one of the major strategies that responsible for the survival and dissemination of this microbe in an aerobic environment. In this study, *Staphylococcus aureus*, *Salmonella enterica*, or *Pseudomonas aeruginosa* was mixed with *C. jejuni* F38011 as cultures to form dual-species biofilms. After four days' exposure to aerobic stress, no viable *C. jejuni* cells could be detected from mono-species *C. jejuni* biofilm. In contrast, at least 4.7 log CFU/cm^2 of viable *C. jejuni* cells could be detected from dual-species biofilms. To elucidate the mechanism of protection mode, the chemical, physical and morphological features of biofilms were characterized. Dual-species biofilms contained a higher level of extracellular polymeric substances with a more diversified chemical composition, especially for polysaccharides and proteins than that of mono-species *C. jejuni* biofilm. The structure of dual-species biofilms was more compact, and their surface was >8 times smoother than that of mono-species *C. jejuni* biofilm which was indicated by the result of atomic force microscopy. Under desiccation stress, the water content of dual-species biofilms decreased slowly and remained at higher levels for a longer time than mono-species *C. jejuni* biofilm. The surface of all biofilms was hydrophilic, but the total surface energy of dual-species biofilms (ranging from 52.5 to 56.2 mJ/m^2) was lower than that of mono-species *C. jejuni* biofilm, leading to more resistance to wetting by polar liquids. This knowledge could aid in developing

intervention strategies to decrease the survival and dispersal of *C. jejuni* into foods or environment.

2.2 Introduction

Campylobacter jejuni is a Gram-negative, microaerophilic bacterium and is one of the leading causes of foodborne gastrointestinal diseases worldwide. *Campylobacter* infection causes acute gastroenteritis characterized by inflammation, abdominal pain, fever and diarrhea (Young et al., 2007). Previous reports indicated that *C. jejuni* infection cases in Canada outnumbered reported cases of *Escherichia*, *Listeria*, *Shigella* and *Salmonella* infections combined (Kalmokoff et al., 2006). The paradox associated with *C. jejuni* is that this bacterium is prevalent in the environment and difficult to eliminate from the food chain; however, as a microaerophile, *C. jejuni* is sensitive to aerobic stress and does not multiply in the aerobic environment. Studies have confirmed that bacteria shed from biofilms could continue to contaminate foods, potentially leading to food poisoning (Kumar and Anand, 1998; Donlan and Costerton, 2002). Under this condition, *C. jejuni* may survive within a biofilm microenvironment and further lead to food contamination (Ica et al., 2012), even though there remain controversies about how *C. jejuni* can resist environmental stress (*e.g.*, temperature fluctuation, aerobic, or shear stress) and form biofilms alone (Teh et al., 2014). In the natural environment, bacterial cells mainly reside in a multispecies culture. According to the previous reports, *C. jejuni* biofilms are present in the gastrointestinal tract of poultry, in water supply and plumbing systems in animal husbandry facilities and food processing plants (Trachoo et al., 2002; Newell and Fearnley, 2003; Hermans et al., 2011; Siringan et al., 2011) along with other foodborne pathogens including *Staphylococcus aureus*, *Salmonella enterica*, and *Pseudomonas aeruginosa*. The biofilms formed

by these microorganisms are believed to protect *C. jejuni* against antimicrobial treatments and aerobic stress (Joshua et al., 2006; Ica et al., 2012).

Biofilms have a complex chemical composition. In the particulate fraction of a biofilm, up to 90% is composed of extracellular polymeric substances (EPS) including polysaccharides, proteins, nucleic acids, lipids, and humic-like substances. Specific chemical components of a biofilm may contribute to its resistance to exogenous stress. For example, hydrophilic polysaccharides and proteins in EPS can hold water and keep entrained microbial cells hydrated limiting the impact of desiccation stress (Roberson and Firestone, 1992; Tamaru et al., 2005). Enzymes within biofilms could inactivate stress inducers and neutralize these in a biofilm microenvironment (Davies, 2003). Unfortunately, it has been difficult to characterize the chemical profiles of biofilms because common methods, such as crystal violet (Reeser et al., 2007) and Congo red staining (Reuter et al., 2010), are destructive and can only be used to evaluate the biofilm formation level. Innovative spectroscopic methods, particularly Raman spectroscopy coupled with confocal technique can provide *in situ* and nondestructive determination of the chemical composition of bacterial biofilms and changes in the composition of biofilms in response to various forms of stress (Ivleva et al., 2008; Ivleva et al., 2010; Lu et al., 2012a).

Besides chemical composition, morphological properties of bacterial biofilms are also important in determining their resistance to the environmental stress. Joshua and coauthors compared biofilms produced by wild-type and mutant *C. jejuni* strains using scanning electron microscopy (SEM) (Joshua et al., 2006). Reuter and coworkers evaluated surface adhesion and microstructure of *C. jejuni* mono-species biofilm formed under microaerobic and aerobic environment using light microscopy after staining (Reuter et al., 2010). Both studies confirmed

that the assemblage structure of biofilms was associated with the survival of encased sessile cells under environmental stress. Due to the destructive sample preparation process (*e.g.*, chemical fixation for SEM, staining for light microscopy), artifacts may be introduced that affect the accurate characterization of biofilms. Atomic force microscopy (AFM) offers an alternative characterization methodology. By recording interaction signals between the probing tip and biofilm surface, AFM can generate high-resolution topographic images that accurately reflect the structural details of morphological information of a biofilm in a nano-scale without sample preparation (Scheuring and Dufrêne, 2010; Ivanov et al., 2011; La Storia et al., 2011; Lim et al., 2011).

Physical properties of biofilms, such as surface wettability (hydrophobicity/hydrophilicity), surface roughness, surface free energy, and water holding capability, play a role in the response of bacterial biofilms to a variety of stresses, such as desiccation and shear stress (Bove et al., 2012; Ng and Kidd, 2013). Wettability is related to the surface area of biofilm that could contact water while a high water holding capability maintains a high relative humidity in biofilms, both of which are important to protect encased cells from desiccation (Allison et al., 1990). Surface roughness predicts the susceptibility of biofilms to shear force, thus the smoother the biofilm surface, the less it is influenced by mechanical shearing forces (Beech et al., 2002; Li and Logan, 2004).

Few studies have been conducted to investigate the effect of mixed bacterial culture on *C. jejuni*-containing biofilms and the susceptibility of *C. jejuni* cells in these multispecies biofilms. Therefore, this study aims to characterize chemical, physical and morphological properties of dual-species *C. jejuni*-containing biofilms and correlate these to the stress resistance of encased *C. jejuni* cells compared to that of mono-species *C. jejuni* biofilm. The knowledge will be

important to further understand the ecology of *C. jejuni* and its survival in the environment and subsequently develop innovative mitigation strategies to more successfully eliminate biofilms and reduce public health risk associated with this microbe.

2.3 Materials and methods

2.3.1 Bacterial strains and cultivation.

C. jejuni F38011 (human clinical isolate), *Staphylococcus aureus* (a clinical isolate used in our previous study) (Lu et al., 2013b), *Salmonella enterica* serovar Enteritidis FDA 3512H, and *Pseudomonas aeruginosa* PAO1 were used in this study. *C. jejuni* strain was stored at -80°C in Mueller-Hinton (MH) broth (BD Difco) containing 12% glycerol and 75% defibrinated sheep blood. Routine cultivation was conducted either on MH agar supplemented with 5% defibrinated sheep blood or in MH broth with constant shaking at 37°C under microaerobic conditions (85% N_2, 10% CO_2, 5% O_2). *S. aureus*, *S. enterica*, and *P. aeruginosa* were individually cultivated overnight in 5 ml tryptic soy broth (TSB) (BD Difco) at 37°C to achieve a concentration of ca. 9 log CFU/ml.

2.3.2 Biofilm cultivation.

One milliliter of overnight bacterial culture was centrifuged at 8,000 ×*g* for 10 min at 22°C. The supernatant was discarded, and the bacterial pellets were washed twice and resuspended in sterile phosphate buffered saline (PBS) (pH = 7.0). The resuspended culture was then diluted to ~10^7 CFU/ml. For dual-species biofilm formation, the mixed culture of *C. jejuni* F38011 was generated by addition of a second bacterial strain listed above on the basis of the same volume and concentration. Biofilms were cultivated at both solid-air interface and solid-liquid interface.

Nitrocellulose membrane (0.45 mm pore size, 47 mm diameter; Sartorius Stedim-type filters) was used as a substrate for biofilm formation at the solid-air interface, as described elsewhere (Lu et al., 2012). *C. jejuni* monoculture or mixed culture (100 µl) was deposited onto the surface of a sterile nitrocellulose membrane with a surface area of ~3×3 cm^2, which was placed onto an agar plate supplemented with 5% defibrinated sheep blood and incubated under a microaerobic environment at 37°C. The membrane was aseptically transferred to a fresh agar plate every 24 h for up to 72 h. 0.2 ml of *C. jejuni* monoculture or mixed culture was added to each well of sterile 96-well polystyrene plate for the cultivation of biofilms at the liquid-solid interface. The plate was incubated under a microaerobic environment at 37°C for up to 72 h.

2.3.3 Survival of *C. jejuni* F38011 and co-cultured bacterial cells in biofilms under aerobic stress.

The survival of *C. jejuni* and co-cultured bacterial cells in mono-species and dual-species biofilms under aerobic stress were determined by selective agar. Briefly, mature biofilms (cultivated under the microaerobic condition for 72 h) formed on nitrocellulose membrane were placed under aerobic environment at 22°C for up to 5 days. Every 24 h, biofilms were detached from nitrocellulose membrane using 0.1% trypsin solution (20 ml) for incubation at 22°C for 20 min. This treatment did not affect bacterial cell viability (data not shown). Following detachment, the bacterial suspension was serially diluted and spread onto selective agar plate. Campy Cefex agar is used for enumeration of viable *C. jejuni* cells (Neal-McKinney et al., 2012). Campy-Cefex agar contains 43 g/l Brucella agar, 0.5 g/l ferrous sulfate, 0.2 g/l sodium bisulfite, 0.5 g/l sodium pyruvate, 33 mg/l cefoperazone, and 0.2 g/l cycloheximide, with a supplement of 5% defibrinated sheep blood (Oyarzabal et al., 2005). Mannitol salt agar (BD BBL) is used for the

enumeration of viable *S. aureus* cells. Xylose lysine deoxycholate (XLD) agar (BD Difco) is used for enumeration of viable *S. enterica* and *P. aeruginosa* cells. The selective agar for *C. jejuni* was placed under a microaerobic environment at 37°C, while selective agars for co-cultured bacterial strains were placed under aerobic environment at 37°C.

2.3.4 Confocal laser scanning microscopy (CLSM).

The survival state of *C. jejuni* cells within a biofilm was further confirmed using CLSM. The SYTO 9 dye (with a green color for live cells) and propidium iodide dye (with a red color for non-viable cells) were diluted according to the manufacturer's instructions and then mixed in equal volume proportions. After exposure to aerobic environment for four days, nitrocellulose membrane with a developed biofilm was transferred from an agar plate to a sterile petri dish with 2 ml of the mixed dye solution, followed by incubation at 22°C for 30 min in the absence of light. The unbound dye was rinsed off of the nitrocellulose membrane with PBS (pH 7.0), and images of stained biofilms were collected using confocal microscopy (FV3000, Olympus, Tokyo, Japan). The wavelengths of excitation laser were set at 488 nm and 543 nm for green channel and red channel, respectively. Images were collected using a 40.0 × 1.0 oil immersion objective lens at a scan speed of 400 Hz.

2.3.5 Crystal violet biofilm assay.

Crystal violet staining was applied to quantify biofilm formation at the liquid-solid interface. After 72 h cultivation, a 96-well plate was washed with sterile deionized water and dried at 37°C for 5 min. Then, 0.2 ml of 0.5% (w/v) crystal violet solution was added to each well of 96-well plate, and the plate was incubated at 22°C for 10 min. Unbound crystal violet was washed off

with sterile deionized water, and the plate was dried at 22°C for another 5 min. Bound crystal violet was dissolved in 0.2 ml of 95% ethanol (v/v) for 10 min. Released crystal violet suspension was measured using a microplate reader at 595 nm (SpectraMax M2, Molecular Devices, Sunnyvale, USA). Broth without bacterial inoculation was stained using the same method as control and subtracted for background correction.

2.3.6 *C. jejuni* share (CJS) index in biofilm formation.

The CJS index is used to semi-quantify the contribution of encased *C. jejuni* cells to the formation of dual-species biofilm compared to the formation of mono-species biofilm. The calculation of CJS index is adapted from a previous publication (Naves et al., 2008):

$$\mathrm{CJS} = \frac{\frac{\mathrm{AB}-\mathrm{NCS}}{\mathrm{C}}}{\frac{\mathrm{AC}-\mathrm{CS}}{\mathrm{CO}}}$$

, in which AB is the optical density of crystal violet stained dual-species biofilms, AC is the optical density of crystal violet stained mono-species *C. jejuni* biofilm, NCS is the optical density of crystal violet stained mono-species non-*C. jejuni* biofilm (*i.e., S. aureus, S. enterica*, and *P. aeruginosa*), CS is the optical density of crystal violet staining without inoculation, C is the viable *C. jejuni* cell counts in the mature dual-species biofilm, CO is the viable *C. jejuni* cell counts in the mature mono-species *C. jejuni* biofilm.

2.3.7 Confocal micro-Raman spectroscopy.

This photonic system includes a Raman spectrometer (Renishaw, Gloucestershire, United Kingdom), a Leica microscope (Leica Biosystems, Wetzlar, Germany) and a diode near-infrared (λ=785 nm) laser (Renishaw, Gloucestershire, United Kingdom). The spectrometer has an

entrance aperture of 50 μm and a focal length of 300 mm and is equipped with 1200-line/mm grating. Raman scattering signals were collected and dispersed by a diffraction grating and finally recorded as a Raman spectrum by a 576-by-384-pixel charge-coupled-device (CCD) array detector, with the size of each pixel 22 by 22 μm. Mono-species and dual-species *C. jejuni* biofilms formed at the solid-air interface were directly transferred onto the microscope stage, which was focused under the collection assembly, and spectra were collected using a 50× objective (numerical aperture [NA] = 0.75, working distance [WD] = 0.37 mm) with a wavenumber range of 1800-400 cm^{-1}. The spectral collection was conducted over a total of 60 s (exposure time) at eight different locations for each biofilm with ~25 mW of incident laser power. Exposure to laser illumination during Raman spectral collection did not cause damage or variations in chemical components of biofilm samples (data not shown).

2.3.8 Raman spectral processing and multivariate analysis.

The polynomial background fits combined with baseline subtractions were carried out to remove fluorescence background derived from biofilms. Spectral binning (2 cm^{-1}) and smoothing (9-point Savitzky-Golay algorithm) were then applied (Feng et al., 2014). Due to the potential minor differences among Raman spectra derived from biological variation among biofilm samples, a second derivative transformation algorithm was applied to amplify the minor spectral variations and separate out overlapping bands (Lu et al., 2011a). Unsupervised PCA models were constructed to quantify the variation among different biofilm samples. *Mahalanobis* distances in the PCA models were calculated to evaluate the variation among different biofilms (Lu et al., 2013b). All these analyses were conducted using MATLAB (Mathworks, USA).

2.3.9 Atomic force microscopy.

The variations in morphological properties between mono-species and dual-species *C. jejuni* biofilms formed at the solid-air interface were determined using a Cypher atomic force microscope (Asylum Research, Santa Barbara, U.S.A.) and TR400PB tip cantilevers from Olympus (Tokyo, Japan; nominal spring constant: k = 0.02 N/m). Topographic images were collected in contact mode in ambient air. The nitrocellulose membrane with a mature biofilm grown (cultivated under a microaerobic condition at 37°C for 72 h) was transferred from agar plate onto AFM specimen disc (15 mm diameter, Ted Pella, Redding, CA). After drying in biological safety cabinet at 22°C at <30% relative humidity for 30 min without air blowing, the specimen disc coated with biofilm was put into an enclosed sample chamber at 22°C at <60% relative humidity. Topographic images were collected at five random locations on the biofilm surface with a surface area of 8 µm × 8 µm at a scan frequency of 1 Hz. The AFM system was operated using Igor Pro 6.31 software (Wavemetrics Inc., Lake Oswego, U.S.A.) and the AFM images were analyzed off-line using WSxM 5.0 software (Nanotec Electronica S.L., Madrid, Spain). Surface root-mean-square (RMS) roughness of biofilms was calculated using height images with a surface area of 8 µm × 8 µm.

2.3.10 Contact angle measurement.

The wettability (hydrophobic/hydrophilic) of biofilm surfaces were determined by contact angle measurement using a sessile drop method (Lamour et al., 2010; Syamaladevi et al., 2013). In this study, sterile deionized water, formamide, and diiodomethane were used as reference liquids. Briefly, mature biofilms (cultivated under the microaerobic condition for 72 h) formed at the solid-air interface were dried at 22°C for 30 min before contact angle measurement. Then, one µl

liquid droplet was deposited onto the biofilm surface and allowed to settle for 5 s. A high-resolution digital camera (D90, Nikon, Tokyo, Japan) was used to capture profile images of contact angles at the equilibrium under a light source. Contact angle (θ) was collected at three random locations for each sample and experiment was conducted in triplicate.

Images were analyzed by software FTA32 Version 2.0 (First Ten Ångstroms, Portsmouth, U.S.A.), as described by Mirvakili and Beyenal (Beyenal et al., 2004; Mirvakili et al., 2013). Biofilm wettability was estimated by contact angle formed by deionized water. Biofilm surface free energy properties [*i.e.*, total surface energy (γ_S), Lewis acid-base component (γ_S^{AB}), Lifshitz-van der Waals (γ_S^{LW}), electron-donor (γ_S^-) and electron acceptor (γ_S^+)] were calculated according to Young-Dupré equation and van Oss approach (Briandet et al., 2001; van Oss, 2002) as follows:

$$\cos\theta = -1 + 2\sqrt{(\gamma_S^{LW}\gamma_L^{LW})}\Big/\gamma_L + 2\sqrt{(\gamma_S^+\gamma_L^-)}\Big/\gamma_L + 2\sqrt{(\gamma_S^-\gamma_L^+)}\Big/\gamma_L$$

$$\gamma_S^{AB} = 2\sqrt{(\gamma_S^+\gamma_S^-)}$$

$$\gamma_S = \gamma_S^{AB} + \gamma_S^{LW}$$

2.3.11 Biofilm water retention assays.

Attenuated total reflectance-Fourier transform infrared (FT-IR) spectroscopy was applied to determine water holding capability of mono-species and dual-species *C. jejuni* biofilms formed at the solid-air interface. After 72 h cultivation, nitrocellulose membranes with developed biofilms were removed from agar plates and immediately mounted onto the crystal cell of Spectrum 100 FT-IR spectrometer (PerkinElmer, Norwalk, U.S.A.). FT-IR spectra of each biofilm were recorded at 22°C at intervals of 5 min until no changes in spectral features. Previous work has shown that spectral features of the nitrocellulose membrane did not affect FT-

IR spectral features of biofilms since the penetration distance of the evanescent wave derived from mid-IR is less than the thickness of biofilm (Lu et al., 2012a).

2.3.12 Statistical analysis.

All the experiments were conducted in at least three replicate trials. Results were reported as the averages of replicates ± the standard deviation with significance ($P < 0.05$) by one-way analysis of variance (ANOVA).

2.4 Results

2.4.1 The survival of *C. jejuni* F38011 and co-cultured bacterial cells in developed biofilms under aerobic stress.

In mature biofilms, the presence of *S. enterica* and *S. aureus* in dual-species biofilms did not affect the growth of *C. jejuni*, and the cell counts of culturable *C. jejuni* in *C. jejuni-S. enterica* and *C. jejuni-S. aureus* dual-species biofilms were not significantly different ($P > 0.05$) compared to that in mono-species *C. jejuni* biofilm thought the biofilm development. However, dual-species biofilm containing *P. aeruginosa* had a significantly lower ($P < 0.05$) number of culturable *C. jejuni* cells, about two orders of magnitude lower compared to the mono-species *C. jejuni* biofilm (**Table 2-1**). On the other hand, the presence of *C. jejuni* in dual-species biofilms did not affect the growth of co-cultured bacterial strains. The co-cultured bacterial cell counts in dual-species biofilms were not significantly different ($P > 0.05$) compared to their mono-species biofilm (**Table 2-2**). In *C. jejuni-S. enterica* and *C. jejuni-S. aureus* biofilms, the viable cell counts of *C. jejuni* were about one order of magnitude less than that of co-cultured bacterial strain. In *C. jejuni-P. aeruginosa* biofilm, the viable cell counts of *C. jejuni* were about three orders of magnitude less than that of co-cultured bacterial strain. In general, *C. jejuni* was not the

dominant strain compared to the co-cultured strains. Under aerobic stress, *C. jejuni* F38011 cell counts in mono- and dual-species biofilms decreased over exposure time, but survival time and rate of decrease varied significantly (**Table 2-1**). *C. jejuni* cells in mono-species biofilm and *C. jejuni-P. aeruginosa* biofilm survived for the shortest time, with no culturable *C. jejuni* cells detected when the biofilms were exposed to aerobic stress at four days and three days, respectively. The initial cell counts of *C. jejuni* in dual-species *C. jejuni-P. aeruginosa* biofilms were two orders of magnitude lower than that in mono-species *C. jejuni* biofilm. The reduction of *C. jejuni* cells in *C. jejuni-P. aeruginosa* biofilm under aerobic condition was more dramatic than that in the mono-species *C. jejuni* biofilm. A large number of *C. jejuni* cells in the other two dual-species biofilms were still culturable at day 5, with the *C. jejuni* cell counts in *C. jejuni-S. enterica* and *C. jejuni-S. aureus* biofilms at 3.9 and 4.2 log CFU/cm^2, respectively. In contrast, the survival of non-*C. jejuni* strains were not affected by aerobic stress. Taken together, the cell counts of *S. enterica*, *S. aureus*, and *P. aeruginosa* did not significantly decrease under aerobic stress.

Table 2-1. Viable *C. jejuni* F38011 cell counts in mature biofilms with aerobic stress.

Time	Biofilms / Viable cell counts (log CFU/cm^2)			
	C. jejuni	*C. jejuni* + *S. enterica*	*C. jejuni* + *S. aureus*	*C. jejuni* + *P. aeruginosa*
Mature (72-h cultivation, Day 0)	8.1 ± 0.1	7.8 ± 0.2	8.2 ± 0.1	5.9 ± 0.2
Day 1	7.4 ± 0.3	7.0 ± 0.3	7.2 ± 0.3	4.6 ± 0.2
Day 2	5.3 ± 0.3	5.9 ± 0.3	6.9 ± 0.7	3.9 ± 0.2
Day 3	4.9 ± 0.1	5.0 ± 0.3	5.2 ± 0.3	ND
Day 4	ND*	4.7 ± 0.1	4.8 ± 0.1	ND
Day 5	ND	3.9 ± 0.1	4.2 ± 0.1	ND

* ND: non-detectable, the limit of detection is 2.7 log CFU/cm^2

Day 1 to Day 5: exposure time of mature biofilm to aerobic environment

Table 2-2. Viable non-*C. jejuni* (*i.e. S. enterica, S. aureus,* and *P. aeruginosa*) bacterial cell counts in mature biofilms under aerobic stress.

Time	Biofilms / Viable cell counts (log CFU/cm^2)					
	C. jejuni + *S. enterica*	*S. enterica*	*C. jejuni* + *S. aureus*	*S. aureus*	*C. jejuni* + *P. aeruginosa*	*P. aeruginosa*
Mature (72-h cultivation, Day 0)	9.4 ± 0.1	9.5 ± 0.2	9.1 ± 0.3	9.0 ± 0.2	8.4 ± 0.1	8.4 ± 0.1
Day 1	9.5 ± 0.1	9.6 ± 0.1	9.2 ± 0.1	9.2 ± 0.1	8.5 ± 0.3	8.5 ± 0.2
Day 2	9.5 ± 0.1	9.5± 0.2	9.1 ± 0.1	9.2 ± 0.0	8.3 ± 0.3	8.4 ± 0.3
Day 3	9.5± 0.1	9.5 ± 0.1	9.4 ± 0.4	9.3 ± 0.2	8.5 ± 0.7	8.3 ± 0.3
Day 4	9.5± 0.0	9.4 ± 0.1	9.4 ± 0.4	9.2 ± 0.1	7.9 ± 0.3	8.2 ± 0.3
Day 5	9.5± 0.1	9.4 ± 0.1	9.2± 0.2	9.2 ± 0.1	8.1± 0.8	7.9 ± 0.3

Day 1 to Day 5: exposure time of mature biofilm to aerobic environment

2.4.2 The viability of *C. jejuni* F38011 cells in biofilms.

The viability of *C. jejuni* F38011 cells in mono-species biofilms under aerobic stress was further determined using live/dead kit coupled with confocal laser scanning microscopy (CLSM). After four days exposure to aerobic condition, no viable cell could be detected by a plating

method. However, live cells (green signal) could still be observed in CLSM images (**Figure 2-1A**). This could due to the amount of live *C. jejuni* cells in mono-species biofilm were lower than the limit of detection of plating assay (2.7 log CFU/cm^2) or these cell were under the non-culturable state. From the vertical layout, the signal of viable cells intensely observed at the bottom layer of biofilm, indicating survived *C. jejuni* cells tend to habit the bottom of biofilm. This particular preference of localization of viable *C. jejuni* cells in biofilms could because bottom biofilm was away from the air-biofilm interface with a low level of oxygen and was suitable for the survival of *C. jejuni* cells (**Figure 2-1B**).

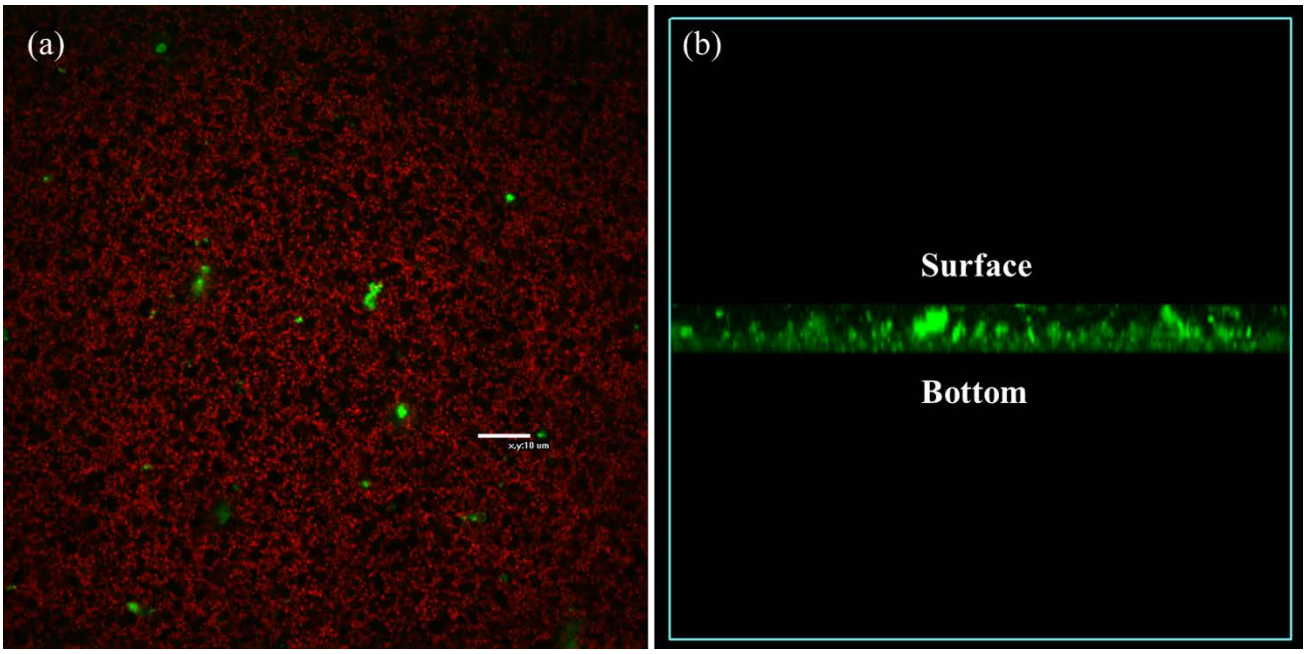

Figure 2-1. The viability and localization of *C. jejuni* cells in mono-species *C. jejuni* F38011 biofilm was determined using live/dead kit coupled with confocal laser scanning microscopy. In this image, green color indicates live *C. jejuni* cells while red color indicates dead *C. jejuni* cells (n = 3). After four days exposure to aerobic stress, there is no viable *C. jejuni* cells could be detected using MH plating method. However, the green signal derived from viable cells still could be observed in biofilm, and most of these viable cells were localized at the bottom layer of biofilm. a) Viable and dead *C. jejuni* cells in mono-species biofilm showed in horizontal layout. b) Viable *C. jejuni* cells in mono-species biofilm showed in vertical layout.

2.4.3 The formation level of *C. jejuni* biofilms.

The formation level of mono- and dual-species *C. jejuni* biofilms in 96-well plate were evaluated using crystal violet staining assay (**Figure 2-2**). Mono-species *C. jejuni* culture only formed a thin biofilm. In contrast, the formation level of all dual-species *C. jejuni* biofilms was

significantly ($P < 0.05$) higher. Among these dual-species biofilms, the biofilm formed by *C. jejuni* with *P. aeruginosa* had the largest biomass, which was approximately 13.5 times higher than that of mono-species *C. jejuni* biofilm (**Figure 2-2**). In addition, the biomass of *C. jejuni-S. enterica* biofilm was similar to that of *C. jejuni-S. aureus* biofilm but significantly higher ($P < 0.05$) than that of mono-species *C. jejuni* biofilm by ~ 4 times.

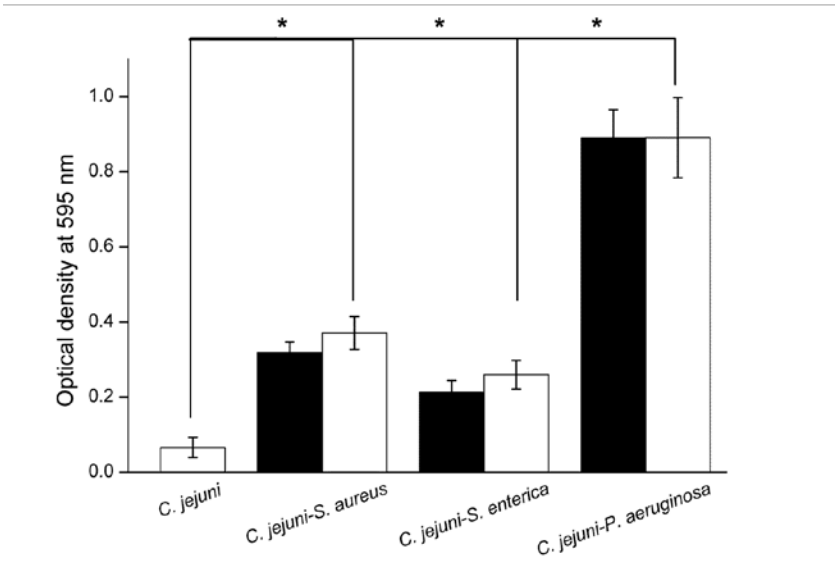

Figure 2-2. The formation level of mono- and dual-species biofilms in 96-well plate was quantified by crystal violet staining assay. (white column: the biofilms formed by *C. jejuni* individually or with other bacteria (*i.e.*, *P. aeruginosa*, *S. enterica*, and *S. aureus*); black column: biofilms formed by non-*C. jejuni* bacteria, including *P. aeruginosa*, *S. enterica*, and *S. aureus*, individually. Asterisk denotes significant difference ($P < 0.05$).

2.4.4 The contribution of *C. jejuni* to biofilm formation.

C. jejuni share (CJS) index was applied to evaluate the weight of *C. jejuni* in the dual-species biofilms (*i.e.*, with *S. aureus*, *S. enterica*, and *P. aeruginosa*) regarding contribution to

biomass. By subtracting the biomass formed by non-*C. jejuni* strain (*i.e.*, *S. aureus*, *S. enterica* and *P. aeruginosa*) in dual-species biofilms, the contribution of *C. jejuni* to dual-species biofilm could be roughly estimated. Subsequently, the contribution of *C. jejuni* to biofilm formation could be determined by comparing the contribution of *C. jejuni* to mono- and dual-species biofilms. According to **Table 2-3**, the contribution of *C. jejuni* to biofilm formation was not affected by the presence of *S. aureus*, *P. aeruginosa*, or *S. enterica*.

Table 2-3. Contribution of *C. jejuni* F38011 cells to the formation of mono- and dual-species biofilms.

C. jejuni share (CJS) index in mono- and dual-species biofilms is summarized.

C. jejuni	*C. jejuni* + *S. enterica*	*C. jejuni* + *S. aureus*	*C. jejuni* + *P. aeruginosa*
1.00	1.07	0.99	0.97

The value is obtained as the ratio of biomass formed by *C. jejuni* alone in the dual-species biofilm to that formed by *C. jejuni* in the mono-species biofilm.

2.4.5 The chemical compositions of *C. jejuni* biofilms.

Raman spectra of mono- and dual-species *C. jejuni* biofilms were collected over a wavenumber region from 1800 to 400 cm^{-1}. A representative Raman spectrum of each biofilm was an average of 24 spectra collected from three independent experiments (**Figure 2-3**). According to the previous studies of band assignments for bacteria and other biological systems (Movasaghi et al., 2007; Lu et al., 2012a), spectral regions depicting four important chemical

components in biofilms are 1800-1500 cm^{-1}: proteins, 1500-1200 cm^{-1}: fatty acids, 1200-900 cm^{-1}: polysaccharides, and 900-400 cm^{-1}: a unique fingerprinting region of mixed constituents.

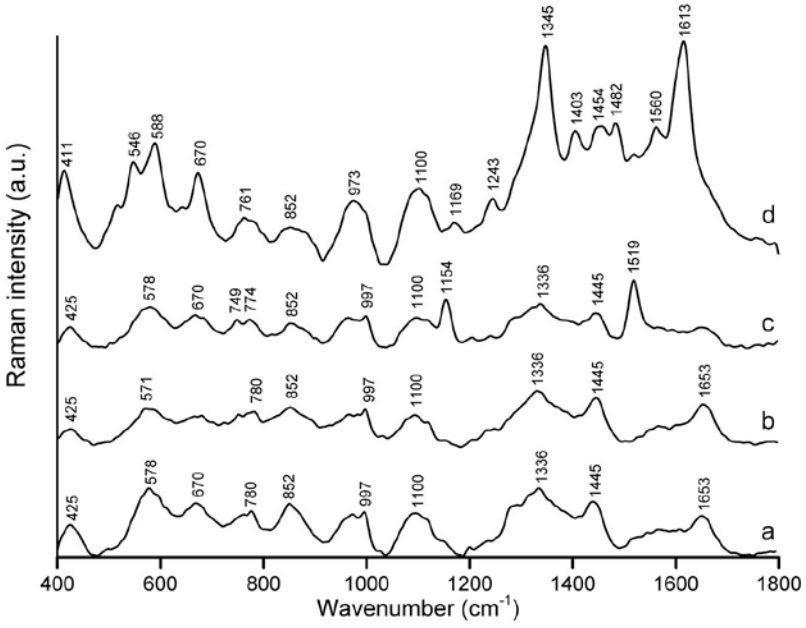

Figure 2-3. The Raman spectra indicated the chemical variations among different biofilms. The Raman spectra were collected using a confocal micro-Raman system with 785 nm laser. The biofilms were prepared on NC membrane and air-dried for 15 mins before spectra collection. Raman spectra showed here were the average of 24 independent replicates: a) the Raman spectra of mono-species *C. jejuni* biofilm; b) the Raman spectra of dual-species *C. jejuni-S. enterica* biofilm; c) the Raman spectra of dual-species *C. jejuni-S. aureus*; d) the Raman spectra of dual-species *C. jejuni-P. aeruginosa*.

C. jejuni-S. enterica biofilm shared a similar Raman spectral pattern as that of mono-species *C. jejuni* biofilm at the bands of 425, 578, 670, 780, 973, 997, 1100, 1336, 1445, and 1653 cm^{-1}, but with higher signal intensity. **Table 2-4** summarizes the major Raman band

assignments of mono- and dual-species *C. jejuni* biofilms, noting the spectral features of both EPS and encased cells within biofilms. Second derivative transformations were performed to magnify the minor variations in raw Raman spectra between mono-species *C. jejuni* biofilm and *C. jejuni-S. enterica* biofilm (**Figure 2-4**). Distinct differences were observed at 425, 578, 780, 855, 997, and 1280 cm^{-1}, as summarized in **Table 2-4**.

Table 2-4. The band assignments of Raman spectra of *C. jejuni* mono-species biofilm and dual-species *C. jejuni-S. enterica* biofilm.

Raman shift (cm^{-1})	Band assignment
425	Symmetric stretching vibration of phosphate
578	tryptophan/cytosine, guanine
670	ring-breathing modes in DNA base
780	ring breathing of nucleotide
855	ring-breathing modes in RNA base
973	C-C backbone of proteins
997	C-O vibration and C-C backbone of polysaccharides
1100	C-C vibration mode of amide III
1280	Backbone of nucleic acids and proteins
1336	CH_3CH_2 wagging of nucleic acids
1445	CH_3CH_2 bending mode of lipids and proteins
1653	amide I and C=C lipid stretch

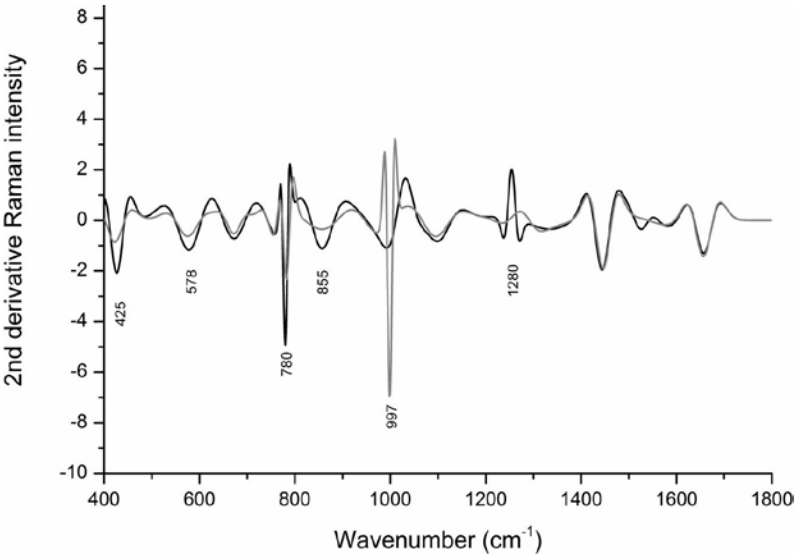

Figure 2-4. The minor chemical variation between *C. jejuni* mono-species biofilm (black) and dual-species *C. jejuni-S. enterica* biofilm (gray) was determined using second derivative transformations of Raman spectra. Distinct differences were observed at 425, 578, 780, 855, 997, and 1280 cm^{-1}.

The chemical compositions of *C. jejuni-S. aureus* and *C. jejuni-P. aeruginosa* biofilms were significantly different from each other, and both of them were varied from that of the mono-species *C. jejuni* biofilm, specifically at bands of lipids, proteins, and polysaccharides. **Table 2-5** summarizes the differences observed in spectral features for these biofilms.

Table 2-5. The assignments for distinct Raman bands between the Raman spectra of *C. jejuni-S. aureus* and *C. jejuni-P. aeruginosa* biofilms.

Biofilms	Raman shift (cm^{-1})	Band assignment
C. jejuni-S. aureus	1519	C=C band stretch of polysaccharides
	1154	C-C stretching of proteins
	774	symmetric breathing of proteins
	749	symmetric breathing of lipids
C. jejuni-P. aeruginosa	1613	tyrosine
	1560	tryptophan
	1482	ring breathing mode of nucleic acids
	1454	CH_3 bending of phospholipids
	1403	methyl group in proteins
	1345	CH deformation of polysaccharides
	1243	amide III
	1169	tyrosine
	761	ring breathing of tryptophan
	588	phospholipids
	546	lipids
	411	phospholipids

The Raman spectra of biofilms formed by non-*Campylobacter* bacteria (*i.e.*, *S. enterica*, *S. aureus*, and *P. aeruginosa*) were regarded as control. Representative Raman spectra of these biofilms were shown in **Figure 2-5**. Biofilms formed by non-*C. jejuni* strains (*i.e.*, *S. enterica*, *S.*

aureus and *P. aeruginosa*) shared similar Raman spectral pattern as that of dual-species biofilms(*i.e., S. enterica* + *C. jejuni*, *S. aureus* + *C. jejuni*, and *P. aeruginosa* + *C. jejuni*), respectively. The Raman spectra of *P. aeruginosa* biofilm only showed two distinct Raman bands at 516 and 1524 cm^{-1} (**Table 2-4 and 5**) that were not observed in the dual-species *P. aeruginosa* + *C. jejuni* biofilm. In addition, the band intensities of Raman spectra of *S. enterica* and *S. aureus* biofilms were lower than that of the dual-species biofilms (*i.e., S. enterica* + *C. jejuni* and *S. aureus* + *C. jejuni*) respectively. The intensities of Raman bands were associated with the quantity of certain functional groups. Hence, the intensities of biofilm Raman bands reflected the quantity of different chemical compositions in different biofilms. In general, dual-species biofilms contained higher biomass than that of mono-species biofilms which were consistent with the result of crystal violet staining assay.

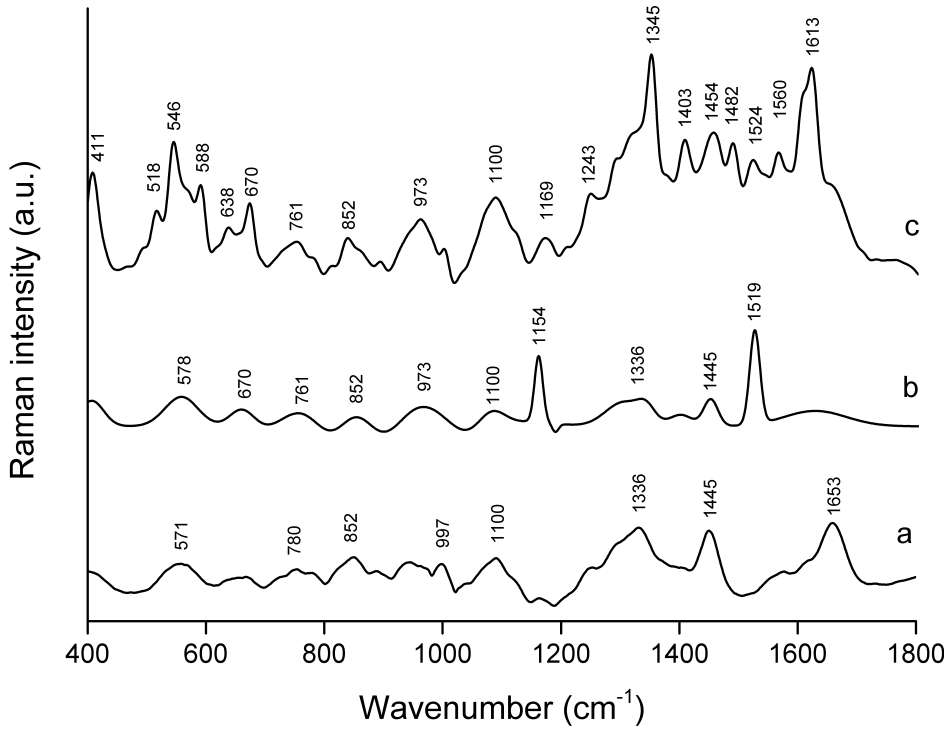

Figure 2-5. The Raman spectra of biofilms formed by non-*Campylobacter* bacteria (*i.e., S. enterica, S. aureus, and P. aeruginosa*) indicated the contribution of non-*Campylobacter* to the chemical composition of dual-species biofilms. The Raman spectra were collected using a confocal micro-Raman system with 785 nm laser. The biofilms were prepared on NC membrane and air-dried for 15 mins before spectra collection. Raman spectra showed here were the average of 24 independent replicates: a) the Raman spectra of *S. enterica* biofilm; b) the Raman spectra of *S. aureus* biofilm; c) the Raman spectra of *P. aeruginosa* biofilm.

The principal component analysis (PCA) was employed to differentiate of mono- and dual-species *C. jejuni* biofilms based on the difference of their Raman spectral patterns (**Figure 2-6**). Each of biofilm had distinctive features as signified by the formation of tight clusters with interclass distances for the biofilms from different species ranging from 4.63 to 13.02 based on

Mahalanobis distance measurements computed between the centroids of groups. Clusters with interclass distance values higher than three are considered to be significantly different ($P < 0.05$) from each other (Lu et al., 2011b).

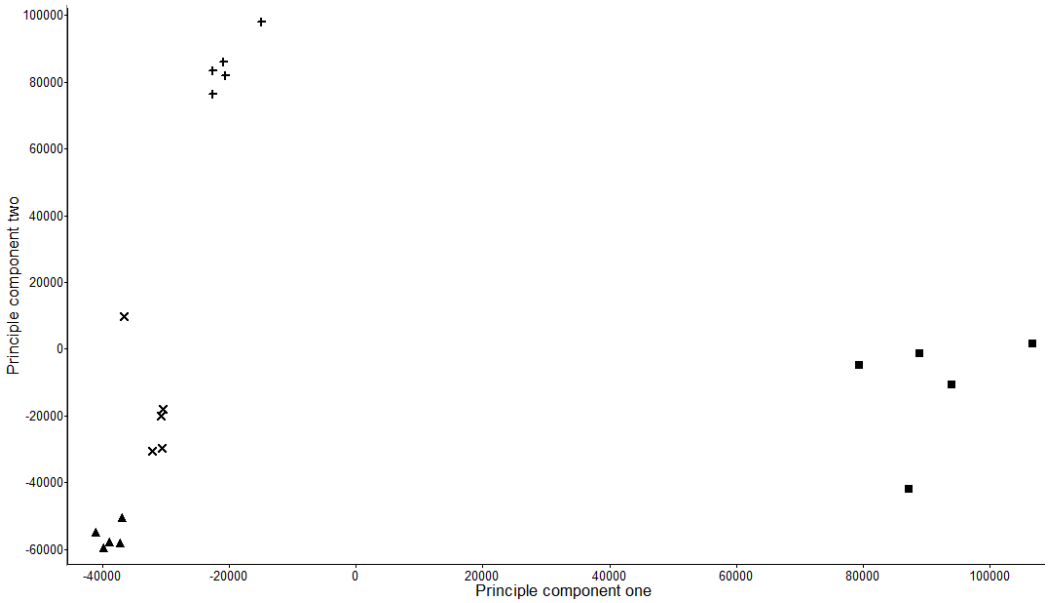

Figure 2-6. The principal component analysis for the segregation of *C. jejuni* mono- and dual-species biofilms based on the difference of their Raman spectra. Cross: *C. jejuni* biofilm; triangle: *C. jejuni-S. enterica* biofilm; plus: *C. jejuni-S. aureus* biofilm; square: *C. jejuni-P. aeruginosa* biofilm.

2.4.6 The morphological and surface roughness of *C. jejuni* biofilms.

The surface mechanical properties of mono- and dual-species *C. jejuni* biofilms were determined using AFM in contact mode. Although AFM contact mode might rupture the surface of biofilm, the trace and retrace images collected from the same spot were perfectly matched (data are not shown), indicating that the interaction between AFM and biofilm surface did not scratch the biofilm, and the morphological properties and surface roughness collected by AFM

were reliable. The representative topographic images of different biofilms were shown in **Figure 2-7**. The deflection images demonstrated the detailed topographic information of biofilm surface. Specifically, the surface of mono-species *C. jejuni* biofilm was loosely structured (**Figure 2-7A**). In contrast, the surface of dual-species *C. jejuni* biofilms was compacted and well organized. In addition, the congested pits (~1×1 μm^2) were randomly arranged on the surface of dual-species *C. jejuni-S. enterica* (**Figure 2-7B**) and *C. jejuni-P. aeruginosa* (**Figure 2-7D**) biofilms; while the surface of dual-species *C. jejuni-S. aureus* biofilm had small shallow pits (**Figure 2-7C**).

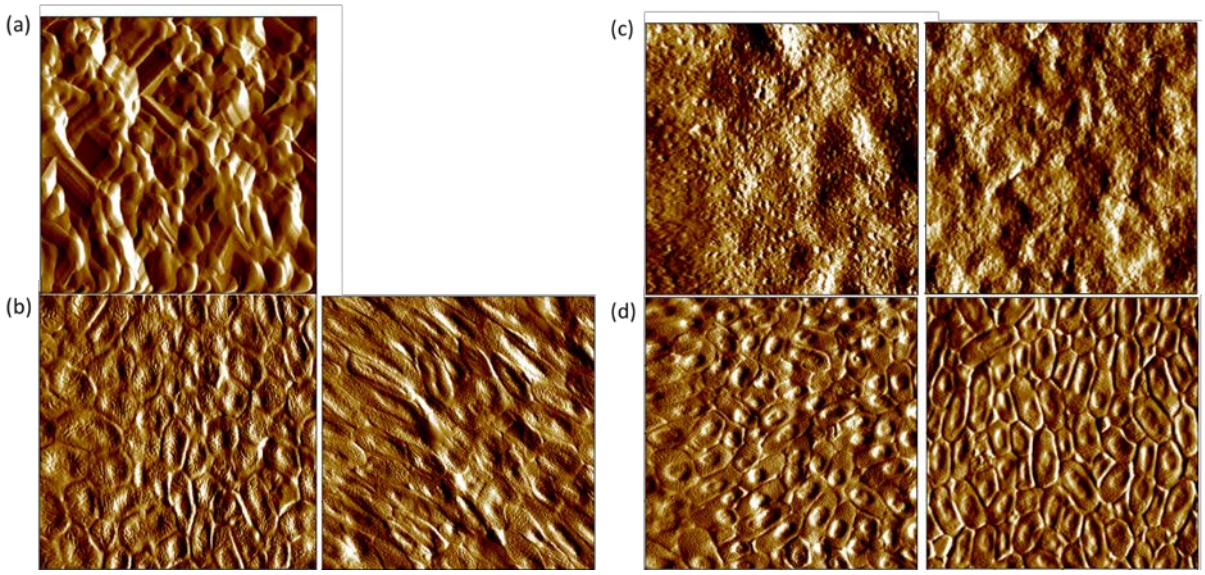

Figure 2-7. Topographic deflection-retrace images of mono- and dual-species *C. jejuni* biofilms obtained by atomic force microscopy in contact mode within 8 μm × 8 μm area: a) *C. jejuni*; b) *C. jejuni-S. enterica*; c) *C. jejuni-S. aureus*; d) *C. jejuni-P. aeruginosa*. (left panels: *C. jejuni*-containing biofilms; right panels: non-*C. jejuni*-containing biofilms) (n = 20).

Topographic information of biofilms formed by non-*C. jejuni* bacteria (*i.e.*, *S. enterica*, *S. aureus* and *P. aeruginosa*) was also measured using AFM (**Figure 2-7**) (n = 20). The surface of these biofilms was all compact. In addition, the surface pattern on the surface of mono-species *P.*

aeruginosa biofilm was similar as that on the surface of dual-species biofilm (**Figure 2-7D**). In contrast, the surface structure of *S. enterica* and *S. aureus* biofilms showed differences with their dual-species biofilm counterparts (*i.e., S. enterica + C. jejuni* and *S. aureus + C. jejuni*) (**Figure 2-7B, C**). Although *S. enterica* biofilm had a similar surface pattern (pits with the size of 1 × 1 μm^2) as that of dual-species *C. jejuni-S. enterica* biofilm, these patterns on the surface of *S. enterica* biofilm were loosely organized. While, compared to dual-species *C. jejuni- S. aureus* biofilm, the surface of *S. aureus* biofilm contained more bumps or protrusions on the surface, but small shallow pits spreading on *C. jejuni-S. aureus* biofilm could not be observed.

The root mean square (RMS) roughness of biofilms were calculated from the AFM height images (**Figure 2-8**). The RMS roughness of mono-species *C. jejuni* biofilm was 257.7 nm, while the RMS roughness of *C. jejuni-S. enterica* biofilm was 17.9 nm; the RMS roughness of *C. jejuni-S. aureus* biofilm was 30.7 nm; the RMS roughness of *C. jejuni-P. aeruginosa* biofilm was 27.4 nm (**Figure 2-9**). This result was consistent with surface morphological properties of biofilms, which indicated that the surface structure of mono-species *C. jejuni* biofilm was rougher and less structured than that dual-species *C. jejuni* biofilms.

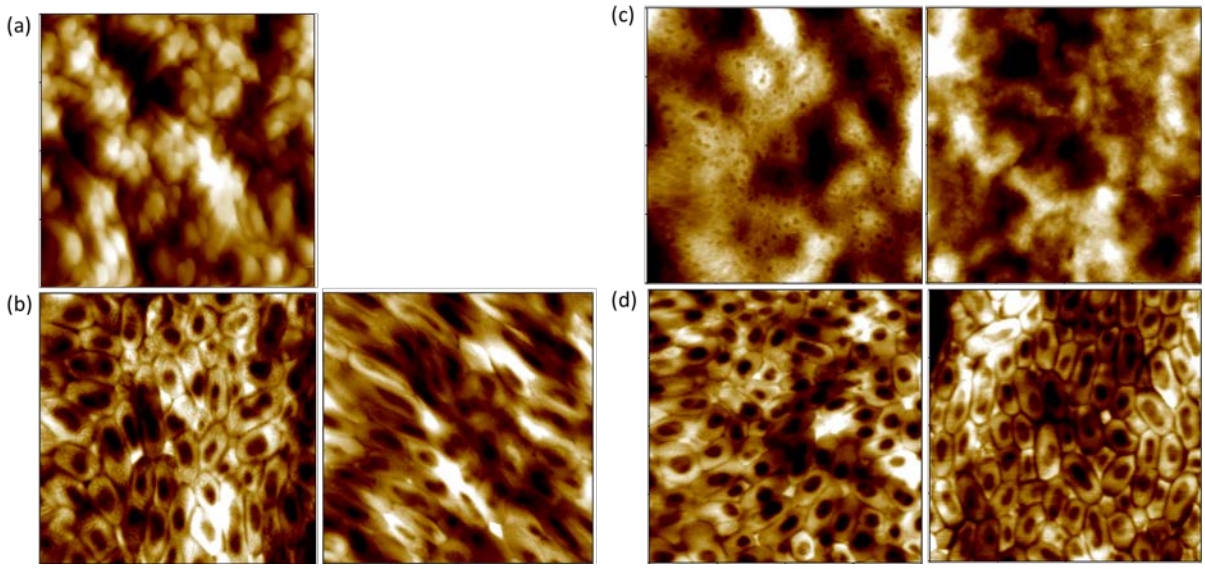

Figure 2-8. The representative topographic height-retrace images of mono- and dual-species *C. jejuni* biofilms were obtained by atomic force microscopy in contact mode. The images were shown in 8 µm × 8 µm area: a) The image of *C. jejuni* biofilm; b) The images of *C. jejuni*-*S. enterica* and *S. enterica* biofilms; c) The image of *C. jejuni*-*S. aureus* and *S. aureus* biofilms; d) The image of *C. jejuni*-*P. aeruginosa* and *P. aeruginosa* biofilms. (left panels: *C. jejuni*-containing biofilms; right panels: non-*C. jejuni*-containing biofilms) (n = 20).

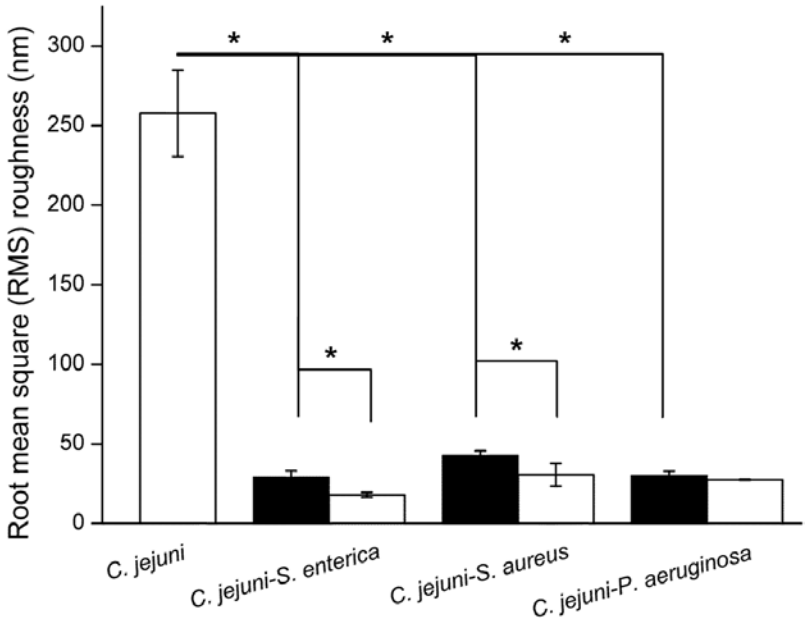

Figure 2-9. The root mean square (RMS) roughness of mono- and dual-species *C. jejuni* biofilms. The RMS roughness value of white column was derived from *C. jejuni* containing biofilms. The RMS roughness value of black column was derived from control biofilms which were *S. enterica*, *S. aureus*, and *P. aeruginosa* biofilms. Asterisk denotes significant difference ($P < 0.05$).

The RMS roughness of biofilms formed by or non-*C. jejuni* bacteria (*i.e., S. enterica*, *S. aureus* and *P. aeruginosa*) were 29.0 nm, 42.8 nm, and 30.2 nm, respectively (**Figure 2-9**). Compared to the dual-species biofilms, the RMS roughness of biofilms formed by *S. enterica* and *S. aureus* were significantly ($P < 0.05$) higher. The RMS roughness of *P. aeruginosa* biofilm was slightly higher compared to its dual-species biofilm counterpart, but no significant difference ($P > 0.05$) was observed.

The three-dimensional reconstruction of the surface structure of mono- and dual-species *C. jejuni* biofilms were shown in **Figure 2-10** which highlighted the variations of surface morphology among different biofilms.

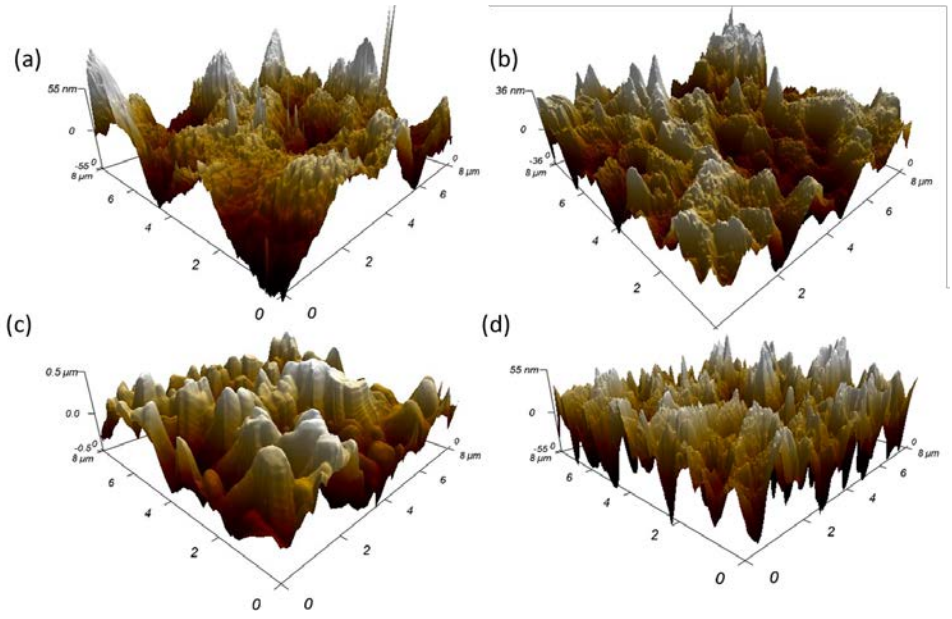

Figure 2-10. The 3D reconstruction images of the surface structure of mono- and dual-species *C. jejuni* biofilms. a) the surface structure of *C. jejuni* biofilm; b) the surface structure of *C. jejuni*-*S. enterica* biofilm; c) the surface structure of *C. jejuni*-*S. aureus* biofilm; d) the surface structure of *C. jejuni*-*P. aeruginosa* biofilm. (n = 20)

2.4.7 The surface wettability and free energy property of *C. jejuni* biofilms.

The contact angle measurement was applied to determine the surface wettability of mono- and dual-species *C. jejuni* biofilms formed on NC membrane. The wettability test was conducted using three reference liquids (*i.e.*, water, formamide, and diiodomethane) (Van Oss, 1993). The contact angle of these reference liquids on biofilms could be used to evaluate the surface

hydrophobicity qualitatively. In general, if the contact angle of a water droplet on a surface was higher than 90°, then this surface could be regarded as hydrophobic. The higher the water contact angle was, the more hydrophobic the surface was. The representative images of the contact angle of different reference liquids on mono- and dual-species *C. jejuni* biofilms were shown in **Figure 2-11**. The water droplets were quickly spread on the surface of mono-species biofilm, forming a contact angle of 13.2°. Dual-species biofilms were more repellent to water droplets, and the contact angle of water on these biofilms was significantly higher ($P < 0.05$) than that on mono-species *C. jejuni* biofilm, ranging from 19.6° to 21.8°. Taken together, water contact angle on all biofilms was lower than 90° (**Table 2-6**), indicating that these biofilms all had a hydrophilic surface and the hydrophilicity of mono-species biofilms was higher than that of dual-species biofilms. The contact angle was higher when the less polar liquids were applied. Specifically, the contact angles of formamide on biofilms ranged from 19.7° to 28.3°; the contact angle of diiodomethane on biofilms ranged from 62.4º to 82.6º.

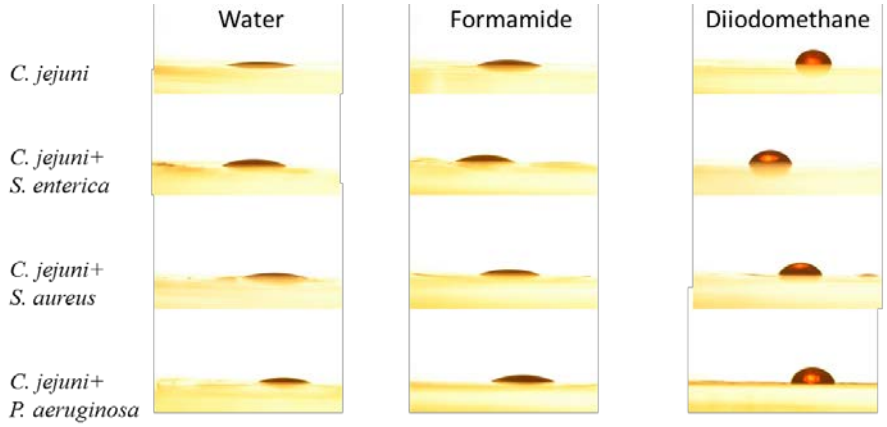

Figure 2-11. Representative images of contact angle formed by three different liquids (water, formamide, and diiodomethane) on the surface of mono- and dual-species *C. jejuni* biofilms (n = 9).

Table 2-6. The contact angle of different reference liquids on mono- and dual-species *C. jejuni* biofilms using sessile drop technique.

Culture	Contact angle		
	Water	Formamide	Diiodomethane
C. jejuni	$13.2^{o} \pm 2.2^{o}$	$19.7^{o} \pm 2.7^{o}$	$82.6^{o} \pm 4.2^{o}$
C. jejuni + S. enterica	$20.5^{o} \pm 2.4^{o*}$	$25.0^{o} \pm 2.5^{o*}$	$65.7^{o} \pm 3.4^{o*}$
S. enterica	$16.5^{o} \pm 3.2^{o}$	$23.7^{o} \pm 2.6^{o}$	$71.5^{o} \pm 5.1^{o}$
C. jejuni + S. aureus	$19.6^{o} \pm 1.8^{o*}$	$22.8^{o} \pm 2.2^{o*}$	$66.6^{o} \pm 2.9^{o*}$
S. aureus	$19.2^{o} \pm 2.4^{o}$	$20.1^{o} \pm 3.7^{o}$	$74.5^{o} \pm 2.4^{o}$
C. jejuni + P. aeruginosa	$21.8^{o} \pm 2.7^{o*}$	$28.3^{o} \pm 2.8^{o*}$	$62.4^{o} \pm 1.9^{o*}$
P. aeruginosa	$21.6^{o} \pm 2.8^{o}$	$27.1^{o} \pm 4.2^{o}$	$65.4^{o} \pm 2.8^{o}$

[*]Significant difference ($P < 0.05$) was observed between mono-species *C. jejuni* biofilm and dual-species *C. jejuni* biofilms. The data was shown as the mean value ± standard deviation. (n=9)

The contact angle measurement was also applied on biofilms formed by non-*C. jejuni* bacteria (*i.e., S. enterica*, *S. aureus* and *P. aeruginosa*). In general, the water contact angles of reference liquids on these biofilms were significantly different ($P < 0.05$) from that of dual-species biofilms (**Table 2-6**). The high contact angle on mono-species biofilms formed by non-*C.*

jejuni bacteria indicated that the hydrophilicity of biofilms formed by non-*C. jejuni* bacteria was higher than that of dual-species *C. jejuni* biofilms.

The surface energy of biofilms can be calculated from contact angle measurement using Young-Dupré equation (**Table 2-7)**. Compared to mono-species *C. jejuni* biofilm, the total surface energy of dual-species biofilms was much lower. In addition, the apolar component (Lifshitz-Van der Waals) and the polar component (Lewis acid-base) of the surface energy of mono- and dual-species *C. jejuni* biofilms varied extensively. Specifically, the apolar component of surface energy of dual-species biofilms ranged from 24.7 to 27.1 mJ/m^2, which was significantly higher ($P < 0.05$) than that of mono-species *C. jejuni* biofilm (16.1 mJ/m^2). This result was consistent with the observation of contact angle measurement in which mono-species biofilm repelled apolar liquid (*i.e.*, diiodomethane) more than that of dual-species biofilms.

Table 2-7. The total surface energy and distribution of energy components of mono- and dual-species *C. jejuni* biofilms.

Biofilms	Total surface energy (mJ/m^2)	Surface energy component distribution (mJ/m^2)	
		Lifshitz-Van der Waals (apolar component)	Lewis acid-base (polar component)
C. jejuni	62.9	16.1	46.7
C. jejuni + *S. enterica*	55.0	25.2	29.8
S. enterica	57.5	22.0	35.4
C. jejuni + *S. aureus*	56.2	24.7	31.5
S. aureus	59.4	20.4	39.0
C. jejuni + *P. aeruginosa*	52.5	27.1	25.4
P. aeruginosa	53.9	25.5	28.5

For biofilms formed by non-*C. jejuni* (*i.e.*, *S. enterica*, *S. aureus* and *P. aeruginosa*), the total surface energy of *S. aureus* and *P. aeruginosa* biofilms were higher than their dual-species biofilm counterparts, but *S. enterica* biofilm had lower total surface energy compared to *C.*

jejuni-S. enterica biofilm. In addition, the apolar component of surface energy of biofilms formed by non-*C. jejuni* was lower than that of dual-species biofilms, ranging from 20.4 to 25.5 mJ/m^2. The polar component of surface energy of biofilms formed by non-*C. jejuni* was higher than that of dual-species biofilms, ranging from 28.5 to 39.0 mJ/m^2.

2.4.8 The water-holding capability of *C. jejuni* biofilms.

The water holding capability of biofilms was critical for the survival of biofilm under desiccation condition. The water holding capability of mono- and dual-species biofilms was evaluated by the decreased water content which was determined using FT-IR spectroscopy (**Figure 2-12**). Water demonstrated a distinct IR absorbance band at 3350 cm^{-1}, the O-H stretch. All biofilms shared the similar water content after three days cultivation on NC membrane, and the intensity of water IR band was ~ 0.3 a.u. (**Figure 2-13**). Along with exposure of biofilms to the atmosphere, the intensity of water IR progressively decreased. The intensity of water IR band of mono-species *C. jejuni* biofilm decreased rapidly to 0.04 a.u. within 25 min. In contrast, the water holding capacity of dual-species *C. jejuni* biofilms was higher. The decrease rate of the intensity of water IR band of dual-species biofilm was much more slowly. Even after 25-min exposure to the atmosphere, the intensity of water IR band of dual-species biofilms was still maintained at a high level which was 0.25 a.u. for *C. jejuni-S. enterica* biofilm, 0.18 a.u. for *C. jejuni-S. aureus* biofilm and 0.20 a.u. *C. jejuni-P. aeruginosa* biofilm, respectively.

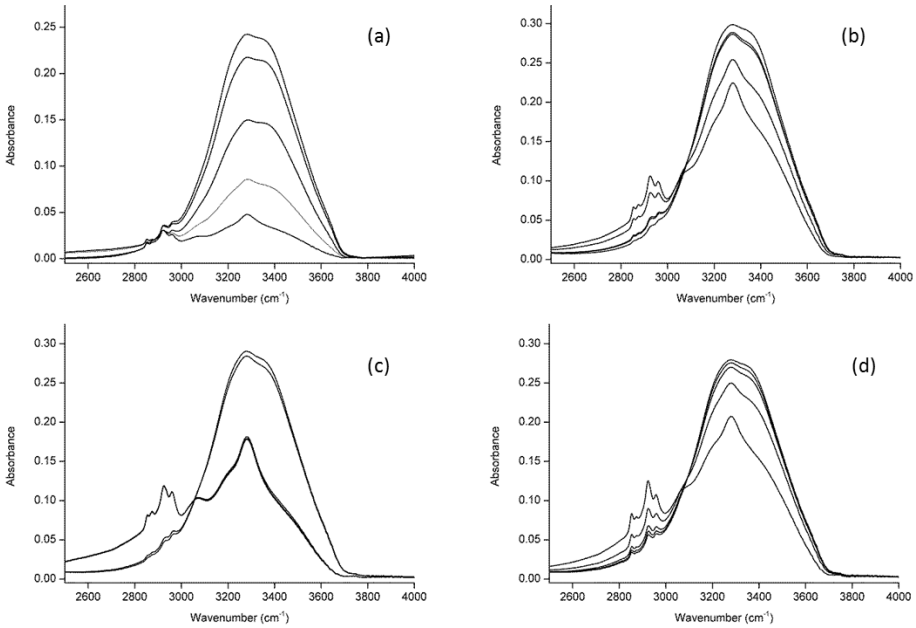

Figure 2-12. The water content of biofilms decreased over time which was reflected by the decrease of the intensity of water IR band at 3350 cm^{-1}. The IR spectra of mono- and dual-species *C. jejuni* biofilms were collected using the Fourier transform infrared spectroscopy at 5-min intervals: a) the IR spectra of *C. jejuni* biofilm, b) the IR spectra of *C. jejuni-S. enterica* biofilm, c) the IR spectra of *C. jejuni-S. aureus* biofilm, d) the IR spectra of *C. jejuni-P. aeruginosa* biofilm.

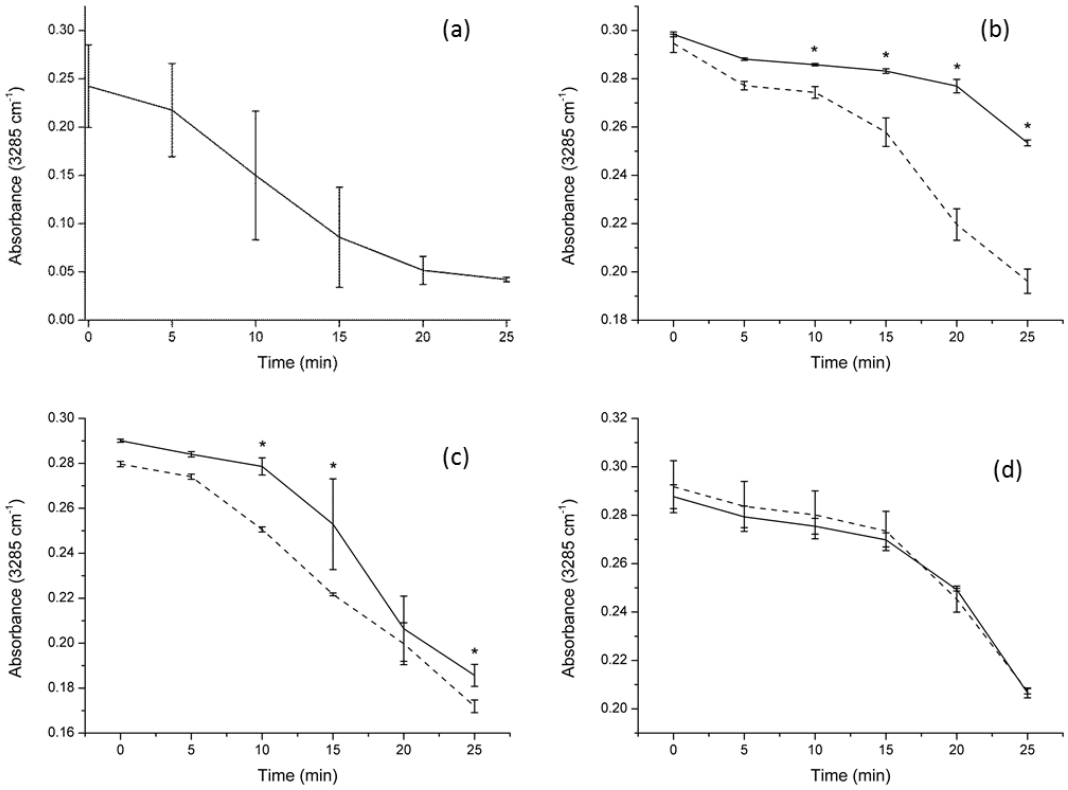

Figure 2-13. The water holding capability of mono- and dual-species *C. jejuni* biofilms was reflected by the decrease of intensity of water IR band. The IR water band of different biofilms was determined by Fourier transform infrared spectroscopy, as indicated by the featured absorbance band at 3350 cm^{-1}: a) the change of the intensity of IR water band of *C. jejuni* biofilm, b) the change of the intensity of IR water band of *S. enterica* and *C. jejuni*-*S. enterica* biofilms, c) the change of the intensity of IR water band of *S. aureus* and *C. jejuni*-*S. aureus* biofilms; d) the change of the intensity of IR water band of *P. aeruginosa* and *C. jejuni*-*P. aeruginosa* biofilms. (solid line: biofilms formed by *C. jejuni* with or without other bacteria, dash line: biofilms formed by *S. enterica*, *S. aureus*, and *P. aeruginosa* individually). Asterisk denotes significant difference ($P < 0.05$).

No significant difference ($P > 0.05$) was observed for water holding capability of biofilms formed by *P. aeruginosa* with or without *C. jejuni*. In contrast, the water capability of biofilms formed by *S. enterica* and *S. aureus* was significantly lower than their dual-species biofilm counterparts (**Figure 2-13**).

2.5 Discussion

C. jejuni could form biofilms on the surface of different materials, including plastics (Trachoo et al., 2002; Asakura et al., 2007a; Reeser et al., 2007), stainless steel (Sanders et al., 2007; Hanning et al., 2008), and glass (Kalmokoff et al., 2006). The biofilm formation capability of *C. jejuni* varied a lot due to different strains. For example, *C. jejuni* RM 1221 was unable to form a biofilm even in a well-controlled laboratory environment; in contrast, *C. jejuni* NCTC 11168 could form a relatively intense biofilm under the same condition (Brown et al., 2015b). *C. jejuni* F38011 used in this study is a human clinical isolate. This strain could only form a thin biofilm at both solid-air interface (on the surface of NC membrane) and solid-liquid interface (in 96-well plate). The biofilm formation capability of *C. jejuni* F38011 was similar to other *C. jejuni* strains reported in the previous studies (Gunther and Chen, 2009; Teh et al., 2010); therefore the result derived from this strain could be representative.

Environmental conditions are critical for the biofilm formation of *C. jejuni*. The aerobic condition was reported to stimulate the biofilm formation of *C. jejuni* at the air-solid interface (Reuter et al., 2010). The high flow rate can generate a high shear force which would increase the structural porosity of *C. jejuni* biofilm formed at liquid-solid interface (Ica et al., 2012). A photonic-based microfluidic platform was recently developed to elucidate the influence of hydrodynamic condition on biofilm formation (Feng et al., 2015). In the current study, these

factors were not included because this will complicate the evaluation of the protection of biofilm to encased *C. jejuni* against aerobic stress.

In the current study, the viability of *C. jejuni* cells in mono-species biofilm could not be detected using plating method over four day's exposure to aerobic stress (**Table 2-1**). However, CLSM result demonstrated a large number of cells at the bottom of biofilm were still alive (**Figure 2-1 A and B**). According to previous studies, *C. jejuni* might lose cultivability and enter the "viable but non-culturable" state in response to unfavorable conditions, such as aerobic stress, desiccation, and starvation (Lázaro et al., 1999; Tholozan et al., 1999). Hence, we speculated that *C. jejuni* cells at the bottom of biofilm might share a viable similarity to VBNC cell and had enhanced tolerance to the aerobic stress.

C .jejuni could also develop multispecies biofilm with other bacteria (Ica et al., 2012) or resides in a pre-established biofilm (Buswell et al., 1998; Trachoo et al., 2002; Sanders et al., 2007; Hanning et al., 2008). Sanders and coauthors reported that the survival of *C. jejuni* cells was prolonged by residing in pre-existing biofilms (Sanders et al., 2007). In another study, *C. jejuni* cells in the pre-established biofilms by microbes in the aquatic environment could survive a doubled longer period than that as dispersed single cells (Buswell et al., 1998). Our current study demonstrated that *C. jejuni* could form a dual-species biofilm with other bacteria. However, *C. jejuni* was not the leading species to form the biofilm. Compared to mono-species *C. jejuni* biofilm, the formation level of dual-species *C. jejuni* biofilms was significantly higher (**Figure 2-2** and **Figure 2-3**). In addition, the dual-species biofilm provided more protection to *C. jejuni* cells than that of mono-species *C. jejuni* biofilm which enabled *C. jejuni* cells to maintain the culturable state for a longer period under aerobic stress (**Table 2-1**).

An interesting observation was that although dual-species *C. jejuni-P. aeruginosa* biofilm was as intense as other dual-species biofilms, the survival period of *C. jejuni* cells in this biofilm were the shortest (**Table 2-1**). Gram-negative bacteria could secret outer membrane vesicles, and this vesicle could inhibit the growth of other bacteria (Flemming and Wingender, 2010). The membrane vesicles of *P. aeruginosa* contained various compounds (*e.g.*, B-band lipopolysaccharide with hemolysin, phospholipase C, and alkaline phosphatase) that could inhibit the growth of other bacteria (Kadurugamuwa and Beveridge, 1995). In a nutrient-limited environment, such as in a biofilm, we believed that *C. jejuni* and *P. aeruginosa* were in a competitive relationship. In the early stage of biofilm formation, *P. aeruginosa* cells could multiply rapidly and take most of nutrient and space which limited the growth of *C. jejuni* cells. Along with the biofilm development, *P. aeruginosa* could progressively secrete secondary metabolites (*e.g.*, hemolysin, phospholipase C, and alkaline phosphatase) which might be toxic to *C. jejuni* cells. This would further negatively affect the survival of *C. jejuni* in the biofilm.

The cells in biofilms usually were more tolerant to stresses. However, the mechanism of this tolerance was not well characterized yet. Researchers had proposed several possible reasons : (1) the chemical compositions of biofilm could chemically react with and neutralize the stresses (Allison and Matthews, 1992); (2) the chemical composition of biofilm could serve as nutrient reservoirs that prolonged the survival of encased biofilm cells (Decho et al., 2005);the particular structure of biofilm can physically trap stresses and delay the penetration of these stresses (Ica et al., 2012). Hence, the understanding of the chemical composition and physical structure of biofilm would be critical to understanding the tolerance of biofilm. Biofilms were mainly composed of proteins, polysaccharides, lipids and nucleic acids (Flemming and Wingender, 2010). These components could react with and neutralize different stresses. In the previous

studies, Raman spectroscopy has been applied to determine chemical components of mono-species *C. jejuni* biofilm (Lu et al., 2012a; Lu et al., 2012b). In this study, Raman spectroscopy was applied to characterize not only mono-species but also dual-species biofilms. We found that the chemical compositions of dual-species biofilms were quite different from that of mono-species biofilm (**Figure 2-3**). Specifically, Raman bands at 1519 and 1345 cm^{-1} could be assigned to polysaccharides which were significant components in *C. jejuni-S. aureus* and *C. jejuni-P. aeruginosa* biofilms, but were not prominent in mono-species *C. jejuni* biofilm. As indicated by the high intensity of Raman bands derived from dual-species biofilms, we believed that dual-species biofilms contained more content of organic substances than that of mono-species biofilm. In addition, Raman spectral patterns of biofilms formed by non-*C. jejuni* bacteria (*i.e., S. enterica*, *S. aureus* and *P. aeruginosa*) were highly similar to that of dual-species biofilms counterparts, indicating that non-*C. jejuni* bacteria contributed more to the chemicals compositions of dual-species biofilms than that of *C. jejuni* did.

The relationship between chemical compositions and its structural properties of the biofilm was also discussed. The previous study found that the presence of a non-cellular protein was one of the prerequisites for the formation of biofilm and closely associated with the stability of biofilm (McSwain et al., 2005). In the current study, the variation of chemical composition could also be correlated with the variation of structural properties between mono- and dual-species biofilms. The results of AFM, FTIR and contact angle measurement (**Figure 2-7**, **Figure 2-9**, **Figure 2-13** and **Table 4**) showed that dual-species biofilms had a compact structure with a smoother surface, a higher water holding capability and lower apolar surface energy than that of mono-species *C. jejuni* biofilm. These distinct surface features of dual-species biofilms could be due to the higher level of polysaccharides and proteins content in dual-species biofilms than that

in mono-species *C. jejuni* biofilm (**Figure 2-3**). In addition, this also suggested that polysaccharides and proteins might contribute more to the structural properties of dual-species biofilms than other components (*e.g.*, lipids and nucleic acids). We speculated that the presence of non-*C. jejuni* bacteria (*i.e., S. enterica*, *S. aureus* and *P. aeruginosa*) could enhance the amount and diversity of biofilm chemical compositions, and these constituents might fill the space of multicellular structure of biofilm, enhance water holding capability and influence the surface energy.

In conclusion, this study confirmed that mono-species *C. jejuni* F38011 culture could form a thin biofilm and protect *C. jejuni* cells against aerobic stress for a short period. The presence of *S. enterica*, *S. aureus,* and *P. aeruginosa* during biofilm formation could significantly remold the on the chemical, physical and morphological perspectives. The dual-species biofilms (1) contained a higher amount of EPS with a more complex chemical compositions; (2) were more compact with a smoother surface; (3) were less hydrophilic but with a higher ratio of apolar component/polar component of surface energy; (4) could hold the water for a longer period. These features were mainly derived from the non-*C. jejuni* bacteria (*i.e.*, *S. enterica*, *S. aureus* and *P. aeruginosa*) in the dual-species culture, and might allow *C. jejuni* F38011 cells to survive the aerobic stress.

Chapter 3: *In-situ* Raman spectroscopic-based microfluidic "lab-on-a-chip" platform for non-destructive and continuous characterization of *Pseudomonas aeruginosa biofilms*

3.1 Summary

The hydrodynamic condition was one of the critical factors that could influence the biofilm formation. We developed and validated a Raman spectroscopic-based microfluidic "lab-on-a-chip" platform for the characterization of bacterial biofilms. This innovative Raman-microfluidic platform could precisely control the flow conditions and mimic the natural hydrodynamic environment. The biofilm formation of *Pseudomonas aeruginosa* was quantified by this label-free platform, and the evaluation of biofilm formation level was well correlated to that derived from a reference techniques confocal laser scanning microscopy. In addition, this Raman-microfluidic platform could also discriminate the distinct formation stages of biofilms.

3.2 Introduction

A biofilm is a consortium of bacteria in which cells associate with each other and attach to a surface (de la Fuente-Núñez et al., 2013). These sessile cells are embedded within a matrix of secreted extracellular polymeric substances (EPS), including exopolysaccharides, proteins, lipids and nucleic acids, which comprise up to 90% of the biofilm (Hall-Stoodley et al., 2004). EPS not only mechanically support the structure of biofilm, but also protect biofilm cells against stresses (Davies, 2003). Biofilms on medical devices and food processing surfaces (*e.g.*, infusion tubes and water pipes) are highly resistant to antimicrobial treatments and disinfectants and thus represent one of the major health risks (Hall-Stoodley et al., 2004; Conlon et al., 2015).

The study of biofilm development is often limited to methods that involve static cultivation conditions, with the low shear flow and no nutrient exchange. On the other hand, cultivation under flow conditions more closely mimics the environment of biofilm formation due to hydrodynamic influences on the structure of biofilm and the accumulation of cell signaling (Kirisits et al., 2007). For example, the biofilm formation of *rpoS*-deficient *Escherichia coli* was impaired using hydrodynamic cultivation, compared to that under static conditions (Ito et al., 2008). The commonly used macro-scale flow cells require large volumes of media, resulting in a relatively expensive system that will not allow for spatial and temporal control of biofilm formation (Webb et al., 2003). By precisely controlling the hydrodynamic conditions, microfluidic platforms can closely simulate the appropriate environmental conditions and allow substantial reductions in the use of reagents. Microfluidic platforms have been recently applied to the study of bacterial biofilms in a high-throughput manner (Benoit et al., 2010; Kim et al., 2012).

The characterization of biofilms in a microfluidic platform is still a challenge. Most of the studies used confocal laser scanning microscopy (CLSM) coupled with staining for the quantitative studies of biofilm development (Shumi et al., 2010; Song et al., 2014). However, the staining process might influence the structure of biofilm. Furthermore, the CLSM assay could not monitor the chemical variations of biofilm continuously. We considered an alternative approach to investigate the biofilm formation using Raman spectroscopy that could observe vibrational, rotational and other low-frequency energies of a molecule in a biological system. When coupled with confocal imaging techniques, Raman spectroscopy can be used *in situ* to determine the chemical composition and

localization of bacterial biofilms in three dimensions, without staining of bacterial cells (Ivleva et al., 2008, 2009).

3.3 Materials and methods

3.3.1 Bacterial strains and growth conditions.

P. aeruginosa PAO1 wild type was cultured in tryptic soy broth (TSB) at 37°C.

3.3.2 Fabrication of microfluidic "lab-on-a-chip" platform.

The Poly-dimethylsiloxane (PDMS) based microfluidic system was fabricated in the Advanced Materials and Process Engineering Lab at UBC using classic soft lithographic techniques (Qin et al., 2010). The microfluidic platform consists of a glass substrate and a PDMS layer. The PDMS layer consists of in/outlet of channels with cultivation chamber. The dimensions of in/outlet were 400µm (width) × 40µm (height).The microchamber for biofilm cultivation is designed as a circle with dimensions of 300µm (radius) × 40µm (height). The PDMS layer was bonded to glass slide after oxygen plasma treatment. The microfluidic device was connected to a synergy pump using tubing.

3.3.3 Biofilm formation in the microfluidic "lab-on-a-chip" system.

An overnight culture of *P. aeruginosa* PAO1 was diluted to a concentration of ~10^7 CFU/ml and introduced into microchamber using a syringe pump. Bacterial culture was maintained in the cultivation chamber by stop pumping for two h to allow the attachment of *P. aeruginosa* PAO1 cells onto the glass surface of the microchamber. Unattached cells

were removed by perfusing TSB medium. The development of biofilm was set in a hydrodynamic condition by flowing media at 0.2 µl/min for 72 h.

3.3.4 Integration of confocal micro-Raman spectroscopy with the microfluidic platform.

A confocal Raman microscope system (Renishaw, Gloucestershire, UK) with 532 nm green diode laser was applied for the characterization of chemical compositions and formation level of *P. aeruginosa* biofilms. The spectrometer was equipped with a 1200-line/mm grating. Laser (0.2 mW laser power on the sample) was introduced through a 50× objective (Leica Biosystems, Wetzlar, Germany) into the microchamber and focused on the biofilm. While Raman signal was collected and dispersed by a diffraction grating, and finally recorded by using a 578- by 385-pixel charge-coupled device (CCD) array detector. An integration time of 30 s was applied for spectral collection over a simultaneous Raman shift range of 1800 to 400 cm^{-1} in an extended mode. The Raman spectrometer was controlled via WiRE software which was also responsible for spectra acquisition and processing (Renishaw, UK).

3.3.5 Confocal laser scanning microscope for biofilm quantification.

Confocal laser scanning microscopy (CLSM) was applied as a reference technique to quantify the formation level of biofilm. Biofilm was stained using a LIVE/DEAD BacLight Bacterial Viability Kit (Molecular Probes, Eugene, OR). A mixture of 1 µM of Syto-9 (green fluorescence for live cells) and 5 µM of propidium iodide (PI; red fluorescence for dead cells) was injected into microchamber at 2 µl/min for 2 hours.

Images were then taken on a Fluoview FV1000 confocal laser scanning microscope (CLSM) (Olympus, Melville, NY) with the multi-laser channel at 488nm (green fluorescence) and 543 nm (red fluorescence). The bio-volume of biofilm, three-dimensional reconstruction, and live/dead cells distribution were conducted using Imaris software (Bitplane, South Windsor, CT).

3.3.6 Chemometric models.

The chemical information obtained from Raman spectroscopy was correlated with the result from CLSM using partial least-squares regression (PLSR) model in MATLAB (Mathworks, USA).

3.4 Results and discussion

Here, we report the *in-situ* characterization of *Pseudomonas aeruginosa* biofilms cultivated in a microfluidic platform using confocal micro-Raman spectroscopy in a non-destructive and continuous manner. The multi-channel microfluidic chip was connected to a pump with bio-compatible tubing. The nutrient broth was continuously infused from the inlet and expelled through the outlet during the biofilm formation. The cultivation chamber containing the biofilm was loaded onto a sample stage, which motorized the chip location at a spatial resolution of 2 μm in the horizontal phase and a 3 μm in vertical phase. The confocal micro-Raman microscope was integrated with the microfluidic platform. Laser introduction and Raman signal collection were conducted through the same 50× objective. The Raman scattering signal was processed through an aperture, passed through a polarizer, and finally collected by a CCD detector (**Figure 3-1**).

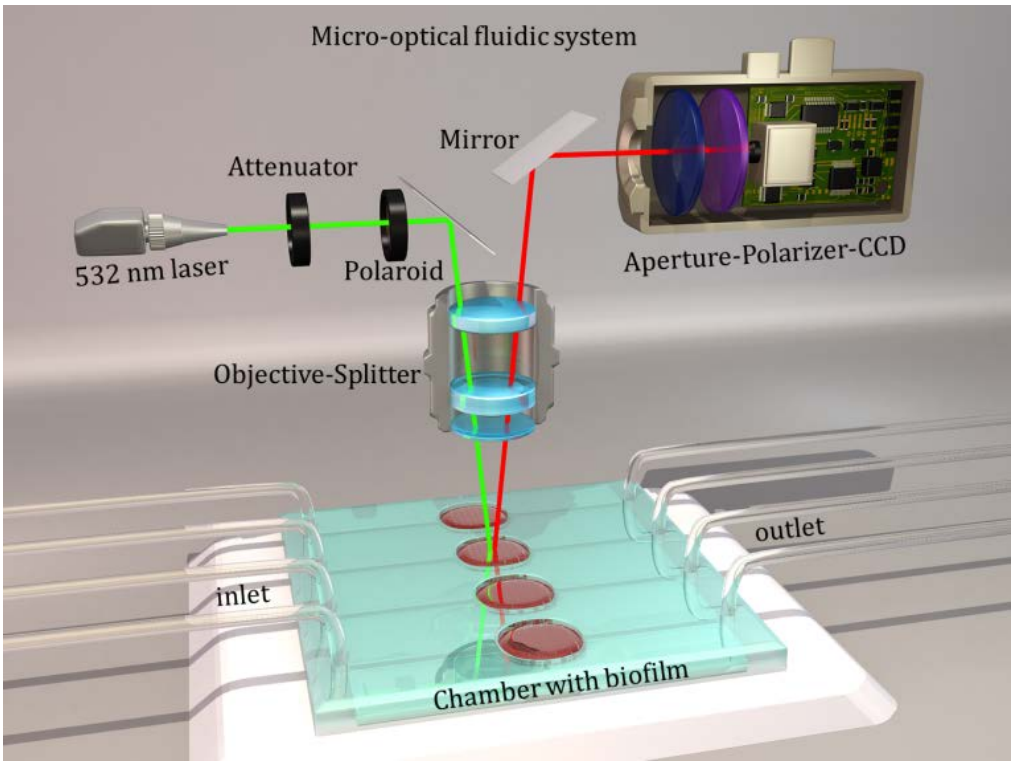

Figure 3-1. Schematic illustration of the Raman spectroscopic-based microfluidic "lab-on-a-chip" platform for cultivation and characterization of bacterial biofilms.

To demonstrate the chemical composition of the biofilm, we need to clarify the Raman signals from chip substrate (*i.e.*, glass slide and polydimethylsiloxane (PDMS) layer) first. The Raman spectra of the substrate were collected by focusing the Raman laser in the microfluidic chip with broth. The substrate of microfluidic chip generated distinct Raman peaks at 485, 610, 703, 785, 860, 1125, and 1402 cm^{-1}. After initial attachment of bacterial cells to the substrate, biofilm started to develop and cover the substrate. The intensity of Raman peaks due to the substrate decreased significantly by 24 h (**Figure 3-2**). Although biofilm continuously accumulated, the peak intensities from the substrate remained relatively constant, indicating no overlap between biofilm peaks and

substrate peaks. Therefore, peaks that were different from substrate peaks and changed during biofilm development could be regarded as deriving from *P. aeruginosa* biofilm.

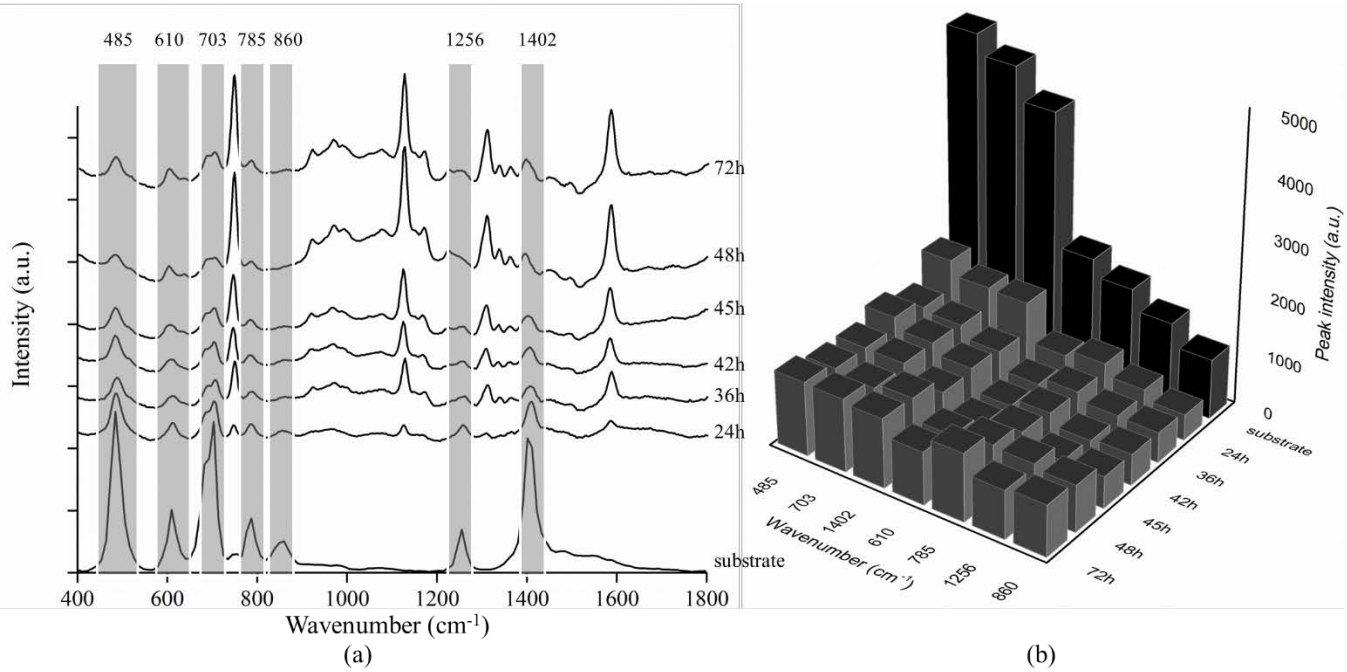

Figure 3-2. Raman spectroscopy determines microfluidic chip substrate as background for biofilm characterization. (a) Prominent peaks in Raman spectra of the substrate and *P. aeruginosa* biofilm grown in the microchamber; (b) Variations in Raman intensities of the corresponding peaks (485, 610, 703, 785, 860, 1256, and 1402 cm^{-1}). Shadow regions highlight variations in peak intensities of microfluidic chip substrate (as background) during *P. aeruginosa* biofilm development.

The characteristic Raman peaks of biofilm were averaged and evident in the wavenumber range of 400 to 1800 cm^{-1} in **Figure 3-3**. Peaks at 746, 1123, 1307 and 1580 cm^{-1} were prominent and could be observed after 24 h cultivation (**Figure 3-3A**). Peaks at 746 and 1580 cm^{-1} were assigned as specific ring structures in nucleic acids (*i.e.*, adenine,

thymine, guanine), while peaks at 1123 and 1580 cm^{-1} referred to C-C stretching and CH_3/CH_2 twisting or bending respectively which widely present in carbohydrates, proteins, and lipids (**Table 3-1**). We defined the first 24 h as the "early stage" of biofilm development. The results demonstrated that nucleic acids, proteins, lipids, and carbohydrates were synthesized when biofilm started to form. Compared to peaks corresponding to other molecules (*i.e.,* proteins, lipids, and carbohydrates), the intensity of peaks corresponding to nucleic acids was higher, indicating that nucleic acids were preferentially synthesized at this stage. Consistent with previous reports, extracellular DNA has been proposed to serve as an important structural component binding surrounding substances and supporting the growth of *P. aeruginosa* biofilms when biofilms initially established (Whitchurch et al., 2002). Our findings validated that extracellular DNA served as the fundamental material in an early developed biofilm in the fluidic environment. After 36 h cultivation, the intensity of the major early peaks (*i.e.*, at 746, 1123, 1307 and 1580 cm^{-1}) increased significantly ($P < 0.05$) and then remained relatively constant to 45 h. The significant change occurred at 36 h could be regarded as a stage switch of biofilm development. Accordingly, we defined 36 h to 45 h as the "mid stage" of biofilm development. The major compositions of biofilm at "mid stage" were almost the same as that of "early stage," but with a higher amount. It indicated that the biofilm had been preliminarily established and synthesis of basic components was temporarily ceased. The intensity of the major early peaks (*i.e.* at 746, 1123, 1307 and 1580 cm^{-1}) increased significantly ($P < 0.05$) up to a maximum at 48 h and then remained relatively constant (**Figure 3-3B**), indicating that 48 h was another critical time point for the stage switch of biofilm development, and the synthesis of basic components in *P.*

aeruginosa biofilm was paused after 48 h. This result indicated that accumulation of basic components into biofilm followed a periodic pattern rather than a continuous pattern.

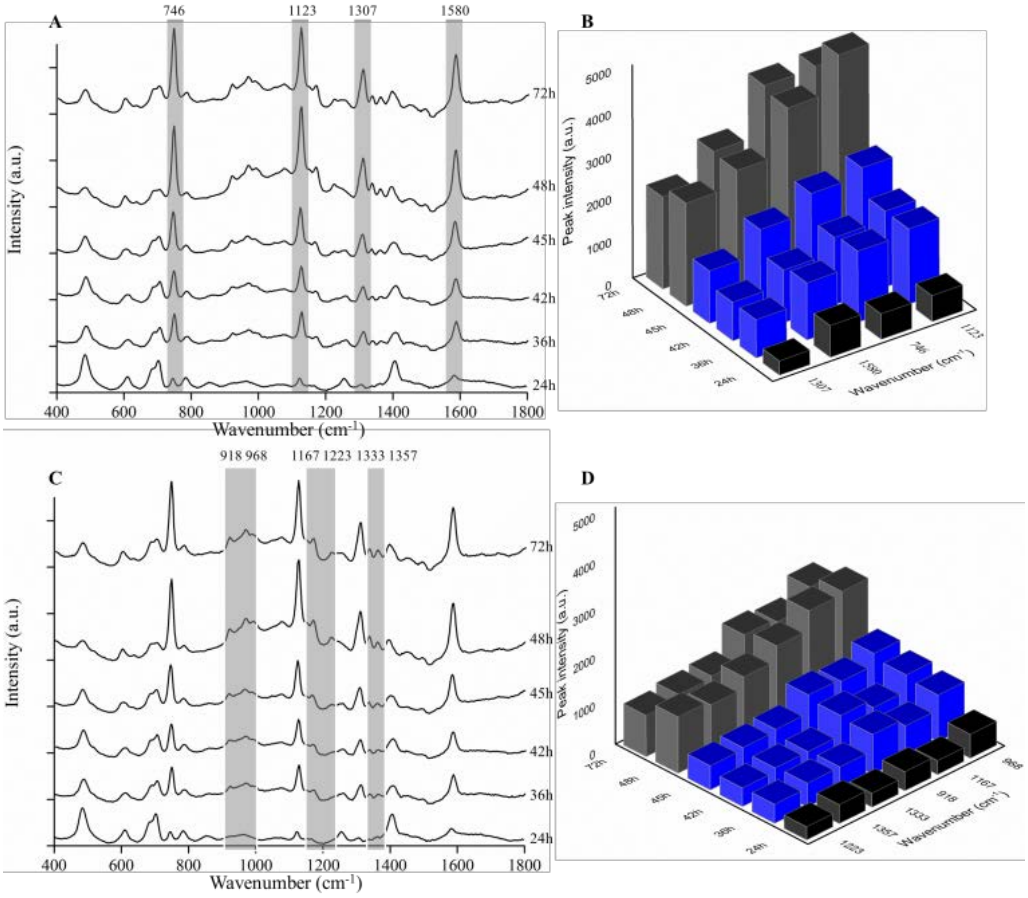

Figure 3-3. Raman spectroscopy monitoring of the development of *P. aeruginosa* biofilm in the microfluidic chamber. (A) Prominent peaks appearing within the first 24 h (early stage) are shaded; (B) Variations in intensities of the corresponding Raman peaks (746, 1123, 1307, and 1580 cm^{-1}) over time. (C) Prominent peaks appearing after 48 h (late stage) are shaded; (D) Variations in intensities of the corresponding Raman peaks (918, 968, 1167, 1223, 1333, and 1357 cm^{-1}) over time.

Table 3-1. Raman band assignments of *P. aeruginosa* biofilm grown in a microfluidic "lab-on-a-chip" platform (De Gelder et al., 2007; Ivleva et al., 2009; Lu et al., 2012b; Tang et al., 2013; Masyuko et al., 2014).

Peaks (cm^{-1})	Assignment			
	Nucleic acids	Proteins	Lipids	Carbohydrates
746	T ring *str*			
918		Proline; hydroxyproline		Glycogen
968			Lipids	
1123		C-C *str*	C-N, C-C *str*	C-C str, C-O-C glycosidic link; ring breath, *sym*
1167		C-C *str*		
1223		Amide III		
1307		CH_3/CH_2 *bend*	CH_3/CH_2 *bend*	
1333		δ(CH)		δ(CH)
1357	G ring *str*			
1580	G, A ring *str*			

Abbreviations. *Bend*: bending, *breath*: breathing, *def*: *deformation*, *scis*: scissoring, *str*: stretching, *asym*: asymmetric, *sym*: symmetric.

P. aeruginosa biofilm also showed Raman peaks at 918, 968, 1167, 1223, 1333, and 1357 cm^{-1} (**Figure 3-3**). Peaks at 918, 1167, 1223, and 1333 cm^{-1} were assigned to carbohydrates and proteins, while peaks at 968 and 1357 cm^{-1} were derived from lipids and nucleic acids (**Table 3-1**). The intensity of these peaks was too weak to be observed until 45 h, but increased substantially from 45 h to 48 h, and then kept relatively constant until 72 h (**Figure 3-3C**). After 48 h of cultivation, biofilm was considered to enter "late stage" development using these peaks as indicators. Compared to the peaks shown in the spectra of biofilm at 24 h cultivation, peaks at 918, 968, 1167, 1223, 1333, and 1357 cm^{-1} in the spectra of biofilm at 48 h cultivation demonstrated 3.1, 3.2, 6.0, 3.7, 3.5 and 1.7 fold increases in intensity, respectively (**Figure 3-3D**). The intensity of peaks assigned to proteins and carbohydrates (918, 1167, 1223, and 1333 cm^{-1}) increased more than those assigned to nucleic acids (968 and 1357 cm^{-1}), indicating proteins and carbohydrates accounted for the largest proportion of synthesized substances at this stage. Taken together, we defined biofilm developmental stages according to the appearance of prominent peaks and the significant increases in peak intensity. The results indicated that *P. aeruginosa* biofilm produced different substances at two different stages (*i.e.,* early stage and late stage).

To confirm the variations of *P. aeruginosa* biofilms developed at different time points shown in the Raman spectra, principal component analysis (PCA) was utilized. PCA was able to cluster samples on the basis of chemical information and enable further differentiation. **Figure 3-4** demonstrates analytical groups for different biofilm samples according to the score plot of principal component 1 (PC1) and component 2 (PC2) from the PCA model. The loading profiles of PC1 and PC2 accounted for 92.85% and 4.78%

of the total variation in spectra, respectively (**Figure 3-5**). The separating lines, derived from a supportive vector machine classification algorithm, clearly separated clusters due to biofilms at 24 h, biofilms at 36 h to 45 h, and biofilms at 48 h to 72 h into three groups. The *Mahalanobis* distance between these groups ranged from 5.57 to 12.83. Clusters with interclass distance values higher than 3 are considered to be significantly different ($P < 0.05$) from each other (Lu et al., 2013a). This result further confirmed the obvious stage switches occurred at 24-36 h (early stage) and 45-48 h (late stage) during biofilm development within the first 72 h (**Figure 3-3**). We accordingly defined the biofilm grown between 24 h and 48 h as the "mid stage."

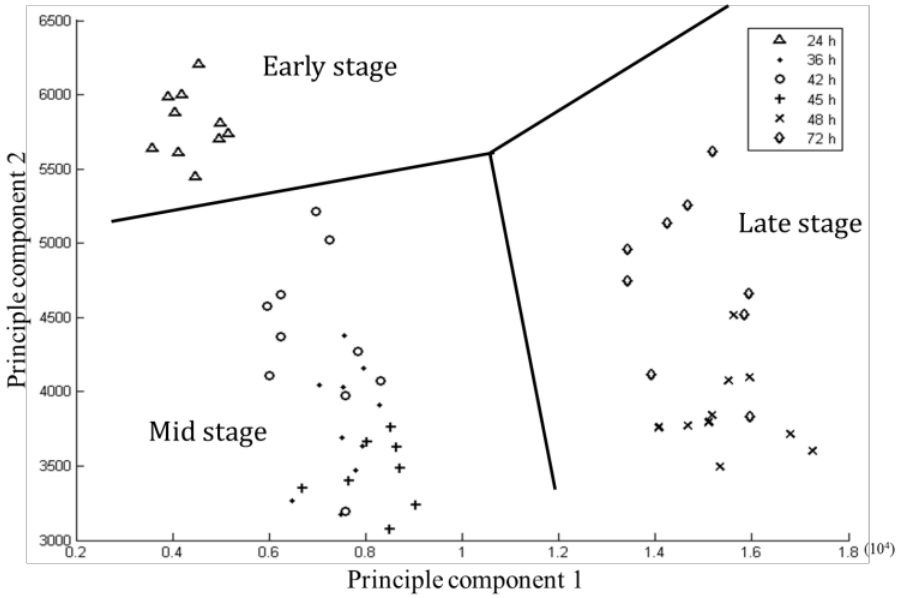

Figure 3-4. The representative two-dimensional principal component analysis for the segregation of *P. aeruginosa* biofilms at different development stages. The boundary lines could be used to cluster different groups.

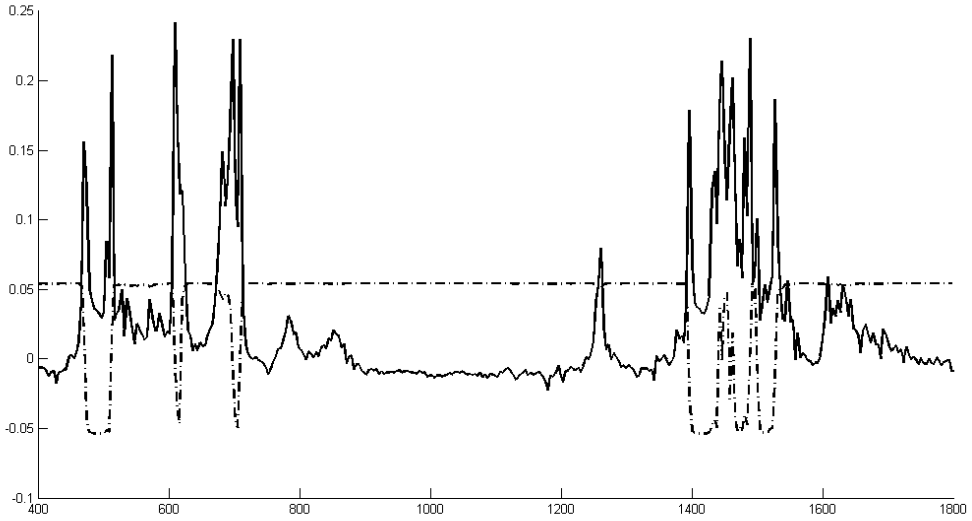

Figure 3-5. The loading profile of principal component analysis. Dash line is the plot of PC1 and solid line is the plot of PC2. Absolute values of peaks (x-axis) represent the contribution in each component (y-axis).

As a parallel study, CLSM was applied to quantify the extent of formation of *P. aeruginosa* biofilm. CLSM coupled with Cyto-9 dye added at various time points to identify biomass of biofilm, optical sectioning, and reconstruction to give a 3D perspective. The formation level of biofilm increased as a function of cultivation time (**Figure 3-6A**). At 24 h, the biofilm consisted of a thin, nearly confluent layer of bacteria without complex structures. At 36 h, the confluent layer had increased more than double in depth. Between 42 and 45 h, the biofilm remained relatively similar to that seen at 36 h, although it must be pointed out that the necessity to stain biofilms for this method means that different biofilms were imaged at each time point. At 48 h, the biofilm increased in thickness, and denser microcolonies started to form. Biofilms were very mature after 72 h

of growth, which is consistent with the results obtained using a more conventional large volume flow cell apparatus (de la Fuente-Núñez et al., 2014). Based on CLSM images, the mean biofilm thickness quantifiably reflect the development of biofilm (**Figure 3-6B**). The total height of cultivation chamber in the microfluidic chip was 50 μm. At 24 h, mean biofilm thickness was 5.24 μm. Up to 36 h, it had a 2.4-fold increase to 12.71 μm and remained constant until 45 h. The mean thickness of biofilm reached a maximum of 24.75 μm at 48 h cultivation, which was 1.95-fold greater than that of biofilm at 36 h.

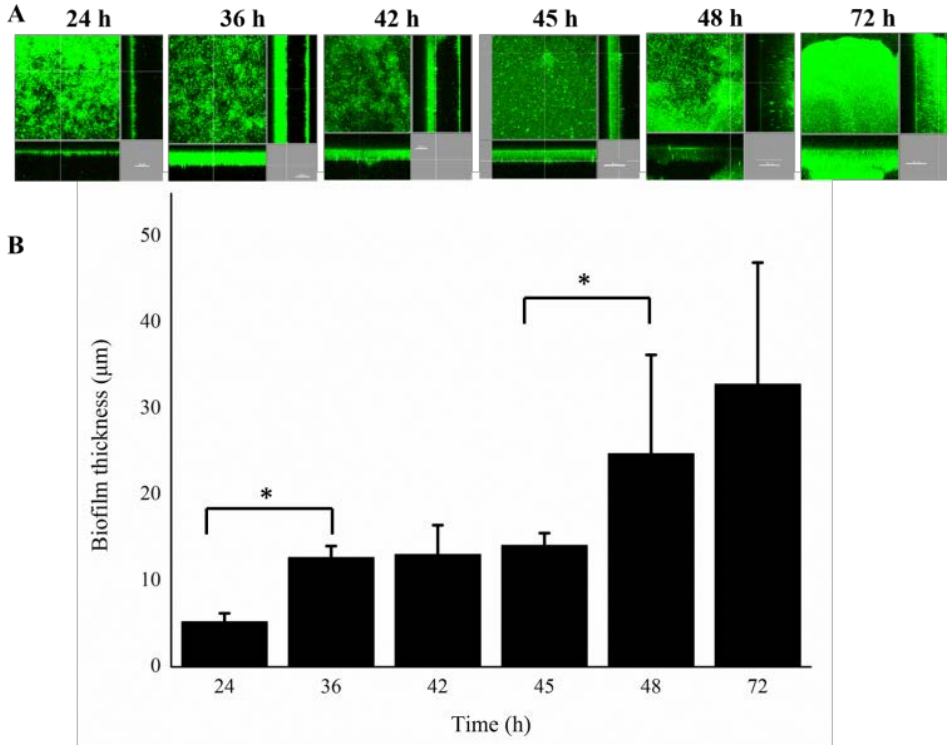

Figure 3-6. Representative confocal laser scanning microscopic images of *P. aeruginosa* biofilms grown in a microfluidic chamber. (A) Each panel shows reconstructions from the top in the large panel and sides in the right and bottom panels (xy, yz, and xz dimensions). Biofilm thickness (μm) increased over time. (B) All the values were measured by confocal laser scanning microscopy. Statistical significance was determined using Student's *t*-test (* denotes $P < 0.05$).

Both the Raman and CLSM results demonstrated that the formation level of *P. aeruginosa* biofilm increased significantly ($P < 0.05$) after 24 h (endpoint of the early stage) and 48 h (starting point of the late stage). Therefore, the correlation between the Raman and CLSM results was examined. Partial least squares regression (PLSR) model was constructed (**Figure 3-7**). When fitted the calculated biofilm thickness (from Raman spectra) to the measured biofilm thickness (from CLSM) in the PLSR model, these two sets of data showed a close correlation, with a regression coefficient (R-square) of 0.9783. Thus, the PLSR result confirmed that chemical variations (Raman) and thickness variations (CLSM) of *P. aeruginosa* biofilms cultivated in the microfluidic chip occurred concurrently.

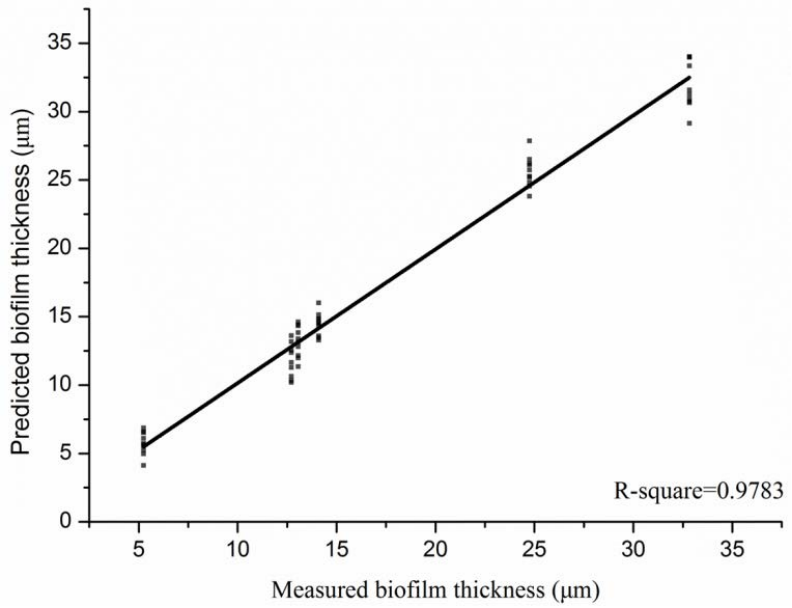

Figure 3-7. Correlation of biofilm thickness measured by confocal laser scanning microscopy and calculated by Raman spectroscopy coupled with partial least-squares regression.

According to previous reports, biofilm development had four major stages, including attachment, accumulation, maturation, and dispersion (Monroe, 2007). Our current study depicted two important stage switches from attachment to early accumulation (early stage to mid stage) and then to maturation (mid stage to late stage) based on chemical and thickness assessments. However, no evidence was obtained to demonstrate any stage switch from maturation to dispersion. This was most likely due to the fact that dispersion usually occurred at the end of a long period of cultivation and was induced by intensive stresses (*e.g.,* starvation and accumulation of toxic wastes) or regulated by signaling molecules (Bjarnsholt et al., 2010; McDougald et al., 2012). In the current study, biofilm was developed in a fluidic environment in which nutrients were supplied continuously. In addition, wastes were continuously expelled to reduce the accumulation of toxic substances and signaling molecules. Hence, it is logical to expect a longer maturation time in this hydrodynamic condition than that in a static condition. Cultivation for 72 h may not be sufficient time to monitor any biofilm switch to the dispersion stage. Another explanation was that accumulation and dispersion within a biofilm might occur simultaneously when the biofilm was fully mature (Klausen et al., 2006). Hence, the biomass and thickness were in a dynamic balance for a long period, and the maturation and dispersion stages could not be differentiated. Long-Term monitoring might be necessary to enable completion of the biofilm dispersion stage. Identification of a specific molecule synthesized at the dispersion stage would provide further evidence for identifying this important stage.

3.5 Conclusions

This study presented an attempt to develop a non-destructive and label-free *in-situ* platform to characterize bacterial biofilms in a precisely controlled hydrodynamic environment. The Raman spectroscopy-based microfluidic "lab-on-a-chip" platform demonstrated the ability to characterize and distinguish *P. aeruginosa* biofilms in different developmental stages (*i.e.,* early, mid, and late stages). In addition, Raman results were well correlated with CLSM analyses, demonstrating its feasibility for quantifying biofilm thickness and determining chemical composition simultaneously. Future work was required to apply this platform to screen antimicrobials for the inactivation of biofilms in a high-throughput manner.

Chapter 4: Environmental stress-induced bacterial lysis and extracellular DNA release contribute to *Campylobacter jejuni* biofilm formation

4.1 Summary

Campylobacter jejuni is a microaerophilic bacterium and supposed to persist in a biofilm to antagonize the environmental stress. This study investigated the influence of environment on *C. jejuni* biofilm formation and the corresponding mechanisms. We report an extracellular DNA (eDNA)-mediated mechanism of biofilm formation in response to aerobic and starvation stresses. The eDNA was determined to be a major constitutions of *C. jejuni* biofilm and closely associated with bacterial lysis. The deletion mutation on the stress response genes *spoT* and *recA* enhanced the aerobic influence by stimulating lysis and increasing eDNA release. Flagella were also involved in biofilm formation but mainly contributed to attachment rather than induction of lysis. The addition of genomic DNA from either *Campylobacter* or *Salmonella* resulted in a concentration-dependent stimulation effect on biofilm formation but not due to forming a pre-coating DNA layer. Enzymatic degradation of DNA by DNase I disrupted biofilm structure and dispersed the encased bacteria. In a dual-species biofilm, eDNA separated *Campylobacter* and *Salmonella* at distinct spatial locations that protect *Campylobacter* away from the oxygen stress. Our findings demonstrated an essential role and multi-functions of eDNA in biofilm formation of *C. jejuni*, including facilitating initial attachment, establishing and maintaining biofilm structure and allocating bacteria cells.

4.2 Introduction

Biofilms are structured bacterial communities encased in a self-produced extracellular polymeric matrix. It is mainly composed of proteins, polysaccharides, lipids and nucleic acids. As one of the well-recognized bacterial survival modes, biofilm owns various physiological capabilities in response to environmental stresses and exhibits inherent tolerance to the host defense system (Costerton et al., 1999). Bacterial cells encased in a biofilm demonstrate significantly elevated tolerance to most of the conventional disinfectants and antimicrobial agents (Fux et al., 2005). Such survival behavior is of potential risk because over 60% of the chronic bacterial infections are associated with biofilm formation (Costerton et al., 1999).

Campylobacter jejuni is recognized as one of the leading causes of bacterial foodborne illness worldwide. Raw meat, untreated water, unpasteurized milk and animals (*e.g.*, birds and pet) are the major reservoirs of *C. jejuni* (Acheson and Allos, 2001). The paradox associated with this fastidious bacterium is that *C. jejuni* is vulnerable to environmental stress, but the incidence of *Campylobacter* infections is high and progressively increases. For example, the reported cases of *Campylobacter* infection in the United States increased by 9% from 2006 to 2015 (CDC, 2016). It is suggested that biofilm may contribute to the survival and distribution of *C. jejuni* in the natural environment (Buswell et al., 1998).

C. jejuni is capable of forming a mono-species biofilm on different substrates (Reeser et al., 2007; Li et al., 2017) as well as residing in a well-developed multispecies biofilm (Hanning et al., 2008). *C. jejuni* cells in the biofilm could survive aerobic stress, and their viability could be maintained twice as long as that in a planktonic state (Feng et al., 2016). In addition, the biofilm is able to facilitate the horizontal transfer of antibiotic resistance genes into *Campylobacter*, such as the ones resistant to kanamycin and chloramphenicol (Bae et al., 2014). It is, therefore,

reasonable to speculate that biofilm is the protection vehicle where *C. jejuni* resides for the survival under the natural environment. The biofilm formation may also explain the high prevalence of *Campylobacter*-associated foodborne diseases worldwide. Recent studies suggest that environmental stresses, such as high oxygen level and relatively low temperature, can stimulate *C. jejuni* biofilm formation to a relatively high level (Reeser et al., 2007; Reuter et al., 2010). The molecular investigation has identified several critical genetic factors that can affect *C. jejuni* biofilm formation, such as *Campylobacter* planktonic growth regulator *cprRS*, stringent response regulator *spoT* and global regulator *csrA* (Gaynor et al., 2005; Reeser et al., 2007; Fields and Thompson, 2008). However, there is still a gap to correlate these genetic factors with the formation of *C. jejuni* biofilm in response to the environmental stresses.

DNA presents in abundance in the environment as a consequence of lysed dead organisms or via active secretion from the living organisms (Nielsen et al., 2007). Bacteria can utilize these free DNA as an important supply of nutrients or integrate the free DNA into the genome for acquiring resistance capacity (Lorenz and Wackernagel, 1994; Thomas and Nielsen, 2005). According to a previous study, *Pseudomonas aeruginosa* progressively released DNA into the environment during biofilm formation (Das and Manefield, 2012). Our recent study identified that the addition of meat juice with a high content of DNA (*e.g.*, chicken juice or pork juice) not only supported the growth of *C. jejuni* cells but also boosted the level of biofilm formation (Li et al., 2017). Therefore, we speculate that eDNA might mediate the biofilm formation in response to different environments. Therefore, the current study aims to characterize the role of eDNA in *C. jejuni* biofilm formation in response to two common environmental stresses, namely aerobic condition, and starvation condition.

4.3 Materials and methods

4.3.1 Bacterial strains and cultivation conditions.

The bacterial strains and plasmid used in the current study are summarized in **Table 4-1**. Routine cultivation of *C. jejuni* was conducted either on Mueller-Hinton (MH) agar supplemented with 5% defibrinated sheep blood (MHB agar) or in MH broth with constant shaking at 37°C under a microaerobic condition (85% N_2, 10% CO_2, 5% O_2). When necessary, kanamycin, chloramphenicol or tetracycline was supplemented either into MHB agar or MH broth at a final concentration of 50 μg/ml, 8 μg/ml or 10 μg/ml, respectively. *Salmonella* and *Escherichia coli* strains were cultivated in Luria-Bertani (LB) broth (BD Difco) at 37°C under aerobic condition. Where indicated, kanamycin or ampicillin was supplemented at a final concentration of 50 μg/ml and 100 μg/ml, respectively.

Table 4-1. Bacterial strains and plasmid used in the current study.

Strain or plasmid	Description	Reference
Strains		
C. jejuni F38011	human clinical isolate	(Feng et al., 2016)
C. jejuni Human 10	human clinical isolate	(Li et al., 2017)
C. jejuni 81116	human clinical isolate	(Neal-McKinney et al., 2010)
C. jejuni ATCC 33560	product, quality control strain	ATCC company
C. jejuni 87-95	human clinical isolate	Laboratory collection obtained from Dr. Michael Konkel (Washington State University)
C. jejuni NCTC 11168	human clinical isolate	(Parkhill et al., 2000)

Strain or plasmid	Description	Reference
C. jejuni 1658	environmental isolate	Laboratory collection obtained from Dr. Gölz, Greta (Free University Berlin)
C. jejuni F38011Δ*spoT*	*spoT* gene deletion mutant of *C. jejuni* F38011 strain, Kan^R	This study
C. jejuni F38011Δ*recA*	*recA* gene deletion mutant of *C. jejuni* F38011 strain, Cm^R	This study
C. jejuni F38011Δ*flaAB*	*flaA* and *flaB* genes deletion mutant of *C. jejuni* F38011 strain, mobility deficiency mutant, Tet^R	(Neal-McKinney et al., 2010)
C. jejuni F38011::*spoT*	*spoT* gene complementary strain of *C. jejuni* F38011, Kan^R&Cm^R	This study
C. jejuni F38011::*recA*	*recA* gene complementary strain of *C. jejuni* F38011, Cm^R&Kan^R	This study
C. jejuni F38011::*flaAB*	*flaA* and *flaB* genes complementary strain of *C. jejuni* F38011, Tet^R&Cm^R	(Neal-McKinney et al., 2010)
C. jejuni GFP	green fluorescent protein expression strain of *C. jejuni* F38011, Kan^R	(Mixter et al., 2003)

S. Typhimurium SL1344	Human clinical isolate	(Knodler et al., 2010)

Strain or plasmid	Description	Reference
S. Typhimurium SL1344 - RFP	Red fluorescent protein expression of *S.* Typhimurium SL 1344 strain, Str^R	(Knodler et al., 2010)
E. coli DH5α	product, generation of recombinant plasmids	Invitrogen
Plasmid		
pUC19	product, suicide vector, Amp^R	Invitrogen
pUC18K2	cloning vector, Kan^R	(Gaynor et al., 2005)
pRY111	cloning vector, Cm^R	(Buelow et al., 2011) A gift from Dr. Michael Konkel (Washington State University)
pRY107	cloning vector, Kan^R	A gift from Dr. Michael Konkel (Washington State University)

Cm^R strands for chloramphenicol resistance (8 µg/ml); Amp^R strands for ampicillin resistance (100 µg/ml); Kan^R strands for kanamycin resistance (50 µg/ml); Str^R strands for streptomycin resistance (100 µg/ml). Tet^R strands for tetracycline resistance (10 µg/ml)

4.3.2 Construction of *C. jejuni* F38011 *spoT* and *recA* knockout mutant strains.

C. jejuni F38011 *spoT* deletion mutant was generated via homologous recombination and subsequent insertion of a kanamycin resistance cassette. The gene sequence of *spoT* in *C. jejuni* F38011 was identical to the gene sequence of *spoT* (*Cj1272c*) in *C. jejuni* 11168, which was

confirmed by nucleotide BLAST. A 430-bp upstream cassette of the *spoT* gene was PCR-amplified using the primer pair of *spoT*-FF/*spoT*-FR. Similarly, a 476-bp downstream cassette of the *spoT* gene was PCR-amplified using the primer pair of *spoT*-RF/*spoT*-RR. The kanamycin resistance gene (Kan^R) was amplified using the primer pair *kan*-F/*kan*-R from the plasmid pUC18K2 (a gift from Dr. Erin Gaynor at the University of British Columbia). The vector pUC19 was digested with EcoRI and XbaI. All the four fragments above were purified using the Gel/PCR purification kit (Froggabio), followed by multiple fragment ligation using NEBuilder® HiFi DNA Assembly Cloning Kit (New England Biolabs® INC.). The pUC19-*spoT*::Kan^R disruption construction was naturally transformed into *C. jejuni* F38011, as *C. jejuni* is a naturally competent bacterium (Davis et al., 2008). Transformants were selected on MHB agar plates supplemented with kanamycin (50 µg/ml). The deletion of *spoT* gene and insertion of Kan^R was identified by PCR.

C. jejuni F38011 *recA* deletion mutant was generated via homologous recombination and subsequent insertion of a chloramphenicol resistance cassette. The gene sequence of *recA* in *C. jejuni* F38011 was identical to the sequence of *recA* (*Cj1673c*) in *C. jejuni* 11168, which was confirmed by nucleotide BLAST. A 428-bp upstream cassette of *recA* gene was PCR-amplified using the primer pair of *recA*-FF/*recA*-FR. Similarly, a 626-bp downstream cassette of *recA* gene was PCR-amplified using the primer pairs of *recA*-RF/*recA*-RR. The chloramphenicol resistance gene (Cm^R) was amplified using the primer pair of *cm*-F/*cm*-R from the plasmid pRY111 (a gift from Dr. Brett Finlay at University of British Columbia). The vector pUC19 was digested with EcoRI and XbaI. All the four fragments above were purified using the Gel/PCR purification kit (Froggabio), followed by the multiple fragment ligation using NEBuilder® HiFi DNA Assembly Cloning Kit (New England Biolabs® Inc.). The pUC19-*recA*::Cm^R disruption construction was

naturally transformed into *C. jejuni* F38011. Transformants were selected on MHB agar plates supplemented with chloramphenicol (8 μg/ml). The deletion of *recA* gene and insertion of Cm^R was identified by PCR. The primer used for mutant construction was listed in **Table 4-2**.

Table 4-2. Primers used in the current study.

Primer	Sequence (5'-3')
spoT-FF	CGGAATTCAAGTGGAGAGCCTTATGCGG
spoT-FR	CTTGGTACCGTCTATGGGCTATTGGGGCA
spoT-RF	GCGGATCCAGCCAGACGTATTAGACAAGTA GC
spoT-RR	GATCTAGATCTCAAAATAATCTACCGCCGA
kan-F	TGTATATGCCCCAATAGCCGGTACCCGGGT GACTAACTAGGAGGAATAA
kan-R	GCTACTTGTCTAATACGTCTGACGGATCCCC GGGTCATTATTCCCTCCAGGTACTA
recA-FF	TTGTAAAACGACGGCCAGTGATTCAACGCC TTTTCCGCCAAATC
recA-FR	AGCAACGCGATCTAGCTATCGCGGCCTAGG GTACC GGAGAGGGTTTAAGCCGTGA
recA-RF	ATATTAGTTCGATTCAACAT GGATCCACATCAAGCGCATGTTCTGC
recA-RR	CAAGCTTGCATGCCTGCAGGTCGACTCTAG

	ATGCTGTGCGTAAAAGTGCAT
Primer	Sequence (5’-3’)
cm-F	TCACGGCTTAAACCCTCTCCGGTACCTTACG
	CCCCGCCCTGCCATCATCGCAGTA
cm-R	GCAGAACATGCGCTTGATGTGGATCCATCG
	AGATTTTCAGGAGCTAAGGAAGCTAA
flaA-F	GCTTATGCTATAAAAGCAGGTTCA
flaA-R	GTCAACCTTACCTATAGTCACACCA
flaB-F	AACAGGAGTTCGTGCAACTT
flaB-R	CATCCGATGTTTTTCCAGACTTTA
rpoA-F	CGAGCTTGCTTTGATGAGTG
rpoA-R	AGTTCCCACAGGAAAACCTA
spoT-CF	CGGTATCGATAAGCTTGATATCGAATTCGC
	GCTGTAGGATCAAACCCT
spoT-CR	GCTCCACCGCGGTGGCGGCCGCTCTAGAAG
	AGCTGTGGAAATTGATGCAG
recA-CF	CGGTATCGATAGGCTTGATATCGAATTCAC
	CACTTGGAACTATGGCCG
recA-CR	GCTCCACCGCGGTGGCGGCCGCTCTAGATT
	GCTCCACTCAAAGCGACT

4.3.3 Construction of *C. jejuni* F38011 *spoT* and *recA* complementary strains.

The complementary plasmid for *spoT* gene was derived from the pRY111 vector (a gift from Dr. Konkel at Washington State University). The insertion fragment containing upstream (500 bp) and downstream (150 bp) regions of *spoT* gene were PCR-amplified using primer pairs of *spoT*-CF/*spoT*-CR. The amplicon containing *spoT* gene was ligated with EcoRI/XbaI-digested pRY111 using NEBuilder® HiFi DNA Assembly Cloning Kit (New England Biolabs® Inc.). The complementary plasmid pRY111-*spoT* was then transformed into the *C. jejuni* F38011 Δ*spoT* mutant. Transformants were selected on MH agar supplemented with chloramphenicol (8 μg/ml). The presence of the vectors in the complementary strain was confirmed by PCR.

The complementary plasmid for *recA* gene was derived from the pRY107 vector (a gift from Dr. Konkel at Washington State University). The insertion fragment containing upstream (500 bp) and downstream (100 bp) regions of *recA* gene were PCR-amplified using primer pairs of *recA*-CF/*recA*-CR. The amplicon containing *recA* gene was ligated with EcoRI/XbaI-digested pRY107 using NEBuilder® HiFi DNA Assembly Cloning Kit (New England Biolabs® Inc.). The complementary plasmid pRY107-*recA* was transformed into the *C. jejuni* F38011 Δ*recA* mutant. Transformants were selected on MH agar supplemented with Kanamycin (20 μg/ml). The presence of the vectors in the complementary strain was confirmed by PCR.

4.3.4 Biofilm formation either in 96-well plate or on nitrocellulose membrane under different environment.

An overnight culture of *C. jejuni* was collected, washed and diluted to 0.003 of OD_{600} (~10^7 CFU/ml) in MH broth and then cultivated in sterile polystyrene 96-well plate in an optimal

growth environment for biofilm formation. A total of 200 µl of the diluted bacterial culture was added to each well of a sterile polystyrene 96-well plate. The 96-well plate was incubated in a microaerobic environment (85% N_2, 10% CO_2, 5% O_2) at 37°C for up to 72 h. To cultivate biofilm in 96-well plate at the starvation condition, *C. jejuni* overnight culture was diluted to 0.003 of OD_{600} in phosphate buffered saline (PBS, pH ~7.0 to 7.2). A total of 200 µl of the diluted bacterial culture was added to each well of a 96-well plate and incubated in a microaerobic condition at 37°C for up to 72 h. *C. jejuni* overnight culture was washed and diluted to 0.003 of OD_{600} in MH broth. A total of 200 µl of the diluted bacterial culture was added to each well of a 96-well plate for biofilm cultivation. The plate was incubated under the aerobic environment (79% N_2, 21% O_2) at 37°C for up to 72 h.

An overnight culture of *C. jejuni* was washed and diluted to 0.003 of OD_{600} in MH broth. A total of 100 µl of the diluted bacterial culture was deposited onto the membrane at a surface area of ~3×3 cm^2 nitrocellulose membrane (0.45-mm pore size, 47-mm diameter; Sartorius Stedim-type filters) for biofilm formation. The membrane was incubated on MHB agar under a microaerobic environment at 37°C and aseptically transferred to a fresh MHB agar plate every 24 h for up to 72 h.

4.3.5 Crystal violet biofilm assay.

Crystal violet staining assay was applied to quantify the formation level of biofilms developed in 96-well plate (Feng et al., 2015). After 72-h cultivation, each biofilm in the 96-well plate was washed with sterile deionized water and air dried for 15 min. A total of 200 µl of 0.5% (w/v) crystal violet solution was added to each well of the 96-well plate to stain the biofilm for 15 min. Unbound crystal violet was then washed off using sterile deionized water. Bound crystal violet

was dissolved in 200 µl of 95% ethanol (v/v) for 10 min. Signals from the released crystal violet were measured using a microplate reader at 595 nm (SpectraMax M2, Molecular Devices). MH broth without bacterial inoculation was stained using the same method as the control. The control signal was subsequently subtracted for background correction.

4.3.6 Fabrication of microfluidic “lab-on-a-chip” platform for biofilm formation.

Polydimethylsiloxane (PDMS)-based microfluidic device was fabricated using the soft lithographic technique (Qin et al., 2010). The schematic image of the fabrication procedure and microfluidic pattern design is described in **Figure 4-1**. The in/outlet-connected cultivation chamber was in the center of the device. The dimensions of inlet and outlet were 400 µm (width) × 60 µm (height) and the cultivation chamber had a circular shape with a dimension of 300 µm (radius) × 60 µm (height). The pattern was molded with PDMS and bonded to a glass slide via oxygen plasma treatment. A syringe pump was applied to control the hydrodynamic condition (*e.g.*, flow rate) in the microfluidic device.

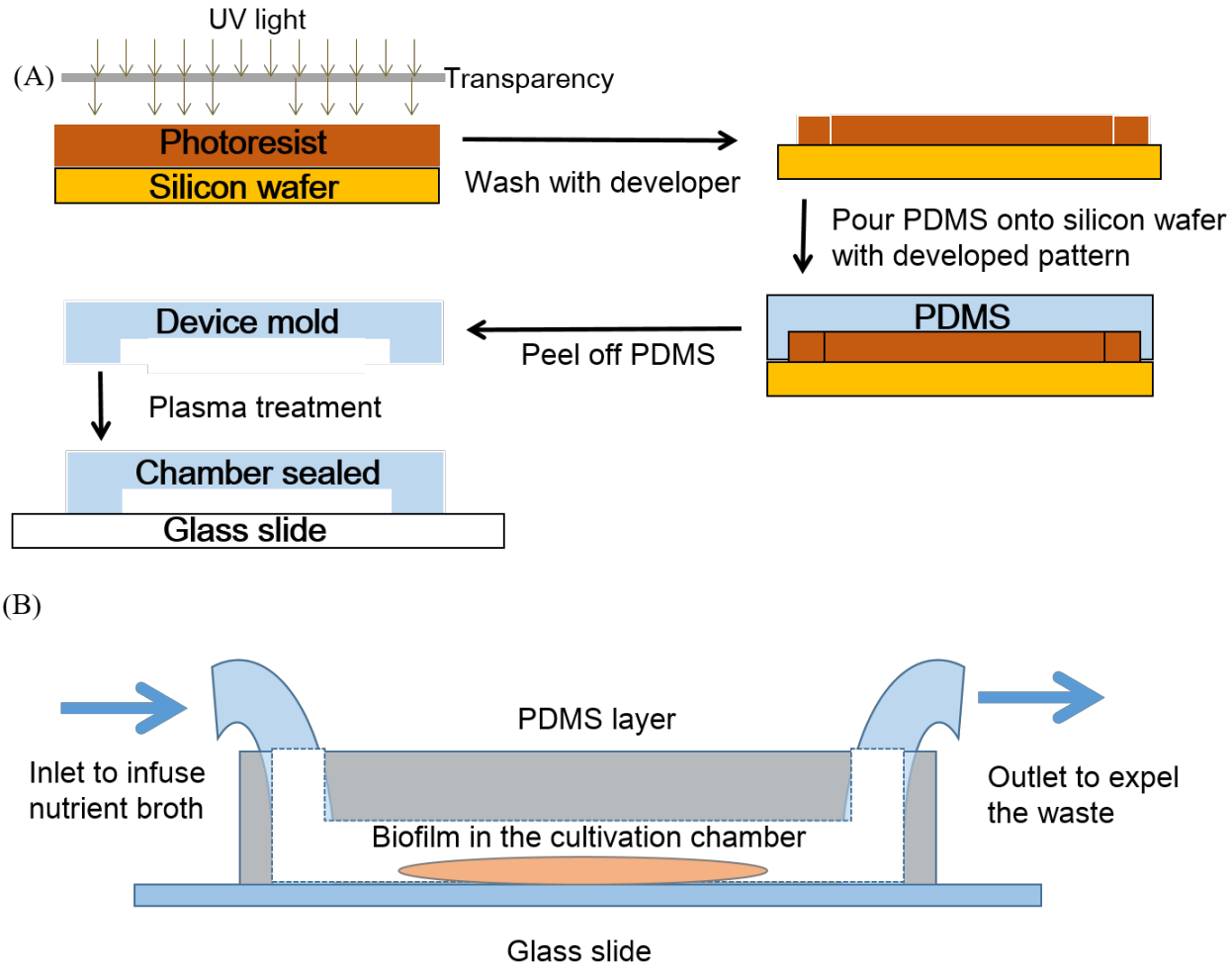

Figure 4-1. Schematic illustration of the fabrication of microfluidic "lab-on-a-chip" platform. (A) The pattern of microfluidic device was printed on a transparency. A total of 1 mL of SU-3050 permanent epoxy negative photoresist was dispensed on a silicon wafer and spun to achieve a thickness of 60 μm with the following program: 500 rpm for 10 sec with the acceleration of 100 rpm/sec and then 3000 rpm for 30 sec with the acceleration of 300 rpm/sec. The photoresist on the silicon wafer was then soft baked on a hot plate for 10 min at 95ºC. The transparency with a pattern was then loaded on the photoresist for UV exposure. The exposure energy was set as 150 mJ/cm^2. After UV exposure, the photoresist was baked again at 65ºC for 1 min and then 95ºC for 5 min. The silicon wafer with photoresist was then washed with the SU-8 developer for 10 min

to remove the unexposed photoresist. The PDMS was then molded on the basis of the pattern on the silicon wafer. The inlet and outlet were drilled on PDMS with a puncher before bond onto a glass slide using the plasma treatment. (B) The microfluidic platform for biofilm cultivation consisted of one inlet for the infusion of nutrient broth, one outlet to expel the waste and one cultivation chamber for biofilm cultivation.

An overnight culture of *C. jejuni* F38011 and *Salmonella enterica* serovar Typhimurium SL1344 was individually washed twice using PBS and diluted to 0.03 of OD_{600} (~10^8 CFU/ml) in MH broth. *C. jejuni* F38011 culture was either individually introduced into the microfluidic chip to form a mono-species biofilm or mixed with *S.* Typhimurium SL1344 to form a dual-species biofilm. Bacterial culture in the microfluidic device was maintained for 2 h to allow for initial bacterial attachment. Biofilm cultivation was conducted by continuously flowing MH broth at a rate of 0.0002 µl/min in aerobic condition at room temperature.

4.3.7 Characterization of *C. jejuni* biofilm in microfluidic platform using confocal micro-Raman spectroscopy.

A confocal micro-Raman spectroscopic system (Renishaw, Gloucestershire, UK) with a 532-nm diode green laser was applied to characterize the chemical composition of *C. jejuni* F38011 biofilm in the microfluidic device. Raman laser was introduced into the cultivation chamber through a 50× objective (Leica Biosystems, Wetzlar, Germany) and focused onto the biofilm with the laser illumination power of 0.2 mW. Raman scattering signal was collected and dispersed by a diffraction grating, and then recorded using a 578 pixel by 384 pixels charge-coupled device (CCD) array detector. An integration time of 20 s was applied for spectral

collection over a simultaneous Raman shift range from 400 to 1800 cm^{-1}. Raman spectrometer was equipped with a 1200-line/mm grating and controlled via WiRE software for spectral acquisition and processing (Renishaw, UK).

4.3.8 Quantification of the released eDNA.

The amount of the released eDNA during biofilm formation was quantified using SYBR Green I dye (Invitrogen) according to the manufacturer's protocol. Briefly, 200 µl of bacterial culture was removed from the 96-well plate and pelleted by centrifugation at 12,000 ×*g* for 2 min. The supernatant was collected for further analysis. SYBR Green I dye was diluted 100 times using TE buffer (10 mM Tris HCl, 1 mM EDTA, pH 8) as the working solution. A total of 5 µl of the SYBR Green I working solution was mixed with 95 µl of the collected supernatant in a well of a black 96-well plate (Greiner Bio-One) and the plate was incubated on an orbital shaker for 5 min. The fluorescence signal was recorded using a TECAN (Infinite 200 PRO, Tecan Life Sciences) with the excitation wavelength at 485 nm and emission wavelength at 535 nm. The amount of eDNA was calculated via a standard curve generated using Lambda DNA (Invitrogen, a series of 10 dilutions from 80 µg/ml to 0.156 µg/ml).

4.3.9 Gel electrophoresis of the released DNA.

Gel electrophoresis was performed to demonstrate the length of the released DNA fragment. After 3-day biofilm cultivation, each bacterial culture in 96-well plate was collected and centrifuged at 16,000 ×*g* for 5 min. A total of 10 µl of the supernatant was mixed with 2 µl of DNA loading dye solution (FroggaBio) and then loaded in 1% agarose gel for electrophoresis. A 1-kb ladder (Invitrogen) was used as the reference. The DNA was stained using SYBR™ safe

DNA gel stain (Life Technologies™) according to the manufacturer's protocol, and the DNA band was visualized on ChemiDoc™ XRS gel documentation system (BIO-RAD).

4.3.10 DNase I treatment on *C. jejuni* F38011 biofilm.

In order to determine the role of eDNA in biofilm formation, DNase I treatment was applied either at the initial bacterial attachment stage or on a well-developed biofilm. The treatment was conducted either in 96-well plate or on a nitrocellulose membrane. To treat biofilm at the initial attachment stage, DNase I (Thermo Scientific™ DNase I) was diluted using DNase and protease-free water and added into the bacterial culture at a final concentration of 2 units/ml before biofilm formation. To test the influence of DNase I on the well-developed biofilm in 96-well plate, the supernatant was removed and then 200 µl of DNase I solution (2 units/ml) was added. The treatment was maintained for 15 min at room temperature. The reduction of biofilm was evaluated using the aforementioned crystal violet assay. To test the influence of DNase I on the well-developed biofilm on a nitrocellulose membrane, the biofilm was immersed in DNase I solution (2 units/ml) for 15 min at room temperature and then washed with PBS. The treated biofilm was air-dried and then analyzed using atomic force microscopy.

4.3.11 Atomic force microscopy.

The morphological variation of the biofilm due to DNase I treatment was determined using a Cypher atomic force microscope (Bruker, Innova™ high-resolution system) with TR400PB tip cantilevers (Bruker, nominal spring constant: k = 0.02 N/m). *C. jejuni* F38011 biofilm developed on a nitrocellulose membrane was air-dried for 30 min before loading onto the AFM specimen disc (15 mm diameter, Ted Pella) for characterization. Topographic images were collected in the

contact mode at 8 random locations on the surface of the biofilm with an area of 8 μm × 8 μm. The scan frequency was maintained at 0.5 Hz. The AFM system was driven using NanoDrive software (Bruker, v8.06) and the AFM images were analyzed off-line using NanoScope software (Bruker, v1.5).

4.3.12 Addition of DNA for biofilm formation.

Genomic DNA of *C. jejuni* F38011 or *S.* Typhimurium SL1344 was individually extracted from the overnight bacterial culture using Presto™ Mini gDNA Bacteria Kit (FroggaBio) according to the manufacturer's protocol. Genomic DNA was quantified using a NanoDrop 2000 spectrophotometer (Thermo Scientific). Addition of DNA for biofilm formation was conducted in two manners: 1) to form a pre-coating layer, 200 μl of DNA solution at different concentrations (20, 10, 5, 2.5 and 0 μg/ml) was individually added into each well of the 96-well plate and maintained for 4 h. The unbounded DNA was then washed out using sterile PBS before bacterial inoculation. 2) DNA was mixed with bacterial culture to a certain final concentration (20, 10, 5, 2.5 and 0 μg/ml) and 200 μl of this mixed culture was cultivated in 96-well plate. The plate was then cultivated in a microaerobic environment at 37°C for up to 72 h.

4.3.13 Autolysis assay.

Autolysis assay was adapted from a previous study with modifications (Kreth et al., 2009). Briefly, autolysis buffer was prepared by diluting Triton X-100 with 0.05 M Tris-HCl to achieve a final concentration of 0.02% (v/v). Bacterial cells were harvested in the late exponential phase by centrifugation at 8,000 ×*g* for 5 min at 4°C, washed twice with chilled water, and resuspended in autolysis buffer to 0.3 of OD_{600}. The reduction of absorbance (OD_{600}) was measured using the

microplate reader (SpectraMax M2, Molecular Devices, Sunnyvale, USA) every 3 min for a total of 90 min.

4.3.14 Motility test.

Motility of *C. jejuni* cells was assessed on the soft agar plates as described previously (Kalmokoff et al., 2006). Briefly, 5 µl of the overnight *C. jejuni* culture was spotted onto the Brucella media supplemented with 0.4% agar. The plate was then incubated under a microaerobic condition at 37°C for 2 days. The halo size of *C. jejuni* cells on the soft agar plate was measured. The results were compared to demonstrate the relative motility among different *C. jejuni* strains.

4.3.15 Quantification of cell lysis.

Genomic DNA is an indicator of bacterial lysis. The cell lysis was quantified via real-time quantitative PCR (qPCR) as described in a previous study (Ma and Wood, 2009). Briefly, *C. jejuni* F38011 wild-type strain and *spoT*, *recA* and *flaAB* deletion mutant strains were individually inoculated in the 96-well plate for biofilm formation as described above. After 3-day biofilm cultivation, the supernatant was collected. Biofilm was detached using 0.1% trypsin solution (Sigma), washed twice with PBS, and pelleted by centrifugation at 10,000 ×*g* for 2 min. The genomic DNA either in the supernatant or the biofilm cells were purified using PicoPure® DNA extraction kit (Applied Biosystems). The qPCR was performed on ABI Prism 7000 Fast instrument (Life Technologies) using a primer pair of a housekeeping gene *rpoA* (Ritz et al., 2009). The percentage of lysis was calculated by dividing the genomic DNA in the supernatant to the sum of genomic DNA in the supernatant and the encased cells in the biofilm.

4.3.16 Real-time qPCR analysis of gene expression.

The real-time qPCR was performed to plot the expression profile of *flaA* and *flaB* in response to the aerobic and starvation conditions in *C. jejuni* F38011 wild-type strain as well as *spoT* and *recA* deletion mutant strains. The total RNA was purified from *C. jejuni* F38011 wild-type strain and *spoT* and *recA* deletion mutant strains using RNeasy mini kit (Qiagen) according to the manufacturer's protocol. Complementary DNA (cDNA) was reverse transcript using RNA as the template by using SensiFAST^{TM} cDNA Synthesis Kit (Bioline) according to the manufacturer's protocol. The qPCR analysis was performed in triplicate using SensiFAST SYBR Lo-ROX Kit (FroggaBio) on ABI Prism 7000 Fast instrument (Life Technologies). The *rpoA* gene was used as the internal control. The arbitrary fold change cut-offs were set as more than 2.

4.3.17 Fluorescence microscopy for the analysis of the role of eDNA in biofilm structure.

Fluorescence microscopy was applied to investigate the spatial distribution of eDNA and bacterial cells in a developed dual-species *Campylobacter–Salmonella* biofilm. The eDNA was stained using 4', 6-diamidino-2-phenylindole (DAPI, Invitrogen) according to the manufacturer's protocol. After 3-days cultivation, the DAPI working solution was prepared as 30 nM in PBS and injected into the microfluidic device with a well-developed dual-species *Campylobacter-Salmonella* biofilm at a rate of 0.0002 µl/min. The microfluidic device was incubated at room temperature for 15 min and then rinsed with flowing PBS at a rate of 0.002 µl/min for 10 min. Images were collected using an Axiovert 200 microscope (Carl Zeiss) equipped with an Axiocam camera (Carl Zeiss) at multi-channels: 405 nm (blue color for DAPI signal), 488 nm (green color for GFP signal), and 543 nm (red color for RFP signal). Analysis of three-

dimensional reconstruction and spatial distribution was conducted using ImageJ software (The National Institutes of Health, USA) and ZEN software (Zeiss, blue edition), respectively.

4.3.18 Statistical analysis.

All the experiments were performed at least in three biological replicates. Results were reported as the averages of replicates ± the standard deviation with significance ($P < 0.05$) by one-way analysis of variance (ANOVA).

4.4 Results

4.4.1 Biofilm formation under different environmental conditions

Biofilm formation of a wide range of *C. jejuni* strains under different environmental conditions (*i.e.*, optimal, aerobic and starvation conditions) was comprehensively evaluated. Under the optimal condition, most of *C. jejuni* wild-type strains including 3 clinical isolates (*C. jejuni* human 10, *C. jejuni* 1658 and *C. jejuni* 87-95) and 4 reference strains (*C. jejuni* 81116, *C. jejuni* ATCC 33560, *C. jejuni* NCTC 11168 and *C. jejuni* F38011) were able to form relatively intensive biofilms (**Figure 4-2A**). Among these wild-type strains, *C. jejuni* F38011 formed the highest level of biofilm, approximately 2.5 times higher than the lowest level of biofilm formed by *C. jejuni* human 10. The biofilm formation of most *C. jejuni* wild-type strains (*i.e., C. jejuni* Human 10, 81-116, NCTC11168, 1658, and F38011) was significantly ($P < 0.05$) stimulated by aerobic condition compared to that under optimal condition. The stimulation effect on the biofilm formation ranged from 142% for *C. jejuni* human 10 to 20% for *C. jejuni* NCTC 11168. The stimulation effect on the biofilm formation by *C. jejuni* F38011 was 30%. In contrast, biofilm formation of *C. jejuni* ATCC 33560 and *C. jejuni* 87-95 under the aerobic condition was

at the same level as that under the optimal condition. Starvation condition significantly ($P < 0.05$) inhibited the biofilm formation for almost all *C. jejuni* wild-type strains except *C. jejuni* human 10. The inhibition effect on biofilm formation ranged from 79% for *C. jejuni* NCTC 11168 to 34% for *C. jejuni* 1658. The inhibition effect on the biofilm formation by *C. jejuni* F38011 was 56%. *C. jejuni* F38011 was used as the representative strain for the following study due to its intense biofilm formation and remarkable response to different environmental conditions.

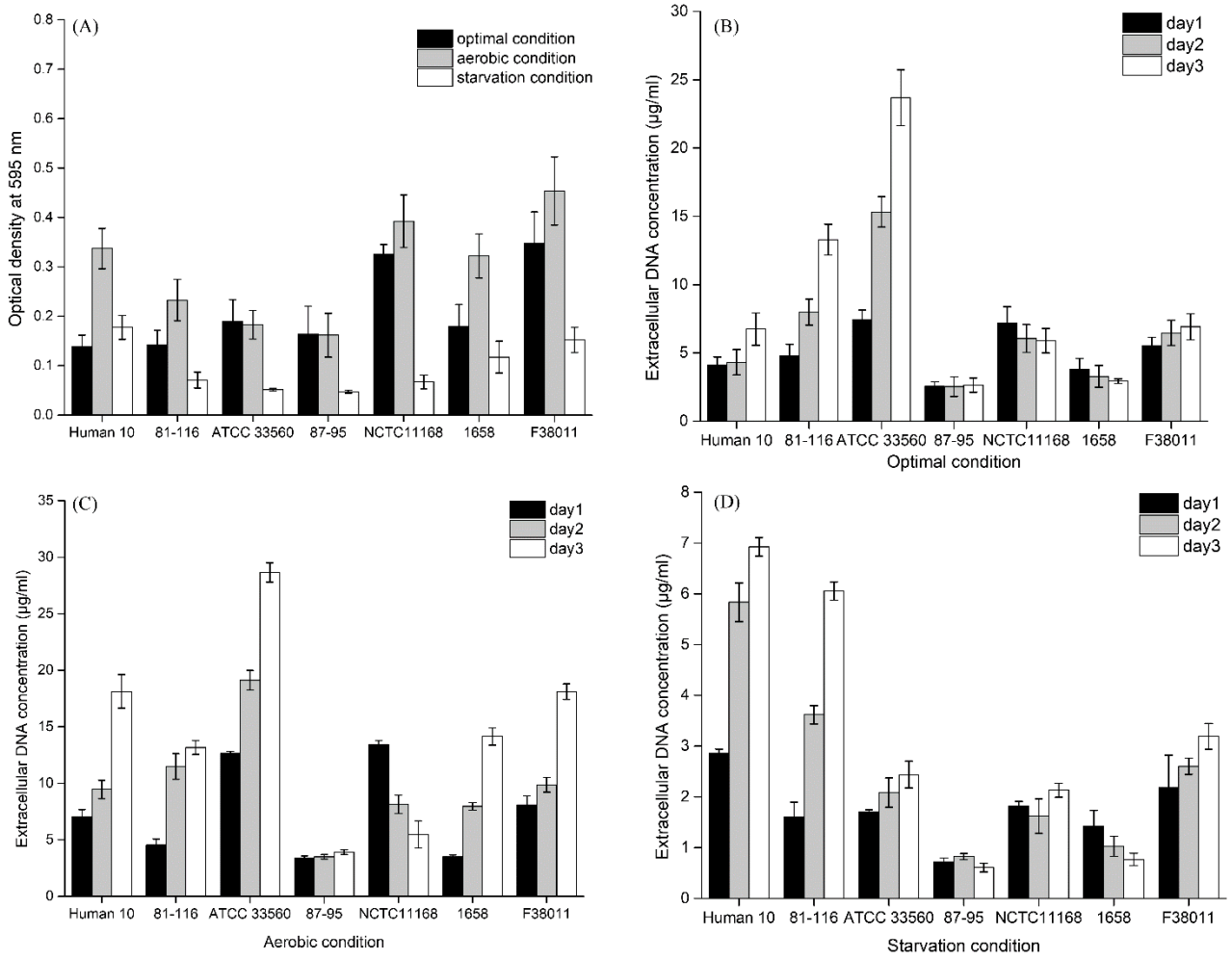

Figure 4-2. Biofilm formation and release of extracellular DNA (eDNA) by wild-type *C. jejuni* strains (*i.e.*, human 10, 81116, ATCC 33560, 87-95, NCTC 11168, 1658, and F38011) under optimal, aerobic and starvation conditions. (A) The level of biofilm formation was evaluated using crystal violet staining. The stained biofilm was released by 95% ethanol and determined by monitoring the value of OD_{595}. The concentration of eDNA during biofilm formation under optimal condition (B), aerobic condition (C) and starvation condition (D) over 3 days was quantified using SYBR Green I dye on the basis of a standard curve generated using a series of 10-fold dilutions of Lambda DNA from 80 μg/ml to 0.156 μg/ml.

Stress response deficiency mutants (mutation on stringent response regulator *spoT* and mutation on DNA repair system *recA*) and motility deficiency mutant (mutation on flagellin protein *flaAB*) were generated using *C. jejuni* F38011 as the parental strain, and their corresponding biofilm formation was tested under different environmental conditions (**Figure 4-3**). Under the optimal condition, the biofilm formation of *recA* and *flaAB* deletion mutants was significantly ($P < 0.05$) lower than that of their parental counterpart by 52% and 55%, respectively, whereas the biofilm formation of *spoT* deletion mutant was significantly ($P < 0.05$) higher than that of its parental counterpart by 24%. These deletion mutants demonstrated a similar response to the environmental stress. Thus, the biofilm formation of the deletion mutants was stimulated under aerobic condition and impaired under starvation condition. Compared to the wild-type strain, the biofilm formation of *spoT* and *recA* deletion mutants under aerobic condition was significantly ($P < 0.05$) higher by 50% and 17%, respectively, whereas the biofilm formation of *flaAB* deletion mutant was significantly ($P < 0.05$) lower by 48%. Under the starvation condition, the biofilm formation of *spoT* and *recA* deletion mutants was significantly ($P < 0.05$) higher by 149% and 72%, respectively, whereas the biofilm formation of *flaAB* deletion mutant was lower by 12%. The biofilm formation of the complementary strains (*i.e.*, *spoT*, *recA*, and *flaAB*) was also tested under an optimal condition in which their biofilm formation was restored to the same level as their wild-type counterpart (**Figure 4-4**). We believed that the complementation restored the capacity of biofilm formation of *C. jejuni* F38011 mutants. These complementary strains are supposed to have the same response as their wild-type counterpart to the environmental stress regarding biofilm formation.

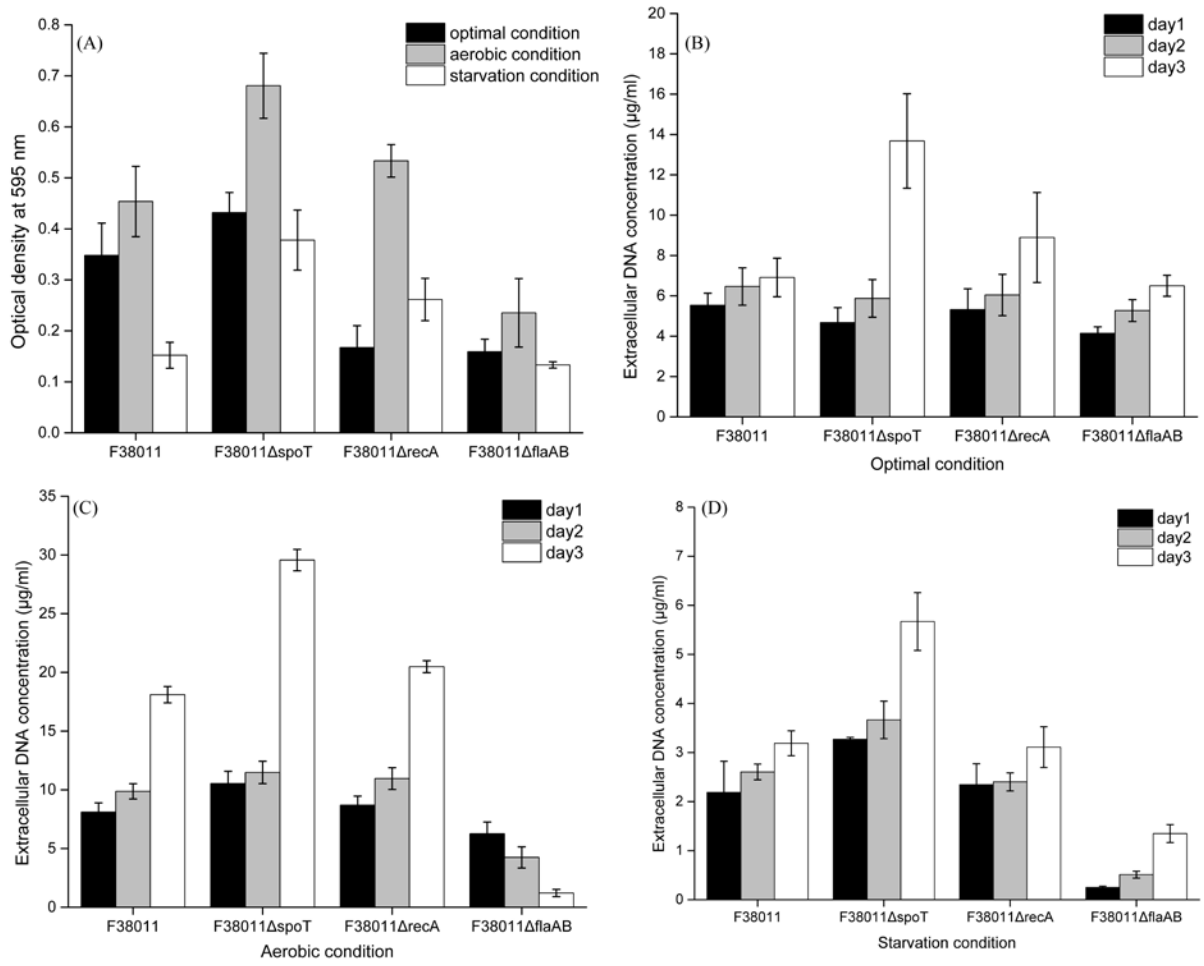

Figure 4-3. Biofilm formation and release of extracellular DNA (eDNA) by wild-type *C. jejuni* F38011 and the corresponding *spoT*, *recA* and *flaAB* deletion mutants under optimal, aerobic and starvation conditions. (A) The level of biofilm formation was evaluated using crystal violet staining. The stained biofilm was released by 95% ethanol and determined by monitoring the value of OD_{595}. The concentration of eDNA during biofilm formation under optimal condition (B), aerobic condition (C) and starvation condition (D) over 3 days was quantified using SYBR Green I dye on the basis of a standard curve generated using a series of 10-fold dilutions of Lambda DNA from 80 μg/ml to 0.156 μg/ml.

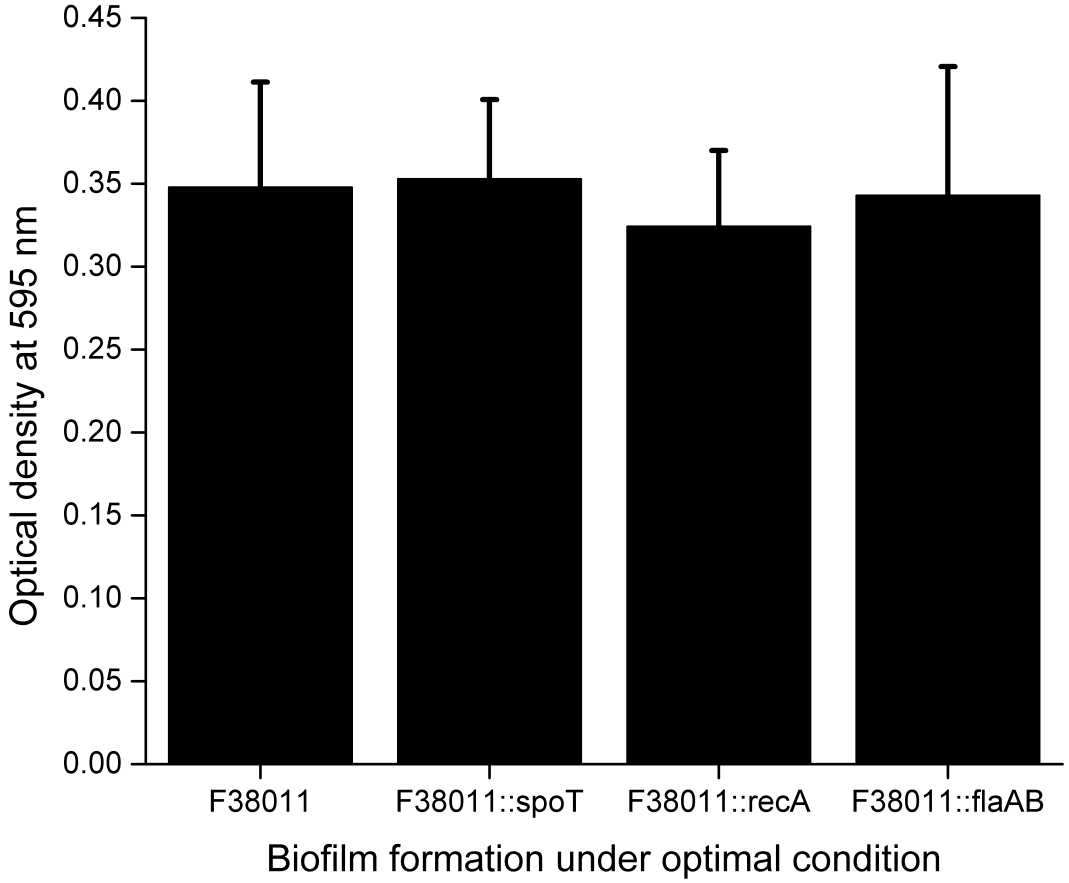

Figure 4-4. The biofilm formation of *C. jejuni* F38011 complementary strains including *spoT*, *recA*, and *flaAB* under optimal condition.

4.4.2 Determination of chemical compositions of *C. jejuni* biofilms in a microfluidic "lab-on-a-chip" device

A microfluidic "lab-on-a-chip" device coupled with confocal micro-Raman spectroscopy was applied to characterize the chemical compositions of the biofilm over a long period of cultivation (up to 216 h) in a continuous and non-destructive manner. The Raman spectral

pattern of *C. jejuni* F38011 biofilm was different from that of the microfluidic substrate (glass and PDMS). The microfluidic substrate could generate intensive Raman scattering signal at 485, 610, 703, 785, 860, 1250, and 1402 cm^{-1} (**Figure 4-5**). After the initial attachment, *C. jejuni* F38011 biofilm progressively accumulated and covered the substrate. In the meanwhile, the intensity of Raman peaks derived from the substrate heavily decreased. Only peaks at 485, 610, 703 and 1402 cm^{-1} from the substrate could still be detected at low levels. In contrast, Raman peaks derived from the biofilm appeared at different wavenumbers and demonstrated a higher intensity than that from the substrate.

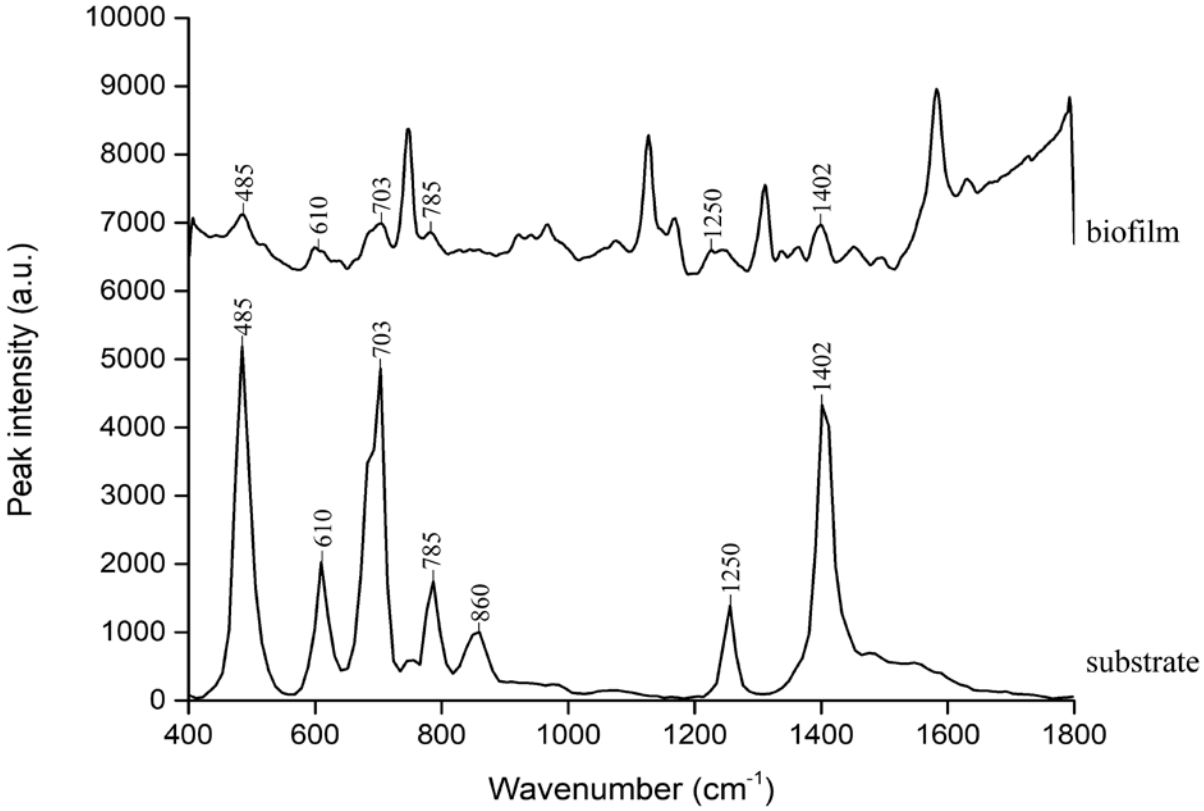

Figure 4-5. The Raman peaks of the microfluidic substrate had no overlap with the peaks of *C. jejuni* F38011 biofilm. Raman peaks of the microfluidic substrate were labeled as a highlight.

The characteristic Raman spectrum of *C. jejuni* F38011 biofilm showed prominent peaks at 746, 918, 968, 1123, 1168, 1310, and 1580 cm^{-1} after 72-h cultivation in the microfluidic chip (**Figure 4-6A**). Peaks at 746 and 1580 cm^{-1} were assigned to thymine ring and pyrimidine ring structures of nucleic acids, while peaks at 918, 968, 1123, 1168 and 1310 cm^{-1} were derived from proline ring, lipid representative band, C-N stretching vibration, C=C vibration, CH_3/CH_2 twisting or bending mode of lipids, respectively (**Table 4-3**). From 72 h to 168 h, the intensity of the prominent Raman peaks (*i.e.* 746, 918, 968, 1123, 1168, 1310, 1580 cm^{-1}) significantly ($P < 0.05$) declined by ~30% at 120 h and then rebounded back at 168 h. Up to 216 h, the intensity of these peaks reached to the highest levels, which were significantly ($P < 0.05$) higher than that at 72 h by 15% (**Figure 4-6B**). Based on Raman band assignment, nucleic acids, lipids, proteins, and polysaccharides were the major compositions of the mono-species *C. jejuni* biofilm. The amount of these components could increase or decrease due to the dynamic development of the biofilm (*i.e.,* dispersion and regrowth), which was reflected by the change of the intensity of Raman peaks from biofilms. The intensity of Raman peaks assigned to nucleic acids was significantly ($P < 0.05$) higher intensity than those derived from proteins, polysaccharides, and lipids, indicating that nucleic acids were the major components in a developed mono-species *C. jejuni* biofilm (**Figure 4-6B**).

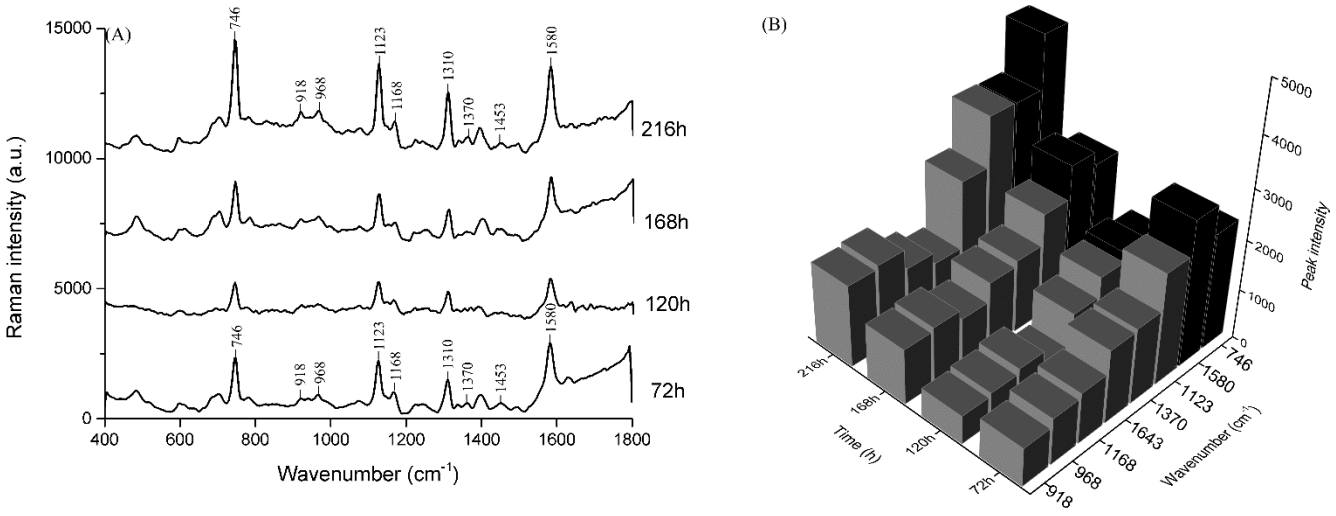

Figure 4-6. Confocal micro-Raman spectroscopy monitors the development of *C. jejuni* biofilm in the microfluidic "lab-on-a-chip" platform. *C. jejuni* biofilm was cultivated in a microfluidic device, and the chemical composition was determined at 72 h, 120 h, 168 h and 216 h using confocal micro-Raman spectroscopy coupled with a 532-nm laser. (A) Prominent Raman peaks during biofilm formation. (B) Variations in the intensity of the corresponding Raman peaks (746, 918, 968, 1123, 1168, 1370, 1580 and 1643 cm^{-1}) over time. The Raman peaks derived from nucleic acids components (746 and 1580 cm^{-1}) are shown in black color, and the Raman peaks derived from other components (*i.e.*, proteins, lipids, and polysaccharides) are shown in gray color.

Table 4-3. Raman band assignments for *C. jejuni* biofilm formed in the microfluidic platform (Naumann, 2001; Movasaghi et al., 2007; Talari et al., 2015).

Raman shift (cm^{-1})	Band assignment
746	T ring breathing mode of DNA/RNA base
918	the amino acid, proline ring
968	lipid representative band
1125	skeletal of acyl backbone in lipid and C-N stretching in protein vibration
1168	lipids υ(C=C) υ(COH)
1310	CH_3/CH_2 twisting or bending mode of lipid/collagen
1370	saccharide representative band
1453	umbrella mode of methoxyl in protein
1580	pyrimidine ring in nucleic acids

4.4.3 Accumulation of eDNA comes along with biofilm development

Since eDNA was identified as the major component of mono-species *C. jejuni* biofilm by confocal micro-Raman spectroscopy, we hypothesized that the release of eDNA was closely associated with the development of *C. jejuni* biofilm. Accumulation of eDNA during biofilm formation was quantified using specific fluorescent double-stranded DNA stain SYBR Green I. The released eDNA could be detected from all *C. jejuni* strains including wild-type and mutant strains since the first day of biofilm formation (**Figure 4-2B, C** and **D; Figure 4-3B, C** and **D**). However, the concentration and accumulation pattern of eDNA varied among different strains and were influenced by the environmental condition as well.

Under the optimal condition, *C. jejuni* 81116 and ATCC 33560 produced the highest amount of eDNA among all wild-type strains and their eDNA concentrations reached to 13.3 and 23.7 μg/ml in a 3-day developed biofilm, respectively (**Figure 4-2B**). In addition, *spoT* deletion mutant produced the highest eDNA among all the mutant strains and its eDNA concentration reached to 13.7 μg/ml in a 3-day developed biofilm (**Figure 4-3B**). From day 1 to day 3, eDNA accumulated in the biofilm of wild-type *C. jejuni* 81116 and ATCC 33560 from ~4 μg/ml to ~23 μg/ml, while the eDNA concentration in the biofilm of *C. jejuni* human 10, 87-95, NCTC 11168, 1658 and F38011 remained relatively constant and was below 10 μg/ml (**Figure 4-2B**). For *C. jejuni* mutant strains, *spoT* and *recA* deletion mutants released a similar amount of eDNA to their wild-type counterpart during biofilm formation at day 1 and day 2, but the released DNA was significantly increased at day 3. Specifically, the concentration of eDNA reached to 13.7 μg/ml for *spoT* mutant and 8.89 μg/ml for *recA* mutant at day 3. In comparison, *flaAB* mutant shared a similar eDNA release pattern to its wild-type parental counterpart during the biofilm formation, and its eDNA concentration was below 6.5 μg/ml (**Figure 4-3B**).

The release of eDNA was stimulated in a well-developed (3-day) biofilm under aerobic condition (**Figure 4-2C** and **Figure 4-3C**). For *C. jejuni* wild-type strains, the release of eDNA in *C. jejuni* human 10, ATCC 33560, F38011 and 1658 was significantly higher ($P < 0.05$) than that under the optimal condition and their concentrations reached to 18.1, 28.7, 18.1 and 14.1 μg/ml, respectively. In contrast, the eDNA concentration of *C. jejuni* 87-95 was not influenced by aerobic condition and remained constant at the same low level as that under the optimal condition (~3.5 μg/ml) during biofilm formation. A distinct release pattern of eDNA was observed for *C. jejuni* NCTC 11168 as its eDNA concentration progressively decreased from 13.4 μg/ml in a 1-day developed biofilm to 5.5 μg/ml in a 3-day developed a biofilm. For mutant

strains, both *spoT* and *recA* deletion mutants produced more significantly ($P < 0.05$) higher amount of eDNA under aerobic condition than that under the optimal condition and their concentrations reached to 29.6 and 20.5 μg/ml, respectively, in a 3-day developed a biofilm. In contrast, *C. jejuni* F38011 *flaAB* deletion mutant produced less eDNA under aerobic condition than that under optimal condition. Starvation condition significantly ($P < 0.01$) inhibited the release of eDNA for all *C. jejuni* strains, including wild-type and deletion mutants, that the eDNA concentration was less than 8 μg/ml (**Figure 4-2D** and **Figure 4-3D**).

Taken all together, a synchronous relationship between eDNA accumulation and biofilm formation was observed. The massive accumulation of eDNA usually came along with a high level of *C. jejuni* biofilm formation under different environmental conditions. In addition, a threshold of eDNA concentration ranging from 10 to 20 μg/ml was identified to associated with the high level of biofilm formation.

4.4.4 Source of eDNA during biofilm formation

Bacterial lysis can release DNA into the environment. Therefore, we speculated that bacterial lysis is responsible for the accumulation of DNA during biofilm formation. The autolysis capacity of *C. jejuni* was tested using 0.02% Triton X-100 autolysis solution, and the reduction rate of OD_{600} was recorded over time (**Figure 4-7**). The autolysis capacity of *Salmonella* was used as the reference. *S.* Typhimurium SL1344 could persist in Triton X-100 solution over 90 min, and only 10% of the total population was lysed. In comparison, *C. jejuni* was extremely vulnerable to Triton X-100 induced autolysis pressure that over 55% of *C. jejuni* cells were lysed within 70 min. In addition, the autolysis capacity of *C. jejuni* F38011 mutants (*i.e., spoT*, *recA,* and *flaAB*) was at the similar level to that of the wild-type counterpart.

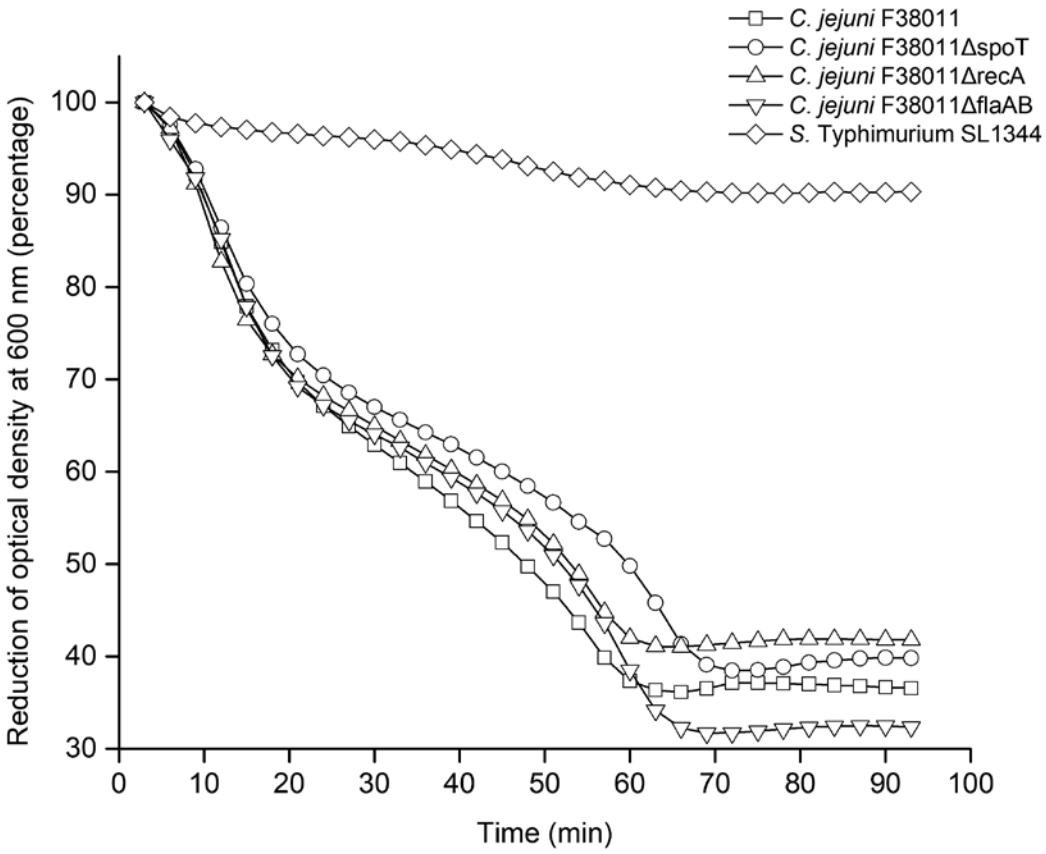

Figure 4-7. Autolysis level of *C. jejuni* induced by Triton X-100 was significantly higher than that of *S.* Typhimurium SL1344 and autolysis level had no significant difference among *C. jejuni* F38011 wild-type, *spoT*, *recA* and *flaAB* deletion mutants. Triton X-100 was dissolved in 0.05 M Tris-HCl to achieve a final concentration of 0.02% (v/v) as the autolysis buffer. Bacterial cells were harvested in the late exponential phase and resuspended in autolysis buffer to 0.3 of OD_{600}. The reduction of OD_{600} value was measured every 3 min for a total of 90 min using a microplate reader.

The release of genomic DNA is an important indicator of bacterial lysis. Using DNA gel electrophoresis assay, the DNA collected from *C. jejuni* F38011 biofilm showed the same length as the genomic DNA extracted from *C. jejuni* F38011 (**Figure 4-8**). We further evaluated the relative lysis level of *C. jejuni* cells under various conditions using qPCR (**Figure 4-9**). Under the optimal condition, *C. jejuni* F38011 wild-type strains, *recA*, and *flaAB* deletion mutants shared the similar lysis level that ~20% to 25% of the total population was lysed in a 3-day developed a biofilm. Further, *spoT* deletion mutant showed a high lysis level which 35.8% of the population was lysed in a 3-day developed biofilm. Compared to the optimal condition, aerobic condition significantly ($P < 0.05$) stimulated bacterial lysis that the lysis level ranged from 32.7% to 54.2%. Among these strains, the lysis level of *recA* deletion mutant was promoted most from 23.6% (optimal condition) to 54.2% (aerobic condition). Under the starvation condition, bacterial lysis was significantly ($P < 0.05$) inhibited. Although *spoT* deletion mutant maintained a relatively high lysis level that accounted for 26.5% of the total population, the lysis level was still lower than that under the optimal condition, which was 35.7%. Other *C. jejuni* F38011 strains (*i.e.*, wild-type, *recA*, and *flaAB*) shared a similarly low level of lysis, which accounted for ~15% of the total population.

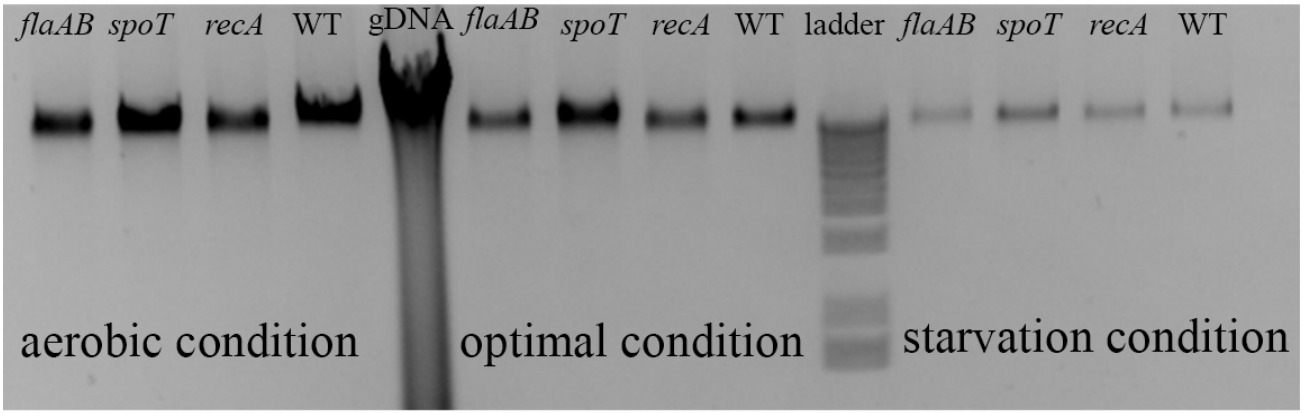

Figure 4-8. The length of DNA fragment present in *C. jejuni* during biofilm formation was similar to that of genomic DNA extracted from *C. jejuni* F38011 planktonic cells. Gel electrophoresis was performed to demonstrate the length of the released DNA fragment. After 3-day biofilm cultivation, each bacterial culture in the 96-well plate was collected. A total of 10 µl of the supernatant was mixed with 2 µl of DNA loading dye solution and then loaded on 1% agarose gel for electrophoresis. A 1-kb ladder was used as the reference. The DNA was stained using SYBR™ safe DNA gel stain and visualized on ChemiDoc™ XRS gel documentation system.

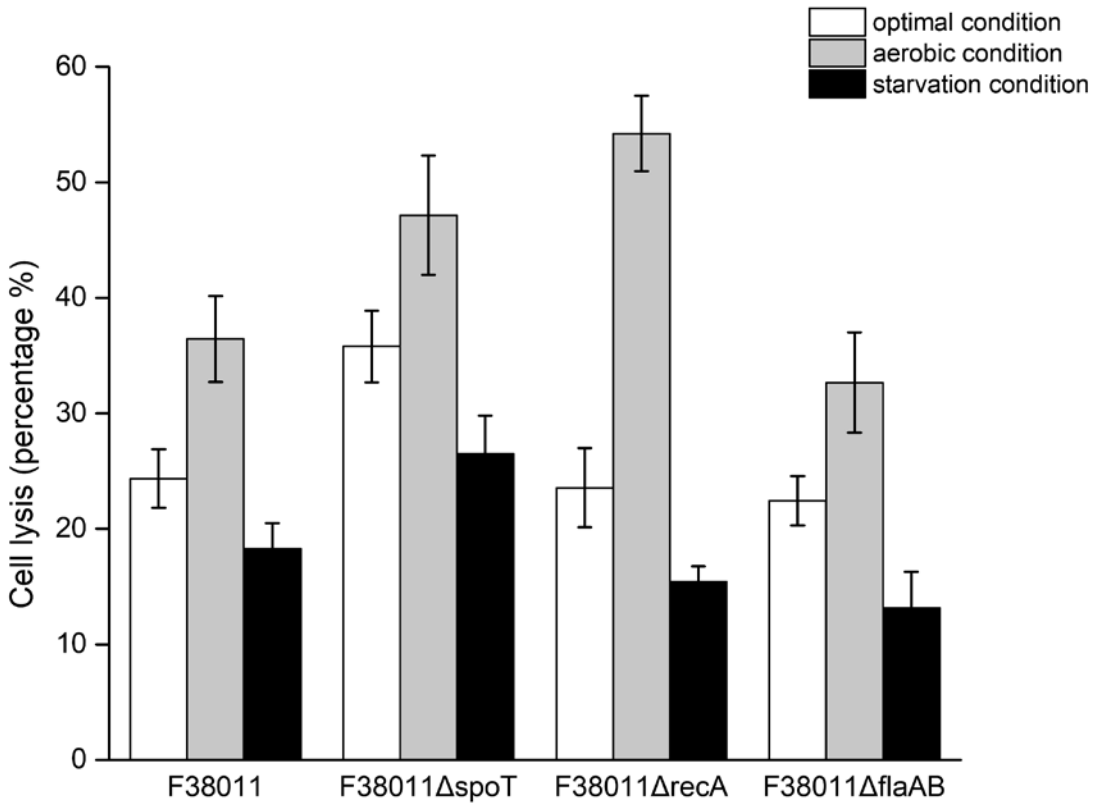

Figure 4-9. Lysis level of *C. jejuni* cells was stimulated by aerobic condition and inhibited by starvation condition during biofilm formation. Genomic DNA is an indicator of bacterial lysis. After 3-day biofilm cultivation, the genomic DNA in the supernatant and biofilm of *C. jejuni* wild-type strain, *spoT*, *recA* and *flaAB* deletion mutant strains were purified. The relative content of genomic DNA in the supernatant and biofilm was individually determined via real-time quantitative PCR (qPCR) using housekeeping gene *rpoA*. The lysis level was calculated by dividing the genomic DNA content in the supernatant to the sum of genomic DNA content in the supernatant and the biofilm.

Interestingly, *flaAB* deletion mutant had a similar level of lysis to that of its parental counterpart but released less DNA. We, therefore, speculated that the expression of *flaA* and *flaB* gene might influence the release of eDNA. Accordingly, the expression profiles of *flaA* and *flaB* were determined using qPCR, and arbitrary fold change cut-offs were set as more than 2 (**Figure 4-10**). Under aerobic condition, both *flaA* and *flaB* genes were significantly (>2 fold and $P < 0.05$) upregulated among *C. jejuni* F38011 wild-type (2.8 fold for *flaA* and 2.2 fold for *flaB*), *spoT* (3.2 fold for *flaA* and 4.1 fold for *flaB*) and *recA* (5.3 fold for *flaA* and 3.0 fold for *flaB*) deletion mutant strains, but the upregulation could only be detected at the first day of biofilm formation. The up-regulation of *flaA* gene reached to 2.8 fold in the wild-type strain, 3.2 fold in *spoT* deletion mutant and 5.3 fold in *recA* deletion mutant while the up-regulation of *flaB* gene reached to 2.2 fold in the wild-type strain, 4.1 fold in *spoT* deletion mutant and 3.0 fold in *recA* deletion mutant. The expression profile of both *flaA* and *flaB* genes were at the same levels among wild-type, *spoT* and *recA* deletion mutant strains under starvation condition compared to that under optimal condition, indicating that the *flaA* and *flaB* genes might play a role under oxidative stress rather than starvation stress.

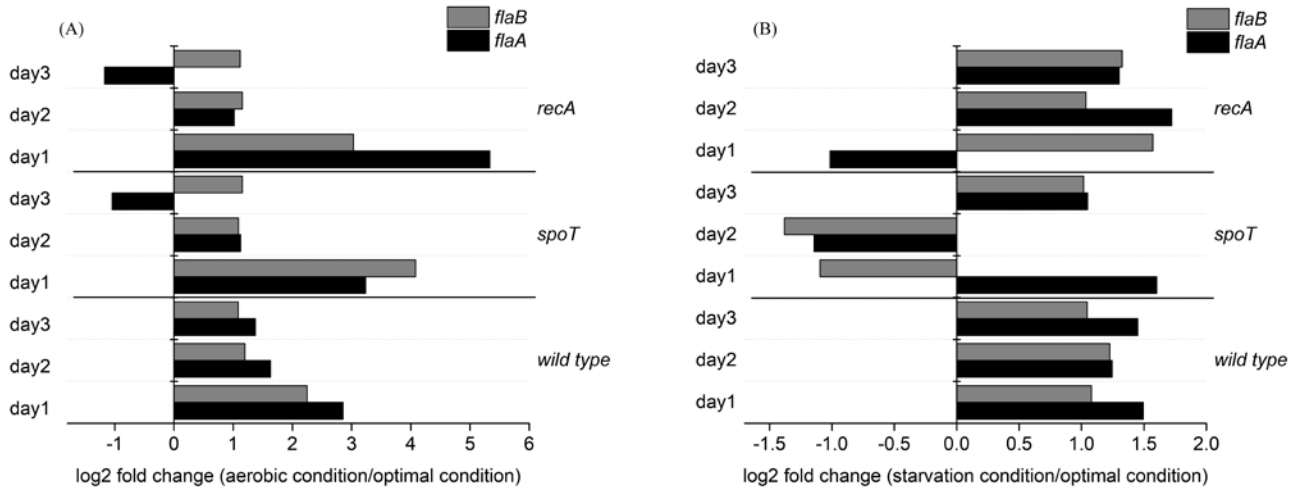

Figure 4-10. The expression of *flaA* and *flaB* genes in *C. jejuni* F38011 wild-type, *spoT* and *recA* deletion mutants was upregulated only at the first day of biofilm formation under aerobic condition. Real-time qPCR was performed to plot the expression profile of *flaA* and *flaB* in response to the aerobic condition (A) and starvation condition (B) in *C. jejuni* F38011 wild-type strain as well as *spoT* and *recA* deletion mutant strains. The *rpoA* gene was used as the internal control. The arbitrary fold change cut-offs were set as more than 2.

4.4.5 Addition of DNA stimulates biofilm formation

We identified a clear correlation between eDNA concentration and biofilm formation (**Figure 4-2** and **Figure 4-3**), but the consequence of DNA release and biofilm formation was not fully clear yet. DNA addition assay was conducted to investigate whether eDNA was the inducing factor or a by-product of biofilm formation. In the natural environment, bacterial cells usually inhabit in a multi-species bacterial community. Therefore, DNA released by other bacterial species may also contribute to biofilm formation. In the current study, genomic DNA of *C. jejuni* F38011 and *S.* Typhimurium SL 1344 was supplemented either by direct addition into the bacterial culture or by forming a pre-coating layer for the subsequent biofilm formation in the

96-well plate. Direct addition of DNA demonstrated a concentration-dependent stimulation effect on *C. jejuni* biofilm formation and this effect could be triggered not only by *C. jejuni* DNA but also *Salmonella* DNA (**Figure 4-11C** and **D**). For *C. jejuni* F38011 wild-type strain, the stimulation effect on biofilm formation was triggered when the concentration of the added DNA reached to 10 μg/ml. For *spoT* deletion mutant, the stimulation effect was observed when the concentration of the added DNA reached to 20 μg/ml. For *recA* deletion mutant, the stimulation effect started from 5 μg/ml and the addition of 10 μg/ml DNA could increase the biofilm formation to the level as that of the wild-type strain. For *flaAB* mutant, the stimulation effect started from the concentration of 2.5 μg/ml and the addition of 10 μg/ml DNA restored biofilm formation to the level as that of the wild-type strain. When the concentration of the added DNA reached to 20 μg/ml, biofilm formation of *C. jejuni* F38011 wild-type and mutant strains was promoted to a similarly high level, indicating that 20 μg/ml was close to the saturation concentration of DNA that could maximize the biofilm formation in the environment. In contrast, forming a pre-coated layer did not enhance biofilm formation regardless of the DNA concentration to generate this pre-coated layer (**Figure 4-11A** and **B**). The biofilm formation level of *C. jejuni* F38011 wild-type, *spoT*, *recA* and *flaAB* deletion mutants on a pre-coated DNA layer was the same as that formed on the untreated substrate. Thus, eDNA was the leading factor for biofilm accumulation and eDNA derived from *Salmonella* could also stimulate the formation of mono-species *C. jejuni* biofilm. Although the initial attachment was the prerequisite for biofilm formation, the pre-coated layer of DNA had little influence on the subsequent biofilm development.

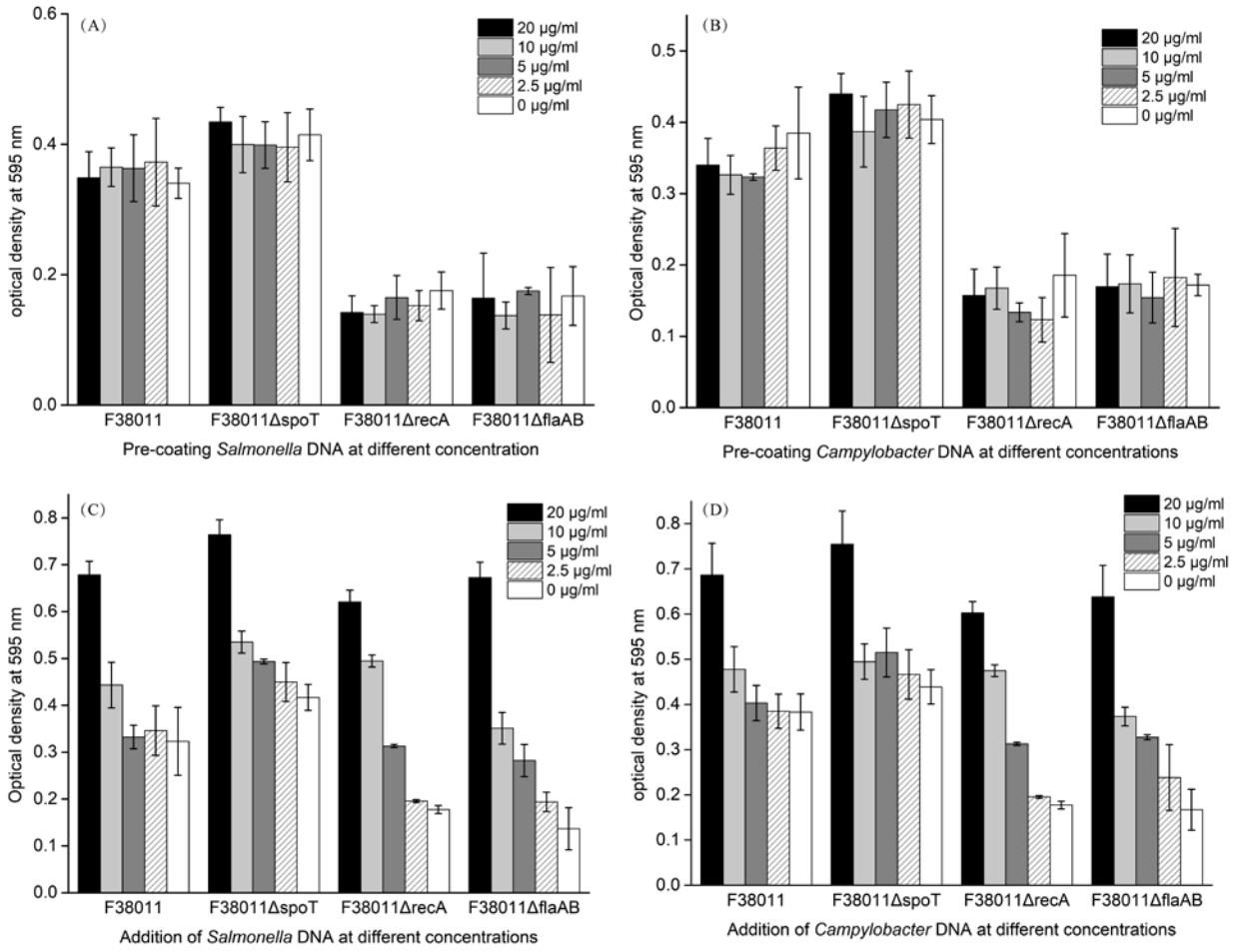

Figure 4-11. Addition of genomic DNA extracted either from *Campylobacter* or *Salmonella* had a concentration-dependent stimulation effect on biofilm formation of *C. jejuni* F38011; the pre-coating layer formed by DNA extracted either from *Campylobacter* or *Salmonella* did not contribute to the development of biofilm formation of *C. jejuni* F38011. Genomic DNA of *C. jejuni* F38011 or *S.* Typhimurium SL1344 was separately extracted and added for biofilm formation. To form a pre-coating layer, 200 μl of DNA *Salmonella* (A) or *C. jejuni* (B) at different concentrations was added to each well of the 96-well plate and maintained for 4 h. The unbounded DNA was washed out before the addition of *C. jejuni* F38011 culture. To directly add DNA for biofilm formation, DNA of *Salmonella* (C) or *C. jejuni* (D) was mixed with *C. jejuni*

F38011 culture to a certain final concentration, and 200 µl of this mixed culture was added into the 96-well plate. The plate was then cultivated in a microaerobic environment at 37°C for up to 72 h.

4.4.6 DNase I treatment prevents biofilm formation and disrupts biofilm structure

DNase I treatment was performed to elucidate the role of eDNA in biofilm formation. The treatment was conducted at two distinct stages, namely initial attachment stage and maturation stage (**Figure 4-12**). Treatment at the initial attachment stage significantly ($P < 0.05$) prevented biofilm formation. Compared to the untreated group, DNase I treatment reduced the biofilm formation level of *C. jejuni* F38011 wild-type (65%), *spoT* deletion mutant (74%), *recA* deletion mutant (61%) and *flaAB* deletion mutant (66%). In comparison, DNase I treatment at the maturation stage significantly ($P < 0.05$) disrupted the well-developed biofilm. The treatment reduced the biofilm biomass of *C. jejuni* F38011 wild-type (77%), *spoT* deletion mutant (64%), *recA* deletion mutant (43%), and *flaAB* deletion mutant (63%).

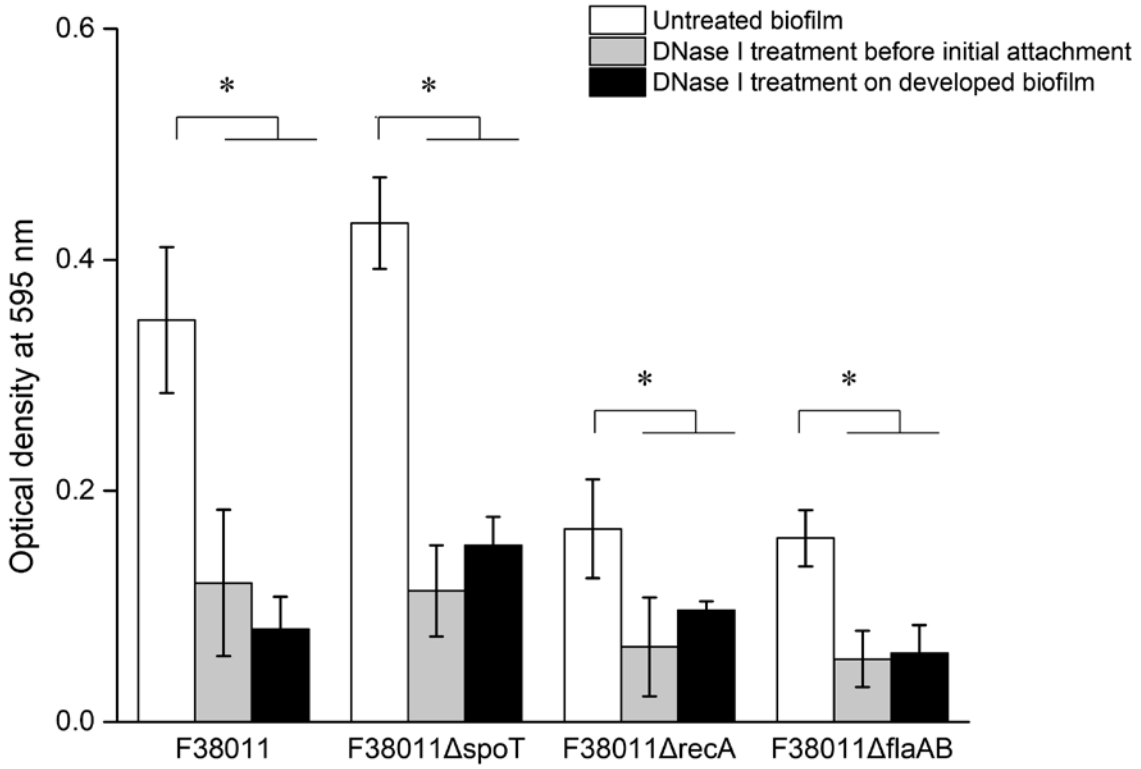

Figure 4-12. DNase I treatment before bacterial initial attachment prevented *C. jejuni* biofilm formation and DNase I treatment on the well-developed *C. jejuni* biofilm disrupted biofilm structure, leading to the reduction of biomass. To treat biofilm at the initial attachment stage, DNase I was mixed with *C. jejuni* culture to a final concentration of 2 units/ml and then added to the 96-well plate for biofilm formation. To treat the well-developed biofilm in the 96-well plate, 200 µl of DNase I solution (2 units/ml) was added into a well with a 3-day cultivated *C. jejuni* biofilm. The treatment was maintained for 15 min at room temperature. The reduction level of biofilm was evaluated using the aforementioned crystal violet staining assay. Asterisk denotes significant difference ($P < 0.05$).

Atomic force microscopy was applied to further investigate the effect of DNase I treatment on *C. jejuni* F38011 biofilm. The topographic images of the treated and untreated biofilms were collected in contact scanning mode. Trace and retrace images were well matched (data not shown), indicating that AFM tips in the contact mode did not scratch biofilm surfaces and the morphological properties derived from AFM characterization were highly reliable. The topographic image of *C. jejuni* F38011 biofilm demonstrated a compact structure and smooth surface. On the top surface of the biofilm, protruding patterns were observed in cell shape with a size of 1.5 × 0.2 μm^2. These cell-shaped patterns were squeezed and highly organized (**Figure 4-13A and B**). DNase I treatment resulted in a morphological variation where the top surface of the biofilm was altered from smooth to rough and from compact to loose. The cell-shaped pattern could still be observed but was concave after the treatment (**Figure 4-13C and D**).

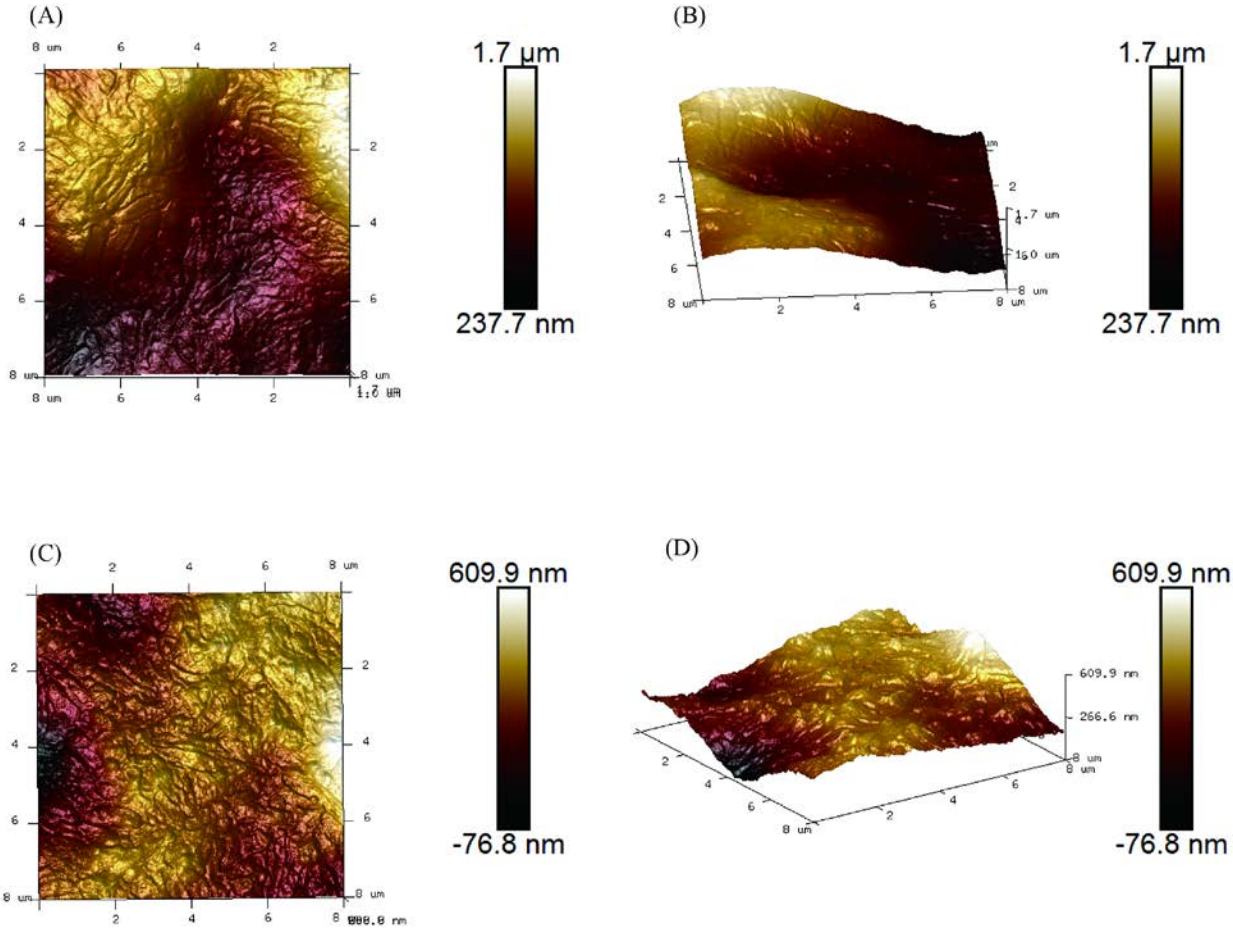

Figure 4-13. Topographic images of *C. jejuni* F38011 biofilms confirmed that the DNase I treatment disrupted biofilm structure and dispersed encased *C. jejuni* F38011 cells. The images were obtained by atomic force microscopy in contact mode within 8 µm × 8 µm area at scan frequency of 0.5 Hz: (A) *C. jejuni* biofilm without DNase I treatment; (B) 3D reconstruction of the untreated *C. jejuni* biofilm; (C) *C. jejuni* biofilm after DNase I treatment ; D) 3D reconstruction of the treated *C. jejuni* biofilm.

The volume and coverage area of the biofilms were also determined on the basis of the 3D reconstruction of biofilm topographic images. According to **Figure 4-14**, DNase I treatment

significantly disrupted biofilm and resulted in the detachment that the volume of the biofilm was reduced from 53.93 μm^3 to 28 μm^3 and the coverage area of the biofilm was reduced from 20.19 μm^2 to 2.68 μm^2. Taken all together, these findings demonstrated the role of eDNA in biofilm formation, which not only facilitated the initial attachment but also maintained the integrity of biofilm structure.

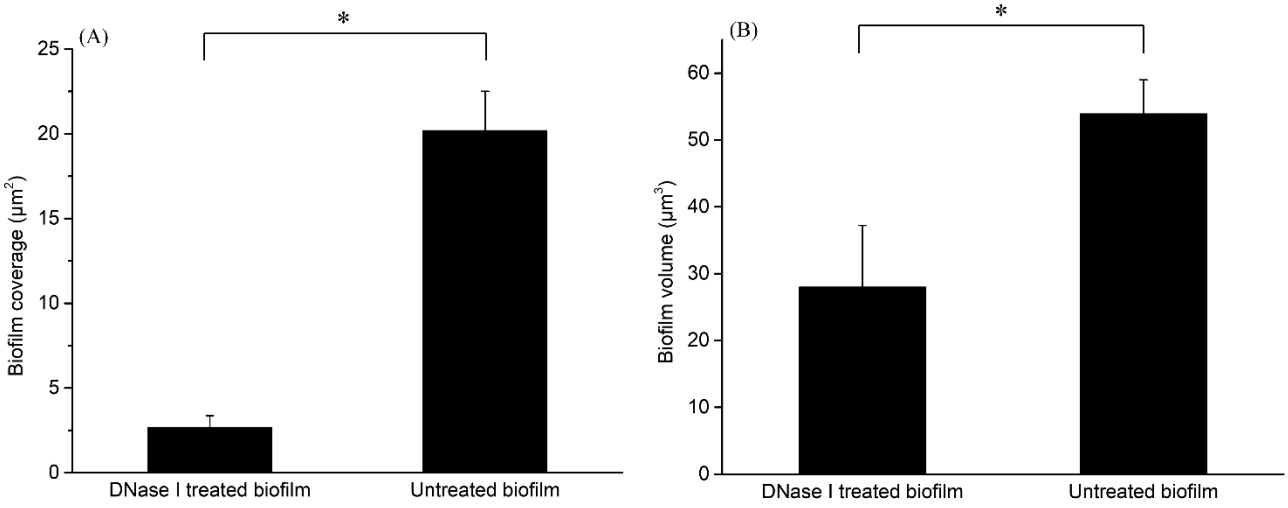

Figure 4-14. DNase I treatment reduced the coverage and volume of *C. jejuni* biofilm. The well-developed (3-day) *C. jejuni* F38011 biofilm on a nitrocellulose membrane was treated with DNase I solution (2 units/ml) for 15 min and then air-dried for the analysis of atomic force microscopy. (A) Coverage reduction caused by DNase I treatment; (B) Volume reduction caused by DNase I treatment. Asterisk denotes significant difference ($P < 0.05$).

4.4.7 DNA allocates *C. jejuni* and *Salmonella* cells in a dual-species biofilm

Multi-species biofilm is the dominant type in the natural environment (Elias and Banin, 2012). In the current study, *Campylobacter-Salmonella* biofilm was used as a representative model to investigate the role of eDNA in a dual-species biofilm. A green fluorescent protein

(GFP)-tagged *C. jejuni* F38011 strain was mixed with a red fluorescent protein (RFP)-tagged *S.* Typhimurium SL 1344 strain and then injected into the microfluidic "lab-on-a-chip" platform. After 3-days cultivation, the biofilm was stained using DAPI, followed by imaging (**Figure 4-148**). *Campylobacter* could co-exist with *Salmonella* and form a dual-species biofilm. Within this dual-species biofilm, *C. jejuni* cells were mainly located at the bottom layer while *S.* Typhimurium cells were mainly located at the top layer. Shown in blue color, a large amount of eDNA was identified in this dual-species biofilm. The eDNA mainly assembled and formed several eDNA-rich areas, although discretely distributed eDNA could still be observed as well.

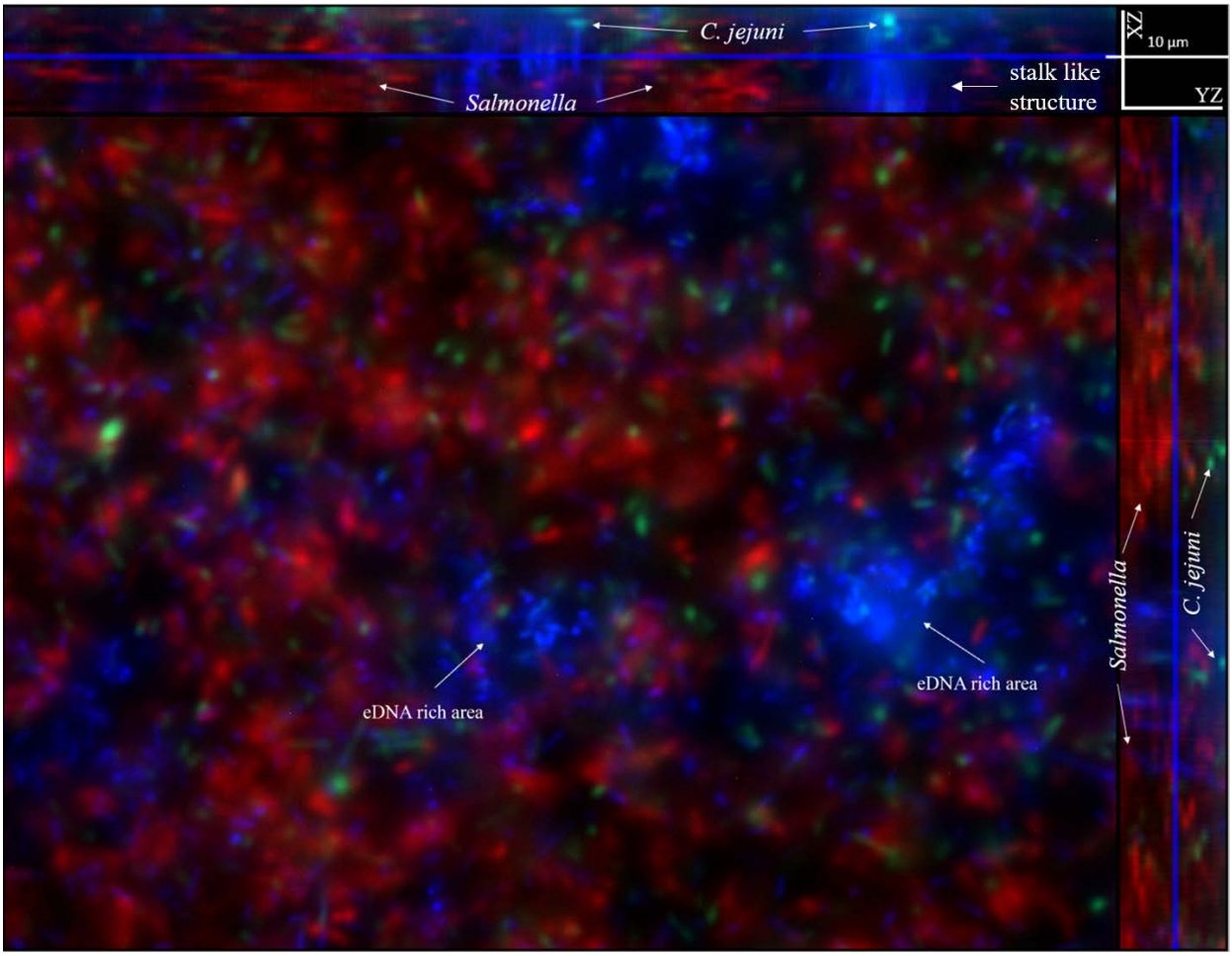

Figure 4-15. Spatial distribution of *C. jejuni* cells, *Salmonella* cells and extracellular DNA (eDNA) within a *Campylobacter-Salmonella* dual-species biofilm formed in the microfluidic platform. Fluorescence microscopy was applied to determine the spatial distribution of eDNA and bacterial cells in a dual-species *Campylobacter–Salmonella* biofilm. After 3-days cultivation, 30 nM of DAPI solution was injected into the microfluidic device to stain eDNA in the biofilm. Images were collected at multi-channels: 405 nm (blue color for DAPI signal), 488 nm (green color for GFP signal), and 543 nm (red color for RFP signal). Within this *Campylobacter-Salmonella* dual-species biofilm, *C. jejuni* cells were mainly located at the bottom while *Salmonella* cells were mainly located at the top layer. The eDNA mainly assembled and formed

several eDNA-rich areas and maintained the spatial distance between *C. jejuni* and *Salmonella* in the biofilm.

The view from spatial perspective identified that eDNA-rich area formed a stalk-like structure and occupied a large space. *C. jejuni* cells were usually associated with the eDNA-rich area and covered by the stalk-like structure. In contrast, *Salmonella* cells were not directly interacted with eDNA, but distributed around the eDNA-rich structure. Therefore, we speculated that eDNA was responsible for allocating different species of bacteria by maintaining a spatial distance between each other.

4.5 Discussion

C. jejuni is a fastidious microaerobic bacterium and extremely vulnerable to the environmental stress. However, this microbe is highly prevalent in the environment and difficult to remove from the food chain. Campylobacteriosis is still the most frequently reported foodborne illness in Canada, outnumbering the reported cases of *Salmonella*, *Listeria monocytogenes*, and Shiga toxigenic *E. coli* infections combined together (Canada, 2017). *C. jejuni* can antagonize stresses by activating internal stress response system. Previous studies demonstrated that stringent response conducted global regulation on bacterial metabolism in reaction to the stresses, especially nutrient starvation. The *spoT* gene in *C. jejuni* 81-176 was reported to be essential for the stringent response. Deletion of this gene significantly inhibited the expression of the genes related to redox balance, metabolism, energy production and conversion pathway (Gaynor et al., 2005). Oxidative stress is a lethal challenge for microaerophilic bacteria because it can induce DNA damage and exert subsequently negative

influences on the microbes (Storz and Imlayt, 1999; Cabiscol Català et al., 2000). A 38-kDa protein encoded by the *recA* gene was identified to mediate both DNA repair and homologous recombination, aiding *C. jejuni* to maintain physiological activities when it encountered the oxidative stress-induced DNA damage. Disruption of the *recA* gene significantly impaired the viability of *C. jejuni* in the DNA damage-induced environment (Gaasbeek et al., 2009). However, bacterial cells (*e.g., C. jejuni*) can only withstand a limited level of stress. As a self-produced bacterial community, biofilm has unique physiological properties, such as tolerance to dehydration, persistence under the harsh environmental condition and resistance to antibiotic treatment, all of which provide remarkable protection to the encased bacteria cells . Apart from the inner stress response system, *C. jejuni* could also survive by forming a biofilm or residing in a mature biofilm against the unfavorable condition. In our previous study, *C. jejuni* could survive a longer period under oxidative stress by forming a biofilm than that as planktonic cells. After 3-day exposure to a high content of oxygen, no viable *C. jejuni* cell could be detected from its planktonic culture, but ~5 log CFU/cm^2 of *C. jejuni* cells were still culturable in the biofilm (Feng et al., 2016). Although biofilm formation of *C. jejuni* has been defined under different conditions, the correlation between stress response system and biofilm formation of *C. jejuni* has only partially been investigated (Reeser et al., 2007; Reuter et al., 2010). In the current study, we further investigated the influence of stress response of *C. jejuni* on the biofilm formation.

Most of the *C. jejuni* wild-type strains shared similar biofilm-forming capability in response to stress. In short, these strains produced more biofilm under aerobic condition and less biofilm under starvation condition (**Figure 4-2A**). This observation was in agreement with a previous study that the biofilm formation of *C. jejuni* increased under the oxygen-enriched condition (Reuter et al., 2010). In addition, another study also reported that the biofilm formation

of *C. jejuni* under nutrient-limited condition (*e.g.*, Brucella or Bolton medium) was significantly inhibited due to the slow growth of *C. jejuni* cells (Reeser et al., 2007).

Biofilm formation of *C. jejuni* F38011 *spoT* deletion mutant was increased by 26% compared to that of its parental counterpart under the optimal condition (**Figure 4-3A**), which was consistent to a previous study that the mutation of the *spoT* gene showed an increased biofilm formation of *C. jejuni* 81-176 (McLennan et al., 2008). In contrast, biofilm formation of the *recA* deletion mutant and *flaAB* deletion mutant was reduced by ~52% and 55%, respectively, compared to their parental counterparts under the optimal condition. Our study demonstrated that the deletion of *recA* inhibited *C. jejuni* biofilm formation. The flagellum is known to be responsible for bacterial attachment onto the surface of a substrate. The loss of flagellar apparatus significantly impairs biofilm formation (Pratt and Kolter, 1998; Joshua et al., 2006; Kalmokoff et al., 2006; Reeser et al., 2007). Consistent with these studies, the deletion of both *flaA* and *flaB* genes in *C. jejuni* F38011 resulted in a significant loss of motility as well as a reduced biofilm formation (**Figure 4-3A and Figure 4-16**).

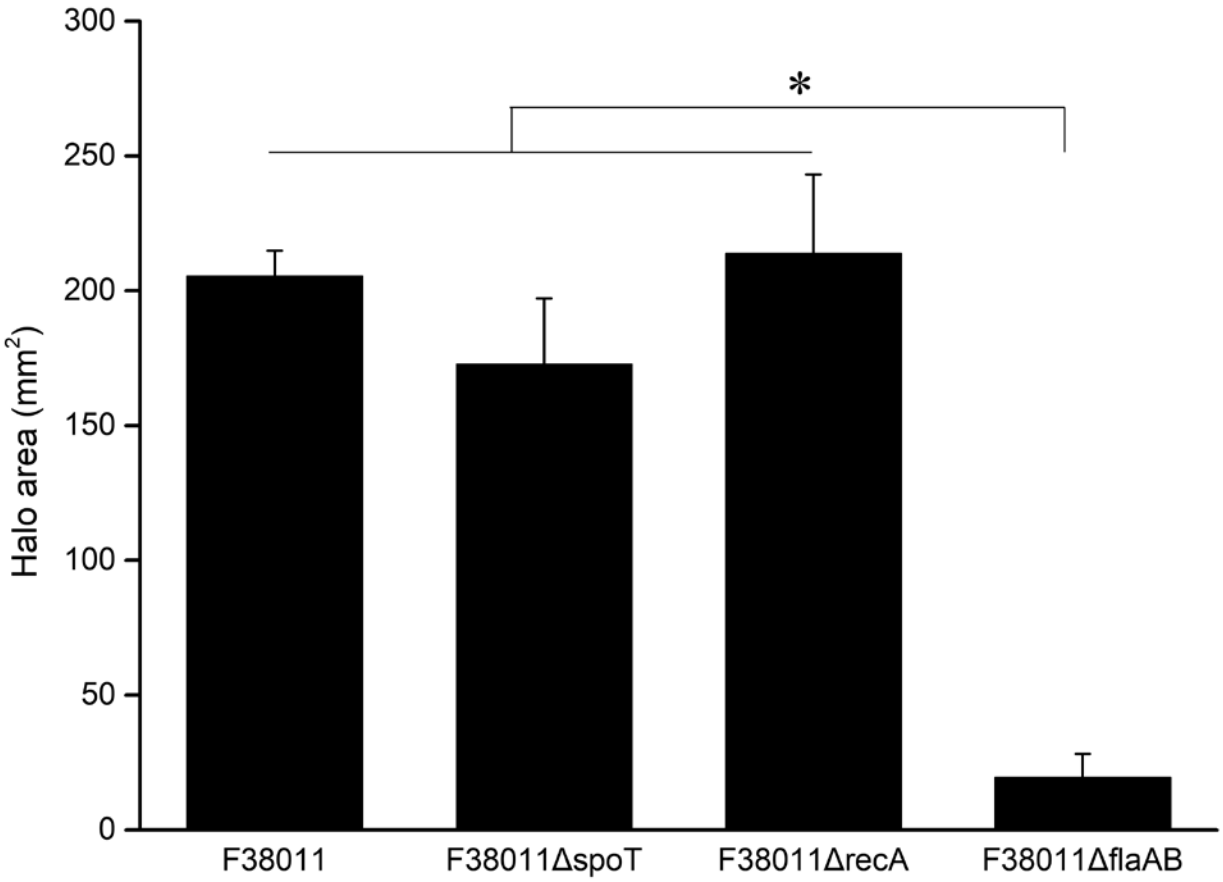

Figure 4-16. The mutations of *flaA* and *flaB* significantly decreased the motility of *C. jejuni* F38011 while the mutations on *spoT* or *recA* did not influence the motility of *C. jejuni* F38011. A total of 5 µl of the overnight bacterial culture was spotted onto the Brucella media supplemented with 0.4% agar. After 2-day cultivation in microaerobic condition at 37ºC, the halo area was measured. Asterisk denotes significant difference ($P < 0.05$).

Compared to *C. jejuni* F38011 flagella deletion mutant (*i.e., flaAB*) strain, *C. jejuni* F38011 stress response deletion mutants (*i.e., spoT* and *recA*) demonstrated a distinctive response to the environmental stress in terms of biofilm formation. Compared to the wild-type strain, the biofilm

formation of *spoT* and *recA* deletion mutants under starvation condition significantly increased by 149% and 72%, respectively, whereas the change in biofilm formation of *flaAB* deletion mutant was not significant. Therefore, we believe that stress response is one of the critical factors to affect biofilm formation of *C. jejuni* more than flagellum does under specific stress condition.

Stress response systems mainly regulate the physiological metabolism inside bacterial cells, whereas biofilm formation occurred outside of bacterial cells. There is likely a factor that can mediate this inside-outside transition. DNA is present in abundance in the environment as a consequence of the lysed dead organisms or via active secretion from the living organisms (Nielsen et al., 2007). Bacteria can use these free DNA as an important supply of nutrients or integrate these free DNA into the genome for acquiring resistant capacity (Lorenz and Wackernagel, 1994; Thomas and Nielsen, 2005). Previous studies identified that bacteria progressively released DNA during biofilm formation. For example, DNA content in a 3-day developed *P. aeruginosa* biofilm reached to 20-25 μg/ml and the concentration of DNA could be up to 220 μg/mg (eDNA/cellular DNA) when the biofilm cultivation extended to 5 days (Steinberger and Holden, 2005; Das and Manefield, 2012).

Our current study also identified the presence of eDNA during the biofilm formation of *C. jejuni*. By Raman spectroscopic analysis, the content of eDNA in the biofilm was determined to be significantly higher than other major biofilm components, such as proteins, lipids, and polysaccharides. In addition, the content of eDNA increased or decreased along with the growth or dispersion of the biofilm, respectively (**Figure 4-6A and B**), demonstrating that eDNA was an important constitutions of *C. jejuni* biofilm.

Bacterial lysis is regarded as the important source of the release of eDNA (Allesen-Holm et al., 2006; Rice et al., 2007). As shown in **Figure 4-7 and 4-8**), *C. jejuni* F38011 was

vulnerable to the induced lysis pressure and the length of the released eDNA fragment was equal to the length of genomic DNA extracted from *C. jejuni* F38011. Taken all together, there was a high possibility that bacterial lysis was the source of the released DNA during the biofilm formation of *C. jejuni*. However, autolysis assay could not fully explain the release of genomic DNA during the biofilm formation of *C. jejuni* F38011 wild-type strain and deletion mutants in response to different stresses. Because Triton X-100 induced a much stronger lysis pressure than that of the environmental stress, autolysis assay only reflected the tendency of bacterial lysis but not the precise proportion of the lysed *C. jejuni* cells during biofilm formation. Accordingly, qPCR was performed to evaluate the lysis level of *C. jejuni* F38011 biofilms under different environmental conditions (**Figure 4-9**). Specifically, aerobic condition significantly ($P < 0.05$) increased the lysis rate by over 32% and starvation condition significantly ($P < 0.05$) decreased the lysis rate by over 25%. The *recA* deletion mutant was vulnerable to the aerobic condition, with 54% of the total population lysed in a 3-day biofilm. The aerobic condition can generate oxidative pressure and induce DNA damage (Storz and Imlayt, 1999). The high lysis rate of *recA* deletion mutant is highly likely due to the lack of function at DNA repair system. The quantitative analysis of eDNA released during the biofilm formation revealed a synchronous response to the environmental stresses (**Figure 4-2** and **Figure 4-3**). For example, the release of eDNA and biofilm formation increased simultaneously under aerobic condition. However, *C. jejuni* ATCC 33560 was an exception. Although over 10 μg/ml of eDNA can be detected from the biofilm of *C. jejuni* ATCC 33560 under aerobic conditions, its biofilm formation levels were significantly less ($P < 0.05$) than that of other *C. jejuni* strains, such as *C. jejuni* F38011 and NCTC 11168, whose eDNA production was ~10 μg/ml. According to a previous study, *C. jejuni* ATCC 33560 contains a single-nucleotide deletion that might lead to the non-function of CmeR

(Hyytiäinen and Hänninen, 2012). CmeR is well characterized as a transcriptional repressor of efflux pump of CmeABC (Lin et al., 2005) and also involved in various metabolic regulations, such as the control of membrane transporters and biosynthesis of periplasmic proteins and capsule (Guo et al., 2008). Therefore, *C. jejuni* ATCC 33560 is more vulnerable and easily lysed under stress conditions, increasing released eDNA. However, the heavy loss of viable cells reduces the initial attachment and subsequently impairs the biofilm formation which might be responsible for the low biofilm formation of *C. jejuni* ATCC 33560 under different stress conditions.

Mutations in the stress response system (*spoT* and *recA*) enhanced the impact of stresses on eDNA secretion and biofilm formation, which was in agreement with the result of cell lysis (**Figure 4-9**). Although the deletion mutation of flagellar apparatus (*flaA* and *flaB*) did not directly affect the stress response capacity of *C. jejuni,* both motility and chemotaxis were significantly impaired (Lertsethtakarn et al., 2011). Hence, the lysis level of *flaAB* deletion mutant was also increased due to the accumulation of redox pressure induced by the aerobic condition. We believe that bacterial lysis was the consequence of stress response, which eventually releases the DNA into the environment. The accumulation of eDNA then facilitated the development of biofilm as the constitutions. To our surprise, not only the DNA from *Campylobacter* but also *Salmonella* could mediate this regulation on biofilm formation. Thus, eDNA was essential to the initial attachment because DNase I treatment at the initial attachment stage almost eliminated biofilm formation. In addition, DNase I treatment on the well-developed biofilm disrupted over 70% of the biomass, confirming that eDNA was the major constitutions in a developed *C. jejuni* biofilm (**Figure 4-12**). AFM analysis revealed that the degradation of eDNA in the biofilm disrupted biofilm structure and resulted in a reduction of ~87% biofilm

coverage and ~48% biofilm volume (**Figure 4-13 and 4-14**). Taken together, eDNA was involved in biofilm formation by performing multi-functions. At the initial stage, eDNA facilitated bacterial initial attachment and established the basis for biofilm formation. At the developing stage, eDNA was included into the biofilm as the major constitutions to build the biofilm structure. In a developed biofilm, eDNA was responsible for maintaining the biofilm structure.

Although the *flaAB* deletion mutant shared a similar lysis rate to that of the wild-type strain under the environmental stresses, its DNA release and the levels of biofilm formation were significantly ($P < 0.05$) lower (**Figure 4-3**). Previous studies reported that both eDNA and flagella were responsible for bacterial attachment and biofilm formation. DNA could facilitate the attachment via an acid-base interaction and flagella-mediated auto-agglutination and immobilize bacteria cell onto a surface (Ritchie et al., 1983; Lillard, 1986; Das et al., 2010; Brown et al., 2015a). The deletion mutation in flagella synthesis gene *flaA* and *flaB* in *C. jejuni* resulted in a biofilm-repressed phenotype (Reeser et al., 2007; Reuter et al., 2010). We believed that the low biofilm formation of the *flaAB* mutant was due to both the deficiency of eDNA and the lack of flagella, but this could not explain why *flaAB* deletion mutant released a low amount of eDNA. Interestingly, it was reported that the expression of flagellin A (*flaA*) and flagellin B (*flaB*) was activated since biofilm formation and their expression level was significantly higher in the biofilms compared to that in the planktonic cells (Kalmokoff et al., 2006). Hence, we hypothesized that there might be a correlation between the synthesis of flagellin and eDNA release. However, the outcome of qPCR assay did not completely support this hypothesis. Aerobic condition up-regulated the expression levels of *flaA* and *flaB* genes in *C. jejuni* F38011 wild-type, *spoT* and *recA* deletion mutant strains, but up-regulation was only shown at the first

day of biofilm formation. In contrast, the expression profiles of *flaA* and *flaB* under starvation condition was maintained at the similar levels as that under optimal condition during biofilm formation. Taken together, although the up-regulation of the *flaA* and *flaB* genes occurred along with the increase of eDNA release under aerobic stress, the down-regulation of *flaA* and *flaB* genes was not observed under the starvation condition where eDNA release was inhibited. Therefore, the correlation between flagellar and DNA release might be more specific to aerobic stress.

In the natural environment, *Campylobacter* is frequently isolated from the environment where *Salmonella* also appears, such as poultry farm and sewage water (Craven et al., 2000; Slader et al., 2002). Our previous study demonstrated that *C. jejuni* survived a longer period in a *Salmonella-C. jejuni* dual-species biofilm than that in a mono-species *C. jejuni* biofilm under aerobic condition (Feng et al., 2016). In the current study, we identified that the distinct spatial distribution of bacteria cells might be responsible for this survival advantage in a dual-species biofilm and eDNA played a role in maintaining spatial distribution by allocating different species of bacteria cells at different locations (**Figure 4-16**). In a well-developed dual-species biofilm, released DNA was identified to assemble and form stalk-like structure. At the bottom layer of the biofilm, eDNA tended to interact with *C. jejuni* cells and form a cover structure on top of *C. jejuni* cells. In contrast, the stalk-like eDNA structure tended to repel *Salmonella* cells and suspend *Salmonella* cells at the top layer of the biofilm. Therefore, *C. jejuni* was allocated at the bottom layer of biofilm away from the aerobic condition, and the top space was occupied by eDNA and *Salmonella* cells that further limit the penetration of oxygen. In the natural environment, the penetration of oxygen would be limited by this unique structure, which facilitates the survival of *C. jejuni* cell under aerobic condition.

4.6 Conclusion

In this study, a comprehensive investigation of *C. jejuni* biofilm formation in response to the environmental stresses was conducted. Oxidative stress and starvation stress could significantly influence the biofilm formation of a broad range of *C. jejuni* isolates, and the synchronous relationship was observed between biofilm formation and eDNA released from bacterial lysis. We propose that environmental stresses may induce a high rate of bacterial lysis and the subsequently released DNA from the dead bacterial cells to promote biofilm formation. This study for the first time reveals the essential role and multi-functions of eDNA in the biofilm formation of *C. jejuni* and provides insights into understanding their molecular mechanisms. The knowledge can aid in developing the intervention strategies to limit the prevalence and distribution of *C. jejuni* in the environment.

Chapter 5: Characterization and transcriptome analysis of *Campylobacter jejuni* persister cells

5.1 Summary

Persister cells account for a small fraction of bacterial populations that demonstrate antibiotic tolerance without developing a resistance mechanism. The presence of persister cells is proposed to be responsible for hard-to-treat infections. As a leading foodborne pathogen, *Campylobacter jejuni* is one of the major causes of human gastroenteritis worldwide. However, the information of *Campylobacter* persister cells is rarely reported. In this study, we validated the presence of *C. jejuni* persister cells and these persister cells demonstrated a multi-drug tolerance. The proportion of persister cells in the whole population varied due to different strains. Among different *C. jejuni* isolates tested in this study, a clinical isolate *C. jejuni* F38011 produced the highest level of persister cells, accounting for ~0.1% of the whole population. The transcriptome analysis by next-generation sequencing (RNA-seq) identified that the genes associated with ATP utilization and amino acid synthesis were considerably down-regulated in the persister cells of *C. jejuni* F38011. The shutdown of these genes indicated the low metabolic activity and the stop of growth which might well explain the tolerance of *C. jejuni* persister cells. This study validated the presence of *C. jejuni* persister cells and provided insight into understanding the formation mechanism of persister cells.

5.2 Introduction

The emergence and spread of antibiotic-resistant bacteria is a serious health risk which could infect human and cause hard to treat diseases (Neu, 1992). However, more and more evidence pointed out that antibiotic-resistant bacteria were not the only cause of chronic

infections. Bacteria can form a highly drug-tolerant subpopulation namely persister cells that might also contribute to the recalcitrance of infections to the chemotherapies (Monack et al., 2004; Mulcahy et al., 2010; Conlon, 2014). Persister cells are phenotypic variants of normal growing bacterial cells that are tolerant to antibiotics but not due to mutations. Hence, the genetic background of persister cells is identical to that of normal growing cells (Bigger, 1944; Keren et al., 2004b). Many pathogens have been validated to be able to form persister cells, such as *Escherichia coli*, *Staphylococcus aureus*, *Salmonella enterica* serovar Typhimurium, and *Pseudomonas aeruginosa* (Keren et al., 2004b).

Several mechanisms have been proposed to decipher the formation of persister cells. The one with the most supportive evidence was that persister cells were the cells in low metabolic activity (*i.e.*, slow or no growth) in response to stresses (Lewis, 2012). Brauner and colleagues systematically discussed the characteristics of antibiotic-resistant cells and persister cells (Brauner et al., 2016). They concluded that the survival mechanism of persister cells under antibiotic treatment was different from that of antibiotic-resistant cells. Specifically, the survival of antibiotic-resistant cells under antibiotic treatment was due to the mutation of antibiotic binding sites. In contrast, persister cells contained intact antibiotic binding sites. However, these persister cells were low in metabolic activity (*i.e.*, slow or non-growing cells) which led to a bad binding between target sites and antibiotics. A study using time-lapse microscopy and microfluidic chamber to investigate the formation of *E. coli* persister cells proved that *E. coli* persister cells were non-growing cells (Balaban et al., 2004). Another study revealed the similar mechanism of formation of persister cells from the molecular perspective that the expression level of biosynthesis and energy metabolism genes was considerably down-regulated in the persister cells of *E. coli*. In addition, fluorescent-labeled bacterial cells demonstrated a low level

of fluorescence when they transited from normal growing cells to persister cells (Shah et al., 2006). All these studies indicated that low metabolic activity was one of the major features of persister cells and might be responsible for the tolerance of persister cells.

Recent studies found the presence of toxin-antitoxin (TA) modules was also get involved in the formation of persister cells. TA modules comprised a pair of closely-linked genes encoding a stable "toxin" protein and a cognate "antitoxin" (the TA were proteins for type II, IV, V TA system; the TA were antisense RNA for type I, III TA system). The expression of RelE toxin in persister cells of *E. coli* was significantly higher than that in the normal growing cells of *E. coli* (Keren et al., 2004a). Another transcriptome analysis revealed that the over-expression of MazF toxin was observed along with the enhanced formation level of persister cells by over 10 times simultaneity (Vázquez-Laslop et al., 2006). Generally, a high proportion of persister cells was usually identified with the over-expression of toxins. However, the deletion of a single TA locus would not influence the formation of persister cells which indicated that that one set of TA module had limited functional effect on the formation of persister cells (Hansen et al., 2008; De Groote et al., 2009; Shan et al., 2015). Conlon and colleagues recently proved this hypothesis. They generated a 10 TA loci knockout mutant of *E. coli* and found a cumulative decrease of the formation level of persister cells along with each deletion of TA locus (Conlon et al., 2016). Hence, these TA systems might have a synergistic effect on influencing the formation of persister cells.

Campylobacter has been recognized as one of the leading causes of human gastrointestinal disease worldwide. Among the 18 species of *Campylobacter* identified so far, *C. jejuni* contributed to over 80% of *Campylobacter*-associated illness. The infectious dose of *Campylobacter* could be as low as 500 cells, and the infection caused by *Campylobacter* was

known as campylobacteriosis (Wilson et al., 2008). Campylobacteriosis has become one of the most reported foodborne illnesses in Canada, outnumbering the infections caused by *Listeria monocytogenes*, *Salmonella*, and *Shiga toxigenic E. coli* combined (Kalmokoff et al., 2006). *C. jejuni* infection is normally self-limiting within a week, and antibiotic treatment (*i.e.*, azithromycin, ampicillin, ciprofloxacin, tetracycline, erythromycin) could rapidly eliminate the *C. jejuni* and resolve the disease. However, more and more cases of *C. jejuni* infections shared similarity with hard to treat diseases which need continuous antibiotic treatment, and the symptoms can last for several weeks (Schwerer, 2002). Hence, these *C. jejuni* cells must be highly tolerant to antibiotics. It is reasonable to speculate that these infections might be caused by some *C. jejuni* cells in a particular survival state, such as persister cells (Cappelier et al., 1999a; Cappelier et al., 1999b). The knowledge about persister cells of *C. jejuni* is still in its infancy. The aims of this study are 1) to identify the presence of *C. jejuni* persister cells; 2) to investigate the formation mechanism of these persister cells.

5.3 Materials and methods

5.3.1 Strains and bacterial cultivation.

C. jejuni isolates used in this study are listed in **Table 5-1**. *C. jejuni* was cultured at 37°C in a microaerobic chamber (85% N_2, 10% CO_2, 5% O_2) on Mueller-Hinton (MH) agar supplemented with 5% defibrinated sheep blood (MHB agar) or in MH broth with constant shaking.

Table 5-1. Bacterial strains and plasmid used in the current study.

Strain	Description	Reference	MIC (μg/ml)	
			Ampicillin	Ciprofloxacin
C. jejuni F38011	human clinical isolate	(Feng et al., 2016)	8	0.08
C. jejuni Human 10	human clinical isolate	(Li et al., 2017)	4	0.08
C. jejuni 81116	human clinical isolate	(Neal-McKinney et al., 2010)	8	0.08
C. jejuni 1554	human clinical isolate	Dr. Michael Konkel (Washington State Univ.)	8	0.08

5.3.2 The minimum inhibitory concentration test.

The minimum inhibitory concentrations (MIC) of ampicillin and ciprofloxacin against different *C. jejuni* isolates were determined using the microtiter broth dilution method as described previously (Wiegand et al., 2008). Briefly, overnight *C. jejuni* culture was diluted in MH broth to a final concentration of ~8 log CFU/ml and challenged by ampicillin or ciprofloxacin in a 96-well microplate. The treatment was maintained for 24 hours at 37°C in a microaerobic condition. The optical density of *C. jejuni* suspension was then measured using a microplate reader at 540 nm (SpectraMax M2, Molecular Devices, Sunnyvale, USA). The MIC values of different antibiotics against *C. jejuni* were defined as the lowest concentration of antibiotics that could inhibit the visible growth of *C. jejuni* cells. In addition, these MIC values were compared with

the breakpoint of MIC against resistant strains to reflect the susceptibility of *C. jejuni* cells used in this study (Luber et al., 2003; Ge et al., 2013).

5.3.3 Kinetics of persister formation.

C. jejuni cells were grown to a late-exponential phase and diluted in MH broth to ~8 log CFU/ml. Then, *C. jejuni* culture was challenged by either ampicillin (100 μg/ml, ~10x MIC) or ciprofloxacin (1 μg/ml, ~10x MIC). The treatment was maintained at 37°C in a microaerobic chamber. At the designated time points, an aliquot of the sample was collected, washed, serially diluted with sterile phosphate buffered saline (PBS, pH ~7.0 to 7.2) and plated on MHB plate. The viable *C. jejuni* cells number was enumerated accordingly.

5.3.4 RNA extraction and RNA-seq analysis of *C. jejuni* F38011 persister cells.

C. jejuni F38011 persister cells and normal growing cells were collected (4 hours antibiotics treatment for persister cells; 4 hours cultivation for normal growing cells) by centrifugation at 8,000 ×*g* for 5 min at 4°C. The cell pellet was then washed twice with cold PBS. The total RNA was extracted using a RiboPure^{TM} RNA purification kit (Life Technologies, Grand Island, NY, USA) and purified using a MICROBExpress^{TM} bacterial mRNA enrichment kit (Life Technologies, Grand Island, NY, USA). The purified mRNA was sequenced in a 2×150 paired-end configuration on Illumine HiSeq 2000 platform (Life Technologies). The raw sequence data was compiled and subjected to CLC genomics workbench software (CLCBio, Cambridge, MA) for analysis. The sequence reads were mapped to the reference genome of *C. jejuni* F38011. The analyzed transcriptomes were sorted by false discovery rate (FDR)-adjusted P values (<0.05) and a relative expression change (>2 fold).

5.3.5 The prediction of type II toxin and antitoxin (TA) module in *C. jejuni* F38011.

The type II TA modules of *C. jejuni* F38011 were predicted using TADB: an updated database of bacterial type II toxin-antitoxin loci (2.0 version) (Shao et al., 2010). Briefly, the annotated genome sequence of *C. jejuni* F38011 was downloaded from GenBank (Accession: CP006851.1) and uploaded onto TADB. The parameters for TA prediction was set as follow: the Expect value (E value) was set as 0.01; the maximum length of potential toxin and antitoxin were set as 500 amino acids; the maximum distance (or overlap) between potential toxin and antitoxin was set as from -50 to 200 nucleotides. The result of TA prediction was validated by another TA prediction tool RASTA-Bacteria according to its guidelines (Sevin and Barloy-Hubler, 2007).

5.4 Results and discussion

5.4.1 *C. jejuni* form multidrug tolerant persister cells

Persister cells are phenotypic variants of normal growing cells that demonstrate the elevated tolerance to the treatment of antibiotics. The biphasic killing curve of bacterial cells under antibiotic treatment is a widely accepted signs that the persister cells present in the whole population. Both ampicillin and ciprofloxacin at bactericide concentration could rapidly eliminate the sensitive *C. jejuni* population and generate a killing curve with a sharp decrease viable cells. According to the MIC of ampicillin and ciprofloxacin against different *C. jejuni* isolates, including *C. jejuni* F38011, 81116, 1554 and human 10 (**Table 5-1**), the MIC of ampicillin was lower than 10 μg/ml (the breakpoint concentration of ampicillin for resistant strain) while the MIC of ciprofloxacin was lower than 1μg/ml (the breakpoint concentration of ciprofloxacin for resistant strain). Hence, none of these wild-type isolates were resistant strains.

Hence, it was possible to investigate the presence of persister cells using the killing curve method. In this study, ampicillin and ciprofloxacin were used to evaluate the presence and the formation level of persister cells of different *C. jejuni* isolates. The concentration of these two antibiotics was maintained at ~10 times of MIC which was 100 μg/ml for ampicillin and 1 μg/ml for ciprofloxacin. It should note that ampicillin and ciprofloxacin were distinct in the mechanism of action. Ampicillin is one of the beta-lactam antibiotics in the penicillin group, which inactivates bacteria by interfering the activity of enzyme transpeptidase and inhibiting the cell wall synthesis. Ciprofloxacin belongs to the fluoroquinolone class that inactivates bacteria by inhibiting DNA gyrase and cell division. Hence, the persister cells survived in both ampicillin and ciprofloxacin treatment could be regarded as multi-drug tolerant. Generally, the killing curves of both ampicillin and ciprofloxacin against several *C. jejuni* isolates including, *C. jejuni* 81116, 1554 and F38011 followed a classic biphasic pattern in which the susceptible population was rapidly eliminated, leaving a high tolerant subpopulation. In contrast, *C. jejuni* human 10 was rapidly eliminated to the level of the limit of detection of plating method by both ampicillin and ciprofloxacin. This results indicated that *C. jejuni* could form persister cells, but the capability of persister cells formation varied due to different strains. For the ampicillin-treated group, *C. jejuni* F38011 demonstrated the highest formation level of persister cells among four *C. jejuni* isolates (*i.e., C. jejuni* human 10, 1554 and 81116) in which persister cells of *C. jejuni* F38011 accounted for ~0.1% (~ Log 4 CFU/ml) of the total population. The level of persister cells of *C. jejuni* 8116 and 1554 was almost the same, which accounted for ~0.01% of the total population (**Figure 5-1A**). For the ciprofloxacin-treated group, persister cells of *C. jejuni* F38011, 81116, and 1554 demonstrated the similar formation level which accounted for ~0.05% of total population (**Figure 5-1B**).

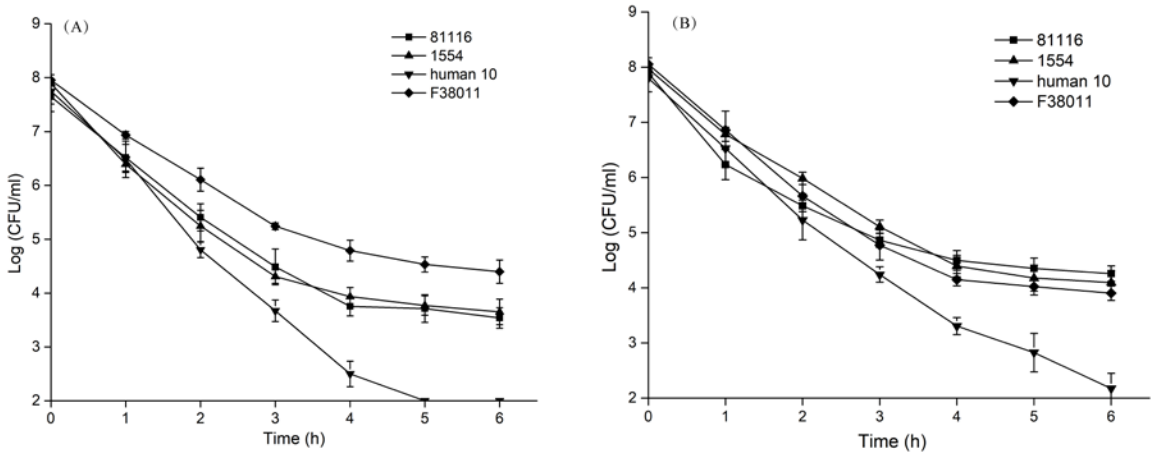

Figure 5-1. The presence of *C. jejuni* persister cells was examined by antibiotics over time. The late-exponentially growing culture of *C. jejuni* was treated with antibiotics (~10 times MIC). The presence of biphasic killing curve indicated that a high tolerant subpopulation could survive the antibiotic treatment. (A) Ampicillin treatment at the concentration of 100 μg/ml. (B) Ciprofloxacin treatment at the concentration of 1 μg/ml.

5.4.2 The transcriptional analysis by next-generation sequencing (RNA-seq) of persister cells of *C. jejuni* F38011.

Among all *C. jejuni* isolates tested for persister cells, *C. jejuni* F38011 demonstrated the highest formation level in both ampicillin and ciprofloxacin-treated groups. Due to this fact, *C. jejuni* F38011 was selected as the representative strain for the transcriptional analysis of persister cells. According to the killing kinetics of antibiotics, the killing curve of ampicillin and ciprofloxacin against *C. jejuni* F38011 was flatted out after 4 hours treatment (**Figure 5-1**). This indicated that persister cells of *C. jejuni* F38011 started to be the majority and accounted for a high proportion of the total population from 4 hours treatment. *C. jejuni* normal growing cells at 4 h (without the addition of antibiotics) were collected as the control. Since various regulations

were involved in the growth of bacteria and bacteria in different growth stages would show distinct expression profiles. In order to clarify the gene expression which was closely associated with the formation of persister cells, the global expression profile of the normal growing cells at 0 h (prior to the antibiotic treatment) and 4 h was measured and analyzed. According to the hierarchical clustering image (**Figure 5-2**), the gene expression profile of “control-0h” and “control-4h” were closely clustered and separated away from that of persister cells, indicating that the gene expression due to bacterial growth could be differentiated from that due to the formation of persister cells.

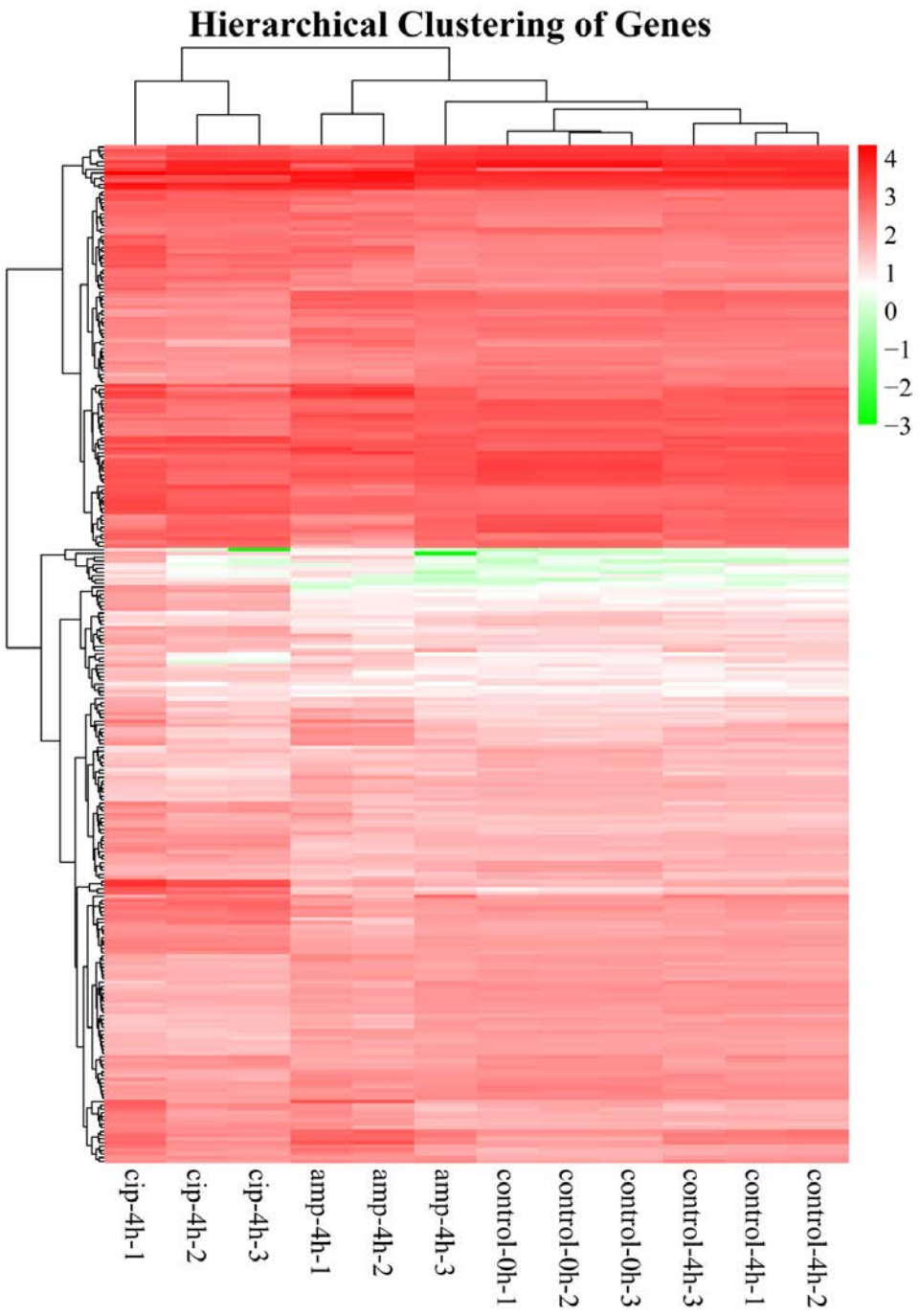

Figure 5-2. The hierarchical clustering of genes expression profile of *C. jejuni* F38011 cells. Each row was referred to a single gene. Each column was referred to a sample or a replicate. The "amp-4h" represented *C. jejuni* F38011 persister cells isolated by 4 hours ampicillin treatment; "cip-4h" represented *C. jejuni* F38011 persister cells isolated by 4 hours ciprofloxacin treatment;

"control-0h" represented *C. jejuni* F38011 normal growing cells prior antibiotic treatment; "control-4h" represented *C. jejuni* F38011 normal growing cells cultivated for 4 hours without antibiotic treatment.

Compared to normal growing cells ("control-4h"), *C. jejuni* F38011 persister cells isolated by ampicillin treatment ("amp-4h") contained 109 differentially expressed genes (> 2 fold change, adjusted *P*-value < 0.01), including 92 up-regulated genes and 17 down-regulated genes. Further analysis by GO enrichment function found that these differentially expressed genes were mainly associated with central metabolism of bacteria. To be specific, the genes involved in the synthesis of oxidoreductase, nitrate reductase, and inorganic anion transmembrane transporter were significantly (> 2 fold change, adjust *P*-value < 0.01) up-regulated while the genes involved in the synthesis of tryptophan were significantly (> 2 fold change, adjust *P*-value < 0.01) down-regulated (**Table 5-2**). In addition, GO pathway analysis identified that these differentially expressed genes were mainly distributed on the pathways of nitrogen metabolism, peptidoglycan biosynthesis, bacterial secretion system, caprolactam degradation, and D-glutamine and D-glutamate metabolism (**Table 5-3**).

Table 5-2. The functional analysis of differentially expressed genes in *C. jejuni* F38011 persister cells isolated by ampicillin treatment on the basis of gene ontology terms.

Gene ontology term	Cluster frequency	Corrected P-value	Genes
oxidoreductase activity, acting on other nitrogenous compounds as donors	4/55 genes, 7.3%	0.00221	CJH_RS06780, CJH_RS03870, CJH_RS03875, CJH_RS03865
nitrate reductase activity	3/55 genes, 5.5%	0.00962	CJH_RS03870, CJH_RS03875, CJH_RS03865
inorganic anion transmembrane transporter activity	3/55 genes, 5.5%	0.17261	CJH_RS05870, CJH_RS02610, CJH_RS02585
tryptophan synthase activity	2/ 55 genes, 3.6%	0.19766	CJH_RS01710, CJH_RS01705

Table 5-3. GO pathway enrichment analysis of DEGs in *C. jejuni* F38011 persister cells isolated by ampicillin treatment.

Pathway	DEGs with pathway annotation	P-value	Pathway ID
Nitrogen metabolism	4/76, 5.26%	005955841	ko00910
Peptidoglycan biosynthesis	4/76, 5.26%	0.04126756	ko00550
Bacterial secretion system	5/76, 6.58%	0.05178325	ko03070
Caprolactam degradation	1/76, 1.32%	0.05608856	ko00930
D-Glutamine and D-glutamate metabolism	2/76, 2.63%	0.08653091	ko00471

Compared to normal growing cells ("control-4h"), *C. jejuni* F38011 persister cells isolated by ciprofloxacin treatment ("cip-4h") contained 139 differentially expressed genes (> 2 fold change, adjusted *P*-value < 0.01), including 79 up-regulated genes and 60 down-regulated genes. Further analysis by GO enrichment function identified that the genes responsible for the synthesis of oxidoreductase, NADH dehydrogenase, and the utilization of pyridoxal phosphate were significantly (> 2 fold change, adjusted *P*-value < 0.01) down-regulated. While the genes associated with the synthesis of amidine-lyase were significantly (> 2 fold change, adjusted *P*-value < 0.01) up-regulated (**Table 5-4**). In addition, GO pathway analysis identified that these differentially expressed genes were mainly distributed on the pathways of alanine, aspartate and glutamate metabolism, oxidative phosphorylation, arginine biosynthesis, and D-Glutamine and D-glutamate metabolism (**Table 5-5**).

Table 5-4. The functional analysis of differentially expressed genes in *C. jejuni* F38011 persister cells isolated by ciprofloxacin treatment on the basis of gene ontology terms.

Gene ontology term	Cluster frequency	Corrected P-value	Genes	
oxidoreductase activity, acting on NAD(P)H	7/84 genes, 8.3%	0.00270	CJH_RS08075, CJH_RS08060, CJH_RS08055, CJH_RS08070	CJH_RS08065, CJH_RS08045, CJH_RS08050,
NADH dehydrogenase activity	5/84 genes, 6.0%	0.02313	CJH_RS08045, CJH_RS08050, CJH_RS08065	CJH_RS08055, CJH_RS08070,
pyridoxal phosphate binding	5/84 genes, 6.0%	0.69163	CJH_RS01595, CJH_RS03015, CJH_RS01495	CJH_RS06960, CJH_RS01120,
amidine-lyase activity	3/84 genes, 3.6%	0.16215	CJH_RS00115, CJH_RS04595	CJH_RS06965,

Table 5-5. GO pathway enrichment analysis of DEGs in *C. jejuni* F38011 persister cells isolated by ciprofloxacin treatment.

Pathway	DEGs with pathway annotation	P-value	Pathway ID
Alanine, aspartate and glutamate metabolism	8/100, 8%	0.0006002362	ko00250
Oxidative phosphorylation	11/100, 11%	0.007054049	ko00190
Arginine biosynthesis	4/100, 4%	0.01571895	ko00220
D-Glutamine and D-glutamate metabolism	2/100, 2%	0.1382485	ko00471

We noticed that *C. jejuni* F38011 persister cells isolated by ampicillin treatment shared various down-regulated genes with *C. jejuni* F38011 persister cells isolate by ciprofloxacin treatment. There shared down-regulated genes were mainly involved in energy metabolism and amino acid synthesis. However, they could not be clustered due to the low frequency of pathway annotation (**Table A-1A for ampicillin group and 1B for ciprofloxacin group independent file**). In addition, a specific term of genes associated with the functions of ATP binding (*i.e.* CJH_RS05510, CJH_RS00725, CJH_RS04985, CJH_RS06245, CJH_RS02020, CJH_RS06235, CJH_RS00715, CJH_RS07595, CJH_RS04600, CJH_RS08050, and CJH_RS08045) and amino acid synthesis (*i.e.* CJH_RS01710, CJH_RS01705, CJH_RS03780, CJH_RS05180, CJH_RS02190, CJH_RS06960, and CJH_RS01595) was found to be significantly down-regulated in both ampicillin-isolated and ciprofloxacin-isolated *C. jejuni* F38011 persister cells. The shutdown of ATP utilization and amino acid synthesis typically indicated a low metabolic

activity. Previous studies indicated that the bacteria with a low level of metabolic activity usually were more tolerant than normal growing cells(Betts et al., 2002; Voskuil et al., 2004; Asakura et al., 2007b). For example, dormant bacterial cells were highly tolerant to antibiotic treatment due to the low metabolic activity (Levin and Rozen, 2006; Dörr et al., 2010). Therefore, we speculated that the tolerance of *C. jejuni* persister cells against ampicillin and ciprofloxacin was due to the low metabolic activities.

Type II TA modules were proposed to play important roles in the formation of persister cells (Gerdes et al., 2005). For example, the activation of *hipBA* TA module could increase the formation level of *E. coli* persister cells (Keren et al., 2004a). For *S.* Typhimurium, 14 type II TA loci had been identified to contribute to the formation of persister cells (Helaine et al., 2014). However, no type II TA modules were predicted either by TADB or RASTA-bacteria, indicating a high probability that the well-recognized type II locus was absent in in *C. jejuni* F38011 genome. There might be some uncharacterized type II modules that were responsible for the formation of *C. jejuni* F38011 persister cells.

In this study, the presence of *C. jejuni* persister cells was validated by the antibiotic treatment. The transcription profile of these *C. jejuni* F38011 persister cells shared a high similarity as that of dormant cells which were low in metabolic activities. However, the signature TA modules that responsible for the formation of persister cells in other bacteria (*i.e., E. coli* and *Salmonella*) were not present in *C. jejuni* F38011. These findings provided new insights into understanding the survival of *C. jejuni* as persister cells and would aid the investigation of anti-persister cells treatments.

Chapter 6: Whole transcriptome sequencing analysis of synergistic antimicrobial effect of metal oxide nanoparticles and ajoene on *Campylobacter jejuni*

6.1 Summary

Campylobacter jejuni is one of the leading foodborne pathogens worldwide. The *Campylobacter* infections are usually associated with the consumption of contaminated poultry meat. Antibiotic are commonly used in poultry farm to prevent the contamination of *Campylobacter* in chicken. Surveillance studies found a close correlation between the use of antibiotic in poultry and emergence of antibiotic-resistant *Campylobacter*. Hence, alternative antimicrobial approaches are highly desired. The significance of our research is in developing an alternative antimicrobial approach against *C. jejuni*. In this study, two metal oxide (*i.e.*, Al_2O_3 and TiO_2) nanoparticles and ajoene, a garlic-derived organosulfur compound, were identified to be effective antimicrobials against *Campylobacter jejuni*. By combining ajoene and metal oxide nanoparticle, a significant synergistic antimicrobial effect was achieved. Whole transcriptome sequencing (RNA-seq) analysis was applied to reveal the antimicrobial mechanism and identify the roles of ajoene and metal oxide nanoparticles in the synergistic treatment. Ajoene and metal oxide nanoparticles mediated a two-phase antimicrobial mechanism. Low concentration of ajoene served as the inducing factor at the first phase that caused damage to cell membranes and increased the susceptibility of *C. jejuni*. Metal oxide nanoparticles served as the active factor at the second phase that directly targeted the injured cells and physically disrupted cell structure. The knowledge of this study can be applied to reduce the prevalence and dissemination of *C. jejuni* in the poultry industry as well as in the environment.

6.2 Introduction

Metal oxide nanoparticles have been widely used in our daily life. For example, aluminum oxide (Al_2O_3) nanoparticles have been approved and used as the material of personal care products (Sadiq et al., 2009). Titanium dioxide (TiO_2) is a common additive in many personal care commodities (*e.g.*, toothpaste), pharmaceuticals and food products, such as chewing gums and candies (Weir et al., 2012). Recent studies have demonstrated that metal oxide nanoparticles could efficiently inactivate a wide range of foodborne pathogens, including *Salmonella*, *Escherichia coli* O157:H7, *Listeria monocytogenes*, and *Campylobacter*, due to their unique electrical, chemical and physical properties (Chen et al., 2014). However, the individual treatment of metal oxide nanoparticles against drug-resistant bacteria might fail. For example, TiO_2 nanoparticles could not completely inactivate the drug-resistant *Cupriavidus metallidurans* due to the overexpression of membrane restoration elements (Simon-Deckers et al., 2009). In addition, the high dose and very-frequently use of nanoparticles could also lead to negative outcomes. For example, Al_2O_3 nanoparticles were found to increase the efficiency of horizontal transfer of antibiotic resistance genes (conjugative transfer of RP4 plasmid) from *E. coli* to *Salmonella* by up to 200 fold (Qiu et al., 2012). Under this circumstances, the modification of metal oxide nanoparticle or the combination treatment with other antimicrobials to achieve a synergistic treatment were highly desired.

Ajoene is an organosulfur compound derived from oil-macerated or ether-extracted garlic oil. As the major components of garlic oil, it has been used in traditional medicine to combat illness for hundreds of years (Goncagul and Ayaz, 2010). Previous studies found that ajoene could significantly inactivate a broad range of Gram-positive and Gram-negative bacteria, including *Cronobacter sakazakii* (Feng et al., 2014), *Helicobacter pylori* (Ohta et al., 1999), *Bacillus*

cereus and *Bacillus subtilis* (Naganawa et al., 1996) and *Staphylococcus aureus* (Yoshida et al., 1998). When it was combined with tobramycin, an aminoglycoside antibiotic derived from *Streptomyces tenebrarius*, a strong synergistic antimicrobial effect against *Pseudomonas aeruginosa* was observed, and this combination treatment was even effective against biofilm (Jakobsen et al., 2012). Compared to other garlic-derived thiosulfinates (*i.e.,* allicin), ajoene demonstrated a more potential to be applied in food industry due to its high stability (Ankri and Mirelman, 1999).

Transcriptome analysis using next-generation sequencing could offer the profiling of gene expression in a high-throughput manner, genome annotation and discovery of non-coding RNA. It has been applied in the investigation of bacterial responses (*e.g.*, *E. coli* O157:H7, *L. monocytogenes* and *Salmonella*) to various stresses, including the oxidative stress (Wang et al., 2009), inorganic and organic acids (King et al., 2010), lysates of lettuce leaves (Kyle et al., 2010), chlorine dioxide (Pleitner et al., 2014), hyperosmotic and low temperature (Durack et al., 2013), dehydration (Gruzdev et al., 2012), starvation in peanut oil (Deng et al., 2012), and chlorine (Wang et al., 2010). In the current study, we tested the individual and synergistic antimicrobial effect of ajoene and metal nanoparticles (Al_2O_3 and TiO_2 nanoparticles) against *C. jejuni*, a leading bacterial cause of human gastroenteritis. The mechanism of the stress and sub-lethal injury of *C. jejuni* by those above single and combined antimicrobial treatments were investigated using high-throughput whole transcriptome sequencing (RNA-seq) analysis. The knowledge from this study can aid the development of innovative antimicrobial treatments to reduce campylobacteriosis and other foodborne illnesses.

6.3 Materials and methods

6.3.1 Chemicals and reagents

Al_2O_3 nanoparticles and TiO_2 nanoparticles were purchased from Sigma-Aldrich (St Louis, MO, USA). The size of Al_2O_3 nanoparticles was in the range of with the size of 30-60 nm and size of TiO_2 nanoparticles were around 21 nm. Ajoene was synthesized according to the protocols described in our previous study (Feng et al., 2014).

6.3.2 Bacterial strains and culture methods

Four *C. jejuni* isolates including, F38011, ATCC 33560, y110539, and z110526, were used in this study. All of these strains were stored at -80°C in Mueller-Hinton (MH) broth containing 75% citrated bovine blood and 12% glycerol. *C. jejuni* cells were routinely cultivated either on MH agar plates supplemented with 5% citrated bovine blood or in 5 ml of MH broth at 37°C for overnight under a microaerobic condition (85% N_2, 10% CO_2, 5% O_2). One milliliter of each *C. jejuni* culture (~ca. 9 log CFU/mL) was centrifuged at 8,000 ×*g* for 10 min at 4°C. The supernatant was discarded, and *C. jejuni* pellets were washed three times using sterile PBS (pH 7.0) and resuspended in sterile MH broth. An equal volume (2 mL) of each *C. jejuni* culture was combined as a cocktail to an initial concentration of ~8 log CFU/ml for the subsequent antimicrobial tests.

6.3.3 Antimicrobial effects of metal oxide nanoparticles and ajoene against *C. jejuni*

The stock solution of Al_2O_3 nanoparticle and TiO_2 nanoparticles were prepared by diluting Al_2O_3 nanoparticle suspension (20% w/v in H_2O) and TiO_2 nanoparticles (in a powder form) independently with sterile deionized water to a final concentration of 1 M. The stock solution

was stored at room temperature. Ajoene was dissolved in DMSO to a final concentration of 0.1 M and stored at 4°C. Different volumes of ajoene were added to *C. jejuni* culture, resulting in the final concentrations of 0.06, 0.125, 0.25, 0.5, and 1 mM. The antimicrobial tests of ajoene and metal oxide nanoparticle against *C. jejuni* were conducted as follow: the working stock of metal oxide nanoparticle suspensions was filtered through an aluminum oxide membrane filter (20 nm pore size, Anodisc; Whatman Inc., Clifton, NJ, USA) to harvest a nanoparticle-free solution. This water and DMSO (1 mM) were used as control groups. The stock solution of ajoene and metal oxide nanoparticles were mixed with *C. jejuni* culture to a series of final concentrations of 0, 0.5, 1, 2, 4, 8, and 16 mM. The treatments were conducted at both 22°C and 37°C for up to 24 h in a microaerobic condition. At 0, 2, 4, 7, 10, and 24 h, viable *C. jejuni* cells were enumerated on MH agar plates supplemented with 5% of defibrinated sheep blood.

6.3.4 Synergistic antimicrobial effect of metal oxide nanoparticle and ajoene against *C. jejuni*

The synergistic antimicrobial treatment was conducted by challenging *C. jejuni* culture with the combination of ajoene and metal oxide nanoparticles (*i.e.*, Al_2O_3 nanoparticles and TiO_2 nanoparticles). The concentration of ajoene in the combination treatment was maintained at 0.06 mM, while the metal oxide nanoparticles were diluted to a series of final concentration from 0, 0.5, 1, 2, 4, 8, to 16 mM. The treatment was conducted at both 22°C and 37°C in a microaerobic condition with constant shaking. At 0, 2, 4, 7, 10, and 24 h, the viable *C. jejuni* cells were enumerated on MH blood agar plates supplemented with 5% of defibrinated sheep blood.

6.3.5 RNA-seq and real-time polymerase chain reaction (qPCR)

C. jejuni F38011 was used as the representative strain for RNA-seq analysis. Overnight *C. jejuni* F38011 culture was diluted to a OD_{540} ~0.3, washed with sterile PBS, resuspended in MH broth and then challenged by (1) 1 mM ajoene, (2) 16 mM Al_2O_3 nanoparticles, (3) 16 mM TiO_2 nanoparticles, (4) a combination of 0.06 mM ajoene and 4 mM Al_2O_3 nanoparticles, and (5) a combination of 0.06 mM ajoene and 4 mM TiO_2 nanoparticles, respectively, for 1 h at 37°C in microaerobic conditions. The samples were collected by centrifugation at 8,000 ×*g* for 5 min at 4°C. The total RNA was extracted using a RiboPure™ RNA purification kit (Life Technologies, Grand Island, NY, USA).

The rRNA was removed using a MICROBExpress™ bacterial mRNA enrichment kit (Life Technologies, Grand Island, NY, USA). The purified mRNA was sequenced on an Ion Torrent sequencing system (Life Technologies).The raw sequencing data were compiled and analyzed using CLC genomics workbench software (CLCBio, Cambridge, MA). The transcriptomes data were sorted by false discovery rate (FDR)-adjusted P values (< 0.05) and a relative fold change of expression (> 2 fold). The differentially expressed genes were submitted to DAVID for cluster analysis. An aliquot of the purified mRNA was used to generate cDNA using SuperScript™ II Reverse Transcriptase (Invitrogen). The quantitative PCR (qPCR) was performed in triplicate using Power SYBR green PCR Master Mix (Applied Biosystems, Warrington, United Kingdom) on ABI Prism 7000 Fast instrument (Life Technologies). The primers used for qPCR were listed in **Table 6-1.** The amplification efficiency of each gene was determined using a standard curve method and the fold change of each gene was determined using the comparative Ct method (Schmittgen and Livak, 2008).

Table 6-1. The primers of selected genes used in qPCR validation

Primer	Sequence (5'-3')
rpoA RT-F	CGAGCTTGCTTTGATGAGTG
rpoA RT-R	AGTTCCCACAGGAAAACCTA
slyD RT-F	TGCGGTTCAAACTTTACCAA
slyD RT-R	GTTTCGCCATTTTCACCTTC
CJH_03855 (Cj0768) RT-F	GGGTACGTGAAATGCCTTTT
CJH_03855 (Cj0768) RT-R	AGCTTGCGATAATAGGAGGG
CJH_05030 (Cj1004) RT-F	ACAACATAATTTCAAAGCGCC
CJH_05030 (Cj1004) RT-R	TTTCCTTCCAAGCTCCATCT
CJH_02460 (Cj0689) RT-F	ATGCTTGAAAGTGCTGCAAA
CJH_02460 (Cj0689) RT-R	GGATTAGCACTAAGTCCGCT
CJH_08660 (Cj1662) RT-F	CGTGGTGCAAAATTTAAGCG
CJH_08660 (Cj1662) RT-R	TGATTGCTTGTGTTTTGGCT
CJH_07030 (Cj1385) RT-F	AGTCTTGTGCCTTTGATGGA
CJH_07030 (Cj1385) RT-R	GGACTAAAGGCAGCTTGTTC
CJH_02840 (Cj0561) RT-F	TTCCTGTGTTTTAGCCTCCA
CJH_02840 (Cj0561) RT-R	TAATATCCCTTGCACCCACA
CJH_08840 (Cj0439) RT-F	AGCGGAAGAGATGAAAATGC
CJH_08840 (Cj0439) RT-R	GCGTTCTTTTGCACCCTTAT

6.3.6 Statistical analysis

All of the experiments were performed at least three times. The results are expressed as the means of the results of three independent replicates ± the standard deviations. The differences between samples were shown to be significant ($P < 0.05$) by one-way analysis of variance (ANOVA) using the Matlab software.

6.4 Results

6.4.1 Antibacterial effect of ajoene against *C. jejuni.*

Ajoene demonstrated a concentration-dependent antimicrobial effect against *C. jejuni* cocktail (**Figure 6-1**). However, the antimicrobial effect of ajoene varied due to different treatment temperatures (*i.e.*, 22°C and 37°C). For example, viable *C. jejuni* cells were reduced to non-detectable levels after 7 h treatment by 1 mM ajoene at 37°C. In contrast, the same treatment could only generate a ~1 log CFU/mL reduction at 22°C. It was obvious that the temperature could influence the metabolic activity of the bacterial cell. Typically, the metabolic activity of bacteria was higher under high temperature than that under low temperature. Hence, we speculated that ajoene was more effective in inactivating the bacteria with high metabolic activity.

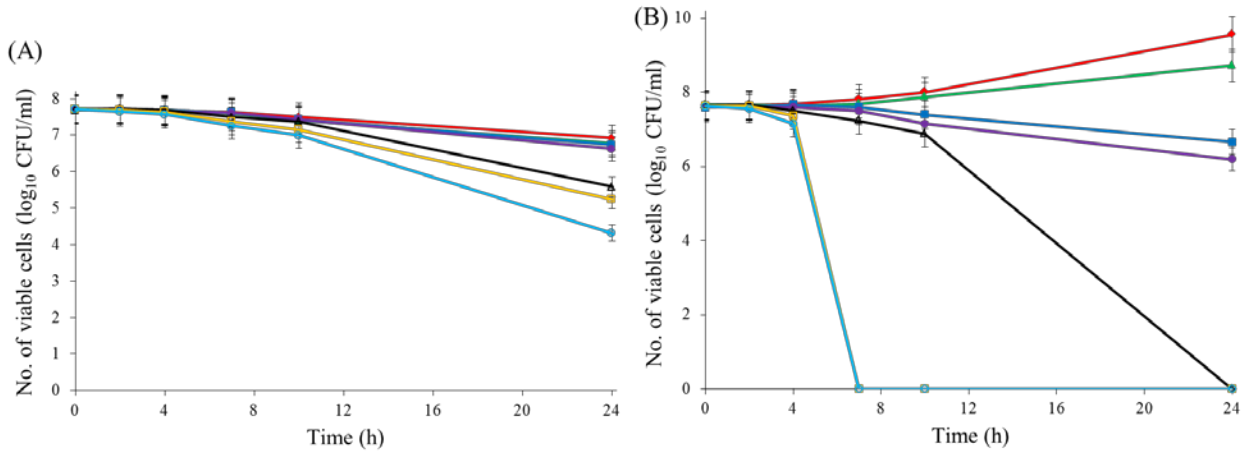

Figure 6-1. The individual ajoene treatment could generate a bacteriostatic effect on *C. jejuni* cocktail at 22°C (A) but a bactericidal effect at 37°C (B). Different colors indicate different samples (red line: control group without treatment; green line: samples treated with DMSO at the concentration of 1 mM; blue line: samples treated with ajoene at the concentration of 0.06 mM; purple line: samples treated with ajoene at the concentration of 0.125 mM; black line: samples treated with ajoene at the concentration of 0.25 mM; orange line: samples treated with ajoene at the concentration of 0.5 mM; light blue line: samples treated with ajoene at the concentration of 1 mM).

6.4.2 Antibacterial effect of metal oxide nanoparticles against *C. jejuni.*

We observed a concentration-dependent antimicrobial effect of individual metal oxide nanoparticle (*i.e.*, Al_2O_3 and TiO_2 nanoparticles) against *C. jejuni.* Compared to Al_2O_3, TiO_2 nanoparticles treatment could cause a better antimicrobial effect against *C. jejuni* when they were applied at the same concentration (**Figure 6-2** and **Figure 6-3**). For example, 16 mM TiO_2 nanoparticles treatment at 22°C could completely inactivate *C. jejuni* cells within 24 h. In contrast, Al_2O_3 nanoparticles treatment at same concentration and temperature could only cause

~2 log CFU/mL reduction of *C. jejuni* cells by 24 h. Similar to ajoene, the antimicrobial effect of Al_2O_3 and TiO_2 nanoparticles also followed a temperature-dependent pattern. For example, the antimicrobial effect of 16 mM TiO_2 nanoparticles at 37°C was significantly ($P < 0.05$) higher than that at 22°C. At 37°C, 16 mM TiO_2 nanoparticles treatment could completely inactivate *C. jejuni* cells within 10 h (**Figure 6-3A**). In order to achieve the same antimicrobial effect, the treatment at 22°C had to be extended to 24h (**Figure 6-2A**).

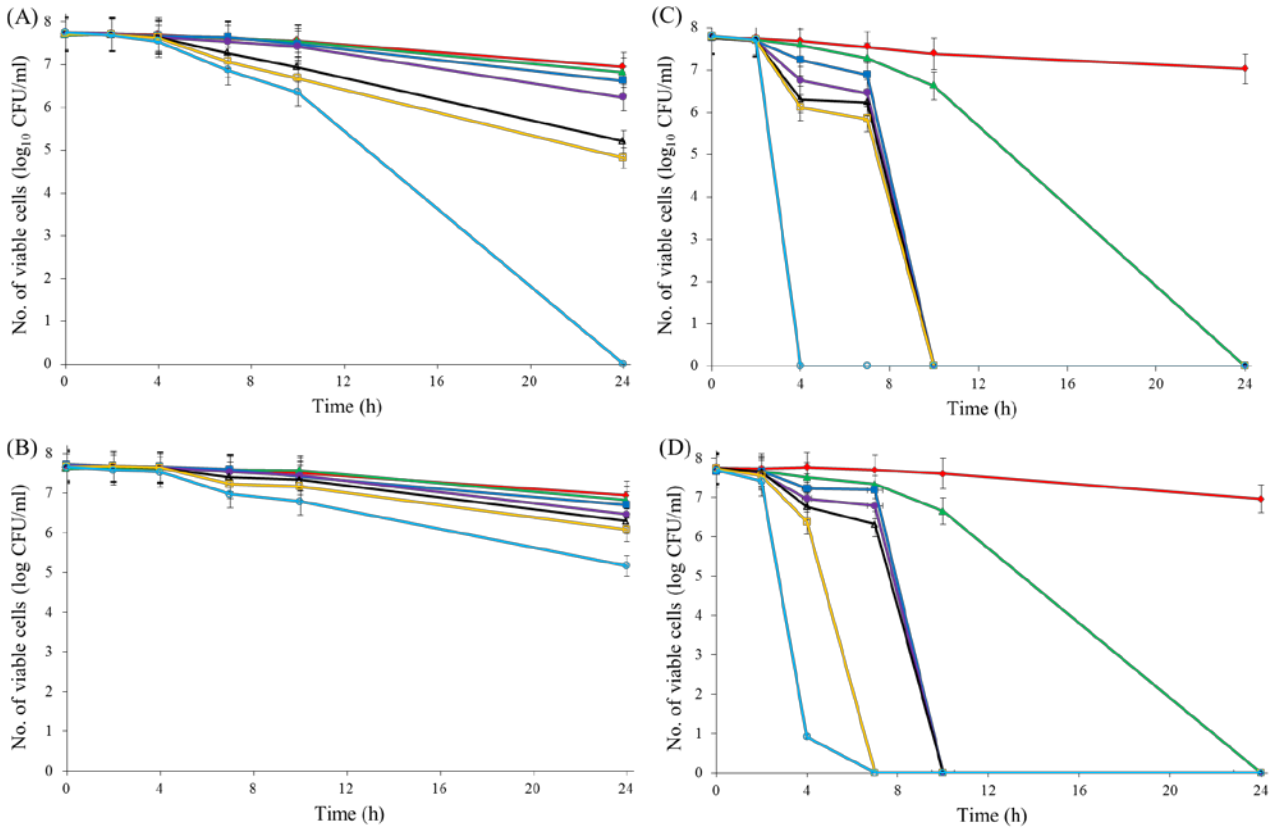

Figure 6-2. Synergistic antimicrobial effect of ajoene and metal oxide nanoparticles against *C. jejuni* at 22°C. Panels: (A) Antimicrobial effect of TiO_2 nanoparticles; (B) Antimicrobial effect of Al_2O_3 nanoparticles; (C) Synergistic antimicrobial effect of 0.06 mM ajoene and TiO_2 nanoparticles; and (D) Synergistic antimicrobial effect of 0.06 mM ajoene and Al_2O_3 nanoparticles. Different symbols indicate different concentrations of metal oxide nanoparticles (red line: 0 mM; green line: 0.5 mM; blue line: 1 mM; purple line: 2 mM; black line: 4 mM; orange line: 8 mM; light line: 16 mM).

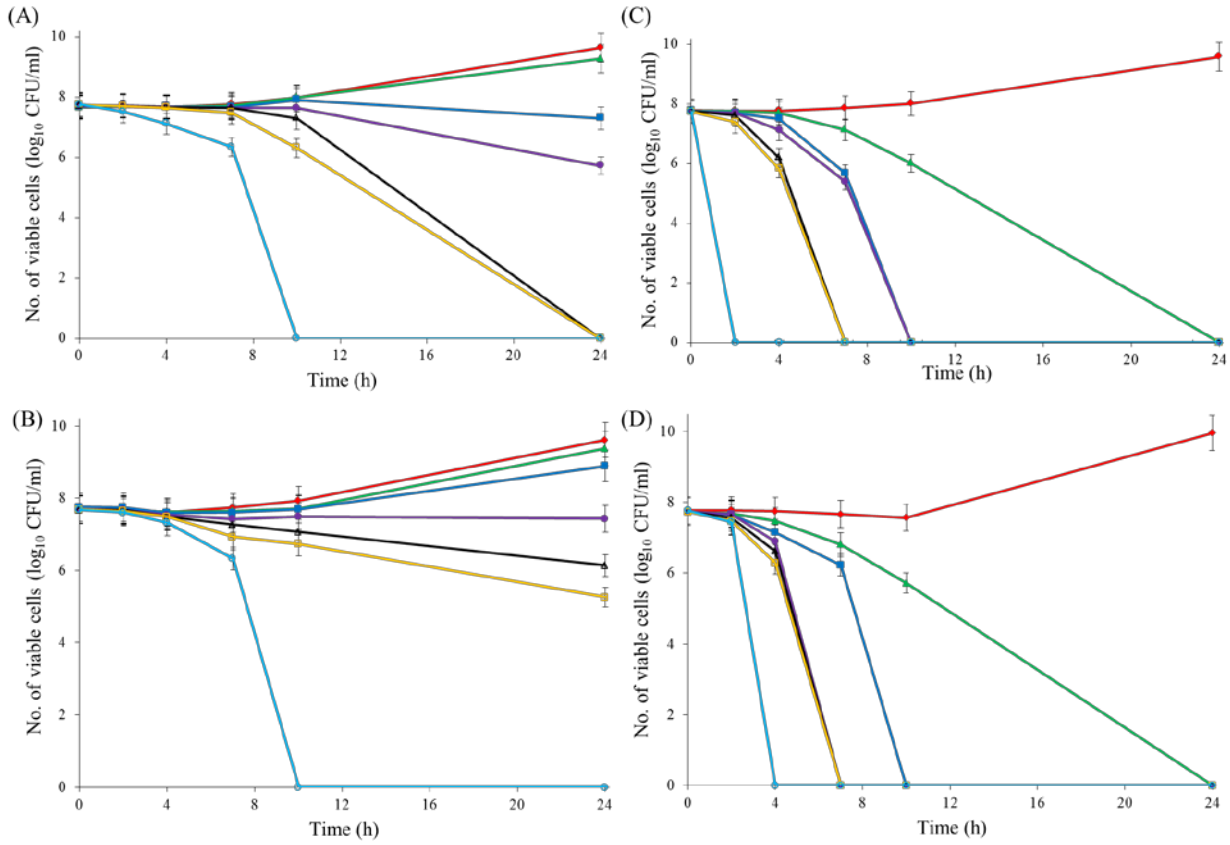

Figure 6-3. Synergistic antimicrobial effect of ajoene and metal oxide nanoparticles against *C. jejuni* at 37°C. Panels: (A) Antimicrobial effect of TiO_2 nanoparticles; (B) Antimicrobial effect of Al_2O_3 nanoparticles; (C) Synergistic antimicrobial effect of 0.06 mM ajoene and TiO_2 nanoparticles; and (D) Synergistic antimicrobial effect of 0.06 mM ajoene and Al_2O_3 nanoparticles. Different symbols indicate different concentrations of metal oxide nanoparticles (red line: 0 mM; green line: 0.5 mM; blue line: 1 mM; purple line: 2 mM; black line: 4 mM; orange line: 8 mM; light blue line: 16 mM).

6.4.3 Synergistic antimicrobial effect of metal oxide nanoparticle and ajoene against *C. jejuni*.

A synergistic antimicrobial effect was observed for the combined treatment of ajoene and metal oxide nanoparticles (*i.e.*, Al_2O_3 and TiO_2 nanoparticles) at both 22°C and 37°C (**Figure 6-2C** and **Figure 6-3D**). The concentration of metal oxide nanoparticles to start a synergistic antimicrobial effect against *C. jejuni* was 0.05 mM. The higher concentration of metal oxide nanoparticles in the combination treatment the better the synergistic antimicrobial effect was. For example, ajoene with 1 mM of Al_2O_3 or TiO_2 nanoparticles achieved a bactericidal effect within 10 h. In comparison, the synergistic treatment completely inactivated *C. jejuni* within 4 h when the concentration of Al_2O_3 or TiO_2 nanoparticles reached to 16 mM. The influence of temperature on the antimicrobial effect almost disappeared in the combination treatment. Thus, the antimicrobial effect of combination treatment at 22°C was similar to that at 37°C. In sum, the synergistic bactericidal effect was mainly associated with the exposure time and antimicrobial concentration rather than temperature.

6.4.4 Transcriptomic response of *C. jejuni* treated with metal oxide nanoparticles and ajoene.

The synergistic antimicrobial mechanism of the combination of ajoene and metal oxide nanoparticles against *C. jejuni* was investigated using RNA-seq analysis. The differentially expressed genes (FDR-adjusted P values (< 0.05) and a relative fold change of expression > 2 fold) derived from different treatment groups were summarized in the **Table A-2** (**independent file**). The RNA-seq results were further validated by qPCR. The expression profiles of selected genes (CJH_02840, CJH_07030, CJH_08840, CJH_03855, CJH_05030, CJH_08660 and

CJH_02460) determined by qPCR were consistent with that determined by RNA-seq (**Figure 6-4**).

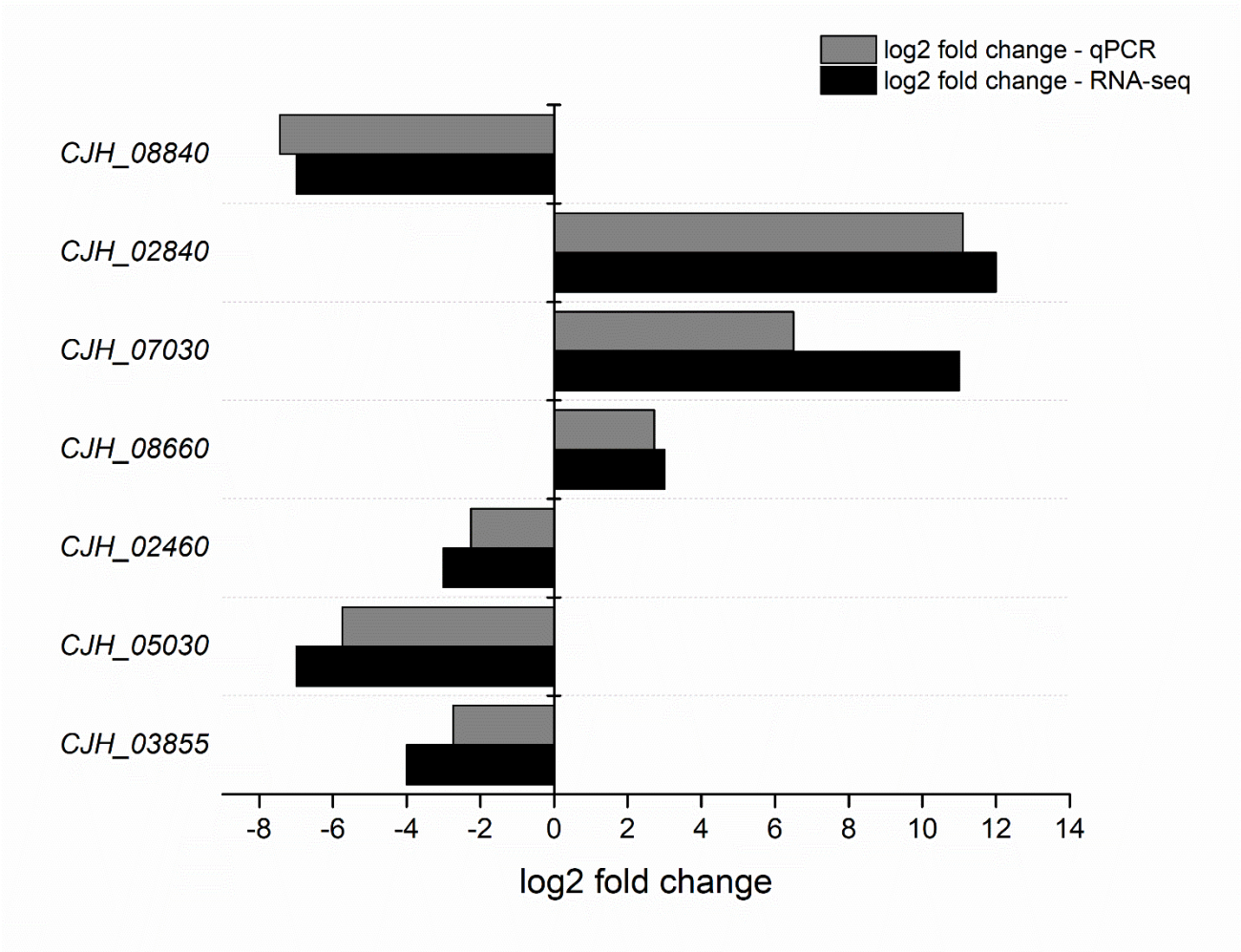

Figure 6-4. RNA-seq results were validated by qPCR. The expression profiles of these 7 genes were selected as the representatives from the treatment of 1 mM ajoene, 16 mM Al_2O_3 nanoparticles, 16 mM TiO_2 nanoparticles, 0.06 mM ajoene and 4 mM Al_2O_3 nanoparticles, and 0.06 mM ajoene and 4 mM TiO_2 nanoparticles.

The differentially expressed genes of *C. jejuni* F38011 due to different treatment were categorized based on the functional terms using DAVID analysis (Huang et al., 2009) and listed in **Table 6-2** and **Table 6-3**. The ajoene treatment induced a relatively wide range of transcriptional response in *C. jejuni* F38011, including 34 up-regulated genes and 18 down-regulated genes. The up-regulated genes could be categorized into two groups on the basis of functional terms: (1) the function responsible for transcription-translation and (2) the function responsible for ATP utilization (**Figure 6-5A** and **B**). In addition, a set of genes responsible for efflux pump, including *cmeA, cmeB,* and *cmeC,* and an oxidative stress response gene *katA* were also significantly (FDR-adjusted P values (< 0.05) and a relative fold change of expression > 2 fold) up-regulated (**Table A-2**). However, due to the low frequency of corresponding functional terms, these genes were not clustered. Down-regulated genes were clustered in one group that referred to the term of the integral cell membrane (**Figure 6-5C**). In addition, a DNA repair-associated gene *recN* and a chemotaxis-associated gene *cheY* were also significantly (FDR-adjusted P values (< 0.05) and a relative fold change of expression > 2 fold) down-regulated (**Table A-2**). Taken together, low concentration of ajoene (1 mM) could induce a mild but not lethal stress in *C. jejuni* F38011.

Table 6-2. The differentially expressed genes in *C. jejuni* F38011 induced by 1 mM ajoene treatment.

Regulation category and annotation cluster	Term and function	Fold enrichment	Benjamini FDR
Upregulation			
1 (enrichment score, 11.56)	GO:0019843; rRNA binding	18	0.00
	GO:0003723; RNA binding	16	0.00
	GO:0019843; rRNA binding	14	0.00
	GO:0005840; ribosome	14	0.00
	GO:0030529; intracellular ribonucleoprotein complex	11	0.00
	GO:0005840; ribosome	13	0.00
	GO:0006412; translation	8.7	0.00
	GO:0003735; structural constituent of ribosome	6.9	0.00
	GO:0005840; ribosome	8.1	0.00
	GO:0015934; large ribosomal subunit	22	0.02
2 (enrichment score, 0.12)	GO:0005524; ATP binding	1.2	1.00
	GO:0000166; nucleotide binding	1	1.00
	GO:0005524; ATP binding	0.8	1.00
downregulation			
Regulation category and	Term and function	Fold	Benjamini

annotation cluster		enrichment	FDR
1 (enrichment score, 0.27)	GO:0016021; integral component of membrane	1.5	0.93
	GO:0016021; transmembrane helix	1.3	1.00
	GO:0016021; transmembrane	1.3	1.00
	GO:0005886; plasma membrane	1.2	1.00

Table 6-3. The differentially expressed genes in *C. jejuni* F38011 induced by 16 mM TiO_2 nanoparticles treatment.

Regulation category and annotation cluster	Term and function	Fold enrichment	Benjamini FDR
Upregulation			
1 (enrichment score, 0.89)	GO:0016021; transmembrane helix	3.1	0.70
	GO:0016021; transmembrane	3.1	0.46
	GO:0005886; plasma membrane	2.8	0.42
	GO:0016021; integral component of membrane	1.8	0.57

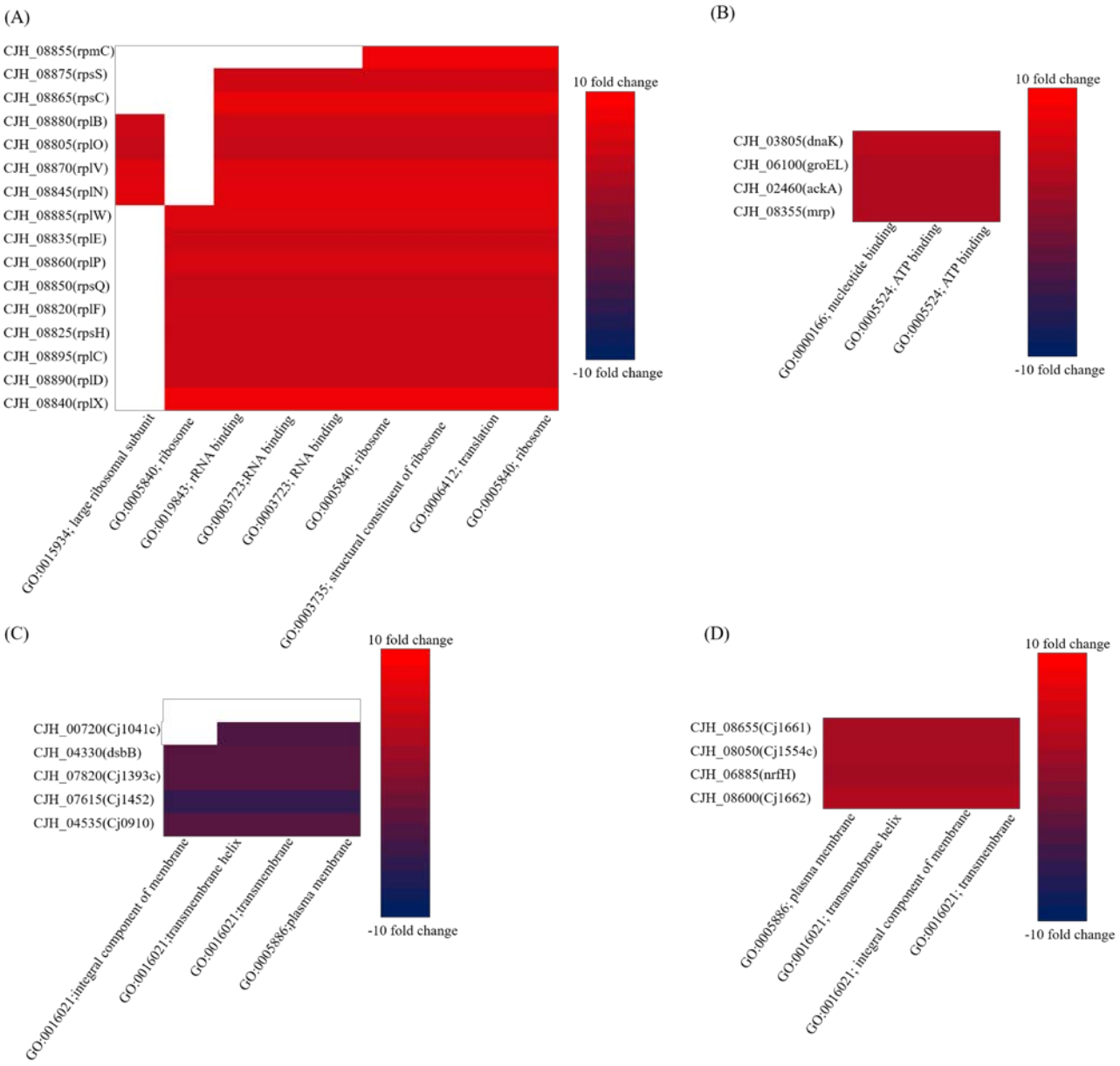

Figure 6-5. Transcriptional response of *C. jejuni* F38011 in response to the different treatments. The differentially expressed genes were categorized on the basis of the functional terms. Panels: (A) Up-regulated genes induced by the treatment of 1 mM ajoene: genes were clustered on the basis of transcription-translation term; (B) Up-regulated genes induced by the treatment of 1 mM ajoene: genes were clustered on the basis of energy utilization term; (C) Down-regulated genes

induced by the treatment of 1 mM ajoene: genes were clustered on the basis of integral cell membrane term; and (D) Up-regulated genes induced by the treatment of 16 mM TiO_2: genes were clustered on the basis of integral cell membrane term. The clusters are shown in white color in panel (A) and (C) indicated that the differentially expressed genes were absent in the certain functional terms.

The treatment of Al_2O_3 nanoparticles barely induced any transcriptional response in *C. jejuni* F38011 regardless of the presence of ajoene. The individual treatment of 16 mM Al_2O_3 nanoparticles alone induced 2 differentially expressed genes, which were CJH_08660 (up-regulated by 3.7 fold) and CJH_05300 (down-regulated by 7.4 fold). The combined treatment of 4 mM Al_2O_3 nanoparticles with 0.06 mM ajoene induced 2 differentially expressed genes (CJH_03855, down-regulated by 3.7 fold, and CJH_00775, up-regulated by 7.8 fold). However, there was no overlap between the differentially expressed genes induced by individual treatment of 16 mM Al_2O_3 nanoparticles and that induced by the combined treatment of 4 mM Al_2O_3 nanoparticles with 0.06 mM ajoene.

The individual treatment of 16 mM TiO_2 nanoparticles induced 6 up-regulated genes and 1 down-regulated gene in *C. jejuni* F38011. The up-regulated genes were categorized in a functional group that referred to the term of the integral cell membrane (**Figure 6-5D**). The combination treatment of 4 mM TiO_2 nanoparticles with 0.06 mM ajoene only resulted in one up-regulated gene (CJH_08660 up-regulated by 3.5 fold).

There was a clear difference between the transcriptional response of *C. jejuni* F38011 to individual treatment of ajoene and individual treatment of Al_2O_3 nanoparticles or TiO_2 nanoparticles. The gene CJH_08660 that encoded a protein for integral cell membrane was up-

regulated in both ajoene-treated group and Al_2O_3 nanoparticles-treated group (**Table A-2**). The treatment of ajoene and the treatment of TiO_2 nanoparticles resulted in the up-regulation of 2 common genes, CJH_08660 (encode integral membrane protein) and CJH_02460 (encode 50S ribosomal protein L24). Taken all together, the up-regulation of CJH_08660 was detected from all three treatment groups (*i.e.,* ajoene, Al_2O_3 nanoparticles and TiO_2 nanoparticles).

The differentially expressed genes (*i.e.,* CJH_03855 and CJH_00775) induced by the combined treatment of ajoene and Al_2O_3 nanoparticles were unique, as they were not detected in either ajoene-treated group or Al_2O_3 nanoparticles-treated group. Combination treatment of ajoene and TiO_2 nanoparticles induced only one differentially expressed gene (CJH_08660), which was also detected in all individual treatment groups.

6.5 Discussion

Developing new antimicrobial and intervention strategies are critical to reducing the prevalence and dissemination of *Campylobacter* in the food industry as well as environment. In the current study, we investigate the potential of using natural product-derived compounds (ajoene) and metal oxide nanoparticles as antimicrobials to inactivate *C. jejuni*. Both individual treatment of ajoene and metal oxide nanoparticles demonstrated antimicrobial effect against *C. jejuni* and the antimicrobial effect was concentration and temperature dependent (**Figure 6-1, 6-2** and **Figure 6-3**).

In order to achieve a better antimicrobial effect, Brown and colleagues functionalized silver and gold nanoparticles with ampicillin. They found that this modified nanocomposite demonstrated a strong bactericidal effect against multidrug-resistant *Staphylococcus aureus.* (Brown et al., 2012) In our previous study, ajoene was synthesized and showed a significant

antimicrobial effect against *Cronobacter sakazakii* at the concentration of 3.88 mM (Feng et al., 2014). Ajoene could easily penetrate the bacterial cell membrane and alter the conformational structure of thiol-containing proteins. Since the mechanism of action of ajoene and nanoparticles were generally different, there would be a potential to achieve a synergistic antimicrobial effect by combining these two compounds. In the current study, we identified a synergistic antimicrobial effect of using a combination treatment of ajoene and metal oxide nanoparticles against *C. jejuni*. Although individual treatment of either 0.06 mM ajoene or 1 mM nanoparticles (both Al_2O_3 and TiO_2 nanoparticles) could only inhibit the growth of *C. jejuni*, the combination treatment could completely inactivate *C. jejuni* within 12 h (**Figure 6-2** and **Figure 6-3**). An interesting observation was that the antimicrobial effect of the combination treatment was not influenced by temperature.

RNA-seq analysis was then applied to plot the transcriptional responses of *C. jejuni* to different treatments. The treatment of individual ajoene induced a relatively broad range of transcriptional response in *C. jejuni* F38011. The up-regulated genes are mainly involved in two pathways responsible for transcription-translation and ATP utilization (**Table 6-2**). Besides, several stress response genes, including *dnak*, *groEL*, *katA*, *cmeA*, *cmeB*, and *cmeC*, were also up-regulated (**Table A-2**). *Dnak* and *groEL* are general stress response genes that can mediate heat and starvation tolerance (Konkel et al., 1998; Klančnik et al., 2006). While *cmeA*, *cmeB*, and *cmeC* together encode an efflux pump that mediates the intrinsic tolerance to a broad range of antimicrobials (Lin et al., 2002; Gibreel et al., 2007). The *katA* gene can mediate the tolerance of bacterial cells to oxidative stress (Grant and Park, 1995; Van Vliet et al., 1999). On the other hand, down-regulated genes were mainly involved in a pathway responsible for the integrity of cell membranes. In addition, a DNA repair associated gene *recN* and a chemotaxis associated

gene *cheY* were also significantly down-regulated (**Table A-2**), suggesting that treatment of ajoene at a low concentration not be lethal stress. The major antimicrobial mechanism of ajoene was proposed to be the inhibition of thiol-containing enzymes via the interaction with thiol groups (Ankri and Mirelman, 1999; Ilić et al., 2011). This interaction was reversible due to its feature of non-covalence. Hence, a low concentration of ajoene would be hard achieve a bactericidal effect, which was validated by a previous study that low concentration of ajoene (< 20 μg/ml) only inhibited the growth of bacteria (Naganawa et al., 1996) Thiol groups, which are also extensively found in the membrane proteins and cell wall-bound proteins, might serve as the reducing compounds to protect the bacterial cell from the oxidative stress (Navarre and Schneewind, 1999; Möller and Hederstedt, 2006; Michelon et al., 2010). Therefore, the interaction between ajoene and thiol groups of membrane proteins might decrease the integrity of cell membrane and increase the susceptibility of cells. In agreement with these studies, the antimicrobial tests found that the treatment of ajoene for a short period (1 h) at a relatively low concentration (0.25 mM) only induced mild stress, rather than immediately lethal stress in *C. jejuni* (**Figure 6-1 and Table 6-2**). The RNA-seq analysis found that the individual treatment of ajoene could induce the up-regulation of RNA binding and ATP binding associated genes, but inhibit the metabolism of the integral cell membrane and chemotaxis (**Table 6-2**). Thus, ajoene could increase the susceptibility of *C. jejuni* to stress by impairing the integrity of cell membrane and the chemotaxis of the cells on the basis of a transcriptional-dependent mechanism.

In this study, individual treatment of metal oxide nanoparticles (Al_2O_3 nanoparticles and TiO_2 nanoparticles) barely induced the transcriptional response of *C. jejuni* F38011. The treatment of Al_2O_3 nanoparticles only induced 2 differentially expressed genes, while the treatment of TiO_2 nanoparticles induced 7 differentially expressed genes, including 4 up-

regulated genes with the similar function to maintain the integrity of cell membrane. Previous studies had proposed several antimicrobial mechanisms of metal oxides nanoparticles. The adhesion of metal oxide nanoparticles onto the surface of bacterial cells was believed to be one of the leading causes of antimicrobial effect. According to Li and coauthors, Al_2O_3 nanoparticles had a positive surface charge at neutral pH that which could interact with the negatively charged surface of *E. coli* cells due to electrostatic interaction. (Li and Logan, 2004) In another study, Pakrashi and colleagues confirmed this statement and identified that Al_2O_3 nanoparticles coagulated at the cell membrane, disrupted cellular structure and subsequently led to the leakage of *Bacillus licheniformis* cells (Pakrashi et al., 2011). In addition, TiO_2 nanoparticles were proposed to a photo-killing mechanism. For example, TiO_2 nanoparticles were highly effective in inactivating *P. aeruginosa*, *E. coli*, and *S. aureus* within 1 h of UV illumination (Maness et al., 1999). Photocatalysis of TiO_2 nanoparticles could enhance the peroxidation of the bacterial cell membrane and shut down respiration of cells (Foster et al., 2011). Our current study illustrated the significant antimicrobial effect of TiO_2 nanoparticles against *C. jejuni* without UV illumination (**Figure 6-2A** and **Figure 6-3A**). Hence, we speculated that the adhesion to and physical disruption of the bacterial cell membrane might be a universal antimicrobial mechanism shared by different types of metal oxide nanoparticles. Previous studies indicated that inducing the generation of ROS could be another important antimicrobial mechanism for metal oxide nanoparticles. For example, the treatment of ZnO nanoparticles could lead to significant up-regulation of oxidative stress genes in *C. jejuni* (Xie et al., 2011). However, we did not observe any gene associated with the oxidative stresses in response to either Al_2O_3 nanoparticles or TiO_2 nanoparticles in this study.

Although the combination treatment of ajoene and metal oxide nanoparticles could generate a synergistic antimicrobial effect against *C. jejuni*, it barely induced any transcriptional response. The combination treatment of Al_2O_3 nanoparticles with ajoene only induced 2 differentially expressed genes (CJH_03855 and CJH_00775), but these 2 genes were not shown in the individual treatment group. The combination treatment of TiO_2 nanoparticles and ajoene only induced 1 differentially expressed gene (CJH_08660) that presented in all individual treatment group. Therefore, metal oxide nanoparticles were regarded as the leading antimicrobial factor in the combination treatment because the combination treatment inactivated *C. jejuni* mainly via the physical disruption conducted by metal oxide nanoparticles. Taken all together, the antimicrobial mechanism of synergistic treatment could be divided into two phases, inducing phase mediated by ajoene and reaction phase mediated by metal oxide nanoparticles. The treatment of ajoene damaged the cell membrane and increased the susceptibility of *C. jejuni* to stresses. Subsequently, the treatment of metal oxide nanoparticles might adhere to the injured cell membrane and physically disrupt *C. jejuni* cells.

6.6 Conclusion

In conclusion, we identified that the combination treatment of metal oxide nanoparticles and ajoene could generate a significant synergistic antimicrobial effect against *C. jejuni*. RNA-seq analysis was applied to investigate the antimicrobial mechanism of this combination treatment. We propose a two-phase antimicrobial mechanism of synergistic treatment of ajoene and metal oxide nanoparticles, utilizing the injury of cell membrane mediated by ajoene and physical disruption mediated by metal oxide nanoparticles. This study provided a novel

intervention strategy to inactivate and limit the prevalence of *C. jejuni* and other foodborne pathogens in the food processing environment.

Chapter 7: Outlook

In this dissertation, we found that *C. jejuni* could survive under stresses as biofilm or persister cells, indicating the importance of this two survival mode. Future work could be focused on the correlation between *C. jejuni* biofilm and persister cells. The microenvironment of biofilm was high acidic with limited nutrient which might facilitate the formation of *C. jejuni* persister cells. The chemical compositions and physical structure of *C. jejuni* biofilm might influence the microenvironment of biofilm and subsequently affect the formation of persister cells. In addition, the identification of candidate genes which were responsible for the formation of *C. jejuni* persister cells could be further extended. Previous studies proposed that type II TA modules played an important role in the formation of persister cells. These type II TA modules and their homologs were absent in *C. jejuni* F38011, although this strain could form a high level of persister cells. We speculated that the formation of *C. jejuni* persister cells could be mediated by genes with similar functions as TA modules. Persister cells were in a state with low of metabolic activity; they could still express virulence gene and should be regarded as a potential risk. Currently, the detection of persister cells was still a challenge. Hence, a rapid and accurate detection method for persister cells could be a future direction. This sensitive detection method could benefit the consumers as well as food industry.

References

Acheson, D., and Allos, B.M. (2001) *Campylobacter jejuni* infections: update on emerging issues and trends. *Clinical infectious diseases* **32**: 1201-1206.

Ades, S.E., Connolly, L.E., Alba, B.M., and Gross, C.A. (1999) The *Escherichia coli* ςE-dependent extracytoplasmic stress response is controlled by the regulated proteolysis of an anti-ς factor. *Genes and development* **13**: 2449-2461.

Ahimou, F., Semmens, M.J., Novak, P.J., and Haugstad, G. (2007) Biofilm cohesiveness measurement using a novel atomic force microscopy methodology. *Applied and environmental microbiology* **73**: 2897-2904.

Allesen-Holm, M., Barken, K.B., Yang, L., Klausen, M., Webb, J.S., Kjelleberg, S. et al. (2006) A characterization of DNA release in *Pseudomonas aeruginosa* cultures and biofilms. *Molecular microbiology* **59**: 1114-1128.

Allison, D., and Matthews, M. (1992) Effect of polysaccharide interactions on antibiotic susceptibility of Pseudomonas aeruginosa. *Journal of applied microbiology* **73**: 484-488.

Allison, D., Brown, M., Evans, D., and Gilbert, P. (1990) Surface hydrophobicity and dispersal of *Pseudomonas aeruginosa* from biofilms. *FEMS microbiology letters* **71**: 101-104.

Ankri, S., and Mirelman, D. (1999) Antimicrobial properties of allicin from garlic. *Microbes and infection* **1**: 125-129.

Asakura, H., Yamasaki, M., Yamamoto, S., and Igimi, S. (2007a) Deletion of *peb4* gene impairs cell adhesion and biofilm formation in *Campylobacter jejuni*. *FEMS microbiology letters* **275**: 278-285.

Asakura, H., Ishiwa, A., Arakawa, E., Makino, S.i., Okada, Y., Yamamoto, S., and Igimi, S. (2007b) Gene expression profile of *Vibrio cholerae* in the cold stress-induced viable but non-

culturable state. *Environmental microbiology* **9**: 869-879.

Ayrapetyan, M., Williams, T.C., and Oliver, J.D. (2015) Bridging the gap between viable but non-culturable and antibiotic persistent bacteria. *Trends in microbiology* **23**: 7-13.

Bae, J., Oh, E., and Jeon, B. (2014) Enhanced transmission of antibiotic resistance in *Campylobacter jejuni* biofilms by natural transformation. *Antimicrobial agents and chemotherapy* **58**: 7573-7575.

Baillon, M.-L.A., Van Vliet, A.H., Ketley, J.M., Constantinidou, C., and Penn, C.W. (1999) An iron-regulated alkyl hydroperoxide reductase (AhpC) confers aerotolerance and oxidative stress resistance to the microaerophilic pathogen *Campylobacter jejuni*. *Journal of bacteriology* **181**: 4798-4804.

Balaban, N.Q., Merrin, J., Chait, R., Kowalik, L., and Leibler, S. (2004) Bacterial persistence as a phenotypic switch. *Science* **305**: 1622-1625.

Beech, I.B., Smith, J.R., Steele, A.A., Penegar, I., and Campbell, S.A. (2002) The use of atomic force microscopy for studying interactions of bacterial biofilms with surfaces. *Colloids and surfaces B: Biointerfaces* **23**: 231-247.

Benoit, M.R., Conant, C.G., Ionescu-Zanetti, C., Schwartz, M., and Matin, A. (2010) New device for high-throughput viability screening of flow biofilms. *Applied and environmental microbiology* **76**: 4136-4142.

Berk, V., Fong, J.C., Dempsey, G.T., Develioglu, O.N., Zhuang, X., Liphardt, J. et al. (2012) Molecular architecture and assembly principles of *Vibrio cholerae* biofilms. *Science* **337**: 236-239.

Betts, J.C., Lukey, P.T., Robb, L.C., McAdam, R.A., and Duncan, K. (2002) Evaluation of a nutrient starvation model of *Mycobacterium tuberculosis* persistence by gene and protein

expression profiling. *Molecular microbiology* **43**: 717-731.

Beyenal, H., Donovan, C., Lewandowski, Z., and Harkin, G. (2004) Three-dimensional biofilm structure quantification. *Journal of microbiological methods* **59**: 395-413.

Bigger, J. (1944) Treatment of *Staphylococcal infections* with penicillin by intermittent sterilisation. *The Lancet* **244**: 497-500.

Bjarnsholt, T., Tolker-Nielsen, T., Høiby, N., and Givskov, M. (2010) Interference of *Pseudomonas aeruginosa* signalling and biofilm formation for infection control. *Expert reviews in molecular medicine* **12**: e11.

Bove, P., Capozzi, V., Garofalo, C., Rieu, A., Spano, G., and Fiocco, D. (2012) Inactivation of the *ftsH* gene of *Lactobacillus plantarum* WCFS1: Effects on growth, stress tolerance, cell surface properties and biofilm formation. *Microbiological research* **167**: 187-193.

Brauner, A., Fridman, O., Gefen, O., and Balaban, N.Q. (2016) Distinguishing between resistance, tolerance and persistence to antibiotic treatment. *Nature reviews microbiology* **14**: 320-330.

Briandet, R., Herry, J.-M., and Bellon-Fontaine, M.-N. (2001) Determination of the van der Waals, electron donor and electron acceptor surface tension components of static Gram-positive microbial biofilms. *Colloids and surfaces B: Biointerfaces* **21**: 299-310.

Brown, A.N., Smith, K., Samuels, T.A., Lu, J., Obare, S.O., and Scott, M.E. (2012) Nanoparticles functionalized with ampicillin destroy multiple-antibiotic-resistant isolates of *Pseudomonas aeruginosa* and *Enterobacter aerogenes* and methicillin-resistant *Staphylococcus aureus*. *Applied and environmental microbiology* **78**: 2768-2774.

Brown, H.L., Hanman, K., Reuter, M., Betts, R.P., and Van Vliet, A.H. (2015a) *Campylobacter jejuni* biofilms contain extracellular DNA and are sensitive to DNase I treatment. *Frontiers in*

microbiology **6**.

Brown, H.L., Reuter, M., Hanman, K., Betts, R.P., and van Vliet, A.H. (2015b) Prevention of biofilm formation and removal of existing biofilms by extracellular DNases of *Campylobacter jejuni*. *PLoS One* **10**: e0121680.

Brown, H.L., Reuter, M., Salt, L.J., Cross, K.L., Betts, R.P., and van Vliet, A.H. (2014) Chicken juice enhances surface attachment and biofilm formation of *Campylobacter jejuni*. *Applied and environmental microbiology* **80**: 7053-7060.

Brown, M.J., and Lester, J.N. (1980) Comparison of bacterial extracellular polymer extraction methods. *Applied and environmental microbiology* **40**: 179-185.

Bryan, F.L., and Doyle, M.P. (1995) Health risks and consequences of *Salmonella* and *Campylobacter jejuni* in raw poultry. *Journal of food protection* **58**: 326-344.

Brzozowska, I., and Zielenkiewicz, U. (2013) Regulation of toxin–antitoxin systems by proteolysis. *Plasmid* **70**: 33-41.

Buelow, D.R., Christensen, J.E., Neal-McKinney, J.M., and Konkel, M.E. (2011) *Campylobacter jejuni* survival within human epithelial cells is enhanced by the secreted protein CiaI. *Molecular microbiology* **80**: 1296-1312.

Buswell, C.M., Herlihy, Y.M., Lawrence, L.M., McGuiggan, J.T., Marsh, P.D., Keevil, C.W., and Leach, S.A. (1998) Extended survival and persistence of *Campylobacter spp*. in water and aquatic biofilms and their detection by immunofluorescent-antibody and-rRNA staining. *Applied and environmental microbiology* **64**: 733-741.

Butzler, J.-P., and Oosterom, J. (1991) *Campylobacter*: pathogenicity and significance in foods. *International journal of food microbiology* **12**: 1-8.

Cabiscol Català, E., Tamarit Sumalla, J., and Ros Salvador, J. (2000) Oxidative stress in bacteria

and protein damage by reactive oxygen species. *International microbiology* **3**: 3-8.

Public Health Agency of Canada. Reported cases from 1924 to 2015 in Canada - Notifiable diseases on-line. http://diseases.canada.ca/notifiable/charts?c=plt. 2017. Date for material retrieve (2017.09.12).

Candon, H.L., Allan, B.J., Fraley, C.D., and Gaynor, E.C. (2007) Polyphosphate kinase 1 is a pathogenesis determinant in *Campylobacter jejuni*. *Journal of bacteriology* **189**: 8099-8108.

Cappelier, J., Magras, C., Jouve, J., and Federighi, M. (1999a) Recovery of viable but non-culturable *Campylobacter jejuni* cells in two animal models. *Food microbiology* **16**: 375-383.

Cappelier, J., Minet, J., Magras, C., Colwell, R., and Federighi, M. (1999b) Recovery in embryonated eggs of viable but nonculturable *Campylobacter jejuni* cells and maintenance of ability to adhere to HeLa cells after resuscitation. *Applied and environmental microbiology* **65**: 5154-5157.

Centers for Disease Control and Prevention. Food Safety Report 2015. https://www.cdc.gov/foodnet/pdfs/foodnet-mmwr-progress-508-final.pdf. Date for material retrieve (2017.09.12).

Chae, M.S., Schraft, H., Hansen, L.T., and Mackereth, R. (2006) Effects of physicochemical surface characteristics of *Listeria monocytogenes* strains on attachment to glass. *Food microbiology* **23**: 250-259.

Chen, C.-W., Hsu, C.-Y., Lai, S.-M., Syu, W.-J., Wang, T.-Y., and Lai, P.-S. (2014) Metal nanobullets for multidrug resistant bacteria and biofilms. *Advanced drug delivery reviews* **78**: 88-104.

Chmielewski, R., and Frank, J. (2003) Biofilm formation and control in food processing facilities. *Comprehensive reviews in food science and food safety* **2**: 22-32.

Chung, J.D., Stephanopoulos, G., Ireton, K., and Grossman, A.D. (1994) Gene expression in single cells of *Bacillus subtilis*: evidence that a threshold mechanism controls the initiation of sporulation. *Journal of bacteriology* **176**: 1977-1984.

Conlon, B.P. (2014) *Staphylococcus aureus* chronic and relapsing infections: evidence of a role for persister cells. *Bioessays* **36**: 991-996.

Conlon, B.P., Rowe, S.E., and Lewis, K. (2015) Persister cells in biofilm associated infections. In *biofilm-based healthcare-associated infections*: Springer, pp. 1-9.

Conlon, B.P., Rowe, S.E., Gandt, A.B., Nuxoll, A.S., Donegan, N.P., Zalis, E.A. et al. (2016) Persister formation in *Staphylococcus aureus* is associated with ATP depletion. *Nature microbiology* **1**: 16051.

Costerton, J.W., Stewart, P.S., and Greenberg, E.P. (1999) Bacterial biofilms: a common cause of persistent infections. *Science* **284**: 1318-1322.

Craig, L., Volkmann, N., Arvai, A.S., Pique, M.E., Yeager, M., Egelman, E.H., and Tainer, J.A. (2006) Type IV pilus structure by cryo-electron microscopy and crystallography: implications for pilus assembly and functions. *Molecular cell* **23**: 651-662.

Craven, S., Stern, N., Line, E., Bailey, J., Cox, N., and Fedorka-Cray, P. (2000) Determination of the incidence of *Salmonella spp*., *Campylobacter jejuni*, and *Clostridium perfringens* in wild birds near broiler chicken houses by sampling intestinal droppings. *Avian diseases*: 715-720.

Das, T., and Manefield, M. (2012) Pyocyanin promotes extracellular DNA release in *Pseudomonas aeruginosa*. *PloS one* **7**: e46718.

Das, T., Sharma, P.K., Busscher, H.J., van der Mei, H.C., and Krom, B.P. (2010) Role of extracellular DNA in initial bacterial adhesion and surface aggregation. *Applied and environmental microbiology* **76**: 3405-3408.

Davies, D. (2003) Understanding biofilm resistance to antibacterial agents. *Nature reviews drug discovery* **2**: 114.

Davis, L., Young, K., and DiRita, V. (2008) Genetic manipulation of *Campylobacter jejuni*. *Current protocols in microbiology*: 8A. 2.1-8A. 2.17.

De Gelder, J., De Gussem, K., Vandenabeele, P., and Moens, L. (2007) Reference database of Raman spectra of biological molecules. *Journal of Raman spectroscopy* **38**: 1133-1147.

De Groote, V.N., Verstraeten, N., Fauvart, M., Kint, C.I., Verbeeck, A.M., Beullens, S. et al. (2009) Novel persistence genes in *Pseudomonas aeruginosa* identified by high-throughput screening. *FEMS microbiology letters* **297**: 73-79.

de la Fuente-Núñez, C., Reffuveille, F., Fernandez, L., and Hancock, R.E. (2013) Bacterial biofilm development as a multicellular adaptation: antibiotic resistance and new therapeutic strategies. *Current opinion in microbiology* **16**: 580-589.

de la Fuente-Núñez, C., Reffuveille, F., Haney, E.F., Straus, S.K., and Hancock, R.E. (2014) Broad-spectrum anti-biofilm peptide that targets a cellular stress response. *PLoS pathogens* **10**: e1004152.

Decho, A.W., Visscher, P.T., and Reid, R.P. (2005) Production and cycling of natural microbial exopolymers (EPS) within a marine stromatolite. *Palaeogeogr, palaeoclimatol, palaeoecol* **219**: 71-86.

Deng, X., Li, Z., and Zhang, W. (2012) Transcriptome sequencing of *Salmonella enterica* serovar Enteritidis under desiccation and starvation stress in peanut oil. *Food microbiology* **30**: 311-315.

Donlan, R.M. (2002) Biofilms: microbial life on surfaces. *Emerging infectious diseases* **8**: 881.

Donlan, R.M., and Costerton, J.W. (2002) Biofilms: survival mechanisms of clinically relevant microorganisms. *Clinical microbiology reviews* **15**: 167-193.

Dörr, T., Vulić, M., and Lewis, K. (2010) Ciprofloxacin causes persister formation by inducing the TisB toxin in *Escherichia coli*. *PLoS biology* **8**: e1000317.

Durack, J., Ross, T., and Bowman, J.P. (2013) Characterisation of the transcriptomes of genetically diverse *Listeria monocytogenes* exposed to hyperosmotic and low temperature conditions reveal global stress-adaptation mechanisms. *PloS one* **8**: e73603.

Dykes, G., Sampathkumar, B., and Korber, D. (2003) Planktonic or biofilm growth affects survival, hydrophobicity and protein expression patterns of a pathogenic *Campylobacter jejuni* strain. *International journal of food microbiology* **89**: 1-10.

Elias, S., and Banin, E. (2012) Multi-species biofilms: living with friendly neighbors. *FEMS microbiology reviews* **36**: 990-1004.

Fang, H.H., Chan, K.-Y., and Xu, L.-C. (2000) Quantification of bacterial adhesion forces using atomic force microscopy (AFM). *Journal of microbiological methods* **40**: 89-97.

Feng, J., De La Fuente-Núñez, C., Trimble, M.J., Xu, J., Hancock, R.E., and Lu, X. (2015) An *in situ* Raman spectroscopy-based microfluidic “lab-on-a-chip” platform for non-destructive and continuous characterization of *Pseudomonas aeruginosa* biofilms. *Chemical communications* **51**: 8966-8969.

Feng, J., Lamour, G., Xue, R., Mirvakliki, M.N., Hatzikiriakos, S.G., Xu, J. et al. (2016) Chemical, physical and morphological properties of bacterial biofilms affect survival of encased *Campylobacter jejuni* F38011 under aerobic stress. *International journal of food microbiology* **238**: 172-182.

Feng, S., Eucker, T.P., Holly, M.K., Konkel, M.E., Lu, X., and Wang, S. (2014) Investigating the responses of *Cronobacter sakazakii* to garlic-drived organosulfur compounds: a systematic study of pathogenic-bacterium injury by use of high-throughput whole-transcriptome sequencing and

confocal micro-raman spectroscopy. *Applied and environmental microbiology* **80**: 959-971.

Fields, J.A., and Thompson, S.A. (2008) *Campylobacter jejuni* CsrA mediates oxidative stress responses, biofilm formation, and host cell invasion. *Journal of bacteriology* **190**: 3411-3416.

Flemming, H.-C., and Wingender, J. (2010) The biofilm matrix. *Nature reviews microbiology* **8**: 623-633.

Foster, H.A., Ditta, I.B., Varghese, S., and Steele, A. (2011) Photocatalytic disinfection using titanium dioxide: spectrum and mechanism of antimicrobial activity. *Applied microbiology and biotechnology* **90**: 1847-1868.

Fux, C., Costerton, J., Stewart, P., and Stoodley, P. (2005) Survival strategies of infectious biofilms. *Trends in microbiology* **13**: 34-40.

Gaasbeek, E.J., van der Wal, F.J., van Putten, J.P., de Boer, P., van der Graaf-van Bloois, L., de Boer, A.G. et al. (2009) Functional characterization of excision repair and RecA-dependent recombinational DNA repair in *Campylobacter jejuni*. *Journal of bacteriology* **191**: 3785-3793.

Gaynor, E.C., Wells, D.H., MacKichan, J.K., and Falkow, S. (2005) The *Campylobacter jejuni* stringent response controls specific stress survival and virulence-associated phenotypes. *Molecular microbiology* **56**: 8-27.

Ge, B., Wang, F., Sjölund-Karlsson, M., and McDermott, P.F. (2013) Antimicrobial resistance in *Campylobacter*: susceptibility testing methods and resistance trends. *Journal of microbiological methods* **95**: 57-67.

Gerdes, K., Christensen, S.K., and Løbner-Olesen, A. (2005) Prokaryotic toxin–antitoxin stress response loci. *Nature reviews microbiology* **3**: 371-382.

Germain, E., Roghanian, M., Gerdes, K., and Maisonneuve, E. (2015) Stochastic induction of persister cells by HipA through (p) ppGpp-mediated activation of mRNA endonucleases.

Proceedings of the national academy of sciences **112**: 5171-5176.

Gibreel, A., Wetsch, N.M., and Taylor, D.E. (2007) Contribution of the CmeABC efflux pump to macrolide and tetracycline resistance in *Campylobacter jejuni*. *Antimicrobial agents and chemotherapy* **51**: 3212-3216.

Goncagul, G., and Ayaz, E. (2010) Antimicrobial effect of garlic (Allium sativum) and traditional medicine. *Journal of animal and veterinary advances* **9**: 1-4.

González-Pastor, J.E., Hobbs, E.C., and Losick, R. (2003) Cannibalism by sporulating bacteria. *Science* **301**: 510-513.

Grant, K.A., and Park, S.F. (1995) Molecular characterization of *katA* from *Campylobacter jejuni* and generation of a catalase-deficient mutant of *Campylobacter coli* by interspecific allelic exchange. *Microbiology* **141**: 1369-1376.

Greenberg, J.T., Monach, P., Chou, J.H., Josephy, P.D., and Demple, B. (1990) Positive control of a global antioxidant defense regulon activated by superoxide-generating agents in *Escherichia coli*. *Proceedings of the national academy of sciences* **87**: 6181-6185.

Gruzdev, N., McClelland, M., Porwollik, S., Ofaim, S., Pinto, R., and Saldinger-Sela, S. (2012) Global transcriptional analysis of dehydrated *Salmonella enterica* serovar Typhimurium. *Applied and environmental microbiology* **78**: 7866-7875.

Gunther, N.W., and Chen, C.-Y. (2009) The biofilm forming potential of bacterial species in the genus *Campylobacter*. *Food microbiology* **26**: 44-51.

Guo, B., Wang, Y., Shi, F., Barton, Y.-W., Plummer, P., Reynolds, D.L. et al. (2008) CmeR functions as a pleiotropic regulator and is required for optimal colonization of *Campylobacter jejuni* in vivo. *Journal of bacteriology* **190**: 1879-1890.

Hall-Stoodley, L., Costerton, J.W., and Stoodley, P. (2004) Bacterial biofilms: from the natural

environment to infectious diseases. *Nature reviews microbiology* **2**: 95-108.

Hanning, I., Jarquin, R., and Slavik, M. (2008) *Campylobacter jejuni* as a secondary colonizer of poultry biofilms. *Journal of applied microbiology* **105**: 1199-1208.

Hansen, S., Lewis, K., and Vulić, M. (2008) Role of global regulators and nucleotide metabolism in antibiotic tolerance in *Escherichia coli*. *Antimicrobial agents and chemotherapy* **52**: 2718-2726.

Harms, A., Maisonneuve, E., and Gerdes, K. (2016) Mechanisms of bacterial persistence during stress and antibiotic exposure. *Science* **354**: aaf4268.

Hayes, F. (2003) Toxins-antitoxins: plasmid maintenance, programmed cell death, and cell cycle arrest. *Science* **301**: 1496-1499.

Helaine, S., Cheverton, A.M., Watson, K.G., Faure, L.M., Matthews, S.A., and Holden, D.W. (2014) Internalization of *Salmonella* by macrophages induces formation of nonreplicating persisters. *Science* **343**: 204-208.

Hermans, D., Van Deun, K., Martel, A., Van Immerseel, F., Messens, W., Heyndrickx, M. et al. (2011) Colonization factors of *Campylobacter jejuni* in the chicken gut. *Veterinary research* **42**: 10.1186.

Hilbert, F., Scherwitzel, M., Paulsen, P., and Szostak, M.P. (2010) Survival of *Campylobacter jejuni* under conditions of atmospheric oxygen tension with the support of *Pseudomonas spp*. *Applied and environmental microbiology* **76**: 5911-5917.

Huang, D.W., Sherman, B.T., and Lempicki, R.A. (2009) Systematic and integrative analysis of large gene lists using DAVID bioinformatics resources. *Nature protocols* **4**: 44.

Hwang, S., Kim, M., Ryu, S., and Jeon, B. (2011) Regulation of oxidative stress response by CosR, an essential response regulator in *Campylobacter jejuni*. *PloS one* **6**: e22300.

Hyytiäinen, H., and Hänninen, M.-L. (2012) Quality control strain *Campylobacter jejuni* ATCC 33560 contains a frameshift mutation in the CmeR regulator. *Antimicrobial agents and chemotherapy* **56**: 1148-1148.

Ica, T., Caner, V., Istanbullu, O., Nguyen, H.D., Ahmed, B., Call, D.R., and Beyenal, H. (2012) Characterization of mono-and mixed-culture *Campylobacter jejuni* biofilms. *Applied and environmental microbiology* **78**: 1033-1038.

Ilić, D.P., Nikolić, V.D., Nikolić, L.B., Stanković, M.Z., Stanojević, L.P., and Cakić, M.D. (2011) Allicin and related compounds: Biosynthesis, synthesis and pharmacological activity. *Facta universitatis-series: physics, chemistry and technology* **9**: 9-20.

Ito, A., May, T., Kawata, K., and Okabe, S. (2008) Significance of *rpoS* during maturation of *Escherichia coli* biofilms. *Biotechnology and bioengineering* **99**: 1462-1471.

Ivanov, I.E., Kintz, E.N., Porter, L.A., Goldberg, J.B., Burnham, N.A., and Camesano, T.A. (2011) Relating the physical properties of *Pseudomonas aeruginosa* lipopolysaccharides to virulence by atomic force microscopy. *Journal of bacteriology* **193**: 1259-1266.

Ivleva, N.P., Wagner, M., Horn, H., Niessner, R., and Haisch, C. (2008) *In situ* surface-enhanced Raman scattering analysis of biofilm. *Analytical chemistry* **80**: 8538-8544.

Ivleva, N.P., Wagner, M., Horn, H., Niessner, R., and Haisch, C. (2009) Towards a nondestructive chemical characterization of biofilm matrix by Raman microscopy. *Analytical and bioanalytical chemistry* **393**: 197-206.

Ivleva, N.P., Wagner, M., Szkola, A., Horn, H., Niessner, R., and Haisch, C. (2010) Label-free in situ SERS imaging of biofilms. *The journal of physical chemistry B* **114**: 10184-10194.

Jacobsen, S.á., Stickler, D., Mobley, H., and Shirtliff, M. (2008) Complicated catheter-associated urinary tract infections due to *Escherichia coli* and *Proteus mirabilis*. *Clinical microbiology*

reviews **21**: 26-59.

Jakobsen, T.H., van Gennip, M., Phipps, R.K., Shanmugham, M.S., Christensen, L.D., Alhede, M. et al. (2012) Ajoene, a sulfur-rich molecule from garlic, inhibits genes controlled by quorum sensing. *Antimicrobial agents and chemotherapy* **56**: 2314-2325.

Jones, D., Sutcliffe, E., Rios, R., Fox, A., and Curry, A. (1993) *Campylobacter jejuni* adapts to aerobic metabolism in the environment. *Journal of medical microbiology* **38**: 145-150.

Joshua, G.P., Guthrie-Irons, C., Karlyshev, A., and Wren, B. (2006) Biofilm formation in *Campylobacter jejuni*. *Microbiology* **152**: 387-396.

Kadurugamuwa, J.L., and Beveridge, T.J. (1995) Virulence factors are released from *Pseudomonas aeruginosa* in association with membrane vesicles during normal growth and exposure to gentamicin: a novel mechanism of enzyme secretion. *Journal of bacteriology* **177**: 3998-4008.

Kalmokoff, M., Lanthier, P., Tremblay, T.-L., Foss, M., Lau, P.C., Sanders, G. et al. (2006) Proteomic analysis of *Campylobacter jejuni* 11168 biofilms reveals a role for the motility complex in biofilm formation. *Journal of bacteriology* **188**: 4312-4320.

Keizer, D.W., Slupsky, C.M., Kalisiak, M., Campbell, A.P., Crump, M.P., Sastry, P.A. et al. (2001) Structure of a pilin monomer from *Pseudomonas aeruginosa* implications for the assembly of pili. *Journal of biological chemistry* **276**: 24186-24193.

Kelly, D. (2001) The physiology and metabolism of *Campylobacter jejuni* and *Helicobacter pylori*. *Journal of applied microbiology* **90**.

Keren, I., Shah, D., Spoering, A., Kaldalu, N., and Lewis, K. (2004a) Specialized persister cells and the mechanism of multidrug tolerance in *Escherichia coli*. *Journal of bacteriology* **186**: 8172-8180.

Keren, I., Kaldalu, N., Spoering, A., Wang, Y., and Lewis, K. (2004b) Persister cells and tolerance to antimicrobials. *FEMS microbiology letters* **230**: 13-18.

Kim, J., Hegde, M., Kim, S.H., Wood, T.K., and Jayaraman, A. (2012) A microfluidic device for high throughput bacterial biofilm studies. *Lab on a chip* **12**: 1157-1163.

Kim, S.-H., Park, C., Lee, E.-J., Bang, W.-S., Kim, Y.-J., and Kim, J.-S. (2017) Biofilm formation of *Campylobacter* strains isolated from raw chickens and its reduction with DNase I treatment. *Food control* **71**: 94-100.

King, T., Lucchini, S., Hinton, J.C., and Gobius, K. (2010) Transcriptomic analysis of *Escherichia coli* O157: H7 and K-12 cultures exposed to inorganic and organic acids in stationary phase reveals acidulant-and strain-specific acid tolerance responses. *Applied and environmental microbiology* **76**: 6514-6528.

Kirisits, M.J., Margolis, J.J., Purevdorj-Gage, B.L., Vaughan, B., Chopp, D.L., Stoodley, P., and Parsek, M.R. (2007) Influence of the hydrodynamic environment on quorum sensing in *Pseudomonas aeruginosa* biofilms. *Journal of bacteriology* **189**: 8357-8360.

Klančnik, A., Botteldoorn, N., Herman, L., and Možina, S.S. (2006) Survival and stress induced expression of *groEL* and *rpoD* of *Campylobacter jejuni* from different growth phases. *International journal of food microbiology* **112**: 200-207.

Klausen, M., Gjermansen, M., Kreft, J.-U., and Tolker-Nielsen, T. (2006) Dynamics of development and dispersal in sessile microbial communities: examples from *Pseudomonas aeruginosa* and *Pseudomonas putida* model biofilms. *FEMS microbiology letters* **261**: 1-11.

Knodler, L.A., Vallance, B.A., Celli, J., Winfree, S., Hansen, B., Montero, M., and Steele-Mortimer, O. (2010) Dissemination of invasive *Salmonella* via bacterial-induced extrusion of mucosal epithelia. *Proceedings of the national academy of sciences* **107**: 17733-17738.

Konkel, M.E., Kim, B.J., Klena, J.D., Young, C.R., and Ziprin, R. (1998) Characterization of the thermal stress response of *Campylobacter jejuni*. *Infection and immunity* **66**: 3666-3672.

Kramer, J.M., Frost, J.A., Bolton, F.J., and Wareing, D.R. (2000) *Campylobacter* contamination of raw meat and poultry at retail sale: identification of multiple types and comparison with isolates from human infection. *Journal of food protection* **63**: 1654-1659.

Kreth, J., Vu, H., Zhang, Y., and Herzberg, M.C. (2009) Characterization of hydrogen peroxide-induced DNA release by *Streptococcus sanguinis* and *Streptococcus gordonii*. *Journal of bacteriology* **191**: 6281-6291.

Kumar, C.G., and Anand, S. (1998) Significance of microbial biofilms in food industry: a review. *International journal of food microbiology* **42**: 9-27.

Kyle, J.L., Parker, C.T., Goudeau, D., and Brandl, M.T. (2010) Transcriptome analysis of *Escherichia coli* O157: H7 exposed to lysates of lettuce leaves. *Applied and environmental microbiology* **76**: 1375-1387.

La Storia, A., Ercolini, D., Marinello, F., Di Pasqua, R., Villani, F., and Mauriello, G. (2011) Atomic force microscopy analysis shows surface structure changes in carvacrol-treated bacterial cells. *Research in microbiology* **162**: 164-172.

Lamour, G., Hamraoui, A., Buvailo, A., Xing, Y., Keuleyan, S., Prakash, V. et al. (2010) Contact angle measurements using a simplified experimental setup. *Journal of chemical education* **87**: 1403-1407.

Lázaro, B., Cárcamo, J., Audícana, A., Perales, I., and Fernández-Astorga, A. (1999) Viability and DNA maintenance in nonculturable spiral *Campylobacter jejuni* cells after long-term exposure to low temperatures. *Applied and environmental microbiology* **65**: 4677-4681.

Lertsethtakarn, P., Ottemann, K.M., and Hendrixson, D.R. (2011) Motility and chemotaxis in

Campylobacter and *Helicobacter*. *Annual review of microbiology* **65**: 389-410.

Levin, B.R., and Rozen, D.E. (2006) Non-inherited antibiotic resistance. *Nature reviews microbiology* **4**: 556-562.

Lewis, K. (2007) Persister cells, dormancy and infectious disease. *Nature reviews microbiology* **5**: 48-56.

Lewis, K. (2010) Persister cells. *Annual review of microbiology* **64**: 357-372.

Lewis, K. (2012) Persister cells: molecular mechanisms related to antibiotic tolerance. In *antibiotic resistance*: Springer, pp. 121-133.

Li, B., and Logan, B.E. (2004) Bacterial adhesion to glass and metal-oxide surfaces. *Colloids and surfaces B: Biointerfaces* **36**: 81-90.

Li, J., Feng, J., Ma, L., de la Fuente Núñez, C., Gölz, G., and Lu, X. (2017) Effects of meat juice on biofilm formation of *Campylobacter* and *Salmonella*. *International journal of food microbiology* **253**: 20-28.

Lillard, H. (1986) Role of fimbriae and flagella in the attachment of *Salmonella typhimurium* to poultry skin. *Journal of food science* **51**: 54-56.

Lim, J., Cui, Y., Oh, Y.J., Park, J.R., Jo, W., Cho, Y.-H., and Park, S. (2011) Studying the effect of alginate overproduction on *Pseudomonas aeruginosa* biofilm by atomic force microscopy. *Journal of nanoscience and nanotechnology* **11**: 5676-5681.

Lin, J., Michel, L.O., and Zhang, Q. (2002) CmeABC functions as a multidrug efflux system in *Campylobacter jejuni*. *Antimicrobial agents and chemotherapy* **46**: 2124-2131.

Lin, J., Akiba, M., Sahin, O., and Zhang, Q. (2005) CmeR functions as a transcriptional repressor for the multidrug efflux pump CmeABC in *Campylobacter jejuni*. *Antimicrobial agents and chemotherapy* **49**: 1067-1075.

Loewen, P.C., Hu, B., Strutinsky, J., and Sparling, R. (1998) Regulation in the *rpoS* regulon of *Escherichia coli*. *Canadian journal of microbiology* **44**: 707-717.

Lorenz, M.G., and Wackernagel, W. (1994) Bacterial gene transfer by natural genetic transformation in the environment. *Microbiological reviews* **58**: 563-602.

Lu, X., Samuelson, D.R., Rasco, B.A., and Konkel, M.E. (2012a) Antimicrobial effect of diallyl sulphide on *Campylobacter jejuni* biofilms. *Journal of antimicrobial chemotherapy* **67**: 1915-1926.

Lu, X., Rasco, B.A., Kang, D.H., Jabal, J.M., Aston, D.E., and Konkel, M.E. (2011a) Infrared and Raman spectroscopic studies of the antimicrobial effects of garlic concentrates and diallyl constituents on foodborne pathogens. *Analytical chemistry* **83**: 4137-4146.

Lu, X., Weakley, A.T., Aston, D.E., Rasco, B.A., Wang, S., and Konkel, M.E. (2012b) Examination of nanoparticle inactivation of *Campylobacter jejuni* biofilms using infrared and Raman spectroscopies. *Journal of applied microbiology* **113**: 952-963.

Lu, X., Wang, J., Al-Qadiri, H.M., Ross, C.F., Powers, J.R., Tang, J., and Rasco, B.A. (2011b) Determination of total phenolic content and antioxidant capacity of onion (*Allium cepa*) and shallot (*Allium oschaninii*) using infrared spectroscopy. *Food chemistry* **129**: 637-644.

Lu, X., Liu, Q., Benavides-Montano, J.A., Nicola, A.V., Aston, D.E., Rasco, B.A., and Aguilar, H.C. (2013a) Detection of receptor-induced glycoprotein conformational changes on enveloped virions by using confocal micro-Raman spectroscopy. *Journal of virology* **87**: 3130-3142.

Lu, X., Samuelson, D.R., Xu, Y., Zhang, H., Wang, S., Rasco, B.A. et al. (2013b) Detecting and tracking nosocomial methicillin-resistant *Staphylococcus aureus* using a microfluidic SERS biosensor. *Analytical chemistry* **85**: 2320-2327.

Luber, P., Wagner, J., Hahn, H., and Bartelt, E. (2003) Antimicrobial resistance in *Campylobacter*

jejuni and *Campylobacter coli* strains isolated in 1991 and 2001-2002 from poultry and humans in Berlin, Germany. *Antimicrobial agents and chemotherapy* **47**: 3825-3830.

Ma, Q., and Wood, T.K. (2009) OmpA influences *Escherichia coli* biofilm formation by repressing cellulose production through the CpxRA two-component system. *Environmental microbiology* **11**: 2735-2746.

Maamar, H., Raj, A., and Dubnau, D. (2007) Noise in gene expression determines cell fate in *Bacillus subtilis*. *Science* **317**: 526-529.

Magajna, B., and Schraft, H. (2015a) Evaluation of propidium monoazide and quantitative PCR to quantify viable *Campylobacter jejuni* biofilm and planktonic cells in log phase and in a viable but nonculturable state. *Journal of food protection* **78**: 1303-1311.

Magajna, B.A., and Schraft, H. (2015b) *Campylobacter jejuni* biofilm cells become viable but non-culturable (VBNC) in low nutrient conditions at 4 ^{o}C more quickly than their planktonic counterparts. *Food control* **50**: 45-50.

Mah, T.-F.C., and O'Toole, G.A. (2001) Mechanisms of biofilm resistance to antimicrobial agents. *Trends in microbiology* **9**: 34-39.

Maness, P.-C., Smolinski, S., Blake, D.M., Huang, Z., Wolfrum, E.J., and Jacoby, W.A. (1999) Bactericidal activity of photocatalytic TiO_2 reaction: toward an understanding of its killing mechanism. *Applied and environmental microbiology* **65**: 4094-4098.

Massé, E., and Gottesman, S. (2002) A small RNA regulates the expression of genes involved in iron metabolism in *Escherichia coli*. *Proceedings of the national academy of sciences* **99**: 4620-4625.

Masyuko, R.N., Lanni, E.J., Driscoll, C.M., Shrout, J.D., Sweedler, J.V., and Bohn, P.W. (2014) Spatial organization of *Pseudomonas aeruginosa* biofilms probed by combined matrix-assisted

laser desorption ionization mass spectrometry and confocal Raman microscopy. *Analyst* **139**: 5701-5709.

McDougald, D., Rice, S.A., Barraud, N., Steinberg, P.D., and Kjelleberg, S. (2012) Should we stay or should we go: mechanisms and ecological consequences for biofilm dispersal. *Nature reviews microbiology* **10**: 39-50.

McLennan, M.K., Ringoir, D.D., Frirdich, E., Svensson, S.L., Wells, D.H., Jarrell, H. et al. (2008) *Campylobacter jejuni* biofilms up-regulated in the absence of the stringent response utilize a calcofluor white-reactive polysaccharide. *Journal of bacteriology* **190**: 1097-1107.

McSwain, B., Irvine, R., Hausner, M., and Wilderer, P. (2005) Composition and distribution of extracellular polymeric substances in aerobic flocs and granular sludge. *Applied and environmental microbiology* **71**: 1051-1057.

Michelon, D., Abraham, S., Ebel, B., De Coninck, J., Husson, F., Feron, G. et al. (2010) Contribution of exofacial thiol groups in the reducing activity of *Lactococcus lactis*. *The FEBS journal* **277**: 2282-2290.

Mirvakili, M.N., Hatzikiriakos, S.G., and Englezos, P. (2013) Superhydrophobic lignocellulosic wood fiber/mineral networks. *ACS applied materials and interfaces* **5**: 9057-9066.

Mixter, P.F., Klena, J.D., Flom, G.A., Siegesmund, A.M., and Konkel, M.E. (2003) *In vivo* tracking of *Campylobacter jejuni* by using a novel recombinant expressing green fluorescent protein. *Applied and environmental microbiology* **69**: 2864-2874.

Möller, M., and Hederstedt, L. (2006) Role of membrane-bound thiol–disulfide oxidoreductases in endospore-forming bacteria. *Antioxidants and redox signaling* **8**: 823-833.

Monack, D.M., Mueller, A., and Falkow, S. (2004) Persistent bacterial infections: the interface of the pathogen and the host immune system. *Nature reviews microbiology* **2**: 747.

Monroe, D. (2007) Looking for chinks in the armor of bacterial biofilms. *PLoS biology* **5**: e307.

Moore, J.E. (2001) Bacterial dormancy in *Campylobacter*: abstract theory or cause for concern? *International journal of food science and technology* **36**: 593-600.

Movasaghi, Z., Rehman, S., and Rehman, I.U. (2007) Raman spectroscopy of biological tissues. *Applied spectroscopy reviews* **42**: 493-541.

Mulcahy, L.R., Burns, J.L., Lory, S., and Lewis, K. (2010) Emergence of *Pseudomonas aeruginosa* strains producing high levels of persister cells in patients with cystic fibrosis. *Journal of bacteriology* **192**: 6191-6199.

Naganawa, R., Iwata, N., Ishikawa, K., Fukuda, H., Fujino, T., and Suzuki, A. (1996) Inhibition of microbial growth by ajoene, a sulfur-containing compound derived from garlic. *Applied and environmental microbiology* **62**: 4238-4242.

Naumann, D. (2001) FT-infrared and FT-Raman spectroscopy in biomedical research. *Applied spectroscopy reviews* **36**: 239-298.

Navarre, W.W., and Schneewind, O. (1999) Surface proteins of gram-positive bacteria and mechanisms of their targeting to the cell wall envelope. *Microbiology and molecular biology Reviews* **63**: 174-229.

Naves, P., del Prado, G., Huelves, L., Gracia, M., Ruiz, V., Blanco, J. et al. (2008) Correlation between virulence factors and *in vitro* biofilm formation by *Escherichia coli* strains. *Microbial pathogenesis* **45**: 86-91.

Neal-McKinney, J.M., Lu, X., Duong, T., Larson, C.L., Call, D.R., Shah, D.H., and Konkel, M.E. (2012) Production of organic acids by probiotic *Lactobacilli* can be used to reduce pathogen load in poultry. *PLoS one* **7**: e43928.

Neal-McKinney, J.M., Christensen, J.E., and Konkel, M.E. (2010) Amino-terminal residues

dictate the export efficiency of the *Campylobacter jejuni* filament proteins via the flagellum. *Molecular microbiology* **76**: 918-931.

Neu, H.C. (1992) The crisis in antibiotic resistance. *Science* **257**: 1064-1074.

Newell, D., and Fearnley, C. (2003) Sources of *Campylobacter* colonization in broiler chickens. *Applied and environmental microbiology* **69**: 4343-4351.

Newell, D.G., McBride, H., and Dolby, J.M. (1985) Investigations on the role of flagella in the colonization of infant mice with *Campylobacter jejuni* and attachment of *Campylobacter jejuni* to human epithelial cell lines. *Epidemiology and Infection* **95**: 217-227.

Ng, J., and Kidd, S.P. (2013) The concentration of intracellular nickel in *Haemophilus influenzae* is linked to its surface properties and cell–cell aggregation and biofilm formation. *International Journal of medical microbiology* **303**: 150-157.

Nielsen, K.M., Johnsen, P.J., Bensasson, D., and Daffonchio, D. (2007) Release and persistence of extracellular DNA in the environment. *Environmental biosafety research* **6**: 37-53.

Nunoshiba, T., Hidalgo, E., Cuevas, C.A., and Demple, B. (1992) Two-stage control of an oxidative stress regulon: the *Escherichia coli* SoxR protein triggers redox-inducible expression of the *soxS* regulatory gene. *Journal of bacteriology* **174**: 6054-6060.

Ohta, R., Yamada, N., Kaneko, H., Ishikawa, K., Fukuda, H., Fujino, T., and Suzuki, A. (1999) In vitro inhibition of the growth of *Helicobacter pylori* by oil-macerated garlic constituents. *Antimicrobial agents and chemotherapy* **43**: 1811-1812.

Oliver, J.D. (2005) The viable but nonculturable state in bacteria. *The journal of microbiology* **43**: 93-100.

Oliver, J.D., and Bockian, R. (1995) In vivo resuscitation, and virulence towards mice, of viable but nonculturable cells of *Vibrio vulnificus*. *Applied and environmental microbiology* **61**: 2620-

2623.

Oyarzabal, O.A., Macklin, K.S., Barbaree, J.M., and Miller, R.S. (2005) Evaluation of agar plates for direct enumeration of *Campylobacter spp*. from poultry carcass rinses. *Applied and environmental microbiology* **71**: 3351-3354.

Pakrashi, S., Dalai, S., Sabat, D., Singh, S., Chandrasekaran, N., and Mukherjee, A. (2011) Cytotoxicity of Al_2O_3 nanoparticles at low exposure levels to a freshwater bacterial isolate. *Chemical research in toxicology* **24**: 1899-1904.

Palyada, K., Sun, Y.-Q., Flint, A., Butcher, J., Naikare, H., and Stintzi, A. (2009) Characterization of the oxidative stress stimulon and PerR regulon of *Campylobacter jejuni*. *BMC genomics* **10**: 481.

Park, S.F. (2002) The physiology of *Campylobacter* species and its relevance to their role as foodborne pathogens. *International journal of food microbiology* **74**: 177-188.

Parkhill, J., Wren, B., Mungall, K., and Ketley, J. (2000) The genome sequence of the food-borne pathogen *Campylobacter jejuni* reveals hypervariable sequences. *Nature* **403**: 665.

Parrish, N.M., Dick, J.D., and Bishai, W.R. (1998) Mechanisms of latency in *Mycobacterium tuberculosis*. *Trends in microbiology* **6**: 107-112.

Parsek, M.R., and Greenberg, E. (2005) Sociomicrobiology: the connections between quorum sensing and biofilms. *Trends in microbiology* **13**: 27-33.

Patel, J.D., Ebert, M., Ward, R., and Anderson, J.M. (2007) *S. epidermidis* biofilm formation: effects of biomaterial surface chemistry and serum proteins. *Journal of biomedical materials research part A* **80**: 742-751.

Pesci, E.C., Cottle, D.L., and Pickett, C.L. (1994) Genetic, enzymatic, and pathogenic studies of the iron superoxide dismutase of *Campylobacter jejuni*. *Infection and Immunity* **62**: 2687-2694.

Pleitner, A.M., Trinetta, V., Morgan, M.T., Linton, R.L., and Oliver, H.F. (2014) Transcriptional and phenotypic responses of *Listeria monocytogenes* to chlorine dioxide. *Applied and environmental microbiology* **80**: 2951-2963.

Pommepuy, M., Butin, M., Derrien, A., Gourmelon, M., Colwell, R., and Cormier, M. (1996) Retention of enteropathogenicity by viable but nonculturable *Escherichia coli* exposed to seawater and sunlight. *Applied and environmental microbiology* **62**: 4621-4626.

Pratt, L.A., and Kolter, R. (1998) Genetic analysis of *Escherichia coli* biofilm formation: roles of flagella, motility, chemotaxis and type I pili. *Molecular microbiology* **30**: 285-293.

Purevdorj, B., Costerton, J.W., and Stoodley, P. (2002) Influence of hydrodynamics and cell signaling on the structure and behavior of *Pseudomonas aeruginosa* biofilms. *Applied and environmental microbiology* **68**: 4457-4464.

Qin, D., Xia, Y., and Whitesides, G.M. (2010) Soft lithography for micro-and nanoscale patterning. *Nature protocols* **5**: 491.

Qiu, Z., Yu, Y., Chen, Z., Jin, M., Yang, D., Zhao, Z. et al. (2012) Nanoalumina promotes the horizontal transfer of multiresistance genes mediated by plasmids across genera. *Proceedings of the national academy of sciences* **109**: 4944-4949.

Raman, S., Song, T., Puyang, X., Bardarov, S., Jacobs, W.R., and Husson, R.N. (2001) The alternative sigma factor SigH regulates major components of oxidative and heat stress responses in *Mycobacterium tuberculosis*. *Journal of bacteriology* **183**: 6119-6125.

Rees, C.E., Dodd, C.E., Gibson, P.T., Booth, I.R., and Stewart, G.S. (1995) The significance of bacteria in stationary phase to food microbiology. *International journal of food microbiology* **28**: 263-275.

Reeser, R.J., Medler, R.T., Billington, S.J., Jost, B.H., and Joens, L.A. (2007) Characterization of

Campylobacter jejuni biofilms under defined growth conditions. *Applied and environmental microbiology* **73**: 1908-1913.

Reuter, M., Mallett, A., Pearson, B.M., and van Vliet, A.H. (2010) Biofilm formation by *Campylobacter jejuni* is increased under aerobic conditions. *Applied and environmental microbiology* **76**: 2122-2128.

Rice, K.C., Mann, E.E., Endres, J.L., Weiss, E.C., Cassat, J.E., Smeltzer, M.S., and Bayles, K.W. (2007) The *cidA* murein hydrolase regulator contributes to DNA release and biofilm development in *Staphylococcus aureus*. *Proceedings of the national academy of sciences* **104**: 8113-8118.

Ritchie, A., Bryner, J., and Foley, J. (1983) Role of DNA and bacteriophage in *Campylobacter* auto-agglutination. *Journal of medical microbiology* **16**: 333-340.

Ritz, M., Garenaux, A., Berge, M., and Federighi, M. (2009) Determination of *rpoA* as the most suitable internal control to study stress response in *C. jejuni* by RT-qPCR and application to oxidative stress. *Journal of microbiological methods* **76**: 196-200.

Roberson, E.B., and Firestone, M.K. (1992) Relationship between desiccation and exopolysaccharide production in a soil *Pseudomonas spp*. *Applied and environmental microbiology* **58**: 1284-1291.

Røder, H.L., Sørensen, S.J., and Burmølle, M. (2016) Studying bacterial multispecies biofilms: where to start? *Trends in microbiology* **24**: 503-513.

Sadiq, I.M., Chowdhury, B., Chandrasekaran, N., and Mukherjee, A. (2009) Antimicrobial sensitivity of *Escherichia coli* to alumina nanoparticles. *Nanomedicine: nanotechnology, biology and medicine* **5**: 282-286.

Samuel, M.C., Vugia, D.J., Shallow, S., Marcus, R., Segler, S., McGivern, T. et al. (2004)

Epidemiology of sporadic *Campylobacter* infection in the United States and declining trend in incidence, FoodNet 1996–1999. *Clinical infectious diseases* **38**: S165-S174.

Sanders, S.Q., Boothe, D.H., Frank, J.F., and Arnold, J.W. (2007) Culture and detection of *Campylobacter jejuni* within mixed microbial populations of biofilms on stainless steel. *Journal of food protection* **70**: 1379-1385.

Sauer, F.G., Mulvey, M.A., Schilling, J.D., Martinez, J.J., and Hultgren, S.J. (2000) Bacterial pili: molecular mechanisms of pathogenesis. *Current opinion in microbiology* **3**: 65-72.

Scheuring, S., and Dufrêne, Y.F. (2010) Atomic force microscopy: probing the spatial organization, interactions and elasticity of microbial cell envelopes at molecular resolution. *Molecular microbiology* **75**: 1327-1336.

Schmittgen, T.D., and Livak, K.J. (2008) Analyzing real-time PCR data by the comparative CT method. *Nature protocols* **3**: 1101.

Schwerer, B. (2002) Antibodies against gangliosides: a link between preceding infection and immunopathogenesis of Guillain-Barre syndrome. *Microbes and infection* **4**: 373-384.

Sevin, E.W., and Barloy-Hubler, F. (2007) RASTA-Bacteria: a web-based tool for identifying toxin-antitoxin loci in prokaryotes. *Genome biology* **8**: R155.

Shah, D., Zhang, Z., Khodursky, A.B., Kaldalu, N., Kurg, K., and Lewis, K. (2006) Persisters: a distinct physiological state of *E. coli*. *BMC microbiology* **6**: 53.

Shan, Y., Lazinski, D., Rowe, S., Camilli, A., and Lewis, K. (2015) Genetic basis of persister tolerance to aminoglycosides in *Escherichia coli*. *MBio* **6**: e00078-00015.

Shao, Y., Harrison, E.M., Bi, D., Tai, C., He, X., Ou, H.-Y. et al. (2010) TADB: a web-based resource for Type 2 toxin–antitoxin loci in bacteria and archaea. *Nucleic acids research* **39**: D606-D611.

Shumi, W., Lim, J., Nam, S.-W., Lee, K., Kim, S.H., Kim, M.-H. et al. (2010) Environmental factors that affect *Streptococcus mutans* biofilm formation in a microfluidic device mimicking teeth. *BioChip journal* **4**: 257-263.

Simões, M., Pereira, M.O., Sillankorva, S., Azeredo, J., and Vieira, M.J. (2007) The effect of hydrodynamic conditions on the phenotype of *Pseudomonas fluorescens* biofilms. *Biofouling* **23**: 249-258.

Simões, M., Simões, L.C., Cleto, S., Pereira, M.O., and Vieira, M.J. (2008) The effects of a biocide and a surfactant on the detachment of *Pseudomonas fluorescens* from glass surfaces. *International journal of food microbiology* **121**: 335-341.

Simon-Deckers, A., Loo, S., Mayne-L'hermite, M., Herlin-Boime, N., Menguy, N., Reynaud, C. et al. (2009) Size-, composition-and shape-dependent toxicological impact of metal oxide nanoparticles and carbon nanotubes toward bacteria. *Environmental science and technology* **43**: 8423-8429.

Siringan, P., Connerton, P.L., Payne, R.J., and Connerton, I.F. (2011) Bacteriophage-mediated dispersal of *Campylobacter jejuni* biofilms. *Applied and environmental microbiology* **77**: 3320-3326.

Sivapalasingam, S., Friedman, C.R., Cohen, L., and Tauxe, R.V. (2004) Fresh produce: a growing cause of outbreaks of foodborne illness in the United States, 1973 through 1997. *Journal of food protection* **67**: 2342-2353.

Slader, J., Domingue, G., Jørgensen, F., McAlpine, K., Owen, R., Bolton, F., and Humphrey, T. (2002) Impact of transport crate reuse and of catching and processing on *Campylobacter* and *Salmonella* contamination of broiler chickens. *Applied and environmental microbiology* **68**: 713-719.

Song, J.L., Au, K.H., Huynh, K.T., and Packman, A.I. (2014) Biofilm responses to smooth flow fields and chemical gradients in novel microfluidic flow cells. *Biotechnology and bioengineering* **111**: 597-607.

Srey, S., Jahid, I.K., and Ha, S.-D. (2013) Biofilm formation in food industries: a food safety concern. *Food control* **31**: 572-585.

Steinberger, R., and Holden, P. (2005) Extracellular DNA in single-and multiple-species unsaturated biofilms. *Applied and environmental microbiology* **71**: 5404-5410.

Stewart, P.S., and Franklin, M.J. (2008) Physiological heterogeneity in biofilms. *Nature reviews microbiology* **6**: 199.

Stoodley, P., Lewandowski, Z., Boyle, J.D., and Lappin-Scott, H.M. (1999) Structural deformation of bacterial biofilms caused by short-term fluctuations in fluid shear: an in situ investigation of biofilm rheology. *Biotechnology and bioengineering* **65**: 83-92.

Storz, G., and Imlayt, J.A. (1999) Oxidative stress. *Current opinion in microbiology* **2**: 188-194.

Sulaeman, S., Le Bihan, G., Rossero, A., Federighi, M., De, E., and Tresse, O. (2010) Comparison between the biofilm initiation of *Campylobacter jejuni* and *Campylobacter coli* strains to an inert surface using BioFilm Ring Test®. *Journal of applied microbiology* **108**: 1303-1312.

Sutherland, I.W. (2001) The biofilm matrix–an immobilized but dynamic microbial environment. *Trends in microbiology* **9**: 222-227.

Svensson, S.L., Pryjma, M., and Gaynor, E.C. (2014) Flagella-mediated adhesion and extracellular DNA release contribute to biofilm formation and stress tolerance of *Campylobacter jejuni*. *PloS one* **9**: e106063.

Syamaladevi, R.M., Lu, X., Sablani, S.S., Insan, S.K., Adhikari, A., Killinger, K. et al. (2013)

Inactivation of *Escherichia coli* population on fruit surfaces using ultraviolet-C light: influence of fruit surface characteristics. *Food and bioprocess technology* **6**: 2959-2973.

Talari, A.C.S., Movasaghi, Z., Rehman, S., and Rehman, I.U. (2015) Raman spectroscopy of biological tissues. *Applied spectroscopy reviews* **50**: 46-111.

Tamaru, Y., Takani, Y., Yoshida, T., and Sakamoto, T. (2005) Crucial role of extracellular polysaccharides in desiccation and freezing tolerance in the terrestrial cyanobacterium *Nostoc commune*. *Applied and environmental microbiology* **71**: 7327-7333.

Tang, L., Pillai, S., Revsbech, N.P., Schramm, A., Bischoff, C., and Meyer, R.L. (2011) Biofilm retention on surfaces with variable roughness and hydrophobicity. *Biofouling* **27**: 111-121.

Tang, M., McEwen, G.D., Wu, Y., Miller, C.D., and Zhou, A. (2013) Characterization and analysis of mycobacteria and Gram-negative bacteria and co-culture mixtures by Raman microspectroscopy, FTIR, and atomic force microscopy. *Analytical and bioanalytical chemistry* **405**: 1577-1591.

Tapia, J., Munoz, J., Gonzalez, F., Blázquez, M., Malki, M., and Ballester, A. (2009) Extraction of extracellular polymeric substances from the acidophilic bacterium *Acidiphilium* 3.2 Sup (5). *Water science and technology* **59**: 1959-1967.

Team, E.E. (2012) The European Union summary report on trends and sources of zoonoses, zoonotic agents and food-borne outbreaks in 2010. *Euro surveillance: bulletin Europeen sur les maladies transmissibles European communicable disease bulletin* **17**.

Teh, A.H.T., Lee, S.M., and Dykes, G.A. (2014) Does *Campylobacter jejuni* form biofilms in food-related environments? *Applied and environmental microbiology* **80**: 5154-5160.

Teh, K.H., Flint, S., and French, N. (2010) Biofilm formation by *Campylobacter jejuni* in controlled mixed-microbial populations. *International journal of food microbiology* **143**: 118-

124.

Thies, F.L., Karch, H., Hartung, H.-P., and Giegerich, G. (1999) Cloning and expression of the *dnaK* gene of *Campylobacter jejuni* and antigenicity of heat shock protein 70. *Infection and immunity* **67**: 1194-1200.

Tholozan, J., Cappelier, J., Tissier, J., Delattre, G., and Federighi, M. (1999) Physiological characterization of viable-but-nonculturable *Campylobacter jejuni* cells. *Applied and environmental microbiology* **65**: 1110-1116.

Thomas, C.M., and Nielsen, K.M. (2005) Mechanisms of, and barriers to, horizontal gene transfer between bacteria. *Nature reviews microbiology* **3**: 711.

Trachoo, N., Frank, J., and Stern, N. (2002) Survival of *Campylobacter jejuni* in biofilms isolated from chicken houses. *Journal of food protection®* **65**: 1110-1116.

Tsuneda, S., Aikawa, H., Hayashi, H., Yuasa, A., and Hirata, A. (2003) Extracellular polymeric substances responsible for bacterial adhesion onto solid surface. *FEMS microbiology letters* **223**: 287-292.

Turonova, H., Briandet, R., Rodrigues, R., Hernould, M., Hayek, N., Stintzi, A. et al. (2015) Biofilm spatial organization by the emerging pathogen *Campylobacter jejuni*: comparison between NCTC 11168 and 81-176 strains under microaerobic and oxygen-enriched conditions. *Frontiers in microbiology* **6**.

Van Oss, C. (1993) Acid—base interfacial interactions in aqueous media. *Colloids and surfaces A: Physicochemical and engineering aspectss* **78**: 1-49.

van Oss, C.J. (2002) Use of the combined Lifshitz–van der Waals and Lewis acid–base approaches in determining the apolar and polar contributions to surface and interfacial tensions and free energies. *Journal of adhesion science and technology* **16**: 669-677.

Van Vliet, A.H., Baillon, M.-L.A., Penn, C.W., and Ketley, J.M. (1999) *Campylobacter jejuni* contains two fur homologs: characterization of iron-responsive regulation of peroxide stress defense genes by the PerR repressor. *Journal of bacteriology* **181**: 6371-6376.

Vatanyoopaisarn, S., Nazli, A., Dodd, C.E., Rees, C.E., and Waites, W.M. (2000) Effect of flagella on initial attachment of *Listeria monocytogenes* to stainless steel. *Applied and environmental microbiology* **66**: 860-863.

Vázquez-Laslop, N., Lee, H., and Neyfakh, A.A. (2006) Increased persistence in *Escherichia coli* caused by controlled expression of toxins or other unrelated proteins. *Journal of bacteriology* **188**: 3494-3497.

Veening, J.-W., Smits, W.K., and Kuipers, O.P. (2008a) Bistability, epigenetics, and bet-hedging in bacteria. *Annual review of microbiology* **62**: 193-210.

Veening, J.-W., Stewart, E.J., Berngruber, T.W., Taddei, F., Kuipers, O.P., and Hamoen, L.W. (2008b) Bet-hedging and epigenetic inheritance in bacterial cell development. *Proceedings of the national academy of sciences* **105**: 4393-4398.

Vora, G.J., Meador, C.E., Bird, M.M., Bopp, C.A., Andreadis, J.D., and Stenger, D.A. (2005) Microarray-based detection of genetic heterogeneity, antimicrobial resistance, and the viable but nonculturable state in human pathogenic Vibrio spp. *Proceedings of the national academy of sciences* **102**: 19109-19114.

Voskuil, M., Visconti, K., and Schoolnik, G. (2004) *Mycobacterium tuberculosis* gene expression during adaptation to stationary phase and low-oxygen dormancy. *Tuberculosis* **84**: 218-227.

Vu, B., Chen, M., Crawford, R.J., and Ivanova, E.P. (2009) Bacterial extracellular polysaccharides involved in biofilm formation. *Molecules* **14**: 2535-2554.

Wang, S., Phillippy, A.M., Deng, K., Rui, X., Li, Z., Tortorello, M.L., and Zhang, W. (2010)

Transcriptomic responses of *Salmonella enterica* serovars Enteritidis and Typhimurium to chlorine-based oxidative stress. *Applied and environmental microbiology* **76**: 5013-5024.

Wang, S., Deng, K., Zaremba, S., Deng, X., Lin, C., Wang, Q. et al. (2009) Transcriptomic response of *Escherichia coli* O157: H7 to oxidative stress. *Applied and environmental microbiology* **75**: 6110-6123.

Wang, W., Chen, J., Chen, G., Du, X., Cui, P., Wu, J. et al. (2015) Transposon mutagenesis identifies novel genes associated with *Staphylococcus aureus* persister formation. *Frontiers in microbiology* **6**.

Webb, J.S., Thompson, L.S., James, S., Charlton, T., Tolker-Nielsen, T., Koch, B. et al. (2003) Cell death in *Pseudomonas aeruginosa* biofilm development. *Journal of bacteriology* **185**: 4585-4592.

Weir, A., Westerhoff, P., Fabricius, L., Hristovski, K., and von Goetz, N. (2012) Titanium dioxide nanoparticles in food and personal care products. *Environmental science and technology* **46**: 2242-2250.

Whitchurch, C.B., Tolker-Nielsen, T., Ragas, P.C., and Mattick, J.S. (2002) Extracellular DNA required for bacterial biofilm formation. *Science* **295**: 1487-1487.

Wiegand, I., Hilpert, K., and Hancock, R.E. (2008) Agar and broth dilution methods to determine the minimal inhibitory concentration (MIC) of antimicrobial substances. *Nature protocols* **3**: 163-175.

Wiegert, T., and Schumann, W. (2003) Analysis of a DNA-binding motif of the *Bacillus subtilis* HrcA repressor protein. *FEMS microbiology letters* **223**: 101-106.

Wilson, D.J., Gabriel, E., Leatherbarrow, A.J., Cheesbrough, J., Gee, S., Bolton, E. et al. (2008) Tracing the source of campylobacteriosis. *PLoS genetics* **4**: e1000203.

Wood, T.K., Knabel, S.J., and Kwan, B.W. (2013) Bacterial persister cell formation and dormancy. *Applied and environmental microbiology* **79**: 7116-7121.

Xie, Y., He, Y., Irwin, P.L., Jin, T., and Shi, X. (2011) Antibacterial activity and mechanism of action of zinc oxide nanoparticles against *Campylobacter jejuni*. *Applied and environmental microbiology* **77**: 2325-2331.

Yaron, S., and Matthews, K. (2002) A reverse transcriptase-polymerase chain reaction assay for detection of viable *Escherichia coli* O157: H7: investigation of specific target genes. *Journal of Applied Microbiology* **92**: 633-640.

Yoshida, H., Iwata, N., Katsuzaki, H., NAGANAwA, R., Ishikawa, K., Fukuda, H. et al. (1998) Antimicrobial activity of a compound isolated from an oil-macerated garlic extract. *Bioscience, biotechnology, and biochemistry* **62**: 1014-1017.

Young, K.T., Davis, L.M., and DiRita, V.J. (2007) *Campylobacter jejuni*: molecular biology and pathogenesis. *Nature reviews microbiology* **5**: 665.